Lecture Notes in Civil Engineering

Varinder S. Kanwar
Sanjay Kumar Shukla *Editors*

Sustainable Civil Engineering Practices

Select Proceedings of ICSCEP 2019

Springer

Lecture Notes in Civil Engineering

Volume 72

Lecture Notes in Civil Engineering (LNCE) publishes the latest developments in Civil Engineering—quickly, informally and in top quality. Though original research reported in proceedings and post-proceedings represents the core of LNCE, edited volumes of exceptionally high quality and interest may also be considered for publication. Volumes published in LNCE embrace all aspects and subfields of, as well as new challenges in, Civil Engineering. Topics in the series include:

- Construction and Structural Mechanics
- Building Materials
- Concrete, Steel and Timber Structures
- Geotechnical Engineering
- Earthquake Engineering
- Coastal Engineering
- Ocean and Offshore Engineering; Ships and Floating Structures
- Hydraulics, Hydrology and Water Resources Engineering
- Environmental Engineering and Sustainability
- Structural Health and Monitoring
- Surveying and Geographical Information Systems
- Indoor Environments
- Transportation and Traffic
- Risk Analysis
- Safety and Security

To submit a proposal or request further information, please contact the appropriate Springer Editor:

– Mr. Pierpaolo Riva at pierpaolo.riva@springer.com (Europe and Americas);
– Ms. Swati Meherishi at swati.meherishi@springer.com (Asia—except China—and Australia/NZ);
– Ms. Li Shen at li.shen@springer.com (China).

Indexed by Scopus and Compendex

More information about this series at http://www.springer.com/series/15087

Varinder S. Kanwar · Sanjay Kumar Shukla
Editors

Sustainable Civil Engineering Practices

Select Proceedings of ICSCEP 2019

Springer

Editors
Varinder S. Kanwar
Chitkara University
Solan, Himachal Pradesh, India

Sanjay Kumar Shukla
Edith Cowan University
Joondalup, WA, Australia

ISSN 2366-2557 ISSN 2366-2565 (electronic)
Lecture Notes in Civil Engineering
ISBN 978-981-15-3676-2 ISBN 978-981-15-3677-9 (eBook)
https://doi.org/10.1007/978-981-15-3677-9

This Springer imprint is published by the registered company Springer Nature Singapore Pte Ltd.
The registered company address is: 152 Beach Road, #21-01/04 Gateway East, Singapore 189721, Singapore

Preface

Increasing population worldwide creates the need to build more infrastructure and develop more resources, and therefore, our environment is under continued deterioration with different types of impact, including depletion of major resources such as air, water and soil, and destruction of the ecosystem. There is a need to understand that the true development cannot be achieved by putting resources and ecology at risk. We need to adopt the sustainability in our progress and growth. Sustainability is often defined as a set of environmental, economic and social conditions in which the society has the capacity and opportunity to maintain and improve its quality indefinitely without degrading the quantity, quality or availability of natural, economic and social resources. Civil engineers must take the lead in applying sustainability to selection, planning, design, construction and maintenance of various elements and components of infrastructure. Historically, sustainability considerations have been approached by engineers as constraints on their designs. However, with its growing importance for civil engineering and its other applied areas such as mining, agriculture and aquaculture, professionals should move towards incorporating sustainability principles into their routine practice. Sustainable design requires a complete assessment of the design in place and time. Sustainable engineering practice should meet the human needs for natural resources, industrial products, energy, food, transportation, shelter and effective waste and material management while conserving and protecting environmental quality and the natural resource base, essential for future development. Civil engineers can contribute solutions to sustainable development by adopting cleaner technology and green design principles. Commitment to this challenge requires that civil engineers acknowledge their professional obligation, extend their knowledge base and participate in all levels of policy decisions.

This international conference, held on 19–20 July 2019, achieved its aims by establishing long-term linkages between the user industries and the providers of clean technologies and sustainable materials for a rapid transformation of the small- and medium-sized enterprises (SMEs). Out of a total of 200 participants who attended this conference, about 60 were SMEs and over 30 were clean technology experts from different areas such as academics, consultancy, equipment manufacturers and

suppliers and environmental technology apart from regulators, administrators and students. The conference has created awareness and appreciation amongst academicians, scientists, researchers and practitioners from various disciplines and sectors about developing and implementing sustainable practices and technologies that minimize the impact on our environment. Deliberations were done on new initiatives in the latest technologies in the fields of infrastructure development and maintenance. This helped participants and regulators to formulate concrete strategies with optimal utilization of available resources for developing these technologies, consolidating the suggestions, strategies and recommendations made during the conference and disseminating the knowledge on the conference themes.

We would like to extend our deep-felt thanks to Dr. Ashok K. Chitkara, Chancellor of Chitkara University; Dr. Madhu Chitkara, Pro-Chancellor of Chitkara University; and Prof. Steve Chapman, CBE, Vice-Chancellor and President of Edith Cowan University for supporting us at all fronts. We are thankful to Dr. Akash Chakraborty, Rini Christy Xavier Rajasekaran and the team of Springer for their full support and cooperation at all the stages of the publication of this book. We wish to extend our special thanks to the contributing researchers/authors, sponsors and all those who supported this conference for making it a milestone in the area of sustainability.

We do hope that this book will create awareness and appreciation amongst academicians, scientists, researchers and practitioners from various disciplines and sectors about the need and the new initiatives towards sustainable infrastructure development. The comments and suggestions from the readers and users of this book are most welcome.

Solan, India — Varinder S. Kanwar
Perth, Australia — Sanjay Kumar Shukla

Contents

About the Editors

Dr. Varinder S. Kanwar Vice Chancellor, Chitkara University, Himachal Pradesh, India, obtained his Master in structural engineering and his Ph.D in civil engineering from Thapar University, Patiala. He also has a Postgraduate Diploma in Rural Development from IGNOU, New Delhi. Dr. Kanwar carries more than 22 years of research, training and administrative experience having previously worked at NIT Hamirpur, Government Polytechnic Hamirpur, Thapar University, Patiala and Punjab Technical University, Jalandhar. He is an active member of various professional societies, including ASCE, Indian Concrete Institute, Institution of Engineers (India) and Punjab Science Congress. He is a Fellow of Institution of Engineers (India). His major research areas include health monitoring of structures and alternate construction materials. He has authored 3 books on Water Supply Engineering, Health Monitoring of Structures & Modern Temples of Resurgent India - Engineering Pilgrimage to Bhakra, Beas and Ranjit Sagar Dams; published 16 journal articles and 20 research papers in conference proceedings and edited 10 conference proceedings. He is also actively involved in joint research activities carried out by Chitkara University, Glasgow Caledonian University, ESTP Paris, Edith Cowan University and Federal University Australia. He was awarded by the Institution of Engineers (India) with the E.P. Nicolaides Prize. He has also been awarded with 'Excellent Contribution in Education Sector' by CMAI Association of India in 2017. His present assignment involves a close interaction with Department of Higher

Education, Government of Himachal Pradesh, Himachal Pradesh Private Educational Institutions Regulatory Commission, University Grants Commission, AIU and other regulatory agencies.

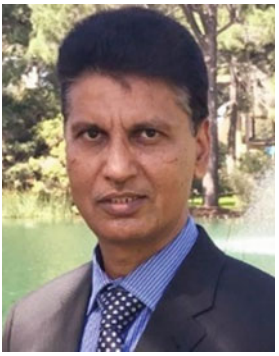

Dr. Sanjay Kumar Shukla is an internationally recognized expert in the field of Civil (Geotechnical) Engineering. He is the Founding Editor-in-Chief of International Journal of Geosynthetics and Ground Engineering. He is also the Founding Research Group Leader (Geotechnical and Geoenvironmental Engineering) at Edith Cowan University, Perth, Australia. He holds the distinguished professorship in Civil Engineering at four international universities, including Fiji National University, Suva, Fiji. He graduated in Civil Engineering from BIT Sindri, India, and earned his MTech in Civil Engineering (Engineering Geology) and PhD in Civil (Geotechnical) Engineering from Indian Institute of Technology Kanpur, India. His primary areas of research interest include geosynthetics and fibres for sustainable developments, ground improvement techniques, utilization of wastes in construction, earth pressure and slope stability, environmental, mining and pavement geotechnics, and soil-structure interaction. He is an author/editor of 14 books, and more than 240 research papers, including over 150 peer-reviewed journal papers. Dr. Shukla's generalized expression for seismic active thrust (2015) and generalized expression for seismic passive resistance (2013) are routinely used by practicing engineers worldwide for designing the retaining structures. He has been honored with several awards, including the most prestigious IGS Award 2018 by the International Geosynthetics Society (IGS), USA, in recognition of his outstanding contribution to the development and use of geosynthetics during the 2014-2017 award period. He is a Fellow of Engineers Australia, Institution of Engineers (India) and Indian Geotechnical Society, and a member of American Society of Civil Engineers, International Geosynthetics Society and several other

professional bodies. He is the Senior Editor of Cogent Engineering (Civil and Environmental Engineering), and serves on the editorial boards of many international journals, including ICE Ground Improvement, Soil Mechanics and Foundation Engineering, and Journal of Mountain Science.

Use of Waste Foundry Sand in Precast Concrete Paver Blocks—A Study with Belgaum Foundry Industry

H. K. Thejas and Nabil Hossiney

Abstract The current study was undertaken at CHRIST (Deemed to be University) in Bangalore to investigate the potential of using waste sand from Belgaum foundries as fine aggregate in the production of precast concrete paver blocks. Concrete paver blocks were manufactured as per the recommendations of IS 15658:2006. M-35 grade of concrete with block thickness of 60 mm was considered as the design parameter. Waste Foundry Sand (WFS) and ground-Granulated Blast Furnace Slag (GGBS) were replaced for manufactured sand and cement, respectively. WFS replacement rates were 15, 30, and 45% by weight of the manufactured sand, and that of GGBS was 30% constant by weight of cement. Obligatory performance tests were conducted as per Indian standards, which included compressive strength, water absorption, and abrasion resistance. Accordingly, paver blocks with 45% WFS showed satisfactory results and can be considered into non-traffic to light-traffic category, which finds application in places like building and monument premises, paths and patios, landscapes, public gardens, and parks. Cost comparison of conventional paver blocks with WFS paver blocks showed approximately 4.8% reduction in the cost of paver blocks containing 45% WFS.

Keywords Waste foundry sand · GGBS · Concrete · Pavers

1 Introduction

In India, Construction is the second largest industry next to agriculture. Construction accounts for more than 40% of national plan outlay and 5% of the gross domestic products [1]. Concrete is one of the most widely used materials in construction industries. Use of sand as fine aggregate has tremendously increased in the present days. Fine aggregate obtained from the natural sources like river bed and manufactured

H. K. Thejas (✉) · N. Hossiney
Faculty of Engineering, CHRIST (Deemed to be University), Bengaluru 560 074, India
e-mail: thejas.hk@christuniversity.in

N. Hossiney
e-mail: nabil.jalall@christuniversity.in

V. S. Kanwar and S. K. Shukla (eds.), *Sustainable Civil Engineering Practices*,
Lecture Notes in Civil Engineering 72,
https://doi.org/10.1007/978-981-15-3677-9_1

sand from quarries are not considered to be sustainable, since quarrying operations are disruptive to the natural ecosystem, wildlife habitats, hydrological resources, etc. Therefore, in this scenario, the use of waste materials in the construction sector can lead to a sustainable practice. Annually, the average per capita consumption of cement worldwide is about 260 kg and that of concrete 1000 kg, while in India it is about 95 and 375 kg, respectively. The cement and concrete consumptions are expected to grow at an average rate of 2 to 3% world over, while in India it is expected to grow at 5 to 6% during the next decade [2].

WFS is generated from ferrous and nonferrous metal-casting industry. The incorporation of such material in concrete helps in reducing the disposal concerns. Partial substitution of sand with WFS in concrete will lower the rate of consumption of natural and manufactured sand. Also replacing cement partially by supplementary materials provides an avenue to reduce the burden on the cement industry. At present, 40–45% of concrete supplied by ready mix plants use fly ash and GGBS for partial cement replacement [3].

Government of India is giving emphasis on infrastructure development with green mobility concept. This importance is given to mobility of non-motorized vehicles and pedestrians, which will reduce the vehicular dependence and increase the quality of living in neighborhoods by reducing carbon emission. It will also increase the safety of pedestrians. But the green mobility concept has increased the demand on materials like cement and crushed aggregate in urban and semi-urban regions of India. Therefore, there is a need to look for alternatives and use of sustainable materials. WFS has shown great potential in the construction industry as a valuable resource [4–9]. In this context, a study on concrete with WFS and GGBS is pursued to evaluate the influence of WFS on mechanical properties of concrete paver blocks. The present study aims at manufacturing paver blocks for non-motorized and pedestrian facility by partially substituting M-sand by WFS and cement by GGBS.

2 Experimental Programme

A standard concrete mix with no WFS and GGBS was designed according to IS 10262-2009 [10]. Additional concrete mix with WFS and GGBS were also proportioned as shown in Table 1. Table 2 presents the concrete mix proportioning the

Table 1 Details of mix specifications

Specifications	Mix type
0% WFS, 0% GGBS	P0
15% WFS, 30% GGBS	P1
30% WFS, 30% GGBS	P2
45% WFS, 30% GGBS	P3
0% WFS, 30% GGBS	P4

Table 2 Details of mix proportions

Mix type	Consumption of design mix propotionsfor M35 concrete					
	Water (Kg/m^3)	Cement (Kg/m^3)	GGBS (Kg/m^3)	Coarse aggregate (Kg/m^3)	M-Sand (Kg/m^3)	WFS (Kg/m^3)
P0	195	430	0	1074	630	0
P1	195	300	130	1074	535.5	94.5
P2	195	300	130	1074	441	189
P3	195	300	130	1074	346.5	283.5
P4	195	300	130	1074	630	0

details. In the past, similar mix proportions were carried with satisfactory results on concrete properties [11]. Therefore, based on results of the past study, concrete mixtures were proportioned for paver blocks. The tests performed on the paver blocks were in accordance with IS 15658-2006 [12] obligatory requirements. These tests include compressive strength, water absorption, and abrasion resistance. The standard requires the tests to be performed after 28 days of moisture curing. Therefore, all the specimens were moisture cured for 28 days before testing.

2.1 Materials

The cement used was OPC grade 53 conforming to standard IS 12269-2013 [13]. Tests were conducted on the cement to determine its physical properties as per IS 4031-1999 [14]. The initial setting time of the cement was 40 min and the specific gravity was 3.15. M-sand was obtained from local quarries which confirmed to zone I according to IS 383-1970 [15], with water absorption of 1%, and specific gravity of 2.65. Similarly, crushed stone with a maximum size of 12 mm obtained from local quarries was used as coarse aggregate. The specific gravity and water absorption for coarse aggregate were 2.65 and 0.5%, respectively. WFS was obtained from a reclamation facility in Belgaum, Karnataka. WFS specific gravity was found to be 2.35. WFS and M-sand particle size distribution are shown in Fig. 1. From the figure, it is clear that WFS is much finer than the M-sand with majority of the particles ranging from 0.3 to 0.075 mm in size. Table 3 presents the chemical composition of M-sand, WFS, and GGBS.

3 Results and Discussions

Figure 2 shows the compressive strength of paver blocks. The compressive strength test of (200 × 100 × 60) mm size paver blocks was conducted after 28 days of

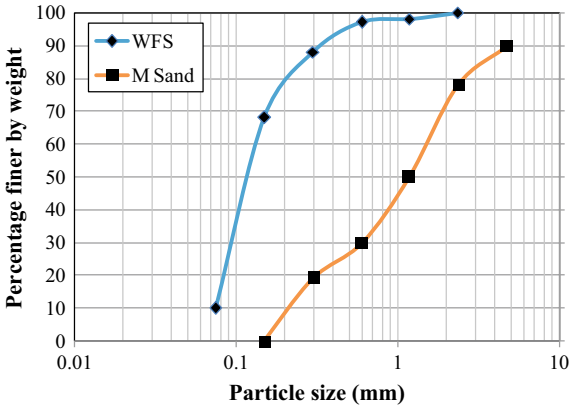

Fig. 1 Particle size distribution of WFS in comparison to M-sand

Table 3 Chemical composition of M-sand, WFS, and GGBS

Material	Values in percentage (%)							
	SiO_2	Al_2O_3	Fe_2O_3	CaO	MgO	TiO_2	Na_2O	K_2O
M-sand	30.73	16.32	0.56	38.47	6.41	–	–	–
WFS	60.21	5.96	6.37	2.22	1.43	0.15	0.19	0.25
GGBS	31.80	17.10	0.50	17.10	6.23	1	0.57	0.31

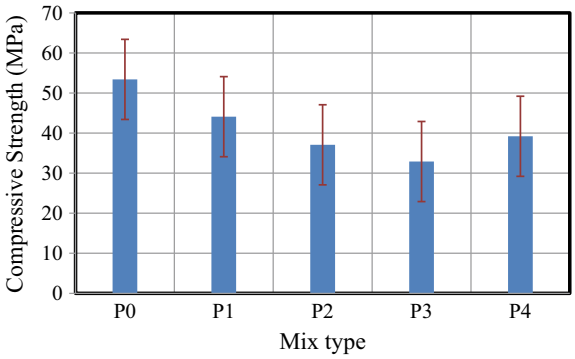

Fig. 2 Compressive strength of paver blocks

curing. A decrease of 17.4, 30, and 38.4% in compressive strength was observed in mix P1, P2, and P3 when compared to P0, respectively. There was a decrease in the strength as the percentage of WFS increased; this decrease in strength can be due to the presence of binders like bentonite in WFS, which can have negative effects on the hydration kinetics of the cement. It is also seen that variations in the compressive strength values of different mix proportions are negligible. The mean value of compressive strength of different mixes was seen as linearly decreasing. All the mixtures containing WFS satisfy the IS 15658-2006 requirement for minimum

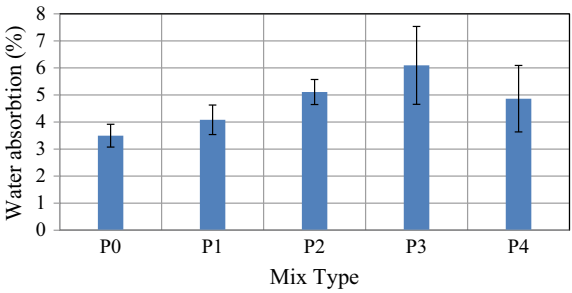

Fig. 3 Water absorption of paver blocks

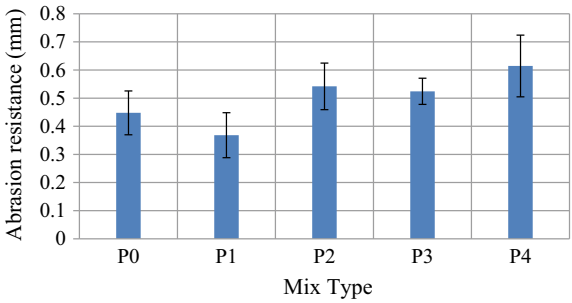

Fig. 4 Abrasion resistance of paver blocks

compressive strength of 30 N/mm^2 for application in non-traffic conditions. Figure 3 shows the water absorption of paver blocks. After 28 days of curing, an increase of 14.3, 31, and 42.6% in water absorption was observed in mix P1, P2, and P3 when compared to reference mix P0, respectively. As WFS has more fine particles, this can lead to greater water absorption, when compared with conventional sand in concrete paver blocks. This high water absorption values for P3 can also be attributed due to WFS coming from the reclamation plant at Belgaum, which consists of very fine dust particles and binders. The abrasion resistance of blocks specimens of (71 × 71 × 60) mm size was conducted after 28 days of curing. Abrasion resistance of concrete paver blocks containing WFS showed very minimal loss due to wear. As per IS 15658-2006 specifications, abrasion resistance measured in terms of loss of thickness should be less than 3 mm. From Fig. 4, it is seen that none of the pavers containing WFS showed thickness loss of more than 1 mm. Therefore, all the paver blocks with WFS satisfy the requirements on abrasion resistance as per the IS 15658-2006.

4 Cost Analysis

Table 4 presents the cost comparison for conventional concrete and WFS concrete paver blocks. The rates mentioned below are based on the Bangalore market price.

Table 4 Cost comparison of conventional concrete and WFS concrete paver blocks

Materials	Paving concrete without WFS (Mix P4)			Paving concrete with 45%WFS (Mix P3)		
	(kg/m^3)	Rate/kg (Rs.)	Amount (Rs.)	(kg/m^3)	Rate/kg (Rs.)	Amount (Rs.)
Cement	300	8.00	2400.00	300	8.00	2400.00
Coarse aggregate	1074	0.60	644.40	1074	0.60	644.40
Fine aggregate	630	0.75	472.25	347	0.75	260.25
WFS	–	–	–	284	0.10	28.40
GGBS	130	2.5	325.00	130	2.5	325.00
Total			3841.65			3658.05

Overhead charges and contractor profit is not included as the charges remain the same irrespective of the materials. Even though WFS is free, a minimum transportation cost of 10 paise/kg is added in the cost comparison. It can be noticed that the difference in amount is Rs. $184/m^3$. This indicates that there will be savings when WFS is utilized for the production of concrete paver blocks. This will encourage the policy makers to utilize WFS in manufacturing paver blocks for pedestrian facilities.

5 Conclusions

The current study shows that WFS can be effectively used in the construction of paver blocks. Based on the experimental study, the following are a few conclusions.

1. The average compressive strength of 32 MPa was obtained for paver blocks when 45% of M-sand was replaced by WFS by weight. For all the paver blocks with WFS, the abrasion loss and water absorption were within 3 mm and 6%, respectively, which satisfied the requirements as per IS 15658-2006.
2. Cost analysis showed that by incorporation of 45% WFS in paver blocks, there was approximately 4.8% reduction in the production cost. Therefore, the use of WFS in paver blocks can provide economic benefits to the industry.
3. WFS paver blocks were categorized in non-traffic to light-traffic category as per IS 15658-2006. It finds application in places like building premises, monument premises, landscapes, public gardens/parks, paths and patios, embankment slopes, sand stabilization area, pedestrian plazas, shopping complexes, ramps, car parks, office driveways, housing colonies, rural roads with low volume traffic, farmhouses, beach sites, and tourist resorts.

Acknowledgements We are thankful to Belgaum Foundry Cluster for providing material and technical support throughout the project. Appreciation is also extended to CHRIST (Deemed to be University) for providing financial support for this research study.

References

1. Panagariya A (2005) India in the 1980s and the 1990s: a triumph of reforms. In: Tseng W, Cowen D (eds) India's and China's recent experience with reform and growth. Procyclicality of Financial Systems in Asia. Palgrave Macmillan, London
2. Hummel RE (2004) Understanding materials science—history, properties, applications, 2nd edn. Springer, United States of America
3. Reddy BS, Ray BK (2010) Decomposition of energy consumption and energy intensity in Indian manufacturing industries. Energy Sustain Dev 14:35–47
4. Hossiney N, Das P, Mohan MK, George J (2018) In-plant production of bricks containing waste foundry sand—a study with Belgaum foundry industry. Case Stud Constr Mater 9:e00170
5. Smarzewski P, Barnat − Hunek D (2016) Mechanical and durability related properties of high performance concrete made with coal cinder and waste foundry sand. Constr Build Mater 121:9–17
6. Nwofor TC, Ukpaka C (2016) Assessment of concrete produced with foundry waste as partial replacement for river sand. J Civil Eng Res 6:1–6
7. Bhimani DR, Pitroda J, Bhavsar JJ (2013) Used foundry sand: opportunities for development of eco-friendly low cost concrete. Int J Adv Eng Technol 4:63–66
8. Salokhe EP, Desai DB (2013) Application of foundry waste sand in manufacture of concrete. IOSR J Mech Civil Eng, 43–48 (Second International Conference on Emerging Trends in Engineering (SICETE). Dr.J.J.Magdum College of Engineering, Jaysingpur)
9. da Silva WRL, Tochetto E, Prudêncio JRLR, Oliveira AL (2011) Influence of foundry sand residues on the fresh and hardened properties of mortars produced with portland cement. IBRACON Struct Mater J 4:642–662
10. IS 10262-2009 (2009) Guidelines for concrete mix design proportioning. Bureau of India Standards, New Delhi, India
11. Jose J, Hossiney N (2016) Characteristics of concrete containing waste foundry sand and slag sand. Int J Earth Sci Eng 9:54–59
12. IS 15658-2006 (2006) Precast concrete blocks for paving-specifications. Bureau of India Standards, New Delhi, India
13. IS 12269-2013 (2013) Ordinary portland cement 53 grade-specification. Bureau of India Standards, New Delhi, India
14. IS 4031-1999 (1999) Methods of physical tests for hydraulic cement. Bureau of Indian Standards, New Delhi, India
15. IS 383-1970 (1970) Coarse and fine aggregates from natural sources of concrete. Bureau of Indian Standards, New-Delhi, India

An Experimental Study on Utilisation of Red Mud and Iron Ore Tailings in Production of Stabilised Blocks

M. Beulah, K. Sarath Chandra, Mothi Krishna Mohan, I. Clifford Dean and G. Gayathri

Abstract Construction of bricks using waste materials is one among the many ways to address the problems encountered in infrastructure. In the present study, various industrial and mining wastes have been used to manufacture stable bricks. These wastes include red mud (RM) from Hindalco, and iron ore tailings (IOT) from BMM Ispat, Bellary. Both RM and IOT were combined in different proportions with ground-granulated blast furnace slag (GGBS) and waste lime. In first series, IOT was replaced in the range of 45% to 60% with increments of 5%, and RM was replaced in the range of 15% to 30% with increments of 5%. In the second series, RM was replaced in the range of 45% to 60% with increments of 5%, and IOT was replaced in the range of 15% to 30% with increments of 5%. Tests were performed as per the Indian and ASTM standards on both the raw material and the developed composites. These tests include liquid, plastic limit, particle size, XRF, XRD, and SEM on raw materials, while tests performed on composites were compressive strength, water absorption, efflorescence, porosity, apparent specific gravity, and bulk density. Results of the study indicate that addition of IOT up to 55% is acceptable as brick material.

Keywords Red mud · Ground-granulated blast slag (GGBS) · Iron ore tailings (IOT) · Lime · Stabilization

1 Introduction

Bricks are one of the desired walling materials in India. Due to rapid growth in population and urbanisation, the demand on building materials like bricks has risen drastically. In a published report "Environmental and energy sustainability: An approach

M. Beulah (✉) · K. Sarath Chandra · M. K. Mohan · I. Clifford Dean
Department of Civil Engineering, Christ (Deemed to be university), Bangalore, Karnataka 560074, India
e-mail: m.beulah@christuniversity.in

G. Gayathri
Department of Civil Engineering, ACS College of Engineering, Bangalore, Karnataka 560074, India

V. S. Kanwar and S. K. Shukla (eds.), *Sustainable Civil Engineering Practices*,
Lecture Notes in Civil Engineering 72,
https://doi.org/10.1007/978-981-15-3677-9_2

for India" by McKinsey &Company, Inc. it was reported by 2030, the construction sector in India would grow at the rate of 6.6%, and 40% of the population will be residing in the urban areas [1]. Another challenge faced is rapid depletion of natural resources. Therefore, to protect the natural resources, use of various industrial wastes to develop a sustainable building material towards green technology would be desirable [2]. Past literatures have already proven the viability of using materials like fly ash and GGBS along with mining waste as sustainable infrastructure materials [3]. Various kinds of mine waste can be used as a sustainable brick-making material [4–6]. Method of geopolymerisation to manufacture IOT bricks with compressive strength of up to 50 MPa has been reported [7]. The researchers have also shown the potential of IOT as aggregates in concrete [8–10]. Studies have also shown the viability of using IOT as fine aggregates in the production of ultra high performance concrete (UHPC) with enhanced strength and frost resistance [9, 11, 12].

The solid waste originated in the aluminium industry by the Bayer's process is red mud or bauxite residue with a pH of 10.5–12.5 which poses serious environmental problems like contamination of underground water due to its leaching property. Many studies proved red mud as an alternative construction material for composite elements like bricks, tiles, roofs and subgrade [13, 14]. The red mud mixture with clay performs as attractive alternative low-cost building material; because of its excellent high mechanical resistance and low absorption properties [15]. Red mud has a potential to produce light weight foamed bricks (LWFB).The LWFB envisaged using in urban construction activities as partitions in the multi-storeyed buildings which reduces the total weight of the wall, foundation cost and building cost [16]. Past studies have been carried on the combination of red mud, fly ash and lime for fired and unfired bricks and proved to be ideal brick material [17, 18]. The RM with geopolymerisation method has already proven to be ideal for bricks [19, 20]. The RM can also be an ideal material for pavement blocks, high grade-base material, embankment and filling material [21–24].In fact, many researchers have reported promising result of RM as a pozzolanic material [25–27]. These studies show an alternative to minimise the environmental impact caused by aluminium industry and mining industry. So far, most of the studies were carried with specific mining waste and there is limited information on the blend of various mining wastes. Therefore, the present study helps to fill the gap in this particular research area.

2 Experimental Investigations

2.1 Materials

In the present study, IOT and RM were used along with GGBS and lime to make standard bricks. Figure 1 shows that the mean particle size of red mud is 36.94 microns and 50% particle size is 10.29micron with a surface area of 0.83 m^2/gm, whereas for IOT, the mean particle size is 22.84 micron, with a surface area of17.88micron

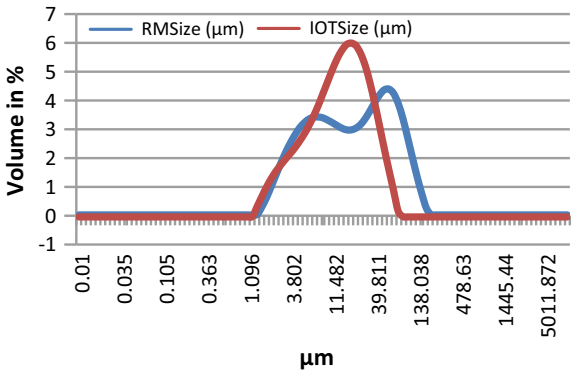

Fig. 1 Particle size distribution of IOT and RM

and 50% particle size with a surface area of 0.59 m^2/gm. Chemical and the physical properties of materials are presented in Tables 1 and 2. As it is seen, the major components in IOT were Fe_2O_3 (66.5%), SiO_2 (9.02%) and Al_2O_3 (9.56%). In RM, the main components are Fe_2O_3 (44.04%), SiO_2 (9.02%) and Al_2O_3 (19.48%) and in GGBS, the components are Fe_2O_3 (1.99%), SiO_2 (34.16%), Al_2O_3 (17.54%) and CaO (37.10%).

Table 2 explicits the physical properties of IOT and red mud and for accuracy, average value obtained from the tests conducted in triplicate was considered. Fineness modulus, specific gravity and consistency limits were determined in accordance with the ASTM C33, D854, D4318 standards, respectively. The optimum moisture content and maximum dry density of RM and IOT were determined by conducting standard compaction test in accordance with the standards ASTM D698. Presence of iron shows the increase in maximum dry density in IOT compared to the RM.

2.2 Experiment and Test Methods

Table 3 presents the details of the mix proportions. In the present study, stabilised blocks were manufactured by using manual-operated block-making machine called "Mardini" which was developed by ASTRA/Department of Civil Engineering, Indian Institute of Science, Bangalore. The standard mould size which was used for making of bricks is 230 × 110 × 100 mm.

The lime solution was maintained constant based on the recommendations in the literature [28], and the concentration of lime solution was designed by the number of trials to optimise the ratio of the lime and water. The brick samples were tested as per the IS and ASTM standards as mentioned in Table 4.

The characterisation of raw materials like mineralogical composition (XRD) and textural behaviour (SEM) was performed. XRD is an analysis technique which is highly used for the determination of crystalline particles that are present in the sample. This test is also used for providing information on unit cell dimensions.

Table 1 Chemical composition of IOT & Red mud

Material	SiO_2	Al_2O_3	Fe_2O_3	TiO_2	CaO	MgO	Na_2O	K_2O	LOI
IOT (%)	9.02	9.56	66.50	1.00	1.96	2.12	0.93	0.25	8.59
RM (%)	9.02	19.48	44.40	6.14	1.96	2.73	4.4.9	0.30	11.42
GGBS (%)	34.16	17.54	1.99	1.00	37.10	7.17	0.57	0.31	0.10

Table 2 Physical properties of IOT and red mud

Properties	Results	
	IOT	Red mud
Fineness modulus	1.8	2.4
Specific gravity	2.34	2.8
Optimum moisture content (%)	9.8	14.95
Maximum dry density (KN/m^3)	21.40	14.80
Liquid limit (%)	26.1	46
Plastic limit (%)	16.56	27
Plasticity index (%)	9.54	19

Table 3 Details of the mix proportions

Brick designation	Mix A	Mix B	Mix C	Mix D	Mix E	Mix F	Mix G	Mix H
IOT (%)	45	50	55	60	30	25	20	15
RM(%)	30	25	20	15	45	50	55	60
GGBS (%)	10	10	10	10	10	10	10	10
Lime (%)	3.75	3.75	3.75	3.75	3.75	3.75	3.75	3.75
Water (%)	11.25	11.25	11.25	11.25	11.25	11.25	11.25	11.25

Table 4 Details of the test specification

Test method	Standards
Compressive strength	IS 1077-1992
Water absorption	IS 3495 (part 2):1992
Apparent porosity	ASTM C20
Apparent specific gravity	ASTM C20
Bulk density	ASTM C20

3 Results and Discussion

Figures 2 and 3 show the SEM micrograph of IOT and RM with irregular particles with high degree of agglomeration. Figure 4 shows SEM micrograph of GGBS which is non-uniform distribution of irregular particles, whereas Fig. 6 shows the XRD pattern of the IOT and the presence of minerals such as quartz (Q), qaolinite (K), calcite (C) and haematite (H). Figure 5 illustrates the XRD pattern of the RM with the combination of $Na_5Al_3CSi3O_{15}$ (Na), calcium carbonate ($Ca(CO_3)$), muscovite (M), haematite (H) and aluminium hydroxide ($Al(OH_3)$). Figure 7 shows the XRD pattern of GGBS signifying as amorphous material.

Table 5 presents the apparent specific porosity, apparent specific gravity, bulk density, water absorption, and compressive strength of bricks. The porosity ranges from 37.30% to 46.96% which has not shown a significant influence on the compressive

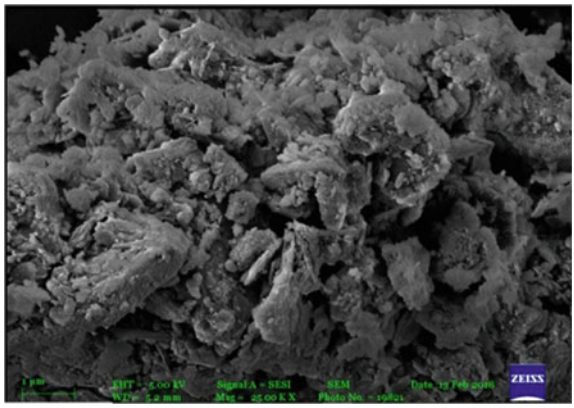

Fig. 2 SEM micrograph of IOT

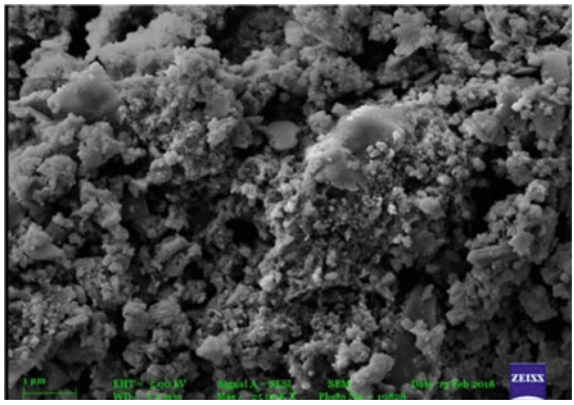

Fig. 3 SEM micrograph of RM

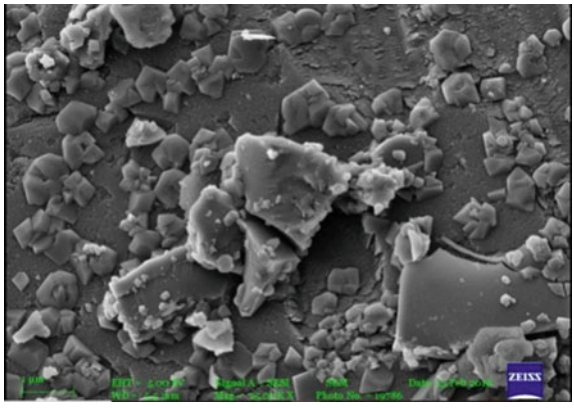

Fig. 4 SEM micrograph of GGBS

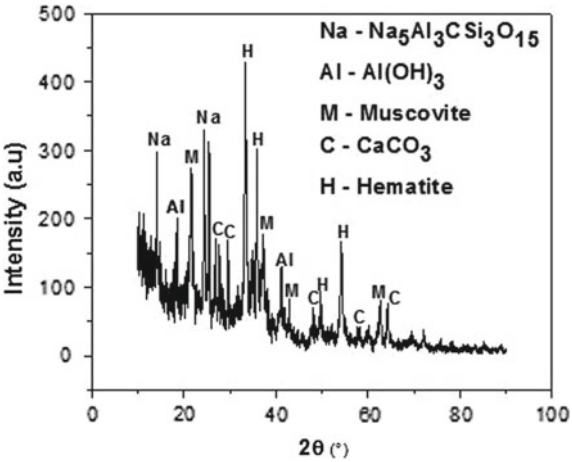

Fig. 5 XRD pattern of RM

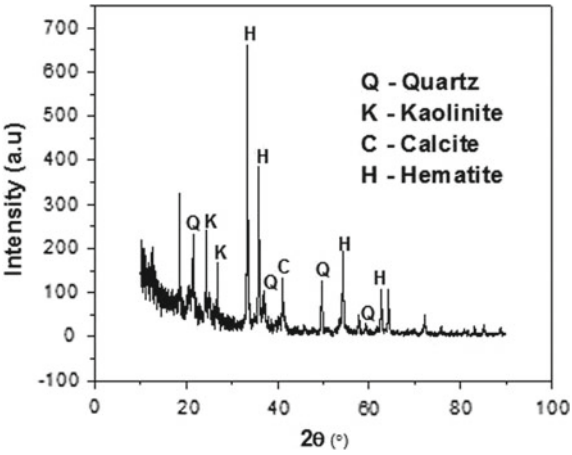

Fig. 6 XRD pattern of IOT

strength. The varying percentage of RM and IOT has not influenced the density of the brick.

The compressive strength was high for sundried brick when compared with ambient temperature-cured bricks. The compressive strength of Mix C with 55% of IOT was increased by 15.10% for sundried bricks in comparison to ambient-cured bricks. It shows that beyond 55% of IOT is not acceptable to use as a brick-making material. The compressive strength of Mixes E–H ranges from 4.79 MPa to 7.80 MPa for room temperature-cured bricks and for sundried bricks, 5.44 MPa to 10.43 MPa. The presence of Al_2O_3 in RM and CaO in GGBS reacted with Sio_2 formed a chemical reaction of Si–Al and Si–Ca which has contributed to high compressive strength for the Mixes E–H. In comparison to Mixes A–D, Mixes E–H was proven to be high quality bricks, even the water absorption values of the Mixes E–H is less than

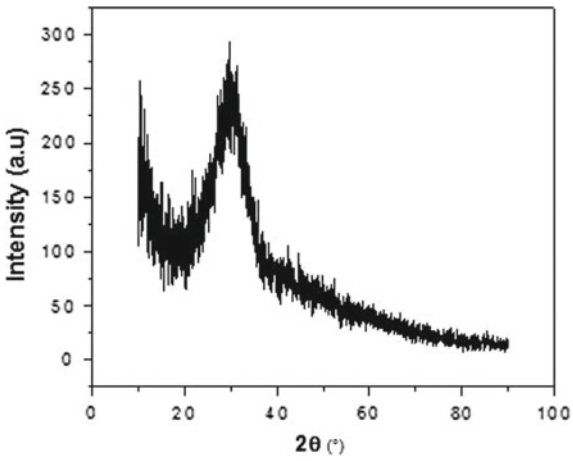

Fig. 7 XRD pattern of GGBS

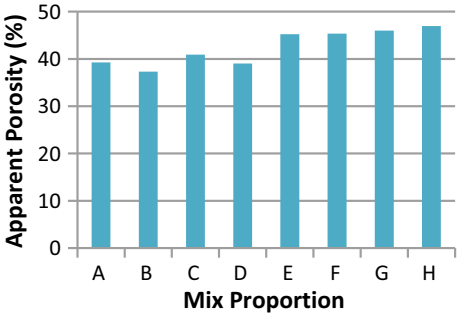

Fig. 8 Apparent porosity of bricks

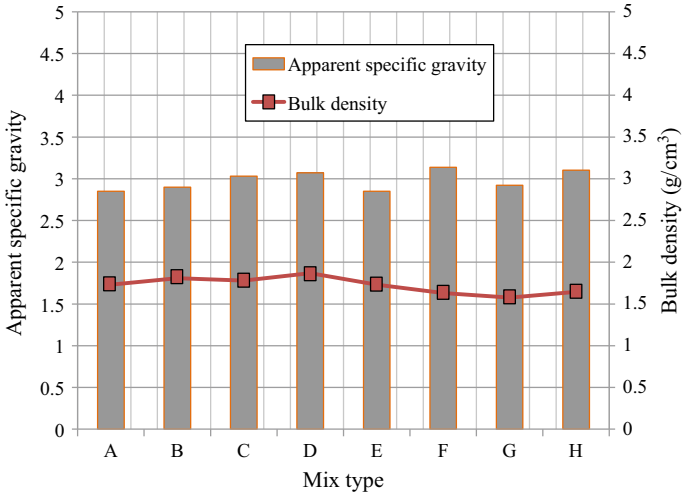

Fig. 9 Specific gravity-bulk density

Table 5 Apparent porosity, apparent specific gravity, bulk density, water absorption and compressive strength

Composition	Apparent porosity (%)	Apparent specific gravity	Bulk density (g/cm^3)	Water absorption (%)	Compressive strength (MPa) (Room temperature)	Compressive strength (MPa) (Sundried bricks)
Mix A	39.27	2.85	1.73	13.6	3.20	3.88
Mix B	37.30	2.90	1.81	17.2	3.54	3.87
Mix C	40.90	3.03	1.78	18.88	3.88	4.03
Mix D	39.01	3.07	1.87	20.61	2.19	2.92
Mix E	45.21	2.85	1.73	16.35	4.79	5.44
Mix F	45.35	3.136	1.630	16.42	5.65	7.00
Mix G	45.97	2.922	1.576	18.16	6.35	7.51
Mix H	46.96	3.102	1.645	19.58	7.08	10.43

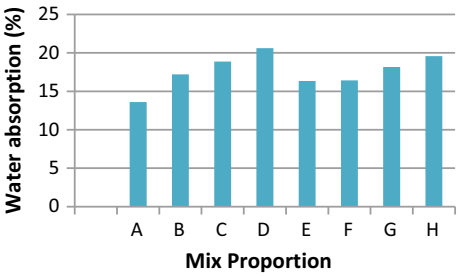

Fig. 10 Water absorption of bricks

20% as per IS code recommendations (Fig. 10). The results of efflorescence of all the mixes falls within the recommendation of IS: 3495-Part [3]. The hardness and dimensionality of all the mixes are within the IS code recommendations of IS: 2185 part [1].

Figures 8 and 9 depict the apparent porosity and bulk density of the IOT and RM bricks. It was noticed that there is an insignificant difference between the bricks of different compositions of IOT and RM. Figure 11 depicts compressive strength of the bricks (sundried and room temperature-cured bricks).

4 Conclusions

The current study presents the production of bricks containing Iron ore tailings and red mud as major materials. Following are a few conclusions drawn from this study

1. The results showed that IOT and RM are suitable materials to produce bricks by adopting local conditions.

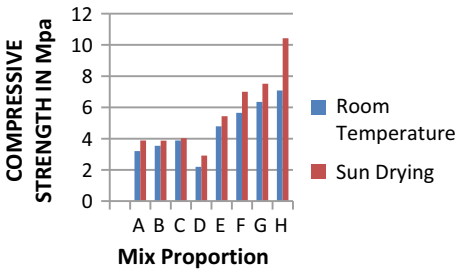

Fig. 11 Compressive strength of bricks

2. There was a significant increase in the compressive strength of the Mix C by 15.1% for sundried bricks in comparison with ambient temperature-cured bricks. This shows that up to 55% of IOT is acceptable.
3. It was observed that there was an increase of 47.8% in compressive strength, as the percentage of red mud increased (Mixes E–H).
4. The presence of IOT and red mud has not influenced the bulk density of the brick.
5. The maximum rate of water absorption is 20.6% for Mix D due to the presence of 60% IOT.
6. The Mixes C, E and F can be classified as class III bricks, whereas Mixes G and H can be classified as class II bricks and based on recommendations of IS 1077 standard specification.
7. The compressive strength of the sundried stabilized bricks was high when compared with room temperature-cured bricks.

References

1. Environmental & Energy sustainability: An approach of India, McKinsey & company Inc
2. Reddy NG, Rao BH (2016) Evaluation of the compaction characteristics of untreated and treated red mud. GSP-272, ASCE, pp 23–32
3. Jiménez-Quero V, Maza-Ignacio OT, Guerrero-Paz J, Campos Venegas K (2017) Industrial wastes as alternative raw materials to produce eco-friendly fired bricks. J Phys Conf Series 792(012065):1–6
4. Nagaraj HB, Shreyasvi C (2016) Compressed stabilized earth blocks using iron mine spoil waste. In: An explorative study, international high—performance built environment conference—a sustainable built environment conference 2016 Series (SBE16), iHBE 2016, Procedia Engineering, pp 1–10
5. Malatse M, Ndlovu S (2015) The viability of using the Witwatersrand gold mine tailings for brick making. J S Afr Inst Min Metall 115:321–327
6. Weishi Li, Guoyuan L, Ya X, Qifei H (2018) The properties and formation mechanisms of eco-friendly brick building materials fabricated from low-silicon iron ore tailings. J Clean Prod 204:685–692
7. Kuranchiea FA, Shuklaa SK, Habibia D (2014) Utilisation of iron ore mine tailings for the production of geopolymer bricks. Int J Mining Reclam Environ 20:1–25
8. Sabat V, Shaikh M, Kanap M, Knadgouda K (2015) Use of Iron ore tailings as a construction material. Int J Conceptions Mech Civil Eng 3(2):1–6

9. Kuranchie FA, Shukla SK, Habibi D, Mohyeddin A (2015) Utilisation of iron ore tailings as aggregates in concrete. Cogent Eng 2(1083137):1–11
10. Lamani SR, Aruna M, Vardhan H, Shanth AT (2015) Development of value added product using iron ore waste for its effective utilization. Int J Adv Appl Sci 2(12):30–35
11. Zhu Zhigang, Li Beixing, Zhou Mingkai (2015) The influences of Iron ore tailings as fine aggregate on the strength of ultra-high performance concrete. Adv Mater Sci Eng 2015:1–6
12. Kuranchie FA (2015) Characterisation and applications of iron ore tailings in building and construction projects. Doctor of Philosophy thesis, Edith Cowan University
13. Kavas T (2006) Use of boron waste as a fluxing agent in production of red mud brick. J Build Environ 17(41):79–83
14. Yang J, Xiao B (2008) Development of unsintered construction materials red mud wastes produced in the sintering alumina process. Constr Build Mater 22:2299–2307
15. HildebrandoI DA, SouzaII JAS, AngélicaIII RS, Neves RF (2013) Application of bauxite waste from amazon region in the heavy clay industry. 16 (6)
16. Najar PAM, Nimje MT, Prajapati SS (2012) Development of light weight foamed bricks from red mud. In: Conference: IBAAS-
17. Rai S, Wasewar KL, Chaddha MJ, Mukhopadhyay J (2013) Utilization of red mud for making bricks. Res J Eng Tech 4(1):12–14
18. Bhaskar M, Akhtar S, Batham G (2014) Development of the bricks from red mud by industrial waste (Red Mud). Int J Emerg Sci Eng 2(4):7–12 (IJESE) ISSN: 2319–6378
19. Ananya A, Avarebeel PB, Sambasivam MC, Aswath MU, Singh S (2015) Experimental Study on Red Mud Based Geopolymer Bricks. Int J Adv Res Eng Sci Technol 2(8):76–83
20. Panias D, Giannopoulou I, Boufounos D (2014) Valorization Of Alumina Red Mud For Production Of Geopolymeric Bricks. Light Met, 155–159
21. Dodoo-Arhin D, Nuamah RA, Agyei-Tuffour B, Obada DO, Yaya A (2017) Awaso bauxite red mud-cement based composites: characterisation for pavement applications. Case Stud Constr Mater 7:45–55
22. Qi JZ, Jiakuan Y, Mei W, Bo X (2005) Experimental research on road materials of red mud. University of Huazhong Science and Technology, Wuhan, China
23. Ghosh PK (2009) Utilization of aluminium waste and Pond ash for construction of embankments. Btech thesis submitted to NIT, Rourkela
24. Yang LG, Yao ZL, Bao DS (1996) Pumped and cemented red mud slurry filling mining method (In Chinese). Mining Res. Develop. 16:18–22
25. Klauber C, Gräfe M, Power G (2009) Review of bauxite residue re-use options. CSIRO Minerals, Waterford, WA, pp 1–77
26. Pontikes Y, Angelopoulos GN (2013) "Bauxite residue in cement and cementitious applications: current status and a possible way forward. Res Conserv Recycl 73:53–63
27. Lima MSS, Thives LP, Haritonovs V, Bajars K (2017) Red mud application in construction industry: review of benefits and possibilities. In: IOP conference series: materials science and engineering, vol 251
28. Dass A, Malhotra SK (1990) Lime-stabilized red mud bricks. Mater Struct 23:252–255 (Matdriaux et Constructions)

Theoretical and Experimental Assessment of Gravel Loss on Unsealed Roads in Australia

Vasantsingh Pardeshi, Sanjay Nimbalkar and Hadi Khabbaz

Abstract Gravel loss is one of the major issues on unsealed roads which attract large annual maintenance. The continual process of gravel loss makes roads environmentally unsustainable. The unsealed road management faces several challenges which are: inaccuracies in behavior prediction, numerous data gathering requirements and exposure in the level of service and maintenance practices. To address these issues, the modified gravel is used on the unsealed road network in Australia. A case study is conducted to assess the gravel loss of unsealed roads. To monitor gravel loss on good quality, gravel monitoring stations are installed. Geographical information system (GIS) is used for finalizing the gravel monitoring station locations. Roughometer is used for surface assessment longitudinally. Roughness will be measured over two years at an interval of every three months. This paper discusses the gravel loss monitoring approaches, data analyses and improved material specification for gravel.

Keywords Gravel loss · Unsealed road · Material quality · Roughness measurement · GIS

V. Pardeshi · S. Nimbalkar (✉) · H. Khabbaz
School of Civil and Environmental Engineering, University of Technology Sydney, City Campus, 15 Broadway, Ultimo, NSW 2007, Australia
e-mail: Sanjay.Nimbalkar@uts.edu.au

V. Pardeshi
e-mail: VasantsinghBhimsingh.Pardeshi@student.uts.edu.au

H. Khabbaz
e-mail: Hadi.Khabbaz@uts.edu.au

V. Pardeshi
Scenic Rim Regional Council, Beaudesert, QLD 4285, Australia

V. S. Kanwar and S. K. Shukla (eds.), *Sustainable Civil Engineering Practices*,
Lecture Notes in Civil Engineering 72,
https://doi.org/10.1007/978-981-15-3677-9_3

1 Introduction

The annual maintenance and rehabilitation expenditure on Australia's roads are about 14B AUD [1]. Unsealed roads are those lacking the wearing layer of spray seal or asphalt. Unsealed roads are also referred as unpaved roads. Australia has unsealed road network with a length of 574,660 km, comprising about 60% of the total length of Australian road transport network and about 25% of the total annual pavement maintenance cost [2]. For this Australian unsealed road network, approximate preservation cost for one year is 1B AUD. Total unsealed road length in Queensland is 51,500 km. It is 39% of the total road network length of Queensland. Scenic Rim Regional Council (SRRC) yearly preservation cost for the unsealed road network is approximately 2 M AUD per year [3]. Most of these unsealed roads are the accountability of local authority, and it is arduous task to maintain those roads.

2 Study Area

SRRC area, selected for this study, is 50 km south of Brisbane, Australia. During March 2017, the rainfall, produced by ex-tropical cyclone Debbie and the cold front meeting over the SRRC, ranged from 350 mm in the West to 800 mm in the East within a 24-h period. The annual average rainfall for SRRC was 892 mm as recorded through Bureau of Meteorology (BoM) weather station in Scenic Rim region. The 24-hr flood event was approximately equal to the annual rainfall. The previous maximum recorded daily rainfall was 419 mm in January 1974. The ETC Debbie event was by far the most significant in a 24-h period on record. The groundwater velocities were very high causing severe scour damage to most unsealed surfaces. Sealed roads suffered very little damage, while unsealed roads and bridges received major damage.

The majority of the unsealed roads have been rated on 3 (from 1 to 5 scale), where 1 is excellent. In many instances, the damage is not immediately apparent as there was no evidence of destructive damage (washes, slips, major erosion). The damage was in the form of loss of surface material (loss of fines) across the entire road surface resulting into loss of shape and rutting along wheel path. The volume of water on the roads in a short period has resulted in surface erosion of almost all of the unsealed roads. The range of restoration treatments proposed was using a minimum of a medium grade; a heavy grade with a 50 mm or 75 mm top; a heavy grade with a 100 mm top and 100 mm resheet or a full 150 mm resheet. For the proposed treatment, there were 986 unsealed road sections with 861 km in length in the SRRC region.

Due to a large amount of unsealed road involved and many roads now demanding maintenance in terms of resheeting, authors in collaboration with SRRC have proposed to advance knowledge in accurate assessment of unsealed roads. The aim of this study is to enhance the existing gravel material specification, measure gravel loss and calibrate the existing gravel loss models and refine existing gravel loss models

to better suit SRRC area, based on those refined models that develop gravel road maintenance strategy.

3 Literature Review

Main concerns related with unsealed road are gravel loss, shape loss and rideability [4]. These three concerns are the consequence of deterioration arising from insufficient drainage capability, dust, corrugations, potholes, ruts, loose gravel and frost damage.

McManus [5] reviewed deterioration models on the basis of lessons learned from different countries around the globe. These models captured the specific characteristics of the local road network in the country where they were initially proposed. Their widespread applicability especially catering for other environments, soil properties and traffic configurations is largely unknown. To make those models suitable for local use, it becomes expensive due to data collection requirements. Roughness measurement is onerous task for longer duration. These issues only pose limitations on the widespread application of these models [5], and use of comprehensive model to suit local conditions is necessary.

Lea [6] analyzed the unsealed road network data using artificial neural networks. He proposed various improvements to the existing prediction models based on neural network output. This data was for unsealed roads in South Africa. The data were analyzed with various networks using forward-fed approach. These results were compared with the results of statistical analysis. The neural network delivered overall approximation measured which can be employed for an extensive presentation of modeling data.

Alzubaidi and Magnusson [4] analyzed the approaches for rating of unsealed roads in New Zealand, Canada, Sweden, Australia, USA and Finland. This learning concluded distress categories and the number of condition class variations. Based on this learning, numerous components relevant to a fresh score system were itemized. Linard [7] proposed a pavement management model following a system dynamics modeling (SDM) approach. He utilized the data reported in the Australian Road Research Board (ARRB) research studies performed on unsealed roads in Australia. He used the SDM approach to analyze the pavement deterioration on the basis of field measurements from 530 sections of unsealed road.

Henning et al. [8] developed a well-planned stratergy for maintenance of unsealed roads. The current asset management systems are not commonly used due to labor-intensive requirements and do not represent true conditions [9]. To predict surface performance, Jones (2015) developed a theoretical approach for unsealed road network in New Zealand based on material properties of surface aggregates. The dependence on condition data collection was ignored by using this system. The study utilized old preservation records and visual examination to rate and forecast mode of failure. Geological data provided precise warning of mode failure based on the Paige-Green [10] theory. The major factors influencing the degree of failure were geometrical

horizontal curvature, average daily traffic and age of the pavement surface. Geological characteristics of the surface aggregate also influenced the results to some extent [11].

3.1 Gravel Loss Model Development

Pavement deterioration models can be grouped under following categories [12]:

1. Performance prediction models to predict the future pavement condition based on the existing data;
2. Remaining life models to accomplish the residual service life of the pavement given the existing condition of deterioration;
3. Effect of maintenance models to forecast the pavement improvement on account of maintenance and age.

Uys [12] selected various internationally recognized gravel loss deterioration models to evaluate gravel loss. These models are listed below:

1. HDM4 model (widespread use internationally)
2. TRH 20 model (based on South African research and experience)
3. Brazilian model (HDM 4 and TRH 20 were preceded by this model)
4. Kenya model (equivalent to ARRB 2000 except difference in gravel types)
5. ARRB model (based on Australian experience).

Henning et al. [8] proposed a gravel loss model for use in New Zealand based on shape loss and slope loss. Martin (2013) established the first nationwide Australian local road deterioration models. These models are result of long-duration monitoring program of 500 sealed and 100 unsealed road locations from Australia. The gravel loss is expressed as (Martin 2013):

$$\mathrm{GL} = k_{\mathrm{gl}} D(-0.00985\,\mathrm{ADT} - 0.02991\,\mathrm{MMP} - 0.00583\,\mathrm{PF}) \tag{1}$$

where GL represents the gravel loss (mm), k_{gl} represents the local calibration factor for gravel loss, D represents the time as hundreds of days (days/100), ADT represents the average daily traffic (total vehicle/day), MMP represents the mean monthly precipitation (mm/month), PF represents the plasticity factor (=PI $\times$ $P_{0.075}$), $P_{0.075}$ is the percentage by mass of material passing 26.5 mm sieve and PI is the plasticity index. An annual shape loss in the cross fall of the pavement is given as (Martin 2013):

$$\mathrm{SL} = k_{\mathrm{sl}}(-1.8353 - 0.0004\,\mathrm{ADT} + 0.0259 P_{0.075}) \tag{2}$$

where SL represents shape loss (%) in pavement cross fall per year and k_{sl} represents local calibration factor for shape loss.

3.2 *Outcome from Models and Research Perspective in Australia and New Zealand*

ARRB Unsealed Roads Manual and Unsealed Roads Tactical Asset Management Manual (August 2015, New Zealand) are the widely used technical guides for unsealed roads in New Zealand and Australia. 'The Unsealed Roads Manual: Guidelines to Good Practice' is management procedures and practices used in both the Australian and New Zealand unsealed road network. ARRB has evidently specified that unsealed roads are currently accomplished with very diminutive technical contribution. Giummarra [13] has accompanied an extensive research on unsealed roads for advancement of this manual.

Figure 1 presents a correlation between the shrinkage product and the grading coefficient which is a schematic presentation for performance of base/wearing course gravel developed by Paige-Green (1996) in South Africa. Shrinkage product is calculated by multiplying linear shrinkage and percentage passing 0.425 mm sieve. Grading coefficient is a percentage derived by multiplying: percentage passing difference between 26.5 and 2.00 mm sieve and percentage passing 4.75 mm sieve. As shown in Fig. 1, the wearing course material is classified into: erodible (A), corrugates and ravels (B), ravels (C), slippery (D) and good (E). This relationship is widely used to select an appropriate type of gravel. The Unsealed Roads Tactical Asset Management Guide [14] provides better representation of material performance based on its properties. Elis and Andrew (2015) optimized gravel choice on a network basis by proposing quarry location and properties.

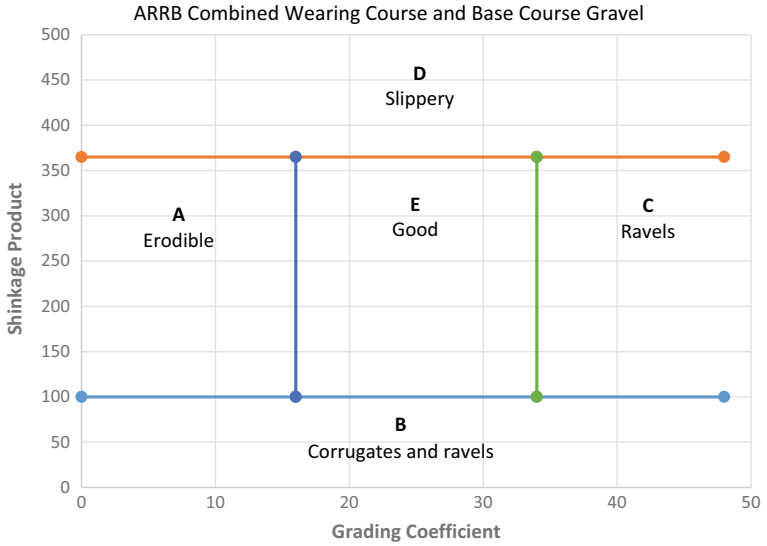

Fig. 1 Relationship between shrinkage product and grading coefficient for base/wearing course

4 Long-Term Gravel Loss Monitoring

About 56 number of total gravel monitoring stations are established within the SRRC area. The flood affected area was divided into six different geographical areas (Southwest A, Northwest, Southwest B, East A1, East A2, East B, Northeast). A list of damaged road sections based on the investigated database was developed. The unsealed road sections were selected from this damaged road sections list. These sections were going to be either graveled or resheeted. Each station was monitored on site for inspecting the geometry of road (horizontal, vertical curve, flat, slope), a number of houses on the road, no through road or connector. Traffic volume was a major consideration before station location was finalized. Actual station location was finalized by a site visit, and chainage was recorded for a particular station. Gravel loss monitoring period for established stations is estimated to be about 2 years. The monitoring station was required to establish the permanent survey control mark. A typical cross section of a road with recorded level measurements is presented in Fig. 4. This figure shows the levels plotted in terms of varying time periods.

By using Eqs. (1) and (2), theoretical gravel loss and theoretical shape loss are calculated, respectively. These equations are developed through the long-term field observations by ARRB and are applicable to the Australian conditions. The monitoring stations are shown in Fig. 2. Regravelling work is completed for these stations to record actual gravel loss. The period for gravel loss and shape loss is the difference

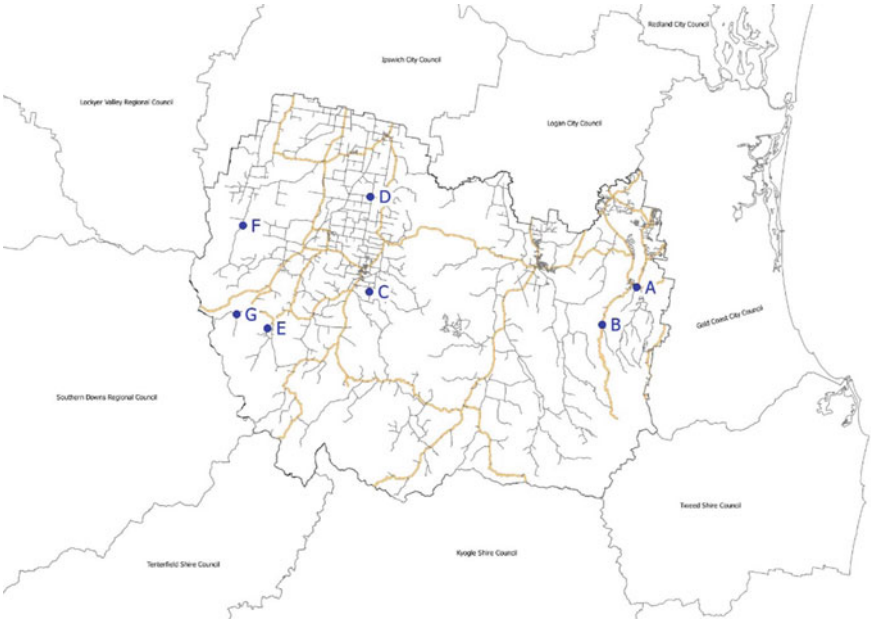

Fig. 2 Gravel monitoring stations within scenic rim regional council, Brisbane, Queensland

Table 1 Actual and theoretical shape loss (SL) monitored from gravel monitoring stations

Monitoring station	A	B	C	D	E	F	G
Actual SL (%)	2.54	−1.26	0.7	− 0.2	0.2	0.6	0.2
Theoretical SL (%)	0.55	0.6	0.69	0.68	0.55	0.65	0.56

between the two recorded dates of gravel level measurements. The mean monthly precipitation (MMP) is obtained from the Bureau of Meteorology rainfall data. Average daily traffic (ADT) is based on council road classification. The gravel test reports were available for each road for the gravel supplied from the quarry. Plasticity factor is derived using the data from a gravel test report. The local calibration factor is based on actual gravel loss at this stage.

Actual gravel loss and shape loss for each location is derived through the level measurements using the gravel loss monitoring stations. The gravel loss is calculated at a particular station on the basis of change in a cross-sectional profile of the road. Shape loss is also calculated using actual level measurements periodically. Table 1 provides the actual and theoretical shape loss for stations shown in Fig. 2. There are noticeable differences between theoretical and actual shape loss. The first level reading was taken immediately after the regravelling, and the second level reading was taken after 3 months. Figure 3 shows actual measured levels plotted on the basis of varying time period.

Both gravel loss and shape loss were measured and compared for the level measurements from the same dates. The theoretical and actual gravel loss reading is plotted in Fig. 4. The values of theoretical and actual gravel loss are also listed in Fig. 4. Out of 7 stations, 4 stations (B–E) exhibited more gravel loss than the theoretical gravel loss. 5 stations (B–G) have more theoretical shape loss than shape loss measured in the field.

This initial data clearly reflects that there is a need for adjustment in the local calibration factor. The local calibration factor used in Martin (2013) equation can be extended to consider the horizontal and vertical geometry of the road as well

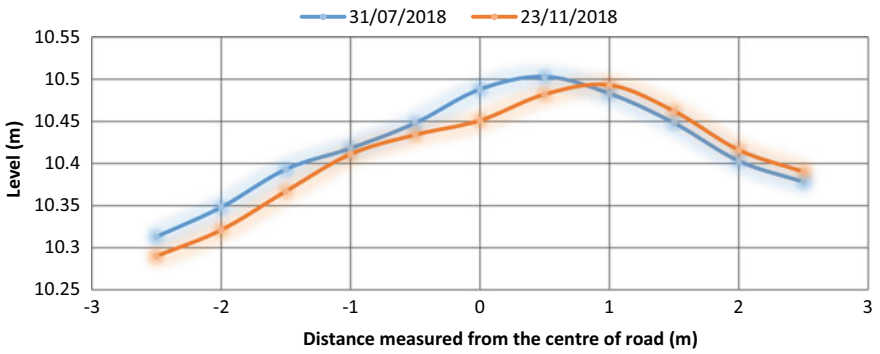

Fig. 3 Typical cross section of recorded levels using gravel monitoring station

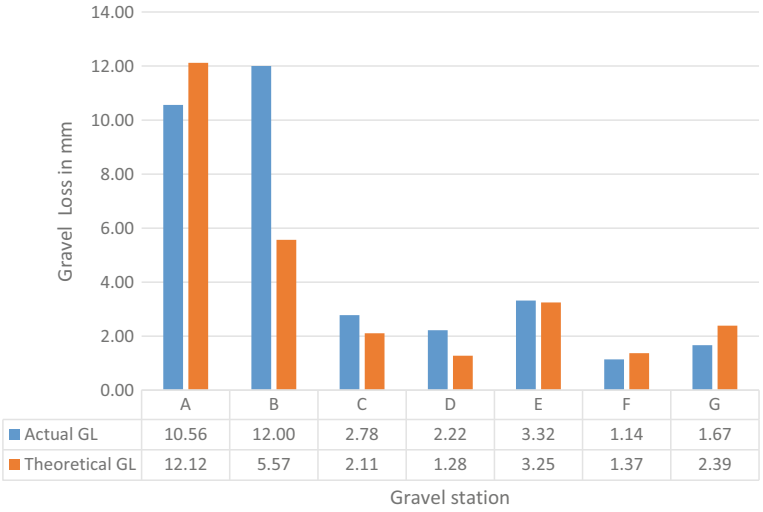

Fig. 4 Predicted and measured gravel loss

as other local conditions. In addition to gravel loss measurement using gravel loss stations, roughness measurements are employed on the road sections where gravel monitoring stations are established. The aim of this roughness measurement is to establish any relationship between gravel loss and roughness on the road. The gravel loss at a particular station provides a cross section of the road over a period of time. Roughness provides the roughness level along the road to driving condition. Mazari [15] has applied a neural network for the prediction of pavement roughness. In this study, Roughometer III is used. Roughometer III reduces the uncertainties related with the vehicle suspension or weight by directly calculating the axle movement with an aid of accelerometer. International Roughness Index (IRI) determination is possible by use of Roughometer III for pavement roughness.

5 Conclusions

There is a huge potential for cost savings by reducing gravel loss on unsealed roads. Most of the studies conclude difficulty in predicting deterioration models precisely for unsealed roads. This is attributed to a number of variables associated and the requirements for time and resources. In view of these, requirement is to advance gravel loss model appropriate for local circumstances. This paper presents initial results of a study on unsealed road network which has shown signs of damage due to ex-tropical cyclone Debbie. In this study,

1. Gravel loss models and maintenance strategy for unsealed road network are discussed.

2. Appropriate modification to gravel material specification is proposed with an aim to reduce gravel loss.
3. For the resheeting and regravelling work, the gravel material is sourced using this modified specification.

Acknowledgements Authors acknowledge Chris Gray, General Manager, Asset and Environmental Sustainability, from Scenic Rim Regional Council for providing his support for this research project.

References

1. Martin T, Choummanivong L (2016) The benefits of long-term pavement performance (LTPP) research to funders. Transp Res Procedia 14:2477–2486
2. Australian RuralRoads Group (2010) Going nowhere: The rural local road crisis Its national significance and proposed reforms. Australian Rural Roads Group, NSW, Australia
3. Scenic Rim Regional Council (SRRC) (2018) 2018–19 community budget report scenic rim regional council, scenic rim regional council, Beaudesert, Australia
4. Alzubaidi H, Magnusson R (2002) Deterioration and rating of gravel roads: state of the art. Road Mater Pavement Des 3(3):235–260
5. McManus KJ (1994) Pavement deterioration models for a local government authority. In: 17th ARRB conference, gold coast, Queensland, 15–19 August 1994; proceedings; volume 17, part 4
6. Lea JD, Paige-Green P, Jones D (1999) Neural networks for performance prediction on unsealed roads. Road and Transp Res 8(1):57
7. Linard K (2010) A system dynamics modeling approach to gravel road maintenance management. In: ARRB conference, 24th, 2010ARRB Group Limited
8. Henning T, Giummarra GJ, Roux DC (2008) The development of gravel deterioration models for adoption in a New Zealand gravel road management system (No. 332)
9. Henning TF, Flockhart G, Costello SB, Jones V, Rodenburg B (2015) Managing gravel-roads on the basis of fundamental material properties (No. 15-2562)
10. Paige-Green P (1989) The influence of the geological and geotechnical properties on the performance of materials for gravel roads (Ph.D. Thesis, University of Pretoria, Pretoria)
11. Jones D, Paige-Green P, Sadzik E (2003) Development of guidelines for unsealed road assessment. Transp Res Rec: J Transp Res BoardBoard 1819:287–296
12. Uys R (2011) Evaluation of gravel loss deterioration models: case study. Transp Res Rec 2205(1):86–94
13. Giummarra G (2009) Unsealed roads manual: guidelines to good practice, 2009th edn. Australian Road Research Board, Melbourne, Victoria, Australia
14. Road Infrastructure Management Support (RIMS) (2015) Unsealed roads tactical asset management guide. RIMS, New Zealand
15. Mazari M, Rodriguez DD (2016) Prediction of pavement roughness using a hybrid gene expression programming-neural network technique. J Traffic Transp Eng (Engl Ed) 3(5):448–455

Experimental Investigation on the Tensile Strength Behaviour of Coconut Fibre-Reinforced Cement Concrete in Fiji and Pacific Region

Samuela Loaloa Vukicea, Swetha Thammadi, Sateesh Pisini and Sanjay Kumar Shukla

Abstract Cement concrete is relatively brittle and its tensile strength is typically only about one-tenths of its compressive strength. It is becoming increasingly popular in various applications to reinforce the concrete with small, randomly distributed fibres. The main purpose is not only to increase the energy absorption capacity, called the toughness of the material, but also to increase the tensile and flexural strength of concrete. This experimental analysis is being carried out to investigate the effects of fibre quantity on tensile strength on coconut fibre-reinforced concrete. Coconut (coir) fibre-reinforced cement concrete with different fibre contents was reviewed together with plain cement concrete and a comparative analysis was made. Tensile strength was investigated for plain concrete mix and coconut fibre-reinforced concrete. The results obtained have been analysed critically and discussed for the practical applications. The results conclude that the addition of 1–4% of coconut fibres increases the tensile strength of plain cement concrete significantly. The fibres also formed a good bonding in the concrete. It can be deduced that the optimum fibre content for enhanced concrete strength is 3% by weight of cement.

Keywords Cement concrete · Tensile strength · Coconut fibre reinforced concrete

1 Introduction

Coconut fibre-reinforced cement concrete is widely known for its versatility and its applications in different branches of engineering, particularly in civil engineering, as a construction material. Coconut fibre is a natural fibre which is abundantly available in tropical regions, including Fiji. It is extracted from the husk of the coconut fruit. The common name is coir, scientific name is cocos nucifera, which belongs to the plant family of arecaceae (Palm). Coconut fibres can be broadly classified as *Brown fibre*

S. L. Vukicea (✉) · S. Thammadi · S. Pisini · S. K. Shukla
School of Building and Civil Engineering, Fiji National University, Suva, Fiji
e-mail: samuela.loaloa@fnu.ac.fj

S. K. Shukla
Discipline of Civil and Environmental Engineering, Edith Cowan University, Perth, Australia

V. S. Kanwar and S. K. Shukla (eds.), *Sustainable Civil Engineering Practices*,
Lecture Notes in Civil Engineering 72,
https://doi.org/10.1007/978-981-15-3677-9_4

which is extracted from matured coconuts and *White fibre* extracted from immature coconuts. While brown fibres are thick and strong, they have high abrasion resistance. On the other hand, white fibres are finer and smoother, but also weaker. For most of the engineering applications, brown fibres are used [2].

Fiji has about 10 million coconut trees scattered or planted in 65,000 hectares of land in the Eastern and Northern Division of Fiji and the coastal area of the main island (Viti Levu). Of these, 70–80% of Fiji's coconut palms are more than 100 years old. Due to the resilience, socio-economic contribution and sustainability of coconut plants, it has been included in the strategic development priority areas in Ministry of Agriculture Sustainable Development Plans: 2018–22. Coconut fibre is widely available in Fiji and the Pacific region which can be potentially used in construction work. Due to the abundance of the availability of coconut fibre, the present research is an attempt to use the available coconut fibre as reinforcement in concrete so as to investigate the effects of fibre quantity on tensile strength of coconut fibre-reinforced concrete.

Several researchers have studied the use of fibres in concrete (Yalley and Kevan [2, 12]; Dhandhania and Sawant [5]; Salain and Nyoman [7]; Nadgouda [4, 6]; Seneviratne and Tharmarajah [8, 9]; Uday and Ajitha [1, 10, 11]. Nadgouda [6] has carried out an experimental analysis on coconut fibre-reinforced concrete and reported that the tensile strength increases with 3% fibre mix. Dhandhania and Sawant [5] reported that the use of coconut fibres had natural cooling effect due to its near zero thermal conductivity. Salain and Nyoman [7] has conducted the experimental study on coconut fibre-reinforced cement concrete and they observed that the addition of coconut fibre in plain concrete improves its mechanical properties, especially its flexural and tensile strength. The magnitude of improvement by an optimal addition can reach to about 16%, 1%, 50% and 15%, respectively, for the split tensile strength, compressive strength, flexural strength and modulus of elasticity. Uday and Ajitha [10] found that the split tensile strength and compressive strength of the cement concrete are maximum with 1% coconut fibre by weight. Seneviratne and Tharmarajah [8] reported that the unit weight of the coir fibre-reinforced concrete was reduced by 3–5% due to the addition of coconut fibres. However, the compressive strength and tensile strength of high strength concrete are decreased by 20–75%. Notably, compressive strength decreased with increase of fibre length. In comparison to flexural strength of high strength plain concrete, only 3–6% enhancement of flexural strength was observed in 2% (25, 40 mm) fibre-added mixes. Yalley and Kevan [12] noticed that the engineering properties of concrete such as torsion, tensile strength, ability to resist cracking and spalling and toughness of coconut fibre-reinforced concrete improved significantly. The addition of fibres to concrete also showed a significant effect on the compressive strength. Veerwal et al. [11] have reported that the slump decreases on addition of fibres to plain cement concrete. As the fibre–cement ratio increases, there is a decrease in slump as water is absorbed by the fibres. Hence, for higher fibre–cement ratios, addition of superplasticizer is recommended as it does not affect any other properties except workability. Coconut fibre is a natural fibre which is low in density due to which the overall weight of the fibre-reinforced

concrete decreases thereby using it as a structural lightweight concrete. The addition of natural fibres including coconut fibres increased the compressive strength of fibre-reinforced concrete compared to plain concrete. Achudhan et al. [1] observed that the compressive strength and split tensile strength of coconut fibre-reinforced concrete increased gradually with increase in fibre content. It has been clearly noted that adding fibre up to 3% slightly increases the strength. The flexural strength of coconut fibre-reinforced concrete increases for 1–3% of fibre for M20 grade compared to conventional concrete. Swathika et al. [9] have found that the maximum compressive strength of coconut fibre-reinforced concrete (CFRC) was achieved at 0.25% coconut fibre. Chandel et al. [4] found that the addition of coconut fibre to Plain Cement Concrete (PCC) increased the compressive strength by nearly 13% while the flexural strength increased by nearly 15% and tensile strength by nearly 40% for CFRC compared to that of PCC. This is a significant increment in strength. The addition of coconut fibre in concrete also suggests that for the same strength of CFRC and PCC, nearly 5% cement by weight can be saved on using CFRC. Thus, CFRC is cost effective when compared to PCC and environmental friendly.

Although there have been studies on the effect of coconut fibre reinforcement in concrete, this study is the first of its kind in Fiji. Reinforcement of concrete enhances its properties, such as impact resistance, flexural and tensile strength and toughness. Therefore, for this study, coconut fibres have been used as reinforcement due to their availability in large quantities in the Oceania tropical region, including Fiji. This study comprises of a comparison of the tensile strength of plain cement concrete and coconut fibre-reinforced cement concrete based on the experiments performed in the laboratory. The results from the experimental studies are then compared to those from literature review.

2 Concrete Tensile Strength

Tensile strength is the ability of concrete to resist elongation. Although the tensile strength of concrete is small in comparison to its compressive strength, it is of importance in unreinforced concrete pavements, floor slabs, etc. Tensile strength is affected by much of the same factors which affect compressive strength and in more or less the same way. The introduction of coconut fibre into the cement concrete will directly affect its tensile strength. The tensile strength of CFRC can be measured in three ways: splitting tension, direct tension and flexural tension. Tensile strength of CFRC should be high enough to resist cracking from shrinkage and temperature changes. Tensile strength of CFRC is affected by the following factors [3]:

(1) Water–cement Ratio
(2) Density (compaction)
(3) Age of concrete
(4) Type of cement
(5) Curing conditions, e.g. moisture and temperature

(6) Fibre content
(7) Aspect ratio and orientation of fibres.

Water–cement ratio is the ratio of the amount of water and cement present in the concrete, i.e. if 1 m^3 of concrete contains 150 kg of water and 300 kg of cement, then the water–cement ratio is 0.5. Density of CFRC is its weight per unit volume. The density of cement concrete depends largely on its major components—sand, coarse aggregate and coconut (coir) fibre. The density of CFRC will be reduced by insufficient compaction. Voids in CFRC were created by excess mixing of water or improper compaction due to which the strength of CFRC as well as the density of concrete decreases. The age of CFRC is one of the factors affecting its strength. The strength of CFRC concrete increases rapidly at first for a few years and more slowly as it becomes older. Therefore, in determining the strength of CFRC, the age at which the test is made must be noted. In most cases, concrete is tested at 28 days which is a compromise between obtaining a strength indication as early as possible and accurately determining the long-term concrete strength. The type of cement also influences the strength of concrete as different types of cement have different rates of strength gain. Concretes made with same water–cement ratio and cured under the same conditions tend to gain the same order of strength. To gain the ultimate strength, concrete must be kept continuously moist so that the water is available for hydration. The importance of curing on strength may be judged from the fact that a concrete curing in air for 28 days may gain only two-thirds of the strength of the same concrete moist cured for the same period. Hydration of cement is a chemical reaction and, like most chemical reactions, the rate at which it proceeds depends upon the temperature. Thus, the temperature at which concrete is cured affects the rate at which it gains strength. Splitting tensile strength test is an indirect method of determining the tensile strength of CFRC using a cylinder which splits across the vertical diameter. The overall objective of the experimental analysis is to find out the splitting tensile strength for CFRC and PCC samples and compare the results. The samples used in the present study were cylindrical with a diameter of 150 mm and a length of 300 mm (Figs. 1 and 2).

3 Materials and Methodology

Mix design was conducted as per AS 1480-1994 to arrive at M20 mix. CFRC was made by mixing the following [3]:

(1) Cement
(2) Water
(3) Coarse and fine aggregates
(4) Coconut (coir) fibres
(5) Admixtures (if required).

Fig. 1 Sample for splitting test of plain cement concrete (PCC)

Fig. 2 Sample for splitting test of coconut fibre-reinforced cement (CFRC) concrete

The type of cement used was PC Type A (AS 1315–1973). The aggregates used were as follows:

Coarse aggregate: crushed rock, gravel or screenings

Fine aggregate: fine and coarse sands and crusher fines.

Water was mixed with cement powder to form a paste which holds the aggregates together like glue. Coconut (coir) fibres were collected from different places and properly shaped in the form of fibres. Uniform length of fibres (40.0 mm) was obtained by using the cutting machine. Typical properties of the fibre are shown in Table 1.

Hand mixing was used for convenient handling of coconut (coir) fibres. Coarse aggregates, coconut (coir) fibre and dry mix of cement and sand were compacted in three layers with 25 blows for each layer. Mixing process had to be done very carefully to avoid the formation of lumps and fibres were randomly oriented in the

Table 1 Properties of fibres

Properties of fibres	
Diameter in mm	0.48
Aspect ratio	3.75
Specific gravity	0.87
Water absorption in %	104.2
Density in kg/m^3	870

mix. The cylinders (150 mm dia. and 300 mm deep) of both the plain (PCC) and fibre-reinforced cement (CFRC) concrete samples were cast. Each layer was compacted with 25 blows using a 16 mm diameter steel rod and the following samples were cast:

(1) Plain cement concrete
(2) 1% of coconut (coir) fibre
(3) 2% of coconut (coir) fibre
(4) 3% of coconut (coir) fibre
(5) 4% of coconut (coir) fibre.

Grade designation: M20
Max nominal size of aggregate: 20 mm
Min cement content: 300 kg/m^3
Max water–cement ratio: 0.55
Workability: 100 mm (slump)
Exposure condition: Mild (for reinforced concrete)
Degree of supervision: Good
Type of aggregate: Crushed angular aggregate
Max cement content: 450 kg/m^3
Chemical admixture type: Superplasticizer.

Cylindrical concrete samples of plain cement concrete cylinders and CFRC cylinders were prepared (Fig. 3). After curing for 28 days, samples have been tested. Incremental axial load has been applied to each sample untill failure (Fig. 4).

The splitting tensile strength of the samples was calculated using

$$T = \frac{2P}{\pi l d} \tag{1}$$

where

T splitting tensile strength (kPa)
P maximum applied load indicated by machine (kN)
l Length (m)
d diameter (m).

Fig. 3 CFRC concrete test samples

Fig. 4 Tensile strength test arrangement

4 Results and Discussion

The cylinder samples were tested on a testing machine in the concrete laboratory at Fiji National University, Derrick campus, Samabula, Suva for determining the split tensile strength of concrete. The results are given in Tables 2 and 3.

The split tensile strength of CFRC and PCC are shown in Fig. 5. It is observed that when compared with PCC, the strength increases gradually in CFRC when the percentage of fibre is increased on a regular interval basis. It is clear that by adding coconut fibres starting at 1% at incremental values of 1%, the strength increases

Table 2 Mix proportions

Cement	Fine aggregate	Coarse aggregate	W/C ratio
1	1.5	3.0	0.5

Table 3 Split tensile strength values for plain cement concrete

Sample	Water–cement ratio	Slump (mm)	28-day strength (N/mm^2)
1	0.5	100	2.61
2			2.62
3			2.63
			Average = 2.62

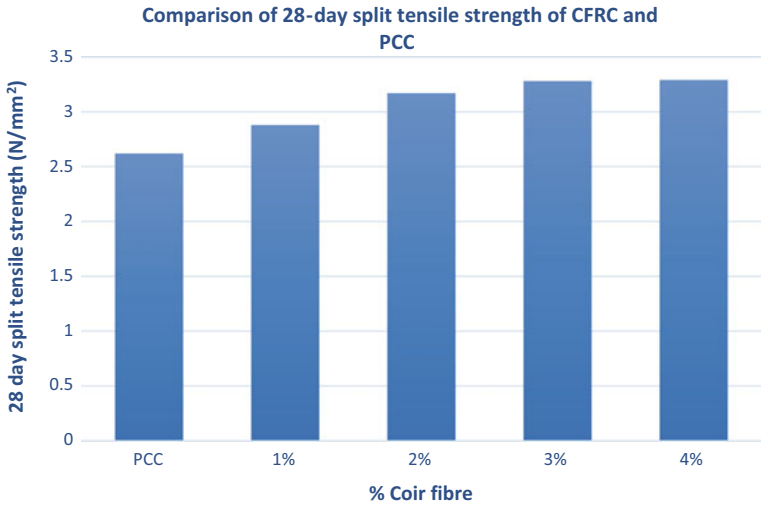

Fig. 5 Split tensile strength of coconut (coir) fibre-reinforced cement concrete

linearly. From 0 to 2%, coir fibre has a linear relationship with split tensile strength and at 3%, there is a gradual decrease in slope and with further increase in coir fibre (e.g. 4%), there is a decrease in split tensile strength. This will usually happen due to displacement of particles present in the concrete. Further addition of coir fibre with concrete mix enhances the binding strength and beyond 3%, the strength of CFRC tends to decrease (Table 4).

The results of the present study are comparable to studies by Nadgouda [6] and Achudhan et al. [1] where they concluded that there is a gradual increase in the split tensile strength of coconut fibre-reinforced concrete with an increase in fibre content. It is evident in our study that adding fibre up to 3% slightly increases the strength. At 4% fibre, it has been observed that there is no significant increase in the tensile strength of concrete. Therefore, it can be concluded that the optimum fibre content for maximum tensile strength of coconut fibre-reinforced concrete is 3%.

Table 4 Split tensile strength values for coconut fibre-reinforced cement (CFRC) concrete

Sample	Water–cement ratio	Coconut fibre (%)	Percentage of superplasticizer used	Slump (mm)	28-day strength (N/mm^2)
1	0.5	1	0.2	110	2.88
2		2	0.4	105	3.17
3		3	0.8	105	3.28
4		4	1.0	105	3.29
					Average = 3.16

5 Conclusions

Based on the results and discussion presented in the previous section, the following general conclusions can be made:

- The split tensile strength of coconut (coir) fibre-reinforced concrete has been tested and the test results show that the strength of the coconut (coir) fibre-reinforced concrete increases with an increase in the fibre content.
- The optimum fibre content for maximum tensile strength of coconut fibre-reinforced concrete is 3%.
- The coconut (coir) fibre-reinforced concrete is more effective than plain cement concrete as shown by the variation of fibre content with the split tensile strength.
- The abundance of coconut fibre in Fiji and Pacific region has the potential for use in construction industry as a replacement of conventional concrete.
- The use of coconut fibre-reinforced concrete is cost effective and environmental friendly.
- This work can be further extended by adding admixtures or superplasticizers to study the flow characteristics of concrete with addition of coconut fibres.
- Another avenue for future work includes the study of compression and flexural strength of coconut fibre-reinforced concrete.

References

1. Achudhan, Ali MJIH, Sankar SS, Saikumar K (2018) Experimental study on coir fibre mixed concrete. Int J Pure Appl Math 118(20):2913–2929
2. Ali M (2010) Coconut fibre—a versatile material and its application in engineering. In: 2nd International conference on sustainable construction materials and technology, pp 1–14
3. CCA (1982) Basic guide to concrete construction, Cement and concrete association of Australia
4. Chandel A, Shah T, Shah T, Vande D (2016) A comparative strength study of Coir Fibre Reinforced Concrete (cfrc) over Plain Cement Concrete (PCC). Int J Mech Civil Eng 13(2):101–103
5. Dhandhania VA, Sawant S (2014) Coir fibre reinforced concrete. J Text Sci Eng 4(5):1–5

6. Nadgouda K (2015) Coconut fibre-reinforced concrete. Int J Mech Prod Eng 3(1):26–28
7. Salain KAMI, Nyoman IS (2014) Mechanical properties of coconut fibre-reinforced concrete. In: 6th international conference of Asian concrete federation, pp 553–558
8. Seneviratne RACJ, Tharmarajah G (2017) Experimental study on addition of pine fibers to high strength concrete. In: 5th international symposium on advances in civil and environmental engineering practices for sustainable development
9. Swathika R, Surya R, Ram MM, Prasad RS (2017) Experimental investigating for coir fibre reinforced concrete with partial replacement of cement by Rice Husk Ash. Int J Sci Dev Res 2(6):397–406
10. Uday SV, Ajitha BA (2017) Concrete reinforced with Coconut fibres. Int J Eng Sci Comput 7(4):10236–10439
11. Veerwal HK, Gupta T, Sharma KR (2017) Utilization of natural fibre in concrete—a review. Int J Adv Eng Res Dev 4(9)
12. Yalley PP, Kevan ASK (2009) Use of coconut fibres as an enhancement of concrete. J Eng Technol 3:54–73

Influence of Flat-Shaped Aggregates in Granular Skeleton on Its Compactness

Koroudji Kamba Ayatou, Irina Pachoukova, Bhartesh Raj and Vikram Kumar

Abstract This paper introduces a study of the compactness properties of granular skeleton depending on the quantity of flat-shaped aggregate. To achieve our goal, we took two granular classes 06/10 and 10/20 from Lilikopé quarry, then we made the determination of the percentages of the flat shapes by the manual method, vernier caliper. The method used for compactness is the method number 61 of LCPC (Laboratoire Central des Ponts et Chaussé de la France/Central Laboratory of Bridges and Roads of France). The determination of the compactness considering granular skeletons is composed of: 0, 25, 50, 75, and 100% of flat-shaped aggregates. A program that highlights the influence of aggregates shapes in a granular skeleton on compactness will bring out later more perspectives for the use of flat aggregates. The objective is often to combine the grains to minimize the porosity in order to minimize the use of a binder. They require the knowledge of some basic data on the optimization of this parameter in addition to other factors.

Keywords Compactness · LCPC · Grain size · Grain shape · Densities

1 Introduction

Granular materials in civil engineering are made from granular fractions available in the denominations of type 0/*D* or *d*/*D* (where *d* is the minimum size and *D* the maximum size in the sense of the sieve). Of all time, the combination of these

K. K. Ayatou (✉) · B. Raj
Department of Civil Engineering, Alakh Prakash Goyal Shimla University, Shimla, H.P. 171009, India
e-mail: ayatoukoroudjik@gmail.com; 100besure100@gmail.com

I. Pachoukova
Civil Engineering Department, Higher National Engineers School, University of Lomé, Lomé, Togo

V. Kumar
Department of Civil Engineering, Gaya College of Engineering, Gaya, Bihar 823003, India

V. S. Kanwar and S. K. Shukla (eds.), *Sustainable Civil Engineering Practices*,
Lecture Notes in Civil Engineering 72,
https://doi.org/10.1007/978-981-15-3677-9_5

fractions, leading to the formulated mixtures, was made on the basis of considerations of dimension, such as described by the particle size. For the realization of these structures (buildings, roads, dams …), some formulation methods rely on questions relevant to know: what is the composition of the granular mixture for a quality concrete? The answer comes through the knowledge of certain parameters of the materials including the compactness, an index that is used to determine the percentage of solid in a granular skeleton.

The current tests used to evaluate the quality and durability of these aggregates are expensive, complex, and long in procedure, especially when installation of new production units is involved. The intrinsic characteristics, such as the mineralogical composition, the porosity, the density and the homogeneity of the gneisses and the granites have been studied and their influence on the mechanical properties of the aggregates resulting from these rocks has been demonstrated [1–4].

The selected working mode comprises of putting a 7 kg test of total inside a cylinder, submitting it to a progression of strokes. After that, repeating these equivalent loads once a steel piston by applying a 10 kPa vertical weight on the upper surface of the sample. The instrumentation of this new test is more direct than that of the past one (which required utilization of a vibration table) and its dimension of reproducibility (which still should be assessed) is likely better [5]. This examination exertion has affirmed the impact of flat shape of aggregate on compactness by LCPC strategy.

2 Materials and Methods

2.1 Characters of the Rock of Lilikopé (TOGO)

The rock of Lilikopé (Fig. 1a, b) has an architecture that is defined by a set of its characters relating to the shape, size and available to its various constituent parts. This quarry brings together:

- Massive rock,
- A foliated texture, and
- A porphyblastic structure characterized by the appearance of large crystals of feldspar.

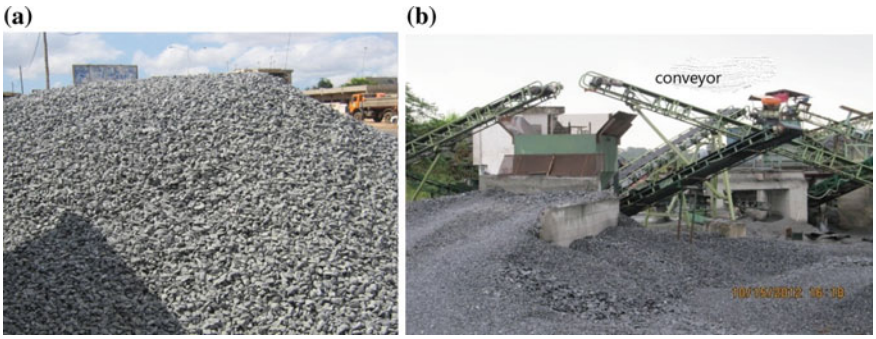

Fig. 1 **a** Crushed aggregate of Lilikopé quarry. **b** Crushed aggregate conveyed by conveyor

2.2 Determination of the Physical Properties of Aggregate Samples

The aims are: first to determine the particle size (Fig. 2a, b), coefficient of cubic shape (Table 1) then the densities of aggregates and second, to determine compactness in accordance with the method no. 61 of LCPC (Laboratoire Central des Ponts & Chaussé/Central Laboratory of Bridges and Roads).

Table 1 gives the coefficient of uniformity (Cu) and the coefficients of curvature (Cc) from the particle size analysis.

The classification in the unified system from the coefficients Cc and Cu, which are all less than 2, groups them in gravel of very tight size, and Cc less than 3 groups the class 0/10 in clean aggregate. The class distribution of aggregates according to the ratio *L*/*E* (Length/Thickness) and regroup the results which detail each granular class in functions of the coefficients of cubic form (Table 2).

2.3 Compactness Test

The outcomes from a noteworthy experimental trial, in which three packing density estimation working modes were actualized on various parts drawn from two sources, are then portrayed, with each test being rehashed an aggregate of multiple times to appraise the normal esteem and standard deviation. The chosen working mode comprises of putting a 7 kg test of total aggregate inside the cylinder, submitting it to a progression of strokes (by methods of shock table), and after that rehashing these equivalent loads once a steel cylinder applying a 10 kPa vertical weight on the upper surface of the example has been situated. The instrumentation of this new test is more clear than that of the past one (which required utilization of a vibration table) and its dimension of reproducibility (which still should be assessed) is presumably better (Fig. 3).

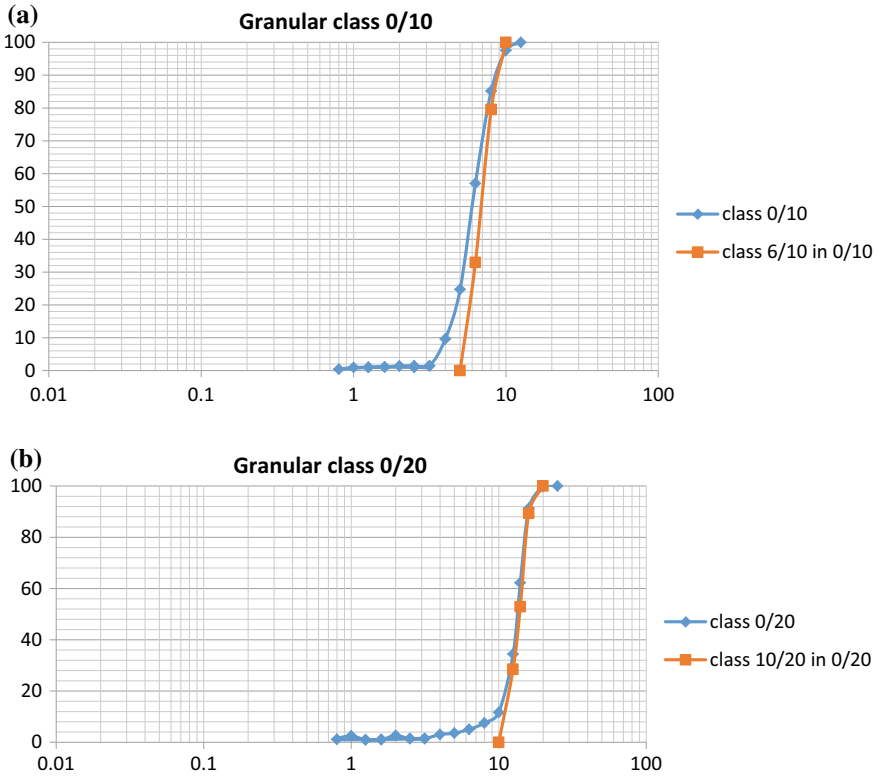

Fig. 2 **a** Grading curve of the granular class 0/10. **b** Grading curve of the granular class 0/20

Table 1 Coefficients of uniformity (Cu) and coefficient of curvature (Cc)

Granular class	Sieve letting the different percentages (mm)			Coefficient of uniformity (Cu)	Coefficient of curvature (Cc)
	D_{10}	D_{30}	D_{60}		
0/10	4.0	5.2	6.5	1.63	1.04
0/20	11.69	12.5	14.0	1.20	0.95
6/10	5.5	6.3	7.5	1.36	0.96
10/20	12	12.5	14.5	1.2	0.89

3 Results and Discussion

To study the influence of the flat-shaped aggregates on its compactness, two modes of implementation are used (LCPC method: method on the vibrating table and method on the table with manual shock).Independently of two different classes, each test and

Table 2 Variations of the *L*/*E* (Length/Thickness) and Fc (Coefficient of cubic) according to the granular classes

Granular class	Coefficient *L*/*E* (%)		Coefficient Fc(%)	
	L/*E* < 3	*L*/*E* > 3	Fc < 4	Fc > 4
06/10	67.5	32.5	75	25
10/20	71.35	28.65	70	30

The aggregate is said to be of cubic shape if it checks both *L*/*E* < 3 and Fc < 4 when the coefficient said "cubic" Fc = L.G.E/E^3

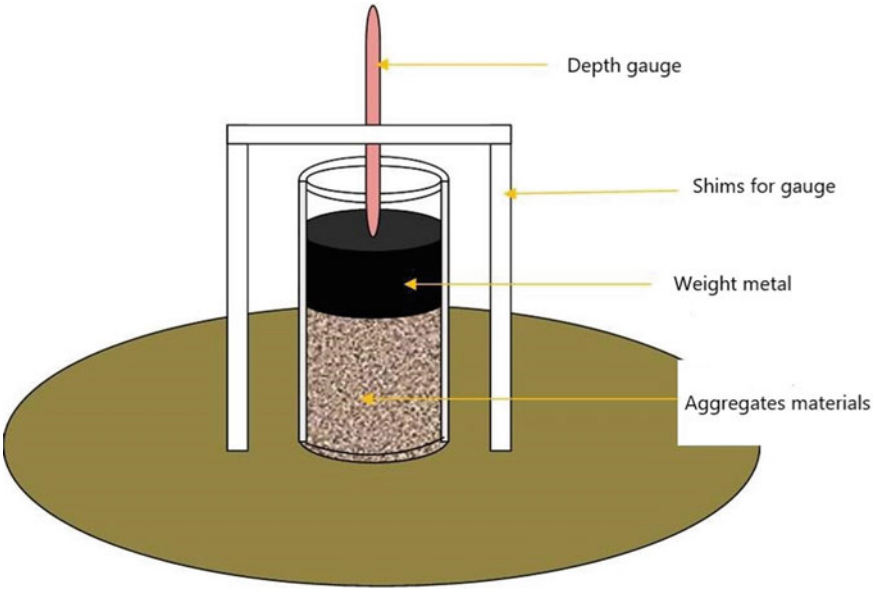

Fig. 3 Top of the shock table or vibrating table

sample is strongly influenced by the quantity of the flat shapes. This is consistent with us the conclusion that the compactness of the materials reduces with many flat shapes.

Overall, we can conclude from Figs. 4 and 5 that only the increase in flat shape will change negatively the compactness of our materials; Tables 3 and 4 summarize, respectively, the experimental results and compactness on the aggregates class 06/10 and 10/20 calculated from the LCPC method.

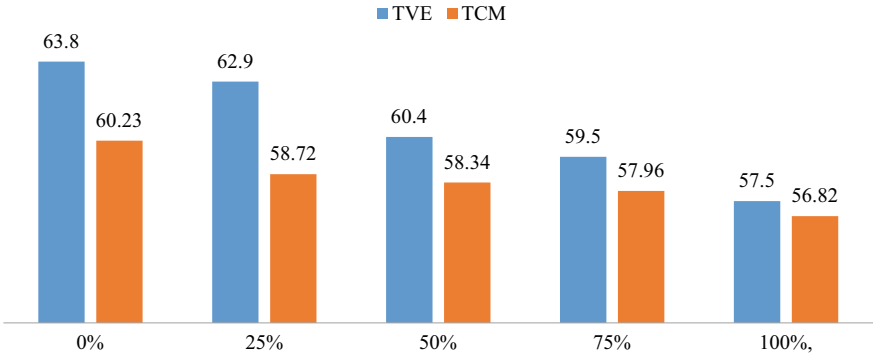

Fig. 4 Paired histogram illustrating the results of compactness of the granular class 06/10 by the shock table and vibrating table method. **TVE**: Electric vibrating table/**TCM**: Manual shock table

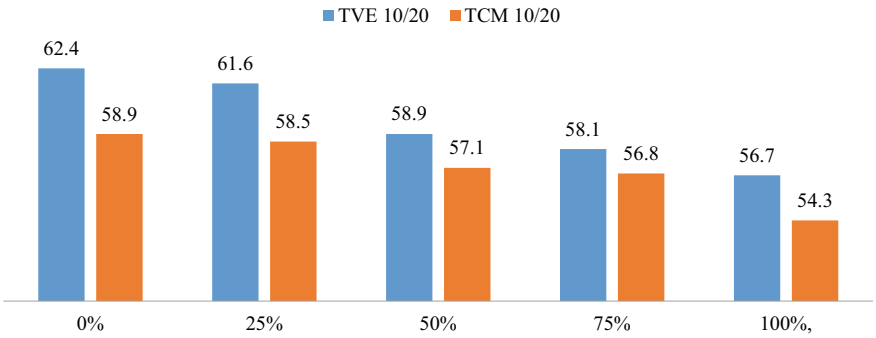

Fig. 5 Paired histogram illustrating the results of compactness of the granular class 10/20 by the shock table and vibrating table method. **TVE**: Electric vibrating table/**TCM**: Manual shock table

Table 3 Results of the compactness test on the granular class 06/10

Percentage of flat shape	0%	25%	50%	75%	100%
Compactness (%) mode shock table	60.23	58.72	58.34	57.96	56.82
Compactness (%) mode of vibrating table	63.80	62.90	60.40	59.50	57.50

Table 4 Results of the test of compactness on the granular class 10/20

Percentage of flat shape	0%	25%	50%	75%	100%
Compactness (%) mode shock table	58.90	58.50	57.10	56.80	54.30
Compactness (%) mode of vibrating table	62.40	61.60	58.90	58.10	56.70

3.1 Compactness Test Results

For the evaluation of the contents of the flat aggregates, the distribution of the aggregates was determined according to the ratioL/E and the coefficient Fc (Table 2). Tables 3 and 4 show, respectively, the results of compactness test on the granular classes 06/10 and 10/20.

Figure 4 based on Table 3 shows, on the one hand, the evolution of the compactness according to the quantities of flat shapes and on the other hand, it compares the methods used (vibrating table method and the method of shock table).

3.2 Analysis and Discussion of Results

The regression line equations found from parameters **a** and **b** of regression formula are presented in Table 3 followed by Figs. 6 and 7 which illustrate them (Table 5).

The following Figs. 5 and 6 give us the point clouds followed by their adjustments.

Where, **TVE**: Electric vibrating table/**TCM**: Manual shock table, **FP**: Flat shape/**FC**: No Flat shape

The analysis of the results allows us to draw the following conclusions:

- The two studied granular classes have a continuous grain size,
- The classification in the unified system from the Cc and Cu coefficients which are all less than 2, group together them into the gravel of tight grain size, and less than 3 Cc includes the class 0/10 in the clean gravel,

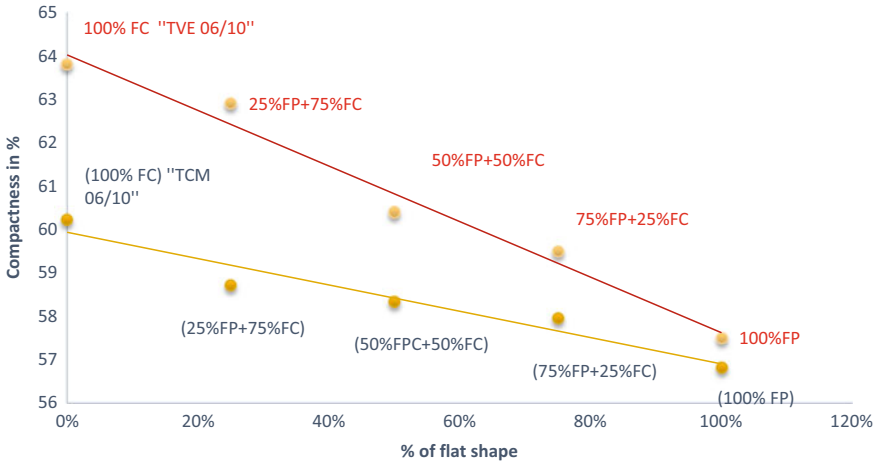

Fig. 6 Variation of the compactness according to the percentage of flat-shaped aggregates for the class 06/10

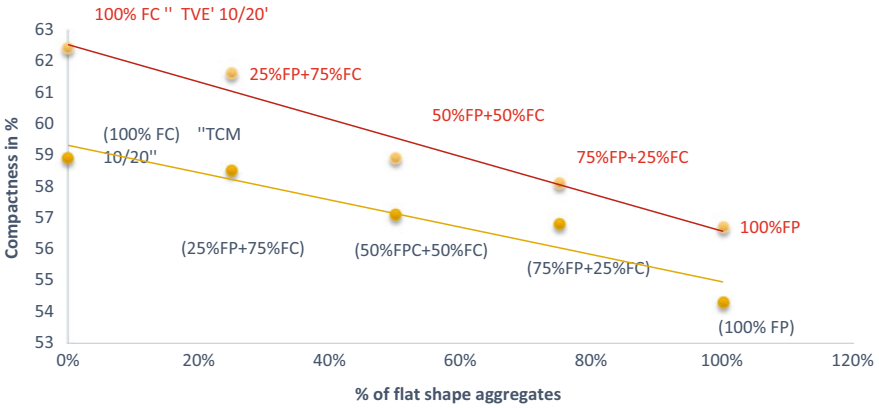

Fig. 7 Variation of compactness based on the percentage of the aggregate of flat shape for the class 10/20

Table 5 Equations of lines of regression to the compactness

Granular class	Line equations	
	Shock table method	Vibrating table method
6/10	$Y = -0.758x + 60.68$	$Y = -1.6x + 65.62$
10/20	$Y = -1.09x + 60.39$	$Y = -1.49x + 64.01$

- The granular class 6/10 has a high percentage of flat shape (32.5%), or 3.85% more than the granular class 10/20.
- Trend in Figs. 6 and 7 curves give the decreasing appearance, which means that more of the flat shape believes more compactness decreases.
- The experimental method using the electric vibrating table allows to reduce the maximum of voids in a granular fraction. This method can be explained by the phenomenon of vibration under compression, as the table in shock is under simple compression.

These results confirm that the presence of flat shape in a material will reduce its compactness when compactness or porosity is one of the important properties that characterize the durability of concrete; a high porosity is detrimental to the strength and permeability of concrete particularly in the cases of concretes cracked in aggressive places.

4 Conclusions

The granular compactness is a problem common to many applications in the field of civil engineering; modelling this characteristic remains the first step for better prediction of other features that depend on this characteristic, such as workability and strength of concrete. Concrete formulation requires optimized compactness of the granular skeleton as well as the pavement layers since the aggregates in the mixture represent 70% of the volume [5]. Indeed, many methods for the formulation of concrete (Féret, Bolomey, Faury, Dreux, etc.) focused on the search for an optimal curve of the mixture which corresponds to the arrangement of the grains offering the maximum compactness of the skeleton.

It is apparent after analysis results that if we increase the quantity of aggregates of flat shape of 25%, the compactness of the granular fraction decreases of:

- For the class 06/10: 0.85% for the table shock method and 1.6% for the method of the electric vibration table
- For the 10/20 class: 1.2% for the table shock method and 1.4% for the method of the electric vibration table.

As a result of all these observations and analyses, we suggest companies to make the choice of aggregates with small quantities of flat shape.

References

1. Marfunin AS (ed) (1994) Advanced mineralogy: volume 1 composition, structure, and properties of mineral matter: concepts, results, and problems. Springer, 23 Aug 23 1994
2. Borchardt-Ott W (1995) Crystallography. Springer Science & Business Media. 12 Dec 1995
3. Jones MP (1987) Applied mineralogy: a quantitative approach. 30 Apr 1987
4. Zhang H (2013) Aspect of rock perméability. Front Struct Civil Eng 7:102–116. SP Heigher Education Press
5. Bouterfas M (2012) Optimization of the compactness of the granular skeleton. Thesis, Magister degree in civil engineering, University Aboubeker Belkard-Tlemcen, Mar 2012

Sustainable Design of Slopes Under Earthquake Conditions

Pragyan Pradatta Sahoo and Sanjay Kumar Shukla

Abstract The consideration of sustainability is very important for the stability assessment of geotechnical structures, including the slopes subjected to the seismic loads. Most seismic stability analyses of the slopes are performed to evaluate the factor of safety by following the conventional deterministic methods where the horizontal earthquake loadings are applied as inertia force to the centre of gravity of sliding mass of the slope. In the past, limited importance has been given to the effect of vertical seismic loading, although it may affect greatly the factor of safety as well as the performance of the slope.

Keywords Horizontal and vertical seismic coefficients · Slope stability · Probabilistic analysis · Earthquake loading

The consideration of sustainability is very important for the stability assessment of geotechnical structures, including the slopes subjected to the seismic loads. Most seismic stability analyses of the slopes are performed to evaluate the factor of safety by following the conventional deterministic methods where the horizontal earthquake loadings are applied as inertia force to the centre of gravity of sliding mass of the slope. In the past, limited importance has been given to the effect of vertical seismic loading, although it may affect greatly the factor of safety as well as the performance of the slope. Therefore, a logical framework is necessary to evaluate the factor of safety which accommodates suitably the occurrence of uncertainty due to vertical seismic coefficient. In the present study, the probabilistic failure analysis has been carried out to compute both factors of safety and probability of failure

P. P. Sahoo (✉)
Discipline of Civil and Environmental Engineering, School of Engineering, Edith Cowan University, Joondalup, Perth, WA 6027, Australia
e-mail: pragyan.pradatta.sahoo@gmail.com

S. K. Shukla
Geotechnical and Geoenvironmental Engineering Research Group, School of Engineering, Edith Cowan University, Joondalup, Perth, WA 6027, Australia
e-mail: s.shukla@ecu.edu.au

Fiji National University, Suva, Fiji

V. S. Kanwar and S. K. Shukla (eds.), *Sustainable Civil Engineering Practices*,
Lecture Notes in Civil Engineering 72,
https://doi.org/10.1007/978-981-15-3677-9_6

under combined horizontal and vertical seismic loadings. The probability of failure due to vertical seismic coefficient as a random variable was first made by using point estimation method. Further, for a given geometrical parameter, the slope is simulated through the Monte Carlo simulation by using commercial limit equilibrium tool for its validity. The design tables of probability of failure due to combined seismic loadings presented herein provide the insight of the vertical seismic coefficient in the seismic design assessment of the slope in order to avoid any risk.

1 Introduction

Design charts are routinely used by the researchers and practitioners for the stability analysis of the slope under static as well as dynamic conditions. In the earthquake-prone area, stability charts are often based on the horizontal seismic coefficient of the inertia loading to compute the factor of safety of slope without giving importance to the effect of the vertical seismic coefficient [5, 11, 12]. The uncertainty in the occurrence of vertical seismic coefficient may alternatively affect the factor of safety of the slope greatly during an earthquake. Recently, many researchers have investigated the effect of the vertical seismic coefficient on the slope and emphasised the inclusion of vertical seismic coefficient for the exact calculation of factor of safety during the earthquake analysis [8, 9]. Therefore, the determination of a realistic factor of safety by quantifying the uncertainty due to vertical seismic coefficient is required in order to avoid the risk for the earthquake geotechnical sustainable engineered system. Recently, the probabilistic methods have been used as a recognising tool to calculate the variation of any random variable associated with conventional slope stability analysis [3, 15]. Duncan [3] evaluated the stability of a retaining wall by using the point estimation method and provided the design tables with probabilistic failures of the walls. Several methods have been developed for reliability analysis of slopes under the horizontal earthquake loading condition to calculate the probability of failure of the slope [2, 6, 16, 17]. If the probabilistic methods for seismic slope stability can further be extended for the variation of the vertical seismic coefficient and its effect on the factor of safety, it will greatly improve the assessment of earthquake-induced slope failure. This can be done by extending the conventional limit equilibrium method and implementing a probabilistic analysis to assess the slope performance. Sahoo and Shukla [10] presented a set of graphs for the variation of factor of safety under combined horizontal and vertical seismic loadings for a homogenous cohesive-frictional soil slope. The method proposed was based on the pseudo-static methods, and the resulting design chart provides factor of safety for a given value of the vertical seismic coefficient. However, the uncertainty due to vertical seismic coefficient on slope stability has not been considered. The primary objective of the present study is to develop the design tables for slopes that quantify the uncertainty of the factor of safety due to change in vertical seismic coefficient in the slope stability analysis. The slopes are analysed by using Rosenblueth's point

estimation method (PEM) for finding statistical moments of the vertical seismic coefficient as a random variable and its corresponding probability of failure of the slope. Further, the Monte Carlo simulation has also been simulated for the better approximation of the result. From the design tables, it is possible to choose the factor of safety for a given slope with the lowest probability of failure due to vertical seismic loading that can be implemented in the slope design. Thus, these design tables can be made more beneficial to the sustainable seismic design practices.

2 Probabilistic Analysis of Cohesive-Frictional Soil Slope

Considering the upward direction of vertical seismic loading is critical to the stability of the slope, the factor of safety (FS) of the cohesive-frictional soil slope subjected to the combined horizontal and vertical seismic loadings is expressed as [10]

$$\mathrm{FS} = \frac{c^* \sec i + [(1 - k_\mathrm{v}) - k_\mathrm{h} \tan i] \tan \varphi}{[(1 - k_\mathrm{v}) \tan i + k_\mathrm{h}]} \tag{1}$$

where c^* is the non-dimensional form of cohesion $\left(= c \big/ \gamma H\right)$; H is the height of the slope; γ is the total unit weight of slope soil; i is the angle of inclination to the horizontal of the slope; φ is the angle of internal friction of the slope soil; k_h is the horizontal seismic coefficient; and k_v is the vertical seismic coefficient of the ground motion.

For a given value of soil strength parameters (c^*,φ), slope geometry and k_h, the value of FS may vary significantly due to the uncertainty in k_v, and hence the value of k_v needs to be selected carefully for the seismic performance of the slope during an earthquake condition. The value of k_v is obtained by referring to the standard seismic manuals or design codes [1, 14]. U.S. Army Corps of Engineers (USACE) [14] has recommended that the value of the vertical seismic coefficient is equal to the half of the value of k_h. In order to compute the probability of failure of the slope, Eq. (1) needs to be converted into the probabilistic framework of analysis for estimating the variability in the FS considering the statistical moments of the random variable k_v. Therefore, following the concepts of Duncan [3] and Rosenblueth [7], the point estimation method (PEM) has been used to evaluate the performance function, $f[\mathrm{FS}]$ at a set of discrete points. This has been performed by computing the mean values (μ) and the standard deviation (σ) of random variable, k_v. For a single random variable, $f[\mathrm{FS}]$ is defined as [7]

$$f[\mathrm{FS}] = \int_{-\infty}^{+\infty} \mathrm{FS}\,\mathrm{d}f(\mathrm{FS}) \tag{2}$$

When FS is a function of single random variables k_v, the first moment (or expected value) $E[\mathrm{FS}]$ and second central moment $E\left[\left\{\mathrm{FS} - E(\mathrm{FS})^2\right\}\right]$ can be determined as

$$E[\mathrm{FS}] = \mu_{\mathrm{FS}} \approx P_{++}\mathrm{FS}_{++} + P_{--}\mathrm{FS}_{--} \tag{3}$$

and

$$E\left[\left\{\mathrm{FS} - E(\mathrm{FS})^2\right\}\right] = \sigma^2[\mathrm{FS}] = E\left[\mathrm{FS}^2\right] - \left(E[\mathrm{FS}]^2\right) \approx P_{++}\mathrm{FS}_{++}^2 + P_{--}\mathrm{FS}_{--}^2 - E[\mathrm{FS}]^2 \tag{4}$$

where the coefficients of P are

$$P_{++} = P_{--} = 0.5 \tag{5}$$

Furthermore, as k_{v} is a single random variable in the present study, the expected FS is computed at the estimating points of $k_{\mathrm{v}+}$ and $k_{\mathrm{v}-}$ such that

$$k_{\mathrm{v}+} = \mu_{k_{\mathrm{v}}} + \sigma_{k_{\mathrm{v}}} \text{ and } k_{\mathrm{v}-} = \mu_{k_{\mathrm{v}}} - \sigma_{k_{\mathrm{v}}} \tag{6}$$

where $\mu_{k_{\mathrm{v}}}$ and $\sigma_{k_{\mathrm{v}}}$ are the mean and standard deviations of the normal distribution function of k_{v}, respectively.

Using Eqs. (1) to (6), the probability of failure (p_{f}) of the slope is computed by estimating the corresponding reliability index (R) of the slope with the use of EXCEL such that

$$p_{\mathrm{f}} = 1 - \mathrm{NORMDIST}(R) = 1 - \mathrm{NORMDIST}\left(\frac{E[\mathrm{FS}] - 1}{\sigma[\mathrm{FS}]}\right) \tag{7}$$

3 Results and Discussion

In the present analysis, k_{v} is assumed to be a single random variable associated with the estimation of p_{f} of slope for a given slope geometry under combined seismic loadings. For a cohesive-frictional soil slope, the value of c^* has been taken in the range of 0–0.2 [13]. In the present analysis, the value of c^* is considered as 0.1, 0.15 and 0.2 for which the probabilistic failure of the slope is computed. The maximum value of k_{h} has been kept as 0.25 while the value of k_{v} has been varied in the range of 0–0.25. For a given geometrical value of the slope, $E[\mathrm{FS}]$ of the slope has been computed corresponding to a particular value of k_{v}, most likely value of k_{v} plus σ and most likely value of k_{v} minus σ of k_{v}. Determination of σ is conveniently expressed in terms of the coefficient of variation (COV) and five different values of COV (20, 40, 60, 80 and 100%) are considered for the estimation of $E[\mathrm{FS}]$ for each discrete values of k_{v}. This has been achieved by using Eqs. (2)–(6) and the probability of failure (p_{f}) of the slope is then computed by using Eq. (7) and presented in the form of design tables.

Figure 1 shows the variation of factor of safety (FS) with the vertical seismic coefficient (k_v) of the cohesive-frictional soil slope for a given value of $\varphi = 35°$, $i = 25°$ and $k_h = 0.25$ corresponding to $c^* = 0.1$, $c^* = 0.15$ and $c^* = 0.25$. It is observed that the FS of the slope reduces significantly as the value of k_v increases for a given value c^*, φ, k_h and i. For example, for $c^* = 0.15$, $\varphi = 35°$, $i = 25°$ and $k_h = 0.25$, the FS is found to be 1.051 for $k_v = 0.15$ while FS is obtained as unity for $k_v = 0.25$. This suggests that stability of the slope reduces greatly with the variation of vertical seismic coefficient.

Tables 1, 2 and 3 present the probability of failure p_f of slope under combined horizontal and vertical seismic coefficients corresponding to the factor of safety (FS) for $c^* = 0.1$, $c^* = 0.15$ and $c^* = 0.25$, respectively. It is noticed that with an increase of COV of k_v with the constant value of k_h, the p_f of the slope increases significantly. For example, in Table 1, for a given value of seismic coefficients,

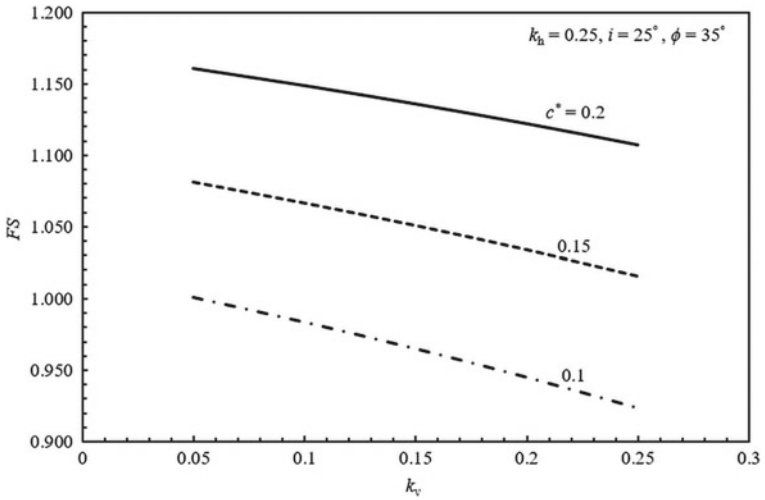

Fig. 1 Variation of factor of safety (FS) of the slope with vertical seismic coefficient (k_v)

Table 1 Probability of failure of slope for $c^* = 0.1$

k_v	FS	$i = 25°, \phi = 35°, c^* = 0.15, k_h = 0.25$				
		COV of k_v				
		20%	40%	60%	80%	100%
0	1.018	0%	0%	0%	0%	0%
0.05	1.001	35%	42%	45%	46%	47%
0.1	0.984	67%	71%	77%	87%	99%
0.15	0.965	72%	77%	84%	93%	100%
0.2	0.945	74%	79%	86%	95%	100%
0.25	0.924	74%	80%	87%	95%	100%

Table 2 Probability of failure of slope for $c^* = 0.15$

k_v	FS	$i = 25°, \phi = 35°, c^* = 0.15, k_h = 0.25$				
		COV of k_v				
		20%	40%	60%	80%	100%
0	1.095	0%	0%	0%	0%	0%
0.05	1.081	0%	0%	0%	0%	0%
0.1	1.066	0%	0%	0%	0%	1%
0.15	1.051	0%	0%	4%	10%	15%
0.2	1.034	1%	12%	21%	28%	32%
0.25	1.016	21%	34%	39%	42%	44%

Table 3 Probability of failure of slope for $c^* = 0.2$

k_v	FS	$i = 25°, \phi = 35°, c^* = 0.2, k_h = 0.25$				
		COV of k_v				
		20%	40%	60%	80%	100%
0	1.172	0%	0%	0%	0%	0%
0.05	1.161	0%	0%	0%	0%	0%
0.1	1.149	0%	0%	0%	0%	0%
0.15	1.136	0%	0%	0%	0%	0%
0.2	1.122	0%	0%	0%	0%	2%
0.25	1.108	0%	0%	1%	4%	9%

$k_h = 0.25, k_v = 0.05$ and $c^* = 0.1, \varphi = 35°, i = 25°$, the p_f of the slope is observed to be 35% for COV = 20% while the p_f is increased to 46% for COV = 80% corresponding to same FS = 1.001. It is also observed that the p_f of the slope is greater for the higher value of k_v while the p_f is minimum for lower value of k_v. For example, from Table 2, considering COV = 20% of k_v, for given value of soil parameters, $c^* = 0.15$, $\varphi = 35°$, $i = 25°$ and $k_h = 0.25$, the probability of failure of the slope is observed as 44% for $k_v = 0.25$ and FS = 1.016 while p_f of the slope is found to be 0% corresponding to $k_v = 0.05$ and $FS = 1.095$. However, with an increase of c^*, the probability of failure of the slope is reduced significantly. For example, from Table 3, for $\varphi = 35°$, $i = 25°$ and $k_h = 0.25$, $k_v = 0.25$ and COV = 60% of k_v, the probability of failure of the slope is obtained as $p_f = 1\%$ corresponding to $c^* = 0.20$ compared to a $p_f = 39\%$ for $c^* = 0.15$ in Table 2. This suggests that the slope is quite stable under higher c^* of soil and the corresponding probability of failure is minimum even though COV = 100% of k_v is taken account.

Figure 2 shows the results of probabilistic failure analysis of a cohesive-frictional slope using the Monte Carlo simulation [4] for a given set of parameters such as $c^* = 0.15$, $\varphi = 35°$, $i = 25°$ and $k_h = 0.25$, $k_v = 0.15$ having COV of k_v as 0.2. The factor of safety and the probability of failure are obtained as 1.098 and 0.2,

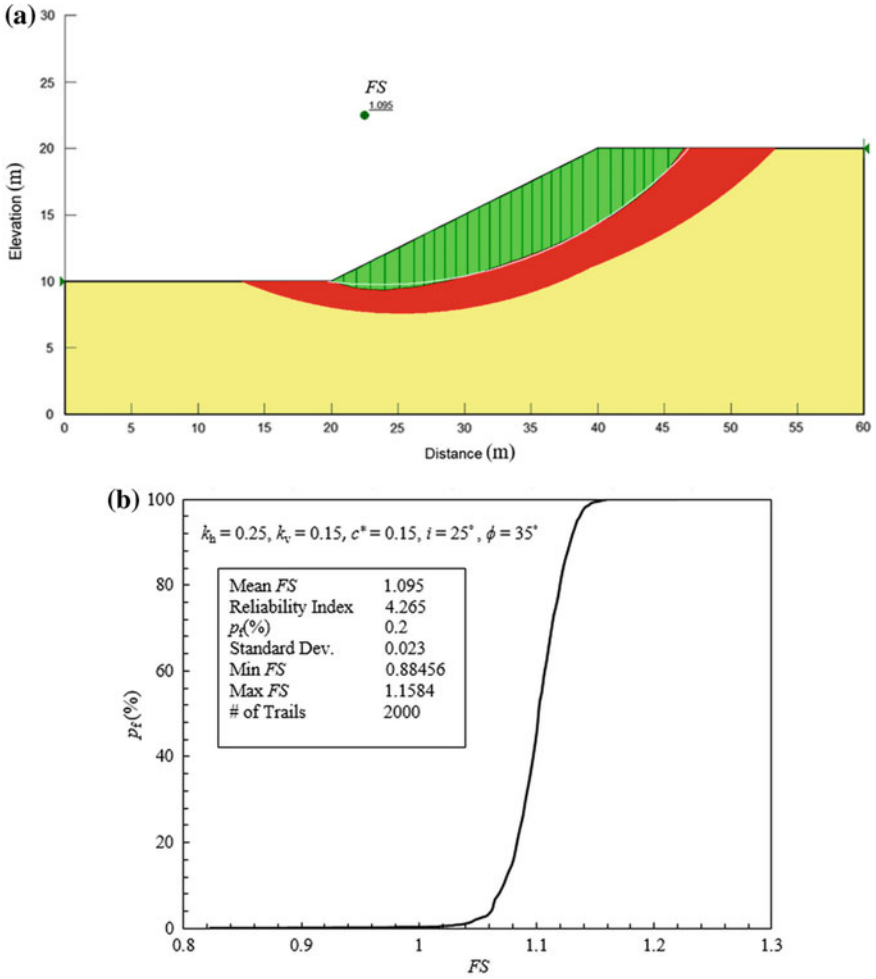

Fig. 2 Monte Carlo simulation of the slope: **a** a slope with a typical failure surface considered for the simulation and **b** variation of probability of failure of the slope with factor of safety

respectively, which is a good agreement with solutions obtained in the design table using the PEM method.

4 Conclusions

In the present analysis, both the factor of safety and the corresponding probability failure of a slope are computed under the combined horizontal and vertical seismic loadings. On the basis of results and discussion presented earlier, the following general conclusions can be drawn:

(a) The probability of failure of the slope increases with an increase of the vertical seismic coefficient.
(b) The higher is the *COV* of k_v, the greater the dispersion in the random variable, k_v. Therefore, a higher probability of failure of the slope is observed even though the factor of safety is greater than unity.
(c) Lower is the cohesion of slope soil, lower is the factor of safety and a 100% probability failure is observed under combined seismic loadings.
(d) With a higher value of cohesion, the probability of failure of slope can be reduced significantly under generalised earthquake condition compared to the slope soil with a lower value of cohesion.

The design tables of factor of safety developed here can be readily used by the practitioners and engineers for the sustainable seismic design of the slope under combined seismic loadings. However, more robust methods can be used to compute the factor of safety of the slope using various numbers of random variables in the design analysis. Further, the numerical modelling can be more useful for simulation of a larger number of random variables compared to the deterministic approach.

References

1. BIS (Bureau of Indian Standards) (2002) IS 1983: Indian standards criteria for earthquake resistant design of structures, part 1. BIS, New Delhi, India
2. Christian JT, Urzua A (1998) Probabilistic evaluation of earthquake-induced slope failure. J Geotech Geoenviron Eng 124(11):1140–1143
3. Duncan MJ (2000) Factors of safety and reliability in geotechnical engineering. J Geotech Geoenviron Eng 126(4):306–316
4. GeoSlope W (2007) Stability modeling with SLOPE/W 2007—an engineering methodology, 2nd edn. GEO-SLOPE/W International, Calgary, Alberta, Canada
5. Majumdar DK (1971) Stability of soil slopes under horizontal earthquake force. Géotechnique 21(1):84–88. https://doi.org/10.1680/geot.1971.21.1.84
6. Rathje EM, Saygili G (2008) Probabilistic seismic hazard analysis for the sliding displacement of slopes: scalar and vector approaches. J Geotech Geoenviron Eng 134(6):804–814
7. Rosenblueth E (1975) Point estimates for probability moments. Proc Nat Acad Sci 72(10):3812–3814
8. Sahoo PP, Shukla SK (2019) Taylor's slope stability chart for combined effects of horizontal and vertical seismic coefficients. Géotechnique 69(4):344–354. https://doi.org/10.1680/jgeot.17.P.222
9. Sahoo PP, Shukla SK, Mohyeddin A (2018) Analytical expressions for determining the stability of cohesionless soil slope under generalized seismic conditions. J Mt Sci 15(7):1559–1571

10. Sahoo PP, Shukla SK (2020) Effect of vertical seismic coefficient on cohesive-frictional soil slope under generalized seismic conditions. Int J Geotech Eng. https://doi.org/10.1080/19386362.2020.1711553
11. Sarma SK (1973) Stability analysis of embankments and slopes. Géotechnique 23(3):423–433. https://doi.org/10.1680/geot.1973.23.3.423
12. Sarma SK (1979) Stability analysis of embankments and slopes. J Geotech Engng Div ASCE 105(GT12):1511–1524
13. Shukla SK, Gupta SK, Sivakugan N (2009) Active earth pressure on retaining Wall for c-ϕ soil backfill under seismic loading condition. J Geotech and Geoenviron Eng 135(5):690–696
14. USACE (US Army Corps of Engineers) (1989) EM 1110-2-2502: Engineering and design of retaining and flood walls. USACE, Washington
15. USACE (US Army Corps of Engineers) (1998) Risk-based analysis in geotechnical engineering for support of planning studies. Engrg. CircularNo. 1110-2-554, Department of the Army, Washington, D.C.. www.usace.army.mil/usace-docs. 27 Feb 1998
16. Wu XZ (2015) Development of fragility functions for slope instability analysis. Landslides 12:165–175
17. Xiao J, Gong W, Martin JR II, Shen M, Luo Z (2016) Probabilistic seismic stability analysis of slope at a given site in a specified exposure time. Eng Geol 212:53–62

Effect of Geosynthetic Reinforcement on Strength Behaviour of Subgrade-Aggregate Composite System

Meenakshi Singh, Ashutosh Trivedi and Sanjay Kumar Shukla

Abstract Geosynthetics have been the most important innovation in the field of geotechnical engineering. This paper presents the results of laboratory California bearing ratio (CBR) tests that were carried out on unreinforced and reinforced soil–aggregate composite systems. The soil used in these tests is locally available soil which is classified as silty sand (SM) as per the Indian Soil Classification System. The improvement in the strength of subgrade-aggregate composite system was determined through the tests conducted in the standard CBR mould in terms of *CBR* value. Unreinforced soil–aggregate composite system is prepared by compacting the soil layer in the mould, and placing the aggregates layer above the soil, where the soil represents the existing subgrade and aggregate layers, represents the base course material of an unpaved road. In reinforced soil–aggregate composite system, the reinforcing layer is inserted at the interface of the soil and aggregate layers. The geosynthetics used in the study as reinforcing layers are geotextile, geogrid and geomat. Some more tests were conducted on reinforced soil–aggregate composite system with double layers of reinforcement such that the first reinforcing layer was placed at the interface of the soil and aggregate layers and another reinforcing layer was placed at the middle half of the compacted aggregate layer. Unreinforced and reinforced soil–aggregate composite systems were subjected to standard penetrating load while performing the tests, and the performance of reinforced soil–aggregate composite system was compared with that of the unreinforced systems. The effect of type of reinforcement on the load–penetration curve and the relative performance of various types of geosynthetics have also been investigated.

Keywords Geogrid · Geotextile · Geomat · Reinforcement

M. Singh (✉) · A. Trivedi
Department of Civil Engineering, Delhi Technological University, Delhi, India
e-mail: meenakshisingh_2k14@dtu.ac.in

A. Trivedi
e-mail: atrivedi@dce.ac.in

S. K. Shukla
School of Building and Civil Engineering, Fiji National University, Suva, Fiji
e-mail: sanjaykshukla1@gmail.com

V. S. Kanwar and S. K. Shukla (eds.), *Sustainable Civil Engineering Practices*,
Lecture Notes in Civil Engineering 72,
https://doi.org/10.1007/978-981-15-3677-9_7

1 Introduction

Geosynthetics have been found as an important innovation in the field of geotechnical engineering. Geosynthetics such as geotextiles and geogrids, which have been used very commonly on various construction sites, can improve the performance and life span of unpaved road when built over weak subgrades. Soil and aggregate are the basic material required for the construction of unpaved roads. Unpaved roads are generally constructed by placing one or more layers of locally available material or good quality granular fill material over a natural subgrade. Since no asphalt or concrete surfacing is provided on the top of unpaved roads, they are prone to problems such as excessive deformations, rutting and potholes, due to which frequent maintenance work is required. Geosynthetic reinforcement can be used to reinforce these roads where reinforcement can be placed at the interface of subgrade and granular fill, increasing its life and reducing maintenance costs [11]. Benefits of reducing granular subbase/base layer thickness are realized if the cost of the geosynthetics is less than the cost of the reduced granular subbase/base layer material [13].

The haul roads as well as the temporary roads can be considered as an unpaved road where subbase/base layers are laid directly on in situ subgrades. These can be referred to as subgrade-aggregate composite systems. Geosynthetic reinforcement has been introduced into a pavement system by placing the geosynthetic layer directly on the unprepared subgrade, and sometimes it is laid on the prepared subgrade before the placement of the subbase/base layer. These systems are referred to as subgrade-geosynthetic-aggregate composite systems. Subgrade-aggregate composite system requires aggregate layer of greater thickness than subgrade-geosynthetic-aggregate composite system to carry the same traffic [3]. It is also observed that the bearing resistance of these soil–aggregate systems is improved by the presence of geosynthetic reinforcement as well as with an increase in quantity or the stiffness of the reinforcement [2].

Several works in the literature have shown the benefits of geosynthetics in reinforcing the paved and unpaved roads by conducting the laboratory model studies and field studies [6, 9]. Some of the analytical studies on reinforced unpaved roads include the works by Giroud and Han [7] and Giroud and Noiray [8]. Limited studies have carried out California bearing ratio (CBR) tests on unreinforced and reinforced soil–aggregate systems to understand the improvement in the CBR value of soil or aggregate with the inclusion of reinforcement [1, 10, 12, 14]. Conventional road design uses the CBR value of the subgrade/subbase/base course material as a measure of the load-carrying capacity of the roads and for the estimation of thickness of granular base course.

The main objective of this study was to conduct a series of CBR tests on unreinforced and reinforced soil–aggregate composite systems. Tests were conducted on soil alone and unreinforced and reinforced soil–aggregate systems. Different types of

geosynthetics used in this study were a geotextile, geogrid and geomat. Geosynthetic layers were placed at the interface of subgrade and aggregate layer and sometimes within aggregate layer also, and a significant improvement in the strength behaviour of system was observed due to the separation and reinforcing action provided by the geosynthetic materials. Effect of various types of geosynthetic as reinforcement on the CBR value was also studied. The test results have been analysed to understand the effect of type of reinforcement on the performance of the subgrade-aggregate composite system in terms of increase or decrease in CBR value. The tests performed in the present study are small-scale tests and were subjected to scale effects.

2 Materials

Locally available soil was collected from the campus of Delhi Technological University that has been used as a subgrade material in the experiments. The soil is classified as silty sand (SM) using the particle-size analysis and Atterberg limit tests as per the Indian Soil Classification System. Maximum dry unit weight (MDU) and optimum moisture content (OMC) of the soil were determined through the standard Proctor compaction test [4], which was obtained as 18.6 kN/m^3 and 13.9%, respectively. The properties of the soil used in the study are given in Table 1. The aggregates having size ranging from 4.75 to 12.5 mm were used as the subbase/base material in the tests. The specific gravity of the aggregates is 2.65.

The geosynthetics used in the experiments to prepare the subgrade-aggregate composite system are geotextile, geogrid and geomat. These three geosynthetics were placed at the interface of subgrade and aggregate layer. The photograph of various geosynthetic reinforcement used in the study are shown in Fig. 1. Woven multifilament polypropylene geotextiles are used and theses are resistant to chemicals and micro-organism normally found in soils and resistant to short-term exposure to ultraviolet radiation. High-strength geogrid was used; the geogrid is coated with a patent-pending elastomeric polymer and self-adhesive glue and had ultimate tensile strength of 115 kN/m. Three-dimensional geomat used in the experiments had peak tensile strength of 3.8 kN/m, and it is formed by laying extruded polypropylene grids in between the two bi-oriented polypropylene grids and tied together by black

Table 1 Properties and classification of subgrade soil

Particulars	Soil
Specific gravity	2.65
Soil classification	SM
Liquid limit and plastic limit (%)	29 and 20
Maximum dry unit weight (kN/m^3)	18.6
Optimum moisture content (%)	13.9

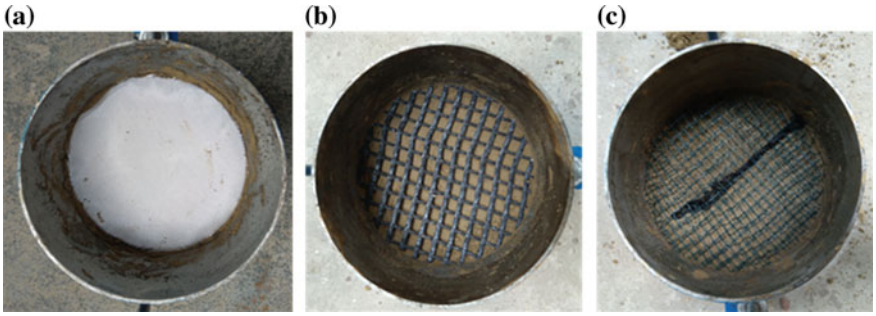

Fig. 1 Geosynthetics used in the study **a** geotextile **b** geogrid **c** geomat

Table 2 Properties of geosynthetics used in experiments

Property	Geotextile	Geogrid	Geomat
Aperture size (mm)	–	12.5 × 12.5	7 × 9
Tensile strength in machine direction (kN/m)	45	115	3.8
Tensile strength in transverse direction (kN/m)	34	115	13
Tensile elongation in machine direction (%)	30	2.5	23
Tensile elongation in transverse direction (%)	28	2.5	23
Mass per unit area (g/m^2)	200	405	180

polypropylene yarn. The properties of geosynthetic materials as provided by the manufacturer are given in Table 2.

3 Experimental Studies

A series of unsoaked laboratory CBR tests were conducted on unreinforced and reinforced subgrade-aggregate composite systems with a single layer and double layers of geosynthetic reinforcement in the conventional CBR mould of 150 mm internal diameter and having the height of 175 mm. To evaluate the effect of geosynthetic reinforcement on the performance of subgrade-aggregate composite system, the single layer of reinforcement was placed at the interface of subgrade and aggregate layer and the double layers of reinforcement was laid in such a way that the first reinforcing layer is placed at the interface of the subgrade and aggregate layer and another reinforcing layer is placed at the middle half of the compacted aggregate layer. These tests were conducted as described in IS: 2720 (Part 16) [5], with single and double layers of reinforcement in order to check the consistency of the obtained results, many of them were repeated. The details of the experiments carried out are given in Table 3. The total height of the prepared specimen was maintained to 125 mm for all the unreinforced and reinforced subgrade-aggregate composite systems. Subgrade

Table 3 Details of the experiments carried out and results of CBR tests

Details of the test	Reinforcement	CBR value (%)
Subgrade only	–	1.67
Subgrade-aggregate composite system	–	8.14
Subgrade-aggregate composite system reinforced with geotextile at the interface	Single layer of reinforcement	11.51
Subgrade-aggregate composite system reinforced with bi-axial geogrid at the interface		9.13
Subgrade-aggregate composite system reinforced with geomat at the interface		4.81
Subgrade-aggregate composite system reinforced with double layers of geotextile, one at the interface and other within the aggregate layer	Double layers of reinforcement	6.35
Subgrade-aggregate composite system reinforced with double layers of bi-axial geogrid, one at the interface and other within the aggregate layer		3.87
Subgrade-aggregate composite system reinforced with double layers of geomat, one at the interface and other within the aggregate layer		2.23

soil was filled in the CBR mould in two lifts, and aggregate was filled in one lift. All these layers were compacted using a rammer of 2.6 kg weight, falling from a height of 310 mm, and the number of blows on each layer was 56. Aggregates were filled in two layers; each layer is compacted with 28 blows, so that the total number of blows for the aggregate layer remained 56. During the compaction of the aggregate layer, a metal plate was used to avoid jumping of the aggregate from the CBR mould. Geotextile, geogrid and geomat were cut in the form of a circular shape of diameter slightly less than the diameter of CBR mould and placed inside it at the interface of subgrade and aggregate layer and sometimes within the aggregate layer also. Figure 2 shows the schematic sketch of the prepared subgrade-aggregate composite systems. Hence, the present study quantifies the improvement in strength of subgrade-aggregate composite system and the beneficial effect of various reinforcing layer at different positions.

The load is applied through a plunger of 50 mm diameter. Before the testing, a surcharge weight of 5 kg was applied on the unreinforced and reinforced subgrade-aggregate composite systems. The plunger was allowed to penetrate the prepared unreinforced and reinforced specimens at a rate of 1.25 mm/min. Based on the load and penetration values recorded, the CBR values were computed from the load–penetration curves.

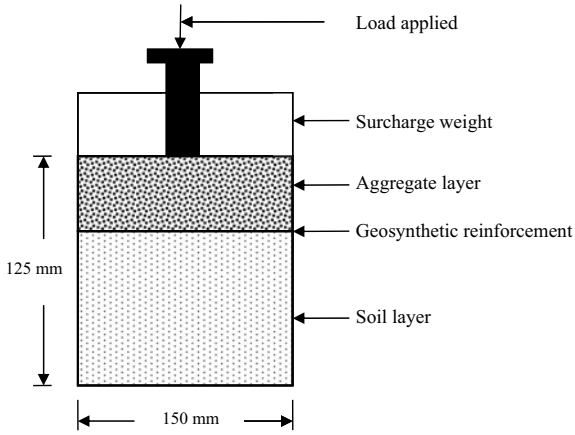

Fig. 2 Schematic diagram of subgrade-aggregate composite system

4 Results and Discussion

4.1 Effect of Geosynthetic Reinforcement

Figure 3 presents the variation of the load–penetration curves obtained from the CBR tests conducted on unreinforced and reinforced subgrade-aggregate composite systems. A clear comparison can be seen in between the unreinforced subgrade-aggregate and reinforced subgrade-aggregate composite systems with a single layer of reinforcement placed at the interface of subgrade and aggregate layer and double layers of reinforcement. The *CBR* values for the various composite systems are given

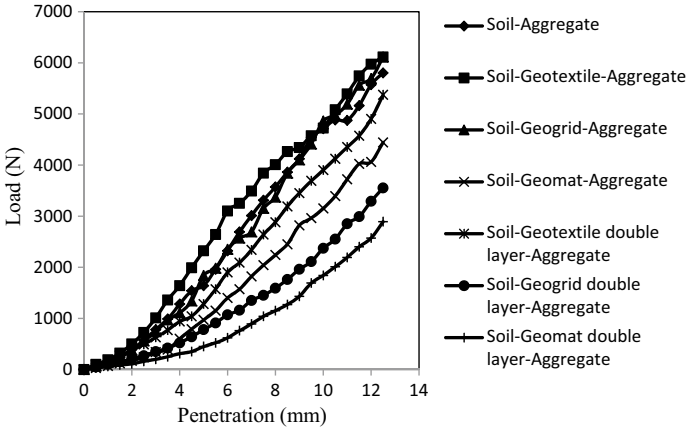

Fig. 3 Load–penetration curve for geosynthetic reinforcement placed at different location

in Table 3. The unreinforced and reinforced subgrade-aggregate composite systems exhibited a good performance when compared to the subgrade only.

The CBR value of the unreinforced subgrade-aggregate composite system was found to be 8.14%, which was increased to 11.51 and 9.13%, when geotextile and geogrid reinforcement was placed at the interface of subgrade and aggregate layer, respectively. Further, placing geomat reinforcement at same interface reduces the CBR value to 4.81%. Reduced *CBR* values were obtained as 6.35, 3.87 and 2.23%, when subgrade-aggregate composite system was reinforced with double layers of geotextile, geogrid and geomat reinforcement, respectively, as shown in Fig. 3. It was observed that an increase in the quantity of reinforcement led to degrade the performance of reinforced subgrade-aggregate composite system because placing the reinforcement layer very near to the load reduces its load-carrying capacity. Only geotextile reinforcement and geogrid reinforcement, when placed at the interface of subgrade-aggregate composite system, perform better than the unreinforced subgrade-aggregate composite systems, and other than these two reinforced systems, all of them performed poorly even in comparison with the unreinforced subgrade-aggregate composite system. The highest increase in *CBR* value was achieved when the subgrade-aggregate composite system was reinforced with geotextile at the interface because it prevents the intermixing of the aggregate and subgrade soil and maintaining a clean separation of the subgrade and aggregate layer. As geogrid and geomet have apertures and geotextile does not have aperture, there is a possibility of aggregates embedded into the subgrade soil during the loading.

4.2 Effect of Type of Reinforcement

To understand the beneficial effect of using reinforcements in subgrade-aggregate composite systems, three geosynthetic materials, namely geotextile, geogrid and geomat, were used at the interface of the subgrade and aggregate layers, and an extra layer is placed within the aggregate layer. Figure 4 shows the comparison of the load–penetration response for subgrade-aggregate composite systems reinforced with geotextile, geogrid and geomat reinforcement at the interface of subgrade and aggregate layer over unreinforced system at optimum moisture content. The experimental results were analysed and compared to evaluate the beneficial effect of various geosynthetic reinforcement in improving the performance of the subgrade-aggregate composite system. It is clear that geotextile reinforced composite system yields the maximum strength and geomat reinforced composite system yields minimum strength even less than the unreinforced composite system. Figure 5 shows the comparison of the load–penetration response for subgrade-aggregate composite systems reinforced with double layers of geotextile, geogrid and geomat reinforcement, over unreinforced system at optimum moisture content. Again geotextile reinforced composite system with double layers of reinforcement yields the maximum strength, but this gained strength is less than the unreinforced subgrade-aggregate composite system.

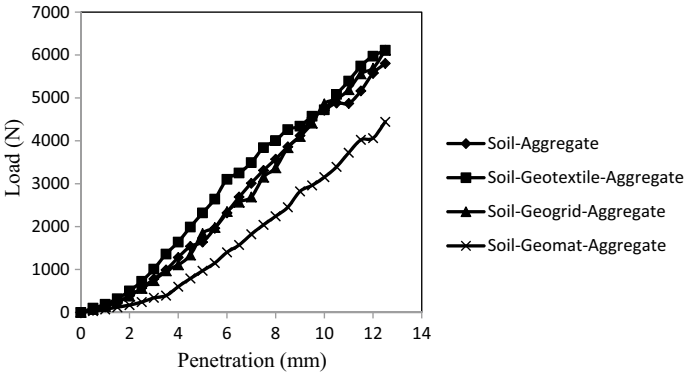

Fig. 4 Load–penetration curve for geosynthetic reinforcement placed at the interface of subgrade and aggregate layer

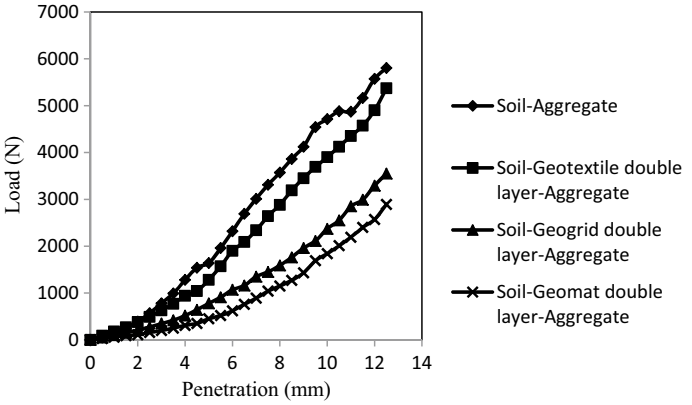

Fig. 5 Load–penetration curve for double layers of geosynthetic reinforcement

Out of three types of geosynthetics used to reinforce the subgrade-aggregate composite system, the best performance was achieved by geotextile reinforcement. The reason for this is the separation function performed by the geotextile placed at the interface of subgrade and aggregate layer, which prevents the intermixing of both the layers. As geogrid and geomat have apertures, they may allow the intermixing of subgrade soil into aggregate layer during loading. Geogrid performance was not better than the geotextile because the few of the aggregates have size almost equal to the aperture size of the geogrid, which reduces the interlocking effect. Geomat results in low CBR because of its least tensile strength as compared to the other geosynthetics. The top layer of geomat was found to be partially damaged after the test. The ascending order of performance improvement was generally observed as geotextile, geogrid and geomat. This order of performance improvement was not the same as the order of increase in the tensile strength of the geosynthetic reinforcement.

Though the tensile strength of geotextile is less than the geogrid, it still performs better than the geogrid because the reinforcing mechanism of geogrids and geotextiles is different. The performance of geotextile and geogrid was more effective than geomat in reinforcing the subgrade-aggregate composite system because of the high tensile strength of geogrid and good separation function served by geotextile. The contribution of geomat in improving the strength/performance is least as compared to the other reinforcements.

5 Conclusions

Based on the results and discussion presented here, the following conclusions can be made:

1. The reinforced subgrade-aggregate composite system with reinforcement at the interface of subgrade and aggregate layer performs better than the reinforced subgrade-aggregate composite system with double layers of reinforcement.
2. Geotextile and geogrid reinforcement proved to be the most effective reinforcement, and the contribution of geomat was least in improving the performance of subgrade-aggregate composite system.
3. The reinforced subgrade-aggregate composite system performs better than the unreinforced subgrade-aggregate composite system only in case of geotextile and geogrid reinforcement placed at the interface of subgrade and aggregate layer.
4. Contribution of geosynthetic reinforcement would be ineffective if it is not implemented at the suitable location.

The present study investigates the effect of geosynthetic reinforcement on the strength of subgrade-aggregate composite system in terms of CBR value. Further, studies are to be carried out for better understanding of the strength behaviour of subgrade-aggregate composite system with multiple layers of reinforcement and by varying the type of geosynthetic reinforcement. This study has been limited to the laboratory tests; thus, the field tests are necessary to validate the results of laboratory work.

References

1. Asha MN, Latha GM (2010) Modified CBR tests on geosynthetic reinforced soil-aggregate systems. In: Indian geotechnical conference-2010, GEOtrendz, IGS Mumbai Chapter & IIT Bombay, 16–18 Dec 2010, pp 297–300
2. Asha MN, Latha GM (2011) Bearing resistance of reinforced soil-aggregate systems. Proc Inst Civil Eng Ground Improv 164(GI2):83–95
3. Bender DA, Barenberg EJ (1978) Design and behaviour of soil-fabric-aggregate systems. Transp Res Rec 671:64–75
4. Bureau of Indian Standards (1980) Methods of test for soils: determination of water content dry density relation using light compaction. New Delhi, India, IS 2720-7

5. Bureau of Indian Standards (1987) Methods of test for soils: laboratory determination of CBR. New Delhi, India, IS 2720-16
6. Fannin RJ, Sigurdsson O (1996) Field observations on stabilization of unpaved roads with geosynthetics. J Geotech Eng ASCE 122(7):544–553
7. Giroud JP, Han J (2004) Design method for geogrid-reinforced unpaved roads. Part I—development of design method. J Geotech Geoenviron Eng 130(8):775–786
8. Giroud JP, Noiray L (1981) Geotextile reinforced unpaved road design. J Geotech Eng Div ASCE 107(9):1233–1254
9. Hufenus R, Rueegger R, Banjac R, Mayor P, Springman SM, Bronnimann R (2006) Full-scale field tests on geosynthetic reinforced unpaved roads on soft subgrade. Geotext Geomembr 24(1):21–37
10. Kamel MA, Chandra S, Kumar P (2004) Behaviour of subgrade soil reinforced with geogrid. Int J Pavement Eng 5(4):201–209
11. Shukla SK (2016) An introduction to geosynthetic engineering. CRC Press, London
12. Singh M, Trivedi A, Shukla SK (2019) Strength enhancement of the subgrade soil of unpaved road with geosynthetic reinforcement layers. Transport Geotech 19:54–56
13. Subaida EA, Chandrakaran S, Sankar N (2009) Laboratory performance of unpaved roads reinforced with woven coir geotextiles. Geotext Geomembr 27:204–210
14. Williams ED, Okine AKO (2008) Effect of geogrid in granular base strength-an experimental investigation. Constr Build Mater 22:2180–2184

Semi-active Control Strategy for Horizontal Dynamic Loading on Wall Retaining Granular Fills

Nisha Kumari and Ashutosh Trivedi

Abstract Dynamic control of smart structures has drawn significant attention in the past decades. Estimation of stress–strain response is essential to access safety and serviceability of smart structure by introducing the sensors and actuators under dynamic loading. The self-actuating and self-diagnostic properties of sensors and actuators control the vibration functions of smart structure. This paper evaluates semi-active control strategy for retaining wall with horizontal dynamic loading. The stress–strain response of retaining wall-PZT system consists of retaining wall interfaced with a PZT patch between the wall and granular backfill have been analyzed. The variation of stress–strain response with modulus ratio of retaining wall and PZT patch is presented graphically. A model is presented to examine the effect of retaining wall-PZT system on vibration induced in retaining structure due to horizontal dynamic loading compared with vertical loading condition.

Keywords Dynamic loading · Stress–strain analysis · PZT patch · Retaining wall

1 Introduction

Recently, the dynamic techniques using semi-active control strategy have become popular worldwide due to its application in reality structures. The semi-active control strategy can be implemented by using the PZT system. It can be achieved by providing a force or displacement that acts in the opposite direction to the original force and displacement. A new method of control aims to make use of piezoelectric ceramics which is a special type of material that utilizes the piezoelectric effect. The piezoelectric effect is an energy transformation acting in such a way that a mechanical deformation causes the rearrangement of the positive and negative

N. Kumari (✉)
Delhi Technological University, Delhi, India
e-mail: nishasoni.ce@gmail.com

A. Trivedi
Civil Engineering Department, Delhi Technological University, Delhi, India
e-mail: atrivedi@dce.ac.in

V. S. Kanwar and S. K. Shukla (eds.), *Sustainable Civil Engineering Practices*,
Lecture Notes in Civil Engineering 72,
https://doi.org/10.1007/978-981-15-3677-9_8

charge within a material. To understand the dynamics of smart structure, the effect of natural frequency of structure, acceleration and displacement have been studied by many researchers. According to the concept of vibration control in a dynamic system, some mechanical properties such as stiffness ratio and mass ratio may be adjusted to minimize the dynamic effect of loads under an acceptable level.

There are two methods adopted to control the structural vibration for retaining structures: by using retaining wall-PZT system and by the use of implements, namely dampers, isolators and actuators for the building. In this study, PZT patch has been used as smart material between the retaining wall and backfill to control the horizontal dynamic load on retaining wall. The stress–strain behavior of retaining wall has been analyzed for various width ratios of PZT and backfill and modulus ratio of PZT and backfill. This is also used stress–strain behavior of composite beam [4] and retaining wall for vertical dynamic loading [3] by considering the modulus of material and thickness of PZT patch.

The objective of this paper is to investigate the behavior of retaining wall composed of granular fill with PZT patch. This study is focused to obtain the average stress and average strain equations for horizontal dynamic loading on retaining wall with PZT patch (Eqs. 5–8). The influence of width and modulus of material has also been numerically evaluated by considering the granular sand as backfill. The effect of modulus ratio on stress and strain curve has been plotted to show the variation between the quantities (Figs. 2, 3, 4 and 5).

2 Stress–Strain Analysis

In this study, a rigid retaining wall of height (h) has been considered. A PZT patch is provided between the retaining wall and granular backfill as shown in Fig. 1. Dynamic loading considered to be applied in the horizontal direction normal to the PZT patch. The width of retaining wall, PZT patch and backfillis are b_R, b_P and b_S, respectively. It is assumed that the contact among retaining wall, PZT patch and granular fill is perfect, and there is no shear moment or separation at the interface. The deformation of retaining wall-PZT system is assumed to be elastic with the consideration of linear elasticity. Table 1 consists of the properties of hard and soft PZT material. The stress inlayer of retaining wall, PZT and backfill is the product of strain and elastic modulus of respective layers. Strain in the layer would depend on the parameters such as frequency coefficient, elastic stiffness and location of neutral surface of retaining wall-PZT system (Table 2).

Assume that the retaining wall-PZT system is under pure bending, that is, displacement in z-direction is zero. In pure bending, stress–strain relationship can be expressed as,

$$\sigma = \mathrm{E}\varepsilon \tag{1}$$

where E, σ and ε is elastic modulus of material, stress and strain, respectively.

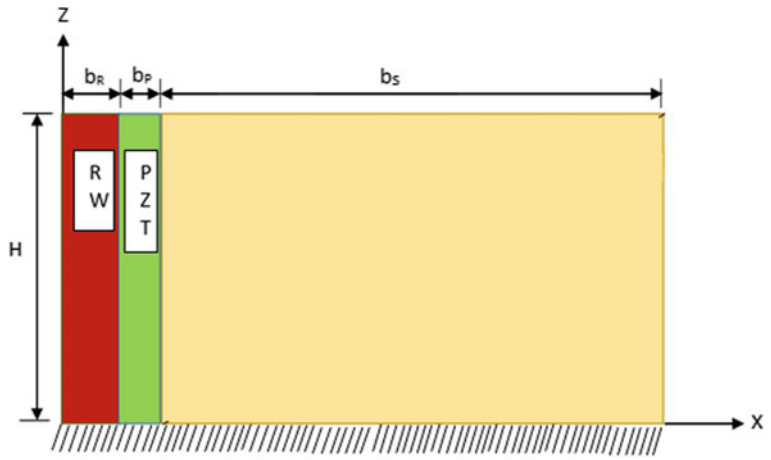

Fig. 1 Schematic of retaining wall bounded with PZT

Table 1 Mechanical properties of PZT[a]

Property	Symbol	Unit	Hard PZT	Soft PZT
Frequency coefficient	N_p	Hz-m	2190–3150	1960–2250
Elastic compliance coefficient	S^E	10^{-2} m^2/N	11.1–14.3	15.0–20.7
Elastic stiffness coefficient	C^D	10^{10} N/m^2	13.6–16.6	10.0–11.1
Mechanical quality factor	Q_m	–	250–2000	50–100

[a]Foley et al. [2]

Table 2 Application of PZT in civil engineering structures

Field	Application
Energy production[a]	Power generated floor, Japan, 2006 Underneath of highway, Israel, 2009
Vibration damping[a]	Used as controller in active structural acoustic control (ASAC), Germany
Sensors[a]	Health monitoring of civil structures As piezoelectric accelerometer in different civil structures
Retaining walls[b]	Application of semi-active control strategy for wall retaining granular fills

[a]Aktan et al. [1], [b]Kumari and Trivedi [3]

The strain of the retaining wall composed of granular fill with PZT patch is expressed as,

$$(\varepsilon)_{\text{avg}} = \frac{M\left(\overline{X} - X\right)}{E_P I_P + E_R I_R + E_S I_S} \tag{2}$$

where $(\varepsilon)_{\text{avg}}$ represents the average strain, M is bending moment of retaining wall-PZT system, X is distance from the neutral axis in x-direction and $\overline{X}$ is location of neutral surface of composite retaining wall. E_P, E_R and E_S is elastic modulus of PZT patch, retaining wall and backfill, respectively. I_P, I_R and I_S is moment of inertia about centroid of PZT patch, retaining wall and backfill, respectively.

For the composite structure with PZT as shown in Fig. 1, we define the ratio of width of PZT and retaining wall (μ), ratio of width of retaining wall and PZT (a), ratio of modulus of PZT and modulus of backfill (n) and ratio of modulus of retaining wall and modulus of PZT (b). That is

$$n = \frac{E_P}{E_S} = \text{Modulus ratio of PZT over backfill}$$

$$\mu = \frac{b_P}{b_S} = \text{Width ratio of PZT over backfill}$$

$$a = \frac{b_R}{b_P} = \text{Width ratio of retaining wall over PZT}$$

$$b = \frac{E_R}{E_P} = \text{Modulus ratio of retaining wall over PZT}$$

The distance between centroid of PZT and neutral axis is expressed as,

$$\left(\overline{X} - X_P\right) = b_S\left[\frac{3\mu + 2 - 12a^2b\mu^2n}{24\mu n(ab+1)+1}\right] \tag{3}$$

The distance between the centroid of the backfill and neutral axis is expressed as,

$$\left(\overline{X} - X_S\right) = -b_P\left[\frac{\mu n\left(3ab - 6a^2b - 6ab\right) - 2n(ab-1)}{12\mu n(ab+1)}\right] \tag{4}$$

By substituting the Eq. (3) into Eq. (2), the average strain for PZT layer is expresses as,

$$(\varepsilon_p)_{\text{avg}} = \frac{36M}{E_S h b_S^2}\left[\frac{(3\mu + 2 - 12a^2b\mu^2n)[24\mu n(a+b)+1]}{\left[3n\mu^3(1+ba^3)+1\right][24\mu n(a+b)+1]^2 + 18\left(3\mu + 2 - 12a^2b\mu^2n\right)[2\mu n(1+ab)+1]}\right] \tag{5}$$

Similarly, by substituting Eq. (4) into Eq. (2), the average strain for backfill layer expressed as,

$$(\varepsilon_s)_{\text{avg}} = \frac{-36M}{E_s h b_s^2}\left[\frac{\left[12\mu^2 n(ab+1)\right]\left[\mu n(3ab-6a^2b-6ab)-2n(ab-1)\right]}{\left[3\mu^3 n(1+ba^3)+1\right][12\mu n(ab+1)]^2} + 18\mu^2\left[\mu n(3ab-6a^2b-6ab)-2n(ab-1)\right]^2[2\mu n(1+ab)+1]\right] \quad (6)$$

The average stress for PZT layer is expressed as,

$$(\sigma_p)_{\text{avg}} = \frac{36nM}{hb_s^2}\left[\frac{(3\mu+2-12a^2b\mu^2n)[24\mu n(a+b)+1]}{\left[3n\mu^3(1+ba^3)+1\right][24\mu n(a+b)+1]^2+18\left(3\mu+2-12a^2b\mu^2n\right)[2\mu n(1+ab)+1]}\right] \quad (7)$$

The average stress for backfill layer is expressed as,

$$(\sigma_s)_{\text{avg}} = \frac{-36M}{hb_s^2}\left[\frac{\left[12\mu^2 n(ab+1)\right]\left[\mu n(3ab-6a^2b-6ab)-2n(ab-1)\right]}{\left[3\mu^3 n(1+ba^3)+1\right][12\mu n(ab+1)]^2} + 18\mu^2\left[\mu n(3ab-6a^2b-6ab)-2n(ab-1)\right]^2[2\mu n(1+ab)+1]\right] \quad (8)$$

3 Results and Discussion

The retaining wall bounded with PZT patch normal to the horizontal dynamic loading was analyzed based on stress–strain relationship. Numerical analysis carried out for PZT layer and granular backfill layer. Equations (5) and (7) represent the average stress–strain for PZT layer respectively. Similarly, Eqs. (6) and (8) represent the average stress–strain for backfill layer depending on the width ratio μ and modulus ratio n. The material used as backfill for analysis is well-graded dense sand. The elastic modulus of dense sand is taken as 250 MPa [5].

Figures 2 and 3 are the strain plots showing the effect of modulus ratio (n) on the strain for PZT layers and backfill layer with four different width ratios (μ) for horizontal dynamic loading.

The height of retaining wall (H) used in analysis is 10 m. The value of modulus of backfill (E_S) and bending moment (M) used in numerical computation of stress–strain for various modulus ratios is $E_S = 250$ MPa and $M = 100$ Nm, respectively. From Eqs. (5)–(7), the value of width ratio of retaining wall over PZT (a) and modulus ratio of retaining wall over PZT (b) also affect the stress–strain behavior of retaining wall-PZT system. In this study, value of $a = b = 2.5$ is used as shown in Table 3.

Figures 2 and 3 represent the strain in the PZT and the backfill with modulus ratio, and when modulus ratio of PZT and backfill (n) is not wide-ranging, the average strain in PZT layer is much larger than that in backfill. It can be observed that from Figs. 2

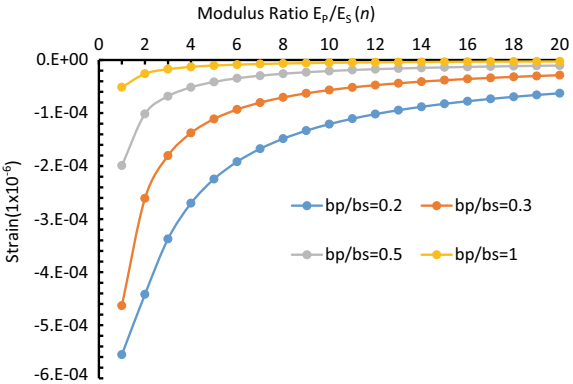

Fig. 2 Variation of average strain with modulus ratio (n) for PZT layer at varied width ratio (μ)

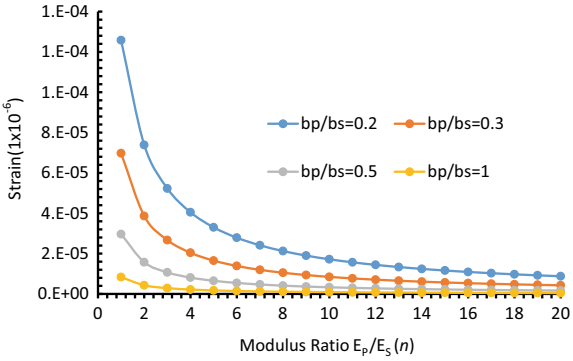

Fig. 3 Variation of average strain with modulus ratio (n) for backfill layer at varied width ratio (μ)

Table 3 Geometric and material properties used in the present study

Property	Symbol	Values
Height of retaining wall	h	10 m
Elastic modulus of backfill	E_S	250 MPa
Bending moment	M	100 Nm
Width ratio of PZT over retaining wall	a	2.5
Modulus ratio of PZT over retaining wall	b	2.5
Width ratio of PZT over backfill	μ	0.2, 0.3, 0.5 and 1
Modulus ratio of PZT over backfill	n	1–20

and 3, average strain decreases with increase in modulus ratio (n) in both PZT layer and backfill layer. For width ratio (μ) = 1, the strain in PZT layer and backfill is equal but with opposite sign. The convention has been adopted such that tension is positive and opposite in compression.

Figures 4 and 5 show the effect of modulus ratio (n) on the stress for PZT layers and backfill layer with four different width ratios (μ) for horizontal dynamic loading. Stress plots are obtained from Eqs. (7) to (8) for PZT layer and backfill layer, respectively.

It is observed from Fig. 4 that the variation of stress in PZT layer and the variation of stain in PZT layer do not have the same trend as shown in Figs. 2 and 4. Figure 4 presented that for width ratio (μ) 0.5 and 1 the stress is constant for modulus ratio (n). Figure 5 shows that the average stress in backfill layer monotonously decreases with increases in modulus ratio (n). It is observed from Figs. 3 and 5 that variation of strain in backfill layer and stress in backfill layer has the same trend. Figures 6 and 7 show the variation of average strain and stress of PZT layer with modulus ratio of PZT over backfill due to vertical dynamic loading [3].

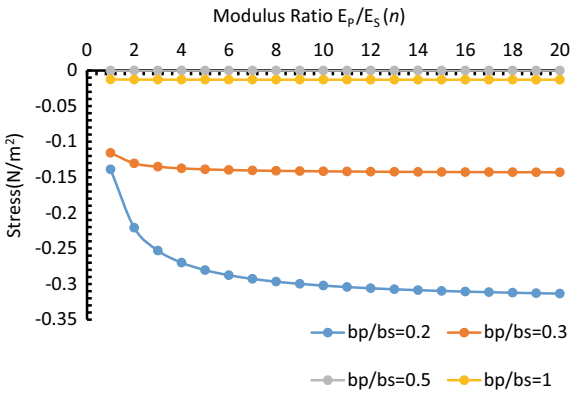

Fig. 4 Variation of average stress with modulus ratio (n) for PZT layer at varied width ratio (μ)

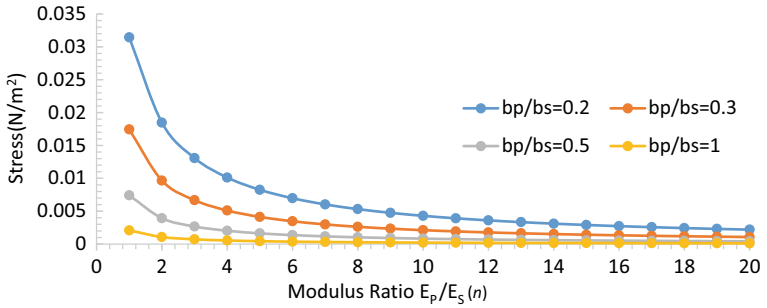

Fig. 5 Variation of average stress with modulus ratio (n) for backfill layer at varied width ratio (μ)

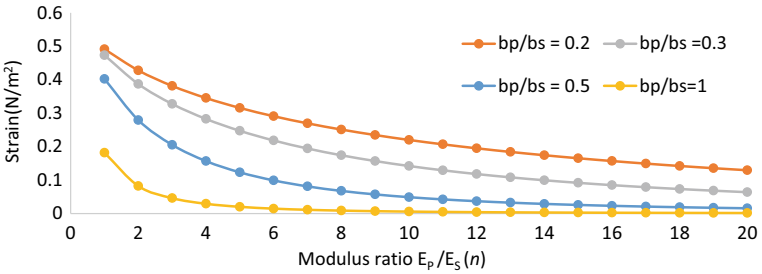

Fig. 6 Average strain in PZT due to vertical loading [3]

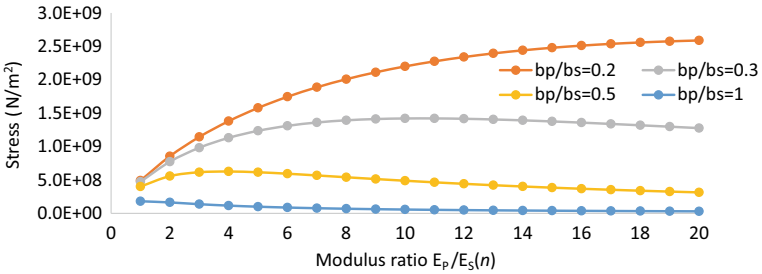

Fig. 7 Average stress in PZT with modulus ratio [3]

4 Conclusions

In this paper, a retaining wall-PZT system was analyzed. The stress–strain equations were obtained through the numerical method for horizontal dynamic loading. According to the results obtained from this study, we draw the following conclusions:

- Stress–strain analysis is performed for varied modulus ratio (n) with four width ratios (μ).
- The relationship of strain with modulus ratio for various width ratios is concave and the relationship stress with modulus ratio for various width ratios is convex. This is due to distance between the centroid of PZT and neutral surface changes with width ratio (μ) increases. For the width ratio (μ) greater than 0.3 variation of stress become constant with variation of modulus ratio (n). The increase of modulus of PZT affect the trend of stress variation.
- The average strain in backfill layer and stress in backfill layer has the same trend of variation, since they are related by constant modulus of backfill (E_S) due to horizontal dynamic loading.
- The average strain in PZT layer decreases and stress in PZT layer increases when modulus ratio of PZT over backfill increases in case of vertical dynamic loading. It is concluded that position of PZT patch in smart structure significant influences the stress–strain behavior.

The present study concluded that the properties of material and geometrical dimensions of the retaining wall-PZT patch have noteworthy influence on the stress–strain behavior of retaining wall-PZT system. The results found in this study are useful in designing of smart structures consisting with PZT patch.

References

1. Aktan AE, Helmicki AJ, Hunt VJ (1998) Issues in health monitoring for intelligent infrastructure. Smart Mater Struct 7(5):674
2. Foley BM, Wallace M, Gaskins JT, Paisley EA, Johnson-Wilke RL, Kim JW, Mckinstry ST, Hopkins PE, Ihlefeld JF (2018) Voltage-controlled bistable thermal conductivity in suspended ferroelectric thin-film membranes. ACS Appl Mater Interf 10(30):25493–25501
3. Kerboua M, Benguediab M, Megnounif A, Benrahou KH, Kaoulala F (2014) Semi active control of civil structures, analytical and numerical studies. Phys Proc 55:301–306
4. Kézdi Á, Rétháti L (1974) Handbook of soil mechanics, vol 1. Elsevier, Amsterdam, p 249
5. Kumari N, Trivedi A (2018) Application of semi-active control strategy for the wall retaining granular fills. In: Proceedings of China-Europe conference on geotechnical engineering, Springer, Cham, pp 978–982

Utilization of Polymers in Improving Durability Characteristics of Open-Graded Friction Course Layer: A Review

Sakshi Sharma and Tripta Kumari Goyal

Abstract Open-graded friction course is a pavement layer laid as a surface course over the dense bituminous macadam layer in flexible pavements. This layer is characterized by a uniform gradation of aggregates, lesser quantity of fines and filler material and higher binder content as compared to conventional hot mix asphalt mixes. The structure of layer thus obtained has large percentage of air voids. The most important benefit lies in upgraded surface drainage as a result of its open-graded structure. The present study intends to give a censorious review of the various problems associated with open-graded friction course and the remedial measures that have been taken in order to tackle these problems in the past. In addition to this, the study also intends to confer some alternative solution to improve the service life of the OGFC pavement which is beneficial to the environment as well as helps in reducing the cost incurred in making an effort to improve the issues of durability and draindown.

Keywords Open-graded friction course · Durability · Sustainable · Polymer · Raveling

1 Introduction

Open-graded friction course (OGFC) has been used in the USA since the middle of the twentieth century for various advantages it imparts to pavements. It comprises a skeleton of uniform size aggregates, minimal amount of fines and higher concentration of bitumen, thus yielding a thin and highly permeable pavement layer. As these mixes have a very less quantity of fine aggregates, the percentage of air voids in the structure is quite high as compared to traditional hot mix asphalt mixes. The ability of pavement to resist heavy loads and carry them without suffering permanent deformation is an attribute imparted by the aggregate skeleton of OGFC layer. In

S. Sharma (✉) · T. K. Goyal
Punjab Engineering College, Chandigarh 160012, India
e-mail: sakshi12109@gmail.com

T. K. Goyal
e-mail: triptagoyal@pec.ac.in

V. S. Kanwar and S. K. Shukla (eds.), *Sustainable Civil Engineering Practices*,
Lecture Notes in Civil Engineering 72,
https://doi.org/10.1007/978-981-15-3677-9_9

addition to this, OGFC layer imparts many positive characteristics to the pavement like high infiltration rate, better traction enhanced surface reflectivity and instant noise reduction. Since OGFC is designed as an open mix, the interconnecting voids present in the structure are responsible for quick and efficient drainage of water in case of heavy rainfalls [1]. The storm water dissipates vertically downwards through the open-graded structure onto an impermeable layer and then flows laterally to the edge of the pavement. Thus, it contributes significantly toward reduction of splash and spray of water and minimization of hydroplaning. The open-graded structure of the layer absorbs sound energy produced at the road surface by movement of vehicles, thereby minimizing the noise levels generated from the pavement surface. Open-graded paving mixtures are light in weight and can cover more surface area in contrast to conventional paving mixes.

One of the most crucial factors in determining economical viability of a new pavement construction method is the service life of pavement. It has been observed that providing an OGFC pavement is 30–35% costlier than providing conventional dense-graded layer due to requirements of extra mix components, additional equipment, increased production temperatures and slower production rates [2]. However, this cost is balanced when whole life cycle costs are considered. According to a survey carried out in six states in the USA, pavements made with open-graded mixes were found to last minimum 19 months longer than conventional pavements and hence proved to be a cost-effective alternative [3]. Performance of OGFC pavements depends on three prime factors: quality of construction, mix design and climate of the region where the pavement is to be provided.

2 Literature Review

Based on visual distress surveys of OGFC roads in different states of America in the 1960s, it was established that the most common problem encountered by these pavements was raveling. The raveling and shoving potential of OGFC mixes was further found to accentuate by extreme hot conditions during the summer of 1980. Due to elevated temperatures, liquid asphalt cement was found to flow downward in the OGFC and the upper layer suffered scarcity of binder, thus making it more susceptible to raveling. Apart from raveling and shoving, detailed pavement damage survey also indicated the presence of other distresses like blistering, slippage, stripping, rutting, loss of texture and delamination of mix immediately below the OGFC layer. Hence, the Department of Transportation of many states reconsidered usage of OGFC on pavements during the early 1980s. However, with good design and construction practices, vast improvements were observed in OGFC pavements [1]. Since OGFC mixes are highly sensitive to temperature variations, it was ensured that ambient temperature be maintained while producing and laying OGFC pavement. It was observed that 80% of the roads built under controlled conditions met with standard OGFC specifications and reported a service life of eight years or more.

To take care of the distresses encountered during the service life of OGFC pavements, DoTs of various Unites States introduced different types of additives which have successfully led to performance enhancement of roads [4]. The ability of asphalt to coat the aggregates was increased by using mineral fibers. Introduction of rubberized asphalt ensured better durability in terms of raveling and shoving. Incorporation of hydrated lime enabled the construction of OGFC pavements in relatively dry areas with freezing temperatures by reducing the stripping of binder from aggregate surface.

The DoT of Georgia (1993) investigated intrusion of moisture into the pavement and accordingly revised the mix design procedure for OGFC layer. The new mix design procedure involves a coarser gradation, use of polymer modified asphalt binder and stabilizing fibers for increased permeability and rut resistance. Use of polymer modifiers and fibers has also enabled laying of OGFC mixes at higher temperatures, thus eliminating the need of maintaining ambient temperature conditions. As a result of these modifications, typical service life of OGFC pavements increased from 8 years to 12 years in Georgia.

Oregon Department of Transportation (ODoT) was one of the first to use OGFC on pavements in the USA in the 1930s. The thickness of OGFC course was kept one and a half inches or less; however, due to issues of durability, rich spots and draindown, ODoT was forced to slow down their usage of OGFC. In 1981, a new mix design procedure was adopted known as Type F mix which used relatively thicker pavements and bigger sized aggregates. As a result, this mix had percentage air voids ranging from 14 to 18%, thus providing better stability and efficient drainage.

OGFC layer was laid in Arizona first in 1954 to improve skid resistance, appearance and rideability. There was a continuous change in gradation of the mix over the years, and the gradation adopted at present lays emphasis on using a single-size aggregate. In the 1980s, reflective cracking was observed on most of the OGFC roads. So Arizona Department of Transportation (ADoT) started modifying hot asphalt with 9–10% crumb rubber in 1988, and this proved successful in addressing the issues of reflective cracking, durability and excessive noise due to tire–pavement interaction. However, this modification increased the cost of OGFC pavements by about 80%, thus allowing its usage only where benefits are more desirable than economics of construction.

New York DoT evaluated the performance of two 7-year-old pavements in 1982 to study the issues faced by traffic traversing these pavements on a daily basis. Traffic volume was used to determine the extent up to which pavement frictional characteristics were improved by OGFC layer. It was observed that wet weather accidents reduced by 61% in case of OGFC pavements as compared to dense-graded pavements. This observation justified the use of OGFCs at wet weather accident sites.

In Europe, the research work on OGFC or porous asphalt pavements has been carried out by contractors instead of the road agencies or DoTs because the contractors in European countries have a close working relationship with centralized authorities of national road agencies. In the 1990s, porous mixes were laid as thick surface course in which coarse gradation with larger top-size aggregate were used.

These pavements encountered severe problems of durability and asphalt draindown and required urgent modification in the mix design procedure. This led to the incorporation of additives in the form of fibers and polymer modifiers in asphalt so as to achieve thicker film coatings and higher asphalt cement content in the mix. The new mix design has same aggregate skeleton as that of stone matrix asphalt mixes excluding the fines. Use of mineral or cellulose fibers was done to prevent the migration of liquid asphalt. This mix design has surfaced better than old design in tackling the issue of draindown and raveling.

Apart from modifications in mix design procedure of OGFC pavements, proper periodic maintenance of pavements laid with OGFC mixes are necessary. All the surface treatments depend on the size and severity of failure. Localized distresses like small cracks and potholes are treated by sealing and patching with dense-graded mix without compromising the surface permeability. Expansive distresses like raveling are treated by milling the existing top layer and overlaying with new OGFC mix.

3 Use of Waste Polymers: A Sustainable Solution

As discussed in the literature above, use of polymers to improve properties of binder increases the cost of pavement by approximately 40%. Due to this reason, highway engineers and contractors are reluctant to use OGFC layer over the existing pavement surface in spite of its numerous advantages. OGFC layers are being used only in those areas where there is absolute necessity and pavements are not able to function without it. So, a more economic solution is required to encourage highway engineers to use open-graded friction course layers.

India is a developing country accounting for approximately 17% of the total population of the world. With the advancement in technology in various fields, the amount of waste polymers to be disposed off is increasing day by day. The different types of polymeric wastes include worn out tyres, soles of shoes, flip flops, discarded carry bags, water bottles, electric fittings and packaging material [5]. These waste products can either be deposited into landfills, incinerated or disposed into large water bodies. However, all of these methods of waste disposal are harmful for the environment and people residing in these areas.

Hence, incorporation of waste polymers in road construction can prove to be an eco-friendly solution for its disposal and can particularly provide an economic solution for improving durability characteristics of OGFC pavements [6]. The use of this innovative technology apart from strengthening road construction will also create a source of income by generating employment for people. Waste plastic has been used in road construction in the past and has proven successful in providing longer fatigue life to roads. However, OGFC roads specifically require stiff binder so as to enhance resistance to cracking and abrasion [7]. Stiffness of binder can be increased by modification with waste polymers in powdered form.

Table 1 Sources of waste polymers

Type of polymer	Source
Low-density polyethylene (LDPE)	Sacks, carry bags, bottles, milk pouches
High-density polyethylene (HDPE)	Household articles, caps of bottles, carry bags
Polyethylene terephthalate	Drinking water bottles
Polypropylene (PP)	Food packaging, bottle caps, microwave trays
Polystyrene	Food trays, egg boxes, disposable cups, protective packaging
Polyvinyl chloride (PVC)	Mineral water bottles, credit cards, toys, pipes, electric fittings, medical disposables

4 Methodology

The polymers primarily used in modification so as to improve the physical properties of bitumen have been listed in Table 1. Waste plastic HDPE, LDPE, PP, crumb rubber can be easily procured from local scrap plastic supplier since these are tremendously consumed by majority of the population in day-to-day life. When these plastics are added into bitumen, various differentiating results have obtained. The addition of this waste is determined by means of weight % of bitumen.

Modification of binder is done by wet process in which powdered waste polymer is directly added to bitumen and the mix is heated to a temperature of 160 °C [8]. Attainment of this temperature is necessary so as to ensure proper dispersion of waste polymer into the binder and hence guarantee a uniform blend of materials. This mix is cooled to a temperature of 120 °C, and then, aggregates are added in the paddling chamber. If the aggregates are added to modified bitumen at 120 °C, air pockets might get formed into small gap of aggregate which reduces the strength of the roads and increases probability of rutting of roads. The process of modification of bitumen by waste polymers has been represented pictorially in Fig. 1.

Experimental studies on modification of bitumen with waste polymers have been carried out to suit the Indian climatic conditions using VG-30 bitumen. Polymers like polyethylene (in shredded form), HDPE plastic waste strands, LDPE plastic waste and crumb rubber powder have been used in percentages varying from 2 to 8% keeping the weight of bitumen constant. Variations in the characteristic properties of bitumen for different waste polymer modifications are given in Tables 2, 3, 4 and 5.

5 Conclusions

- The issue of enhanced cost of construction can be taken care of by using waste polymers in binder modification. This modification provides dual benefits in terms of improving the durability characteristics of OGFC pavements as well providing

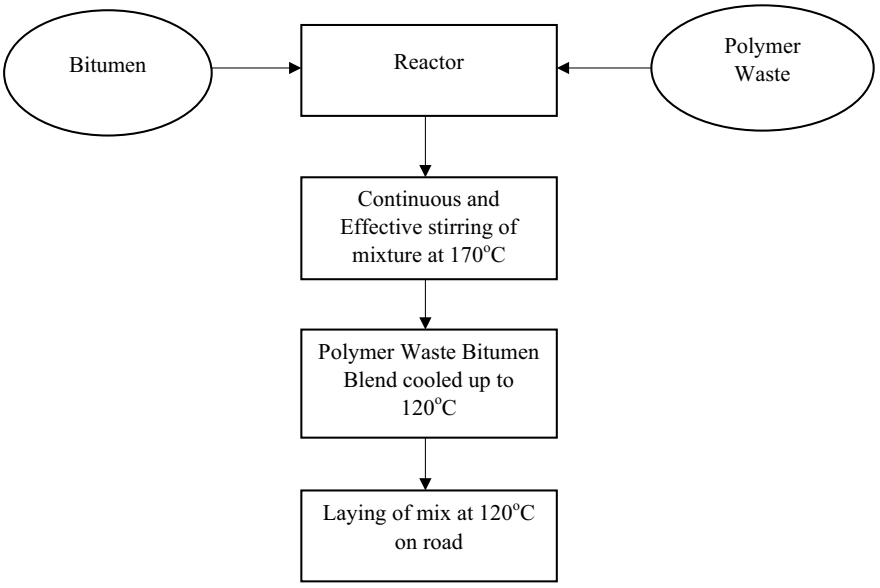

Fig. 1 Process of modification of bitumen with polymer additives

Table 2 Modification of bitumen with polyethylene

% Weight of polyethylene	Bitumen (g)	Penetration (mm)	Ductility (cm)	Softening point (°C)
0	200	69	75	42
2	200	68.5	70	43
4	200	63	65	54
6	200	58	63	56
8	200	44	57	62

Table 3 Modification of bitumen with HDPE plastic waste

% Weight of HDPE waste	Bitumen (g)	Penetration (mm)	Ductility (cm)	Softening point (°C)
0	200	69	75	42
2	200	68	68	48.2
4	200	66.3	63	52.5
6	200	62	58	55.3
8	200	46	48	60.5

Table 4 Modification of bitumen with LDPE plastic waste

% Weight of LDPE waste	Bitumen (g)	Penetration (mm)	Ductility (cm)	Softening point (°C)
0	200	69	75	42
2	200	66	69	47
4	200	64	66	51
6	200	60	64	53
8	200	48	58	57

Table 5 Modification of bitumen with crumb rubber

% Weight of crumb rubber	Bitumen (g)	Penetration (mm)	Ductility (cm)	Softening point (°C)
0	200	69	75	42
2	200	68.9	74.5	42
4	200	68.2	74.2	44
6	200	67	74.8	45
8	200	61	74.6	45.3

an alternative for efficient method of disposal of ever-increasing plastic waste reserve of the country.

- Bitumen modification with crumb rubber can be effectively carried up to 6% as further increase in percentage of crumb rubber yields a nonuniform mix which affects the surface of the pavement.
- HDPE waste plastic was not dispersed uniformly in bitumen at percentages greater than 4%. Further increase in HDPE loading led to reduced ductility of bitumen.
- The addition of LDPE waste exhibited similar results as that of HDPE modification.
- Crumb rubber and HDPE waste polymer in conjunction exhibited optimum results at 8% loading after which the properties of bitumen fall considerably. Hence, maximum amount of polymer waste that can be added to bitumen is 8%.
- The cost of using fresh polymers in binder modification can be entirely eliminated by using waste polymers, and burden of waste disposal by incineration or into landfills can be considerably reduced. Thus, it provides added benefit to the environment in terms of reducing pollution. The problem of raveling and rutting of roads can also be tackled effectively as modified binder forms thick coating around the aggregates and reduces the binder stripping potential.

References

1. Cooley LA, Mallick RB, Kandhal PS, Watson DE (2000) Design, construction and performance of new-generation open-graded friction courses. In: Proceedings of the annual meeting of the association of asphalt paving technologists, Reno, Nevada, March 13–15, 2000
2. Hanson DI, Shuler S (1990) Improving durability of open-graded friction courses. Transp Res Rec 11(1):35–41
3. Shankar AR, Suresha SN, Varghese G (2008) A comparative study on properties of porous friction course mixes with neat bitumen and modified binders. Constr Build Mater 23(2):1211–1217 (Elsevier)
4. Taylor GJ (2014) Open graded friction courses (OGFC). http://www.info@cedengineering.com
5. Haron HE, Musa EA (2014) Effect of the low density polyethylene carry bags waste on the asphalt mixture. Int J Eng Res Sci Technol 3:2
6. Nemade SN, Thorat PV (2013) Utilization of polymer waste for modification of bitumen in road construction. Sci Rev Chem Commun 3(4):198–213
7. Molenaar JMM, Molenaar AAA (2000) An Investigation into the contribution of the bituminous binder to the resistance to ravelling of porous asphalt. In: 2nd Eurasphalt and Eurobitume Congress, Barcelona, Spain, pp 500–508
8. Al-Orami S, Hassan HF, Taha R (2005) Evaluation of open-graded friction course mixtures containing cellulose fibers and styrene butadiene rubber polymer. J Mater Civ Eng—ASCE 7(3):416–422

Laboratory Study on the Effect of Plastic Waste Additive on Shear Strength of Marginal Soil

B. A. Mir

Abstract The shear strength of marginal soils can be enhanced by means of stabilization methods using various additives or waste materials. Among various waste materials, plastic bottles and carry bags are tremendously used and thrown away as a waste material onto the ground, which being non-biodegradable material pollutes the environment. Therefore, for an eco-friendly and sustainable environment, there is a dire need for proper use of plastic waste as an admixture in various engineering applications. In this paper, investigation has been carried out to enhance the engineering characteristics of Campus soil by randomly mixing with the plastic strips/chip of different aspect ratios and proportions (0.25, 0.75, 1 and 1.5%) by weight of dry soil. A series of laboratory tests consisting of compaction, CBR and shear strength tests were conducted on composite samples. The test results showed that the addition of 1% plastic waste material with aspect ratio of 3 enhanced the shear strength and California bearing ratio (CBR) of the Campus soil. It was also concluded that base course thickness of a road pavement can be significantly reduced if plastic waste strips are used as soil stabilizing agent for sub-grade material for flexible pavements in highway sub-base construction.

Keywords Marginal soils · Waste materials · Soil stabilization · Sustainable environment

1 Introduction

Plastic waste is being increased many-fold day by day due to rapid increase in industrialization and its peculiar characteristics such as leak proof and light weight. The plastic bottles of transparent polyethylene terephthalate (PET) material are commonly used for mineral water, soda waters, soft drinks, oil containers, etc. The large quantity of plastic waste is generally produced in the form transparent polyethylene terephthalate (PET) bottles, low-density polyethylene (LPDE) bags, high-density

B. A. Mir (✉)
Department of Civil Engineering, National Institute of Technology Srinagar, Srinagar, J&K, India
e-mail: p7mir@nitsri.net

V. S. Kanwar and S. K. Shukla (eds.), *Sustainable Civil Engineering Practices*,
Lecture Notes in Civil Engineering 72,
https://doi.org/10.1007/978-981-15-3677-9_10

(a) Types of plastic wastes

(b) Disposal and environmental problems imposed by plastic wastes

Fig. 1 Types of plastic wastes and disposal problems

polyethylene (HDPE) containers and bottles, polypropylene (PP) foil bags, expanded polystyrene (EPS) sheets, food containers and wrappers, PVC and plastic bags used for transport and packing materials, etc. (Fig. 1a). However, plastic wastes are non-biodegradable and pollute the environment causing severe health problems (Fig. 1b). Therefore, there is a dire need for scientific use of this non-biodegradable waste in various geotechnical applications for sustainable environment. This plastic waste can be used as source material for thermal insulation.

Among various plastic wastes, the bottled water is the fastest growing beverage industry in the world and about more than 2 million tons of plastic is used to bottle water every year [15]. Thus, the huge quantity of plastic waste not only requires lot of land for its disposal, but also pollutes the environment. Therefore, there is a dire need for characterization of such waste materials for improvement of marginal soil deposits to be used either as foundation medium or as an engineered construction material for building various infrastructures. Thus, for a sustainable development of environment, there is dire need for proper use of plastic waste as an additive in various engineering applications. Unlike other additives such as fly ash, fibre reinforcement and human hair [8, 18–20, 24, 26], plastic waste has also been a promising material to improve locally available marginal soils as well as enhances the properties of stabilized soils [21]. Many researchers (e.g. Ghavami et al. [14], Consoli et al. [9, 10]) have concluded that plastic waste in the form of polyethylene terephthalate fibre

when added to marginal soils improved the engineering properties significantly. Peddaiah et al. [23] investigated the effectiveness of polyethylene terephthalate (PET) in improving the behaviour of silty sand and concluded that the engineering properties were considerably improved. They further concluded that both shear strength parameters increased using roughed surface plastic strips. Similar results were also reported by Nsaif [22] and Mercy Joseph et al. [16]. Dutta and Rao [13] have reported that adding LDPE strips to locally marginal soils increased load bearing capacity of soil to support design maximum loads. Choudhary et al. [11] used high-density polyethylene (HDPE) for improvement of weak soils to enhance the engineering properties of sub-grade soil. Thus, the weak/marginal soils could be significantly improved effectively admixed with plastic wastes. Therefore, in this paper, an attempt was made to utilize waste plastic bottle (PET bottle) strips/chips by randomly mixing with clayey soil to investigate the suitability of plastic waste as an additive for stabilization of marginal soils.

2 Environmental Issues and Sustainability Aspects

Environment is lifeline of livelihood for all living species and any sort of exploitation with its resources will imbalance life cycle of all living species. Since due to rapid urbanization and increase in population, lot of waste material is produced every day. If the waste material is not disposed off scientifically, it will create severe health and environmental problems. Since the environmental issues are multidimensional and dynamic, researchers, designers and engineers should adopt sustainable engineering practices, which can meet the human aspirations and needs for natural environmental balance and effective waste material management and utilization.

3 Materials

3.1 Soil Samples

In the present study, soil samples were collected from three locations in the Institute Campus (henceforth termed as Campus soil). At each site, soil samples were collected, sealed and transported with utmost precaution for studying their in situ properties. All the required tests on undisturbed and disturbed (remoulded) soil samples were conducted base on Codal procedures (IS 2720 part 3 (10, 4, 6, 7, 10 & 16) [1–7]).

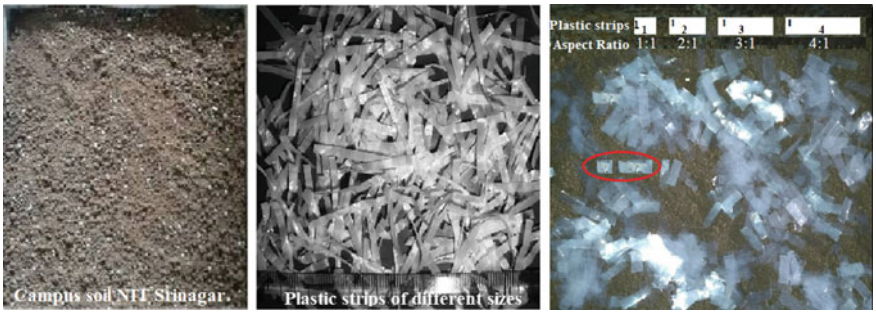

Fig. 2 Soil and plastic material used in the study

3.2 Plastic Material

In this study, the plastic material was collected from solid waste disposal site of NIT Srinagar Campus. It was mainly low-density polyethylene (LDPE).

4 Experimental Program and Methodology

In this study, all the basic tests were conducted on the untreated Campus soil as per standard codal procedure (IS 2720). After analysing the test results, the weakest sample was chosen out of three samples tested for stabilization with plastic waste. The plastic strips were cut into lengths of 10 mm (aspect ratio: AR = 1:1), 20 mm (AR = 2:1), 30 mm (AR = 3:1) and 40 mm (AR = 4:1) as shown in Fig. 2. During testing of composite test specimens, it was ensured that there is no boundary influence and the plastic strips deform freely. The plastic strips were added by weight of dry soil in different proportions so as to achieve an optimum plastic content for stabilization of marginal soils. The CBR and strength tests were carried out at different plastic strip contents of 0.25%, 0.75%, 1% and 1.5% by weight of dry soil, respectively.

5 Test Results and Discussions

5.1 Physical and Index Properties of Campus Soil

The soil samples collected from three locations were analysed as per IS 1470-1948. The specific gravity tests of these soil samples were carried out as per IS 2720-part 3. A series of trials were taken on the three samples, and the average values of specific gravity are 2.60 for JH, 2.62 for JKB and 2.61 for MED sites, respectively. It was observed that the test specimens exhibit lower specific gravity than standard value

of 2.65 for natural soils. The soil grading (IS 2720-part 4) for Campus soils was carried out as per standard codal procedures (Fig. 3). From Fig. 3, it is observed that the Campus soil is fine-grained dominated by silt content. Atterberg limits such as liquid limit, plastic limit and shrinkage limits for the Campus soils were determined in accordance with IS 2720-part 5. From the test results, the Campus soil is classified as clayey soil with medium plasticity. It is also seen that the soil collected from Jhelum Hostel (JH) site is weaker than other two soil samples having higher rate of loss of shear strength (Fig. 4).

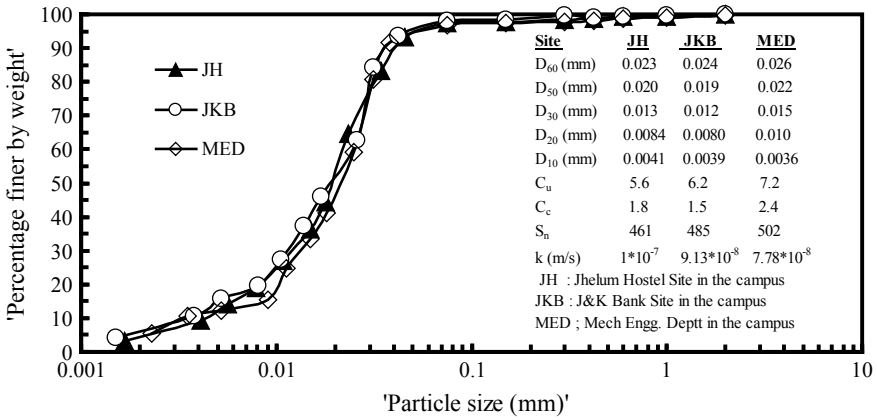

Fig. 3 Particle size distribution curves for Campus soils, NIT Srinagar

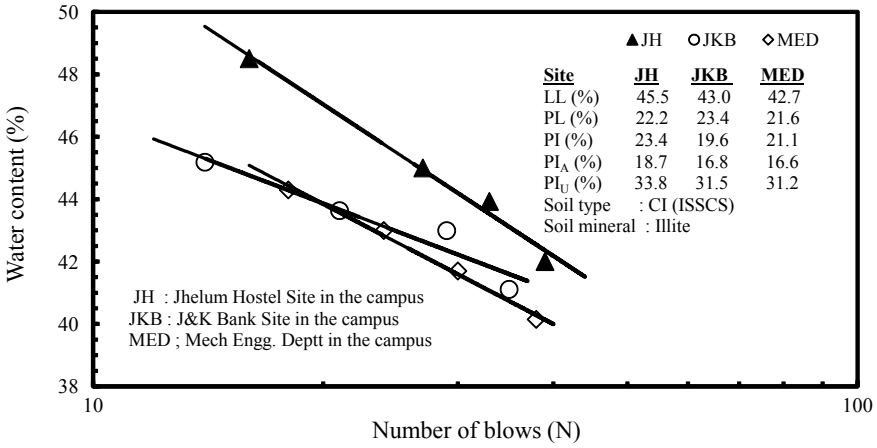

Fig. 4 Flow curves for Campus soils, NIT Srinagar

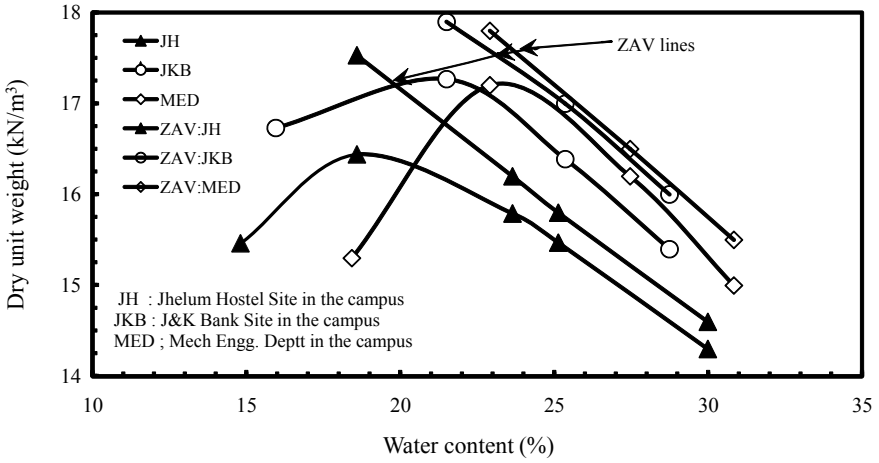

Fig. 5 Compaction curves for Campus soils, NIT Srinagar

5.2 Compaction Characteristics of the Campus Soil

The standard compaction tests were conducted to determine the compaction characteristics such as optimum moisture content (OMC) and the maximum dry unit weight (MDU) for all the three soil samples (JH, JKB and MED) (IS 2720-part 7) as shown in Fig. 5. From Fig. 5, the values of optimum moisture content and maximum dry unit weight obtained are 19%, 21.7%, 23.6% and 16.4 kN/m^3, 17.2 kN/m^3, 17.1 kN/m^3, respectively. Since the dry unit weight is relatively less as expected for stable soil deposits (generally >17.5 kN/m^3), the soil need to be improved for sustainable construction of infrastructures.

5.3 Effect of Plastic Stabilization on California Bearing Ratio (CBR)

Among the available methods of design of flexible pavements, the California bearing ratio (CBR) method is the most reliable method of evaluating the strength of the sub-grade material [17]. In this study, plastic strips were blended with the soil and then mixed thoroughly until homogeneous mix was obtained. A series of unsoaked and soaked CBR tests were conducted on plastic stabilized soil samples and the load penetration curves are shown in Figs. 6 and 7, respectively. From Fig. 6a, it is observed that unsoaked CBR increases with the addition of plastic strips in different proportions and aspect ratios. The test results showed that maximum value of CBR is obtained for an optimum plastic content of 1% with an aspect ratio of 3:1. On increasing aspect ratio beyond 3, the CBR values decreased. This may be attributed

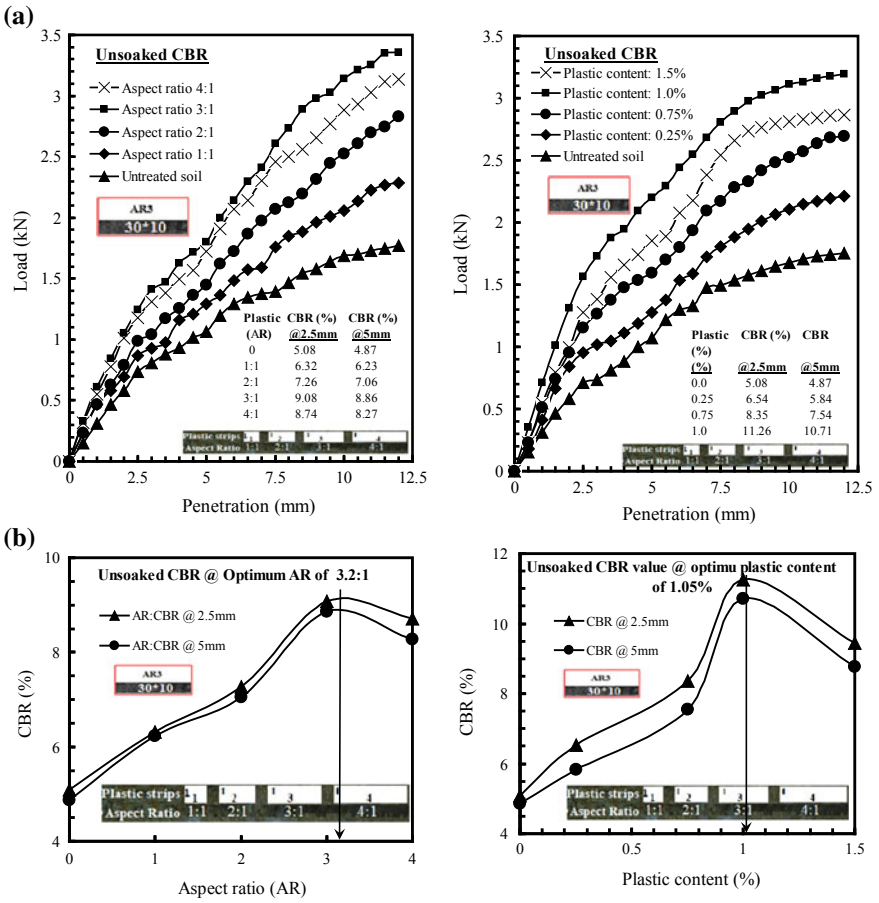

Fig. 6 **a** Unsoaked CBR curves for stabilized campus soil, NIT Srinagar. **b** Variation of unsoaked CBR with aspect ratio and plastic content

due to the fact that plastic strips interaction is more slippery than soil–soil interaction. The higher aspect ratio of plastic strips results in decrease of frictional resistance and hence lowers CBR of composite soil. The variation of unsoaked CBR with aspect ratio and plastic content is shown in Fig. 6b. Similar trend is observed for soaked CBR tests as illustrated in Fig. 7a, b. Similar results have also been reported by Craig and Khire [12], Mir [17] and Rawat and Kumar [25].

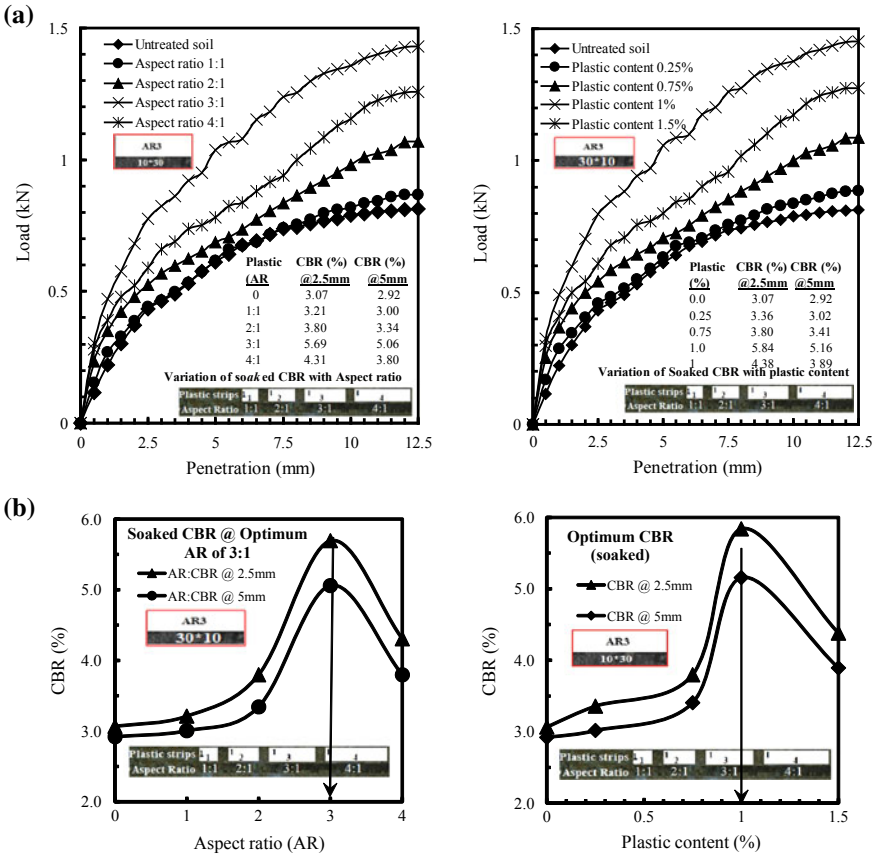

Fig. 7 **a** Soaked CBR curves for stabilized campus soil, NIT Srinagar. **b** Variation of soaked CBR with aspect ration and plastic content

5.4 *Effect of Plastic Waste Content on the Unconfined Compressive Strength*

In this paper, the unconfined compression tests were conducted on plastic admixed soil specimens as per IS 2720-part-10 for "Immediate" test series under a constant strain rate of 0.625 mm/min. In both cases, the composite test specimens of height 7.6 cm and diameter 3.8 cm were prepared by statically compacting the mixtures in a mould at 0.95 $\gamma_{d\max}$ and corresponding water content dry side of optimum. The effect of increasing plastic content with aspect ratio of 3 on stress–strain behaviour of composite soil specimens is illustrated in Fig. 8. From test results, it is seen that the unconfined compressive increases with addition of plastic content. The test results showed that the maximum value of UCS is obtained for 1% plastic content with an aspect ratio of 3:1. On increasing plastic content 1%, the UCS values decrease.

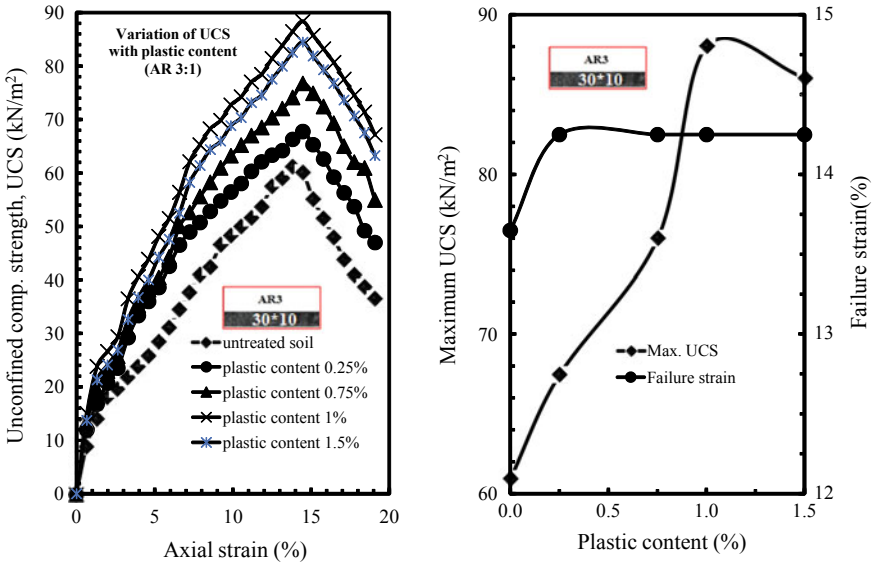

Fig. 8 Variation of unconfined compressive strength with plastic content

However, there is a negligible effect on failure strain, which remains constant with increasing plastic content. This may be attributed due to the fact that plastic strips crossing the failure plane increase and resistance towards the deformation of soil along the failure plane enhances the failure strain.

6 Conclusions

Based on the test results and discussions, the following conclusions can be made:

1. The CBR values of the Campus soil are significantly altered by the addition of plastic waste material in the form of different proportions and aspect ratios.
2. The extent of variation depends on the aspect ratio and the plastic content. A proper mix proportion improves the CBR and shear strength values.
3. It has been observed that 1% of plastic content with an aspect ratio of 3 is the optimum amount required to maximize the CBR and shear strength of the Campus soil.
4. The thickness of sub-grade can be reduced significantly by way of mixing soils with suitable amount of LDPE strips.
5. Thus, a marginal soil with the proper quantity of plastic waste is recommended for use in various geotechnical works for sustainable environment and cost-effective infrastructures.

Future Scope of Work

For complete characterization of marginal soils and stabilization with plastic waste material as an additive, further tests such as permeability, consolidation and triaxial tests need to be performed to study the final behaviour of plastic reinforced soil.

References

1. Bureau of Indian Standards (1970) IS 1498: classification and identification of soils for general engineering purposes. Bureau of Indian Standards, New Delhi
2. Bureau of Indian Standards (1980) IS 2720-part 3(1): determination of specific gravity of fine grained soils. Bureau of Indian Standards, New Delhi
3. Bureau of Indian Standards (1985) IS 2720-part 4: determination of grain size distribution. Bureau of Indian Standards, New Delhi
4. Bureau of Indian Standards (1985) IS 2720-part 5: determination of Atterberg limits. Bureau of Indian Standards, New Delhi
5. Bureau of Indian Standards (1980) IS 2720-part 7: determination of water content-dry density relation using light compaction. Bureau of Indian Standards, New Delhi
6. Bureau of Indian Standards (1979) IS 2720-part 16: laboratory determination of CBR. Bureau of Indian Standards, New Delhi
7. Bureau of Indian Standards (1986) IS 2720-Part 10: laboratory tests procedure for unconfined compressive strength test. Bureau of Indian Standards, New Delhi
8. Butt WA, Mir BA, Jha JN (2016) Strength behaviour of clayey soil reinforced with human hair as a natural fibre. Geotech Geol Eng 2016(34):411–417
9. Chouksey SK, Babu GLS (2011) Stress-strain response of plastic waste mixed soil. Waste Manage (New York NY) 31(3):481–488
10. Consoli NC, Montardo JP, Prietto PDM, Pasa GS (2002) Engineering behaviour of a sand reinforced with plastic waste. J Geotech Geoenviron Eng ASCE 128(6):462–472
11. Choudhary AK, Jha JN, Gill KS (2010) A study on CBR behaviour of waste plastic strip reinforced soil. Emir J Eng Res 15(1):51–57
12. Craig HB, Khire MV (1994) Reinforcing sand with strips of reclaimed high density polyethylene. Jr Geotech Eng 120(5):838–855
13. Dutta R, Rao GV (2004) Ground improvement with plastic waste. In: Proceeding 5th international conference on ground improvement technique, Kaulalumpur, Malaysia, pp 321–328
14. Ghavami K, Filho R, Barbosa P (1999) Behaviour of composite soil reinforced with natural fibres. Cement Concr Compos 21:39–48
15. Maurya R, Kumar U (2015) Utilization methods of polymer waste in geotechnical applications. Int J Sci Res Publ 5(10):1–7
16. Mercy Joseph P, Haneef FM, Jacob MT, Krishnan R, Rajan S (2014) Effect of plastic granules on the properties of soil. Int J Eng Res Appl 4(4):160–164
17. Mir BA (2005) Effect of dredged material on the CBR behaviour of fine grained soils. In: Proceedings of international conference on structural and road transportation engineering (START 2005). Elite Publishing House Pvt Ltd., New Delhi, pp 542–550
18. Mir BA, Sridharan A (2013) Physical and compaction behaviour of clay soil–fly ash mixtures. Geotech Geol Eng 31(4):1059–1072
19. Mir BA (2015) Some studies on the effect of fly ash and lime on physical and mechanical properties of expansive clay. Int J Civil Eng Trans B: Geotech Eng-Geotech 13(3&4B):203–212
20. Mir BA, Sridharan A (2019) Mechanical behaviour of fly ash treated expansive soil. In: Proceedings of the institution of civil engineers-ground improvement, vol 172, no 1. ICE-UK, pp 12–24

21. Muntohar AS (2009) Influence of plastic waste fibers on the strength of lime-rice husk ash stabilized clay soil. Civil Eng Dimens 11(1):32–40
22. Nsaif MH (2013) Behaviour of soils strengthened by plastic waste materials. J Eng Dev 17(4):182–194
23. Peddaiah S, Burman A, Sreedeep S (2018) Experimental study on effect of waste plastic bottle strips in soil improvement. Geotech Geol Eng 36(5):2907–2920
24. Puppala AJ, Musenda C (2000) Effects of fibre reinforcement on strength and volume change in expansive soils. Transp Res Rec TRB 1736(2000):134–140
25. Rawat P, Kumar A (2016).Study of CBR behaviour of soil reinforced with HDPE strips. In: Proceedings of Indian geotechnical conference IGC 2016. IIT Chennai, pp 1–4
26. Tang CS, Shi B, Gao W, Chen FJ, Cai Y (2007) Strength and mechanical behaviour of short polypropylene fiber reinforced and cement stabilized clayey soil. Geotext Geomembr 25:194–202

An Overview of Utilization of E-waste Plastic in Road Construction

Abhitesh Sachdeva and Umesh Sharma

Abstract Recent advancements in science and technology have produced uncontrolled electronic waste (E-waste) into the developing world. Illegitimate E-waste exports into India by developed countries have played key role in aggravating this problem. E-waste disposal is directly related to environmental deterioration. The countries which are on road to development see it as an issue of major concern. Therefore, there is a need to explore new innovative disposal techniques that are economically feasible and capable enough to deal with such huge rate of E-waste generation. The latest effort in this direction is about incorporation of E-waste plastic in pavement construction. Polymer obtained from discarded E-waste can be effectively used to enhance pavement durability and performance. The present study highlights overall E-waste management and recycling issues followed by a censorious review of various benefits and methods of using E-waste plastic as construction material. Utilization of E-waste plastic in road construction is an economical way to tackle environmental degradation, human health exploitation as well as in reducing the undue pressure on natural construction materials.

Keywords Environment · Management · Health and safety · Pavement design · Recycling and reuse of materials

1 Introduction

The twenty-first century witnesses everyday advancements in electronics, information and other technologies which motivate the users to replace these items in a very short period of time. E-waste is thus referred to the various electronic items such as computers, televisions, mobile phones, and others which either got exhausted, damaged or just discarded by the users. With such an alarming rate of generation, E-waste

A. Sachdeva (✉) · U. Sharma
Punjab Engineering College (Deemed to Be University), Chandigarh 160012, India
e-mail: sachdeva.abhitesh@gmail.com

U. Sharma
e-mail: umesh1651@gmail.com

V. S. Kanwar and S. K. Shukla (eds.), *Sustainable Civil Engineering Practices*,
Lecture Notes in Civil Engineering 72,
https://doi.org/10.1007/978-981-15-3677-9_11

accumulation has now emerged as one of the greatest concerns for the environmentalists from all over the world. Global estimation depicts about 50 million metric tons (MMT) of electronic waste generation per year which makes it an extensive part of the daily municipal waste [1]. Recent research concludes that accumulation of electronic waste in India has increased to around 30 lakh MT, and the current generation rate is around 18.5 lakh MT per year. Thus, the disposal of such huge quantities of E-waste has developed into a cumbersome issue. In usual practice, the methods adopted for disposing E-waste plastic are incineration, landfilling or disposal in water bodies [2].

E-waste comprises 50% metallic portion, 21% plastic, 10% nickel alloys, about 6% of solder scrap and about 13% of other nonferrous metals. The major polymers of electronic waste plastic are high impact polystyrene (HIPS) and acrylonitrile butadiene styrene (ABS) with certain percentage of polypropylene (PP) as shown in Fig. 1 [3]. The present work was carried to analyze the effect of utilizing E-waste plastic in bituminous as well as concrete mixes in order to tackle various problems such as overexploitation of natural aggregate reserves, increased traffic volume on roads, E-waste plastic disposal and at the same time to encourage sustainability in road construction. HIPS and ABS polymers have desirable engineering properties and therefore can be effectively used for fine aggregate replacement in both types of mixes [4]. However, E-plastic granules used for coarse aggregate replacement had high flakiness index and therefore do not provide enough interlocking and result in formation of weak mixes.

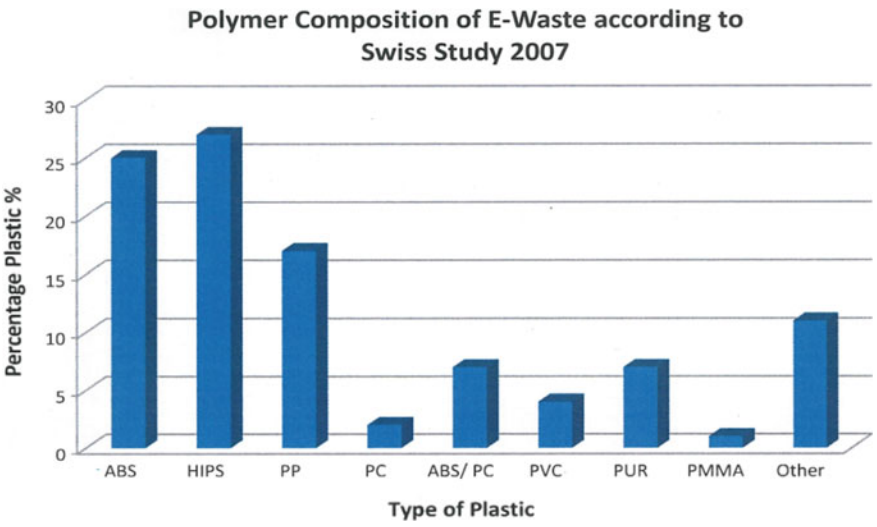

Fig. 1 Polymeric composition of E-waste

2 Utilization of E-waste Plastic in Road Construction

Extensive research has been carried out for a long time to develop alternative methodologies for efficient disposal of variety of polymers such as low-density polyethylene (LDPE) and high-density polyethylene (HDPE), polyethylene terephthalate (PET), polyvinyl chloride (PVC) and styrene-butadiene-styrene (SBS) [5]. Recently, researchers have tried to adopt similar methodologies for E-waste plastic. High rate of generation, ineffective recycling and poor disposal methods are the main factors that have led to the exploration of new methodologies for an effective E-waste plastic disposal [6]. Moreover, ongoing practices for E-waste plastic disposal like incineration and landfills have deteriorated the environment. Utilization of E-waste plastic in pavement construction seems to be an efficient disposal method because these polymers have high tensile strength, stiffness and considerable impact resistance [7]. This methodology can not only accommodate large quantities of E-waste plastic but also provide considerable improvement in pavement life and performance.

3 Benefits of Using E-waste Plastic in Road Construction

- Utilization of E-waste plastic in pavement construction can be an efficient alternative to tackle the issue of its disposal [8, 9].
- Evolution of such constructive disposal methodology will also motivate people to install more and more authorized E-waste recycling plants which in turn limits the involvement of unskilled workers [10].
- The incorporation of E-waste plastic in pavement construction reduces the consumption of bitumen as well as the haulage cost of material and can significantly enhance the Marshall Stability Value (MSV) and Marshall Quotient (MQ) of the bituminous mixes [11].
- Research studies have also highlighted the incorporation of E-waste plastic in concrete mixes as it produces a nonbearing lightweight concrete that may be used as concrete panels in facades [12].
- Modification with E-waste plastic contributes to impart ductility to conventional concrete mixes, which significantly enhances its ability to deform prior to failure [13].
- It also improves the chemical and corrosive resistance, ease of placement, longevity, low permeability and thermal stability of concrete mixes, thus encouraging the use of E-waste plastic-modified mixes for precast components, bridge deck overlays, artificial marble and as a repair material for concrete structures [13].

Table 1 Characterization of E-waste plastic

Characteristics	Value
Type	Crushed
Maximum size	20 mm
Specific gravity (20 mm)	1.1
Water absorption (20 mm)	0%
Fineness modulus of aggregates (above 20 mm)	7.59
Fineness modulus of aggregates (20 mm)	8.2
Fineness modulus of aggregates (below 20 mm)	9.18

4 Methodologies for Incorporation of E-waste Plastic

Method of material replacement has been a topic of great interest among research aspirants. E-waste plastic may be utilized as a replacement material for fine as well as coarse aggregates (in various percentages of the total quantity of cement) to form concrete mixes of desired strength [12]. Various physical properties of E-waste plastic aggregates which mark their suitability for use as stone aggregates are given in Table 1.

Utilizing E-waste plastic as a major component (coarse aggregate) and fly ash in the form of filler material can be another approach for preparation of concrete mixes. Both materials can be used in various percentages for replacing coarse aggregates and cement, respectively. Incorporation of E-waste plastic in Geopolymer concrete has proved to be beneficial in enhancing the mechanical properties of these mixes. Fine aggregates are replaced by nonmetallic fractions obtained from crushed printed circuit boards (PCBs), and various industrial waste products are used for cement replacement [14].

Modification of bitumen with E-waste plastic is an innovative technique to obtain superior modified binder. Bitumen is modified by adding E-waste plastic in powdered form in varying percentages to produce a modified binder having better adhesion properties [15, 16].

E-waste plastic can also be used in various bituminous mixes so as to increase the durability and performance of flexible pavements. Bituminous mixes are modified by partially replacing certain amount of coarse or fine aggregates with shredded E-waste plastic [11, 17].

5 Utilization of E-waste Plastic in Concrete Mixes

Modification of E-waste plastic significantly reduces various strength parameters of conventional concrete mixes. Various factors responsible for strength reduction are discussed below:

- In case of coarse aggregate replacement, the E-waste plastic granules do not have enough thickness and therefore are flaky in nature. Hence, the modified mix is not able to bear higher compressive, flexural and splitting tensile loads.
- The smooth texture of E-waste plastic granules reduces the cohesive strength of cement mortar. Due to the absence of frictional properties, the mortar is unable to stick firmly to the E-plastic granules, and thus on load application, it strips off easily which results in failure.
- There is a great possibility that shredded E-waste plastic granules do not have the desired shape to ensure sufficient aggregate interlocking. This may increase the overall percentage voids and therefore reduce the load-bearing capacity of the modified concrete mix.
- E-plastic is hydrophobic in nature and therefore has negligible water absorption. This affects the water–cement ratio, and hence, the modified mix is pulverulent in comparison with the conventional concrete mix.

Effect on strength parameters of E-waste plastic-modified concrete mixes:

(a) **Compressive Strength**

Use of E-waste plastic granules as a replacement material for coarse aggregates in concrete mixes results in a decrease in compressive strength. It has been observed that as the percentage of E-waste plastic is increased, the compressive strength of modified mixes decreases. However, the modified mixes do not show brittle failure as observed in conventional concrete mixes. The modified mixes deform significantly before the final failure. At 20% aggregate replacement in conventional M20 concrete mix, the compressive strength decreased by 52.89% [13].

(b) **Split tensile strength**

The modified mixes had lower split tensile strength as compared to the conventional concrete mixes. A decrease of 47.98% has been reported for E-waste plastic-modified mixes at 50% aggregate replacement in conventional M25 concrete mix [18]. However, the tensile property of E-waste plastic imparts ductility to the modified mixes. Due to this property, the modified mixes having higher percentage replacements show ductile failure [19]. The modified mixes have improved resistance to the splitting load as compared to the conventional mixes. In modified mixes, the failure occurs gradually, and therefore, specimens do not breakdown completely.

(c) **Workability**

Incorporation of E-waste plastic reduces the workability of conventional concrete mix. A decrease of 41.40% has been observed in the modified concrete mix with water–cement ratio of 0.5 and mix proportion of 1:1.4:2.4 [13].

(d) **Flexural strength**

A similar behavior is seen in the flexural strength of modified mixes. The strength reduces with increasing replacement percentages of E-waste plastic. The modified

mixes have lower flexural strengths, and failure is ductile in nature. A decrease of 42.89% in flexural strength has been observed in E-waste plastic-modified mixes [18].

6 Utilization of E-waste Plastic in Bituminous Mixes

Incorporation of E-waste plastic in conventional bituminous mixes improves all the strength parameters. The modified mixes are lighter in weight and therefore can help in reducing material haulage cost for any flexible road construction project.

7 Effect on Strength Parameters of E-waste Plastic-Modified Bituminous Mixes

(a) **Marshall Stability Value**

E-waste plastic-modified mixes have higher MSV as compared to the conventional bituminous mixes. The modified mix possesses improved resistance to distortion, shearing stresses. Therefore, these mixes are capable of taking much higher loads. The MSV of modified mix increases with increasing percentages of E-waste plastic replacement, attains a maximum value and then decreases [20]. Experimental studies have reported that at 3% coarse aggregate replacement and 5.5% bitumen content, the MSV of modified mix increases up to 70%. Similarly, at 8% fine aggregate replacement and 5.5% optimum bitumen content (OBC), the MSV of modified mix increases up to 185% [11].

(b) **Flow**

Flow value denotes the vertical deformation corresponding to MSV. The modified mixes have lower flow values, and it is observed that the flow value decreases with increasing percentages of E-waste plastic [11]. This indicates that the modified mixes have better resistance to plastic deformation as compared to the conventional bituminous mixes and therefore provide better performance characteristics during service life of the pavement.

(c) **Bulk density (γ_b)**

It is observed that the specific gravity of E-waste plastic being 1.06 is very less as compared to the conventional aggregates. Therefore, incorporation of E-waste plastic lowers the (γ_b) of modified mix. In comparison with the conventional bituminous mix, a decrease of 9.3% was observed in the (γ_b) of modified mix when 3% of coarse aggregates were replaced by E-waste plastic at 5.5% OBC. Similarly, at 8% fine aggregate replacement and 5.5% OBC, (γ_b) of modified mix was decreased by 11.60% [11].

(d) **Percentage air voids (V_a)**

A minimum percentage of air voids are necessary in all bituminous mixes so as to accommodate additional layer compaction by traffic loads and temperature variations. For both coarse and fine aggregate replacement, it is observed that with addition of E-waste plastic, (V_a) increases as compared to the conventional bituminous mix [11, 21].

(e) **Voids in mineral aggregate (V_{ma})**

V_{ma} is the pocket where bitumen gets deposited, and therefore, it is desirable to have only a minimum amount of (V_{ma}). Excess V_{ma} results in an uneconomical bituminous mix. Experimental studies have shown that E-waste plastic-modified mixes have lower V_{ma} in comparison with the conventional bituminous mix.

(f) **Voids Filled with Bitumen (V_{fb})**

It expresses the bitumen-void ratio of the bituminous mix. A certain percentage of V_{fb} is necessary to achieve a durable bituminous mix, but excess V_{fb} results in unreasonable bitumen consumption. Also, such a mix can over-densify and bleed under traffic loads. It is observed that E-waste plastic-modified mixes have lower percentage of V_{fb} as compared to the conventional bituminous mixes. As the percentage of E-plastic increases, the V_{fb} of modified mix decreases [11, 21].

8 Sustainability Aspects of Utilizing E-waste Plastic in Road Construction

From the literature review of various research articles, it can be inferred that utilization of electronic waste plastic in road construction is an economical way for handling E-waste management and disposal issues. The methodology is capable of accommodating huge amounts of E-waste plastic and thus will be efficient to curb the present hazardous methods of E-waste disposal. It has numerous benefits in motivating both government as well as corporate sectors to install more number of authorized E-waste collection and recycling centers. Therefore, it seems to be a brilliant way to handle environmental as well as human health exploitation [22].

9 Conclusions

- E-waste plastic can be effectively used as a modifier for conventional bituminous mixes to enhance their low as well as high temperature performances at optimum blending conditions. E-waste-modified bituminous mixes have increased viscosity, blending and mixing temperatures but are comparatively less rut susceptible.

- The use of E-waste plastic as aggregate replacement in bituminous mixes is a sustainable approach to tackle E-waste disposal problems. It improves pavement life and performance by increasing both MSV and MQ.
- Experimental studies have proved that incorporation of E-waste plastic as aggregate replacement in concrete mixes is only viable for lightweight nonbearing mixes as it significantly reduces various strength parameters.
- However, E-waste plastic can easily be used in certain geopolymer concrete mixes as it considerably enhances various mechanical properties of these mixes.
- It is found that incorporation of E-waste plastic in road construction is a very recent subject of research, and till date, very few studies have been conducted on this topic. Keeping all the benefits in mind, a comprehensive research is strongly recommended for further improvisation and advancement of methodologies by which this hazardous waste can be effectively utilized in construction of sustainable and durable pavements.

References

1. Geyer R, Jambeck JR, Law KL (2017) Production, use, and fate of all plastics ever made. Am Assoc Adv Sci 3(7):1–5
2. Awasthi AK, Awasthi MK, Li J, Wang M, Wang Z (2018) E-waste management in India: a mini-review. Waste Manage Res 36(5):408–414
3. Boni H, Buser A, Morf L et al (2009) Recycling of plastics from waste electrical and electronic equipment (WEEE)—tentative results of a swiss study. In: R'09 world congress, vol 2, no 13. Davos, Switzerland, pp 12–24
4. Anandhan S, Bandyopadhyay S, Bhowmick AK, De PP, De SK (2002) Novel thermoplastic elastomers based on acrylonitrile-butadiene-styrene terpolymer (ABS) from waste computer equipment and nitrile rubber. Rubber Chem Technol 76(5):1145–1163
5. Abdelaziz M, Niloofar KZ, Rehan KM (2012) A review of using waste and virgin polymer in pavement. Constr Build Mater 33:55–62
6. Espinosa DCR, Holuszko M, Kumar A (2017) E-waste: an overview on generation, collection, legislation and recycling practices. Resour Conserv Recycl 122:32–42
7. Adam AP, Goncalves JV, Robinson LC, Rosa LC, Schneider EL (2017) Recycling and mechanical characterization of polymer blends present in printers. SciELO 20(2):202–208
8. Kadam DB, Tapase A, Tapase R (2014) Performance evaluation of polymer modified bitumen in flexible pavement. J Environ Res Dev 8(3):504–509
9. Chidambaram R, Needhidasan S, Samuel M (2014) Electronic waste—an emerging threat to the environment of urban India. J Environ Health Sci Eng 12(1):113–121
10. Terazono SM, Abe N, Inanc B, Moriguchi Y, Sakai S (2006) Current status and research on e-waste issues in Asia. J Mater Cycles Waste Manage 8:1–12
11. Laxman PJ, Sopan BS (2017) Effect of E-waste plastic as aggregate replacement on marshall mix design of dense bituminous macadam. Indian Highw 8(1):51–59
12. Gavhane A, Patil P, Soni S, Sutar D (2016) Utilisation of e-plastic waste in concrete. Int J Eng Res Technol 5(2):594–601
13. Manjunath ABT (2016) Partial replacement of E-plastic waste as coarse-aggregate in concrete. Procedia Environ Sci 016(35):731–739
14. Li J, Lu H, Guo J, Xu Z, Zhou Y (2007) Recycle technology for recovering resources and products from waste printed circuit boards. Environ Sci Technol 41:1995–2000

15. Agar E, Hinislioglu S (2003) Use of high density polyethylene as bitumen modifier in asphalt concrete mix. Mater Lett 58(3):267–271 Elsevier
16. Colbert BW, You Z (2012) Properties of modified asphalt binders blended with electronic waste powders. J Mater Civ Eng-ASCE 24(10):1261–1267
17. Koushik K, Sarang G, Shankar AR (2013) Performance studies on bituminous concrete mixes using waste plastics. Highw Res J, Indian Roads Congr 6(1):1–11
18. Baskar K, Kumar KS (2014) Recycling of e-plastic waste as a construction material in developing countries. J Mater Cycles Waste Manag 17(4):718–724
19. Lakshmi R, Nagan S (2010) Studies on concrete containing e-plastic waste. Int J Environ Sci 1(3):270–281
20. Ranadive MS, Shinde MK (2012) Performance evaluation of E-waste in flexible pavement-an experimental approach. Int J Civ, Struct, Environ Infrastruct Eng Res Dev, Trans Stellar J Publ 2(3):1–11
21. Murugan L (2018) Use of E-plastic waste in bituminous pavements. Gradevinar 70(7):607–615
22. Brune MN, Fiona CG, Kristen G et al (2013) Health consequences of exposure to E-waste: a systematic review. Lancet Glob Health 1:350–361

Signal Coordination in Transportation Engineering by Using Microsimulation Tool

N. T. Imran and M. I. Nayyer

Abstract The growing advancement in the features of microsimulation models has encouraged their use in transportation engineering and planning. Traffic simulation models are a practical approach to analyse traffic operations. Traffic simulation models allow visualizing the existing or future traffic conditions and test strategies that would be difficult or impossible in roadway conditions. They also used to evaluate corridor improvement measures. The main objective of this study is to make improvements in the study corridor such that traffic congestion is relieved. The study aims to evaluate the present traffic conditions in the study corridor by using the microsimulation tool VISSIM. Data collection was done in the planning area which was used as input for the software. The corridor was first evaluated based on the present traffic conditions. After proper calibration, by considering average travel time as the calibrating parameter, the corridor was evaluated again by coordinating the signals along the corridor. Three different signal plans were done for signal coordination. The evaluation was done in terms of queue length, travel time and delay at intersections. All the three signal plans showed better results as compared to the present field condition.

Keywords PTV VISSIM software · Signal coordination · Corridor improvements

1 Introduction

Due to rapid urbanization and economic development, use of motorized vehicle has increased leading to road traffic congestion. Congestion above a certain limit results in an increase in travel time, thereby reducing mobility, accessibility and leading to loss of productivity and environmental degradation. The rapid increase

N. T. Imran (✉)
School of Civil Engineering, KIIT University, Bhubaneswar, India
e-mail: naziaimran.imran879@gmail.com

M. I. Nayyer
Department of Management Studies, Indian Institute of Technology Madras, Chennai, India
e-mail: ms17d004@smail.iitm.ac.in

V. S. Kanwar and S. K. Shukla (eds.), *Sustainable Civil Engineering Practices*,
Lecture Notes in Civil Engineering 72,
https://doi.org/10.1007/978-981-15-3677-9_12

in vehicle ownership accompanied by the growth of infrastructure has resulted in space constraint. It is necessary to design and manage transportation systems more efficiently while improving the use of the existing infrastructure. Signal coordination is one such measure which could be helpful in managing traffic. It is desirable to coordinate the pre-timed traffic signals of adjacent intersections such that platoons of vehicles can get through a number of intersections without being stopped. For this purpose, offset is used in addition to cycle length, phase sequence and phase duration to coordinate adjacent traffic signals.

Parikh [1] studied that the traffic signal retiming has proved to be a beneficial measure for improving traffic flow conditions and reducing fuel consumption. This research focuses on measuring CO_2 and NO_x from light-duty vehicles to verify the effectiveness of traffic signal synchronization as a measure for the reduction of emissions. Stevanovic and Martin [2] observed that various simulation models, when calibrated and validated, yield similar outputs for the current traffic conditions, but their estimates for future conditions, such as increased traffic, may vary significantly. Stevanovic and Martin [3] studied the effect of Sydney Coordinated Adaptive Traffic System (SCATS) that is installed by Utah Department of Transportation (UDOT) in Park City, Utah, on its network of 14 signalized intersections. The results showed the travel times, and delays on the major route in the Park City network were always shorter with SCATS control than with time of day (TOD) plans. Ofosu [4] evaluated the operating conditions of traffic control by retiming and coordinating the existing traffic signals. The new signal timing plans and coordination showed improvement in progression by 11% and on the coordinated segments, and there was a reduction in fuel consumption by 19–40%. Park and Chen [5] studied the benefits of coordinated actuated traffic signal systems by analysing before-and-after data. The analysis showed an improvement in the performance of the coordinated actuated system over the actuated isolated system (the before condition), including a 30% reduction in travel time.

Gomes et al. [6] provided the procedure for constructing and calibrating a detailed model of a freeway by using VISSIM. Authors concluded that with few and well-reasoned modifications to its driver behaviour parameters, the simulation model in VISSIM is capable of reproducing the field measured response on mixed flow lanes. Doina and Chin [7] observed that VISSIM has ability to display and visualize complex traffic flow in a graphical way. It is able to cope with the analyses of various traffic and transit operations under various conditions and also helpful in the assessment of impact on traffic in transportation planning when physical and operational alternatives are applied. Zhizhou et al. [8] found a suitable combination of VISSIM parameters for calibration. The authors observed that the average desired distance between stopped cars (CC0), the headway time (in second) that a driver wants to keep at a certain speed (CC1), and safety distance a driver allows before he intentionally moves closer to the car in front (CC2) were used specifically to calibrate the model. Further Jie et al. [9] described traffic characteristics that should be used for the calibration of parameters in VISSIM, includes saturation flow rates distributions, dependence of saturation flow rates on intersection characteristics, link speed

distributions, and speed—acceleration patterns. Patel et al. [10] suggested a methodology for the pre-timed signal coordination at the network level by adopting different phase plans to reduce the vehicular delay. Equal phase timings and proper selection of phase sequence can reduce delay considerably in signal coordination. For the closer intersections, a shorter cycle is more beneficial. Cunningham and Archer [11] described the construction, calibration and validation of a model using the VISSIM microsimulation software package. The methodology applied firstly included the definition of the modelling area and simulation scenario then data analysis (and data collection), followed by definition of output indicators for evaluation and analysis, network modelling, model calibration and model validation—analysis and comparison of simulation results. Finally, the authors observed that by increasing the levels of details in the input provides more accurate results and is more representative of model behaviour. Woody [12] focused on two elements associated with the calibration and validation process, i.e. calibration and validation methods for microsimulation traffic models and adjustment of calibration parameters for freeway models. Manjunatha et al. [13] proposed a methodology for calibrating a microsimulation model for mixed traffic. Calibration parameters were identified using multi-parameter sensitivity analyses, and the optimum values were obtained by minimizing the error between the simulated and field delay by use of genetic algorithm.

With the above literature review, traffic signal retiming emerges as an excellent solution to reduce the impact of traffic congestion. This study is taken up to identify the different signal coordination measures that can be implemented in the study area and further simulate and assess the impacts of signal retiming in the study area with a microscopic simulation model, VISSIM. Travel time, queue length and delay time are used as the performance measures.

2 Methodology

The study corridor where the study is to be carried out was selected. The corridor to be analysed was selected on the basis of the composition of traffic, the speed of traffic density and the traffic congestion conditions during peak hours. The selected corridor lies from Kazipet railway station junction to Nakkalagutta junction. This stretch consists of five intersections out of which two intersections were un-signalized, and rest were signalized. After the study area was selected, the next step was to collect data required for the model building process in VISSIM tool. The data included geometric element, traffic volume, existing traffic signals, average travel time and average speed. Geometric elements data included link length, road widths, lane width and the number of lanes. Likewise, in traffic volume, the data required were turning the movement of vehicles at all intersections, traffic volumes at morning and evening peaks and their vehicle compositions. Data needed for existing traffic signals include the position of signals at the intersections, phasing of the existing signals control and signal timings, which included cycle times and green times. The average travel

time was obtained by moving car observer method, and for average speed, spot speed surveys were carried out.

Once the data collection was done, the next step was to process the data, and data was used as input for VISSIM software. The network was built in VISSIM in which the first step was to load a Google map image and to scale it accordingly. Links and link connectors were then traced on this background image. The tracing of links and connectors should be done in such a way that they should match the actual field conditions. The next step in the model building was to give vehicle inputs for each leg. The vehicle input should be given at the beginning of each leg in the intersection, and also, the vehicle composition should also be mentioned in it. In vehicle composition, vehicle type, relative flow and desired speed were also mentioned. The next step was to give the corresponding routing decision and also provides vehicle input in each direction. The next step in the model building was to mention the conflicting areas in the network. Conflict areas are usually given for un-signalized intersections and also merging and diverging conflicts for the signalized intersection. Signal program at each intersection was defined based on the actual signal timings as observed in the field. Travel time sections were defined from the beginning of the corridor to the end of the corridor in both the directions. At each intersection, also the travel time sections and queue counters were mentioned. Queues are counted from the location of the queue counter on the link or connector upstream to the final vehicle, that is, in queue condition.

The model building process is followed by the calibration process. Calibration is defined as the adjustment of computer simulation model parameters to reflect prevailing conditions of the roadway network accurately. In the given study, average travel time to travel through the study corridor was selected as the calibration parameter. By using the Wiedemann 99 model, the parameters used to modify for calibration include CC0 (standstill distance), CC1 (Headway time) and CC7 (Oscillation acceleration). The simulation was run by varying the values of the above parameters. The present condition of the corridor was simulated, and the results obtained from the simulation were compared with the survey data. This process was continued until the simulated result and observed field result difference is obtained to be below 10%.

After the model calibration is done, the model replicates the actual field condition. The next step is to coordinate all the signalized intersection present along the corridor by three different signal plans and to see the impact of each plan over the travel time, queue length and delay time. Out of all the three signal plans, first, the signal is coordinated by simultaneous coordination, i.e. all the signals along a given street always display the same indication to the same traffic stream at the same time.

3 Results and Discussion

After the model building process and calibration process is complete, the next process is to make changes in the present corridor to increase its efficiency. By making the necessary changes in the model, the results obtained were determined in terms

of the average travel time, queue length and delay time. Comparisons were made between the present and modified conditions in terms of performance measures. This comparison showed better performance at the intersections for a decrease in travel time, queue length and delay times. Figure 1 shows a comparison of travel times in seconds which slightly decreases in all the intersections, and the average travel time decrease is found to be 20%. In Fig. 2, the queue length for each intersection

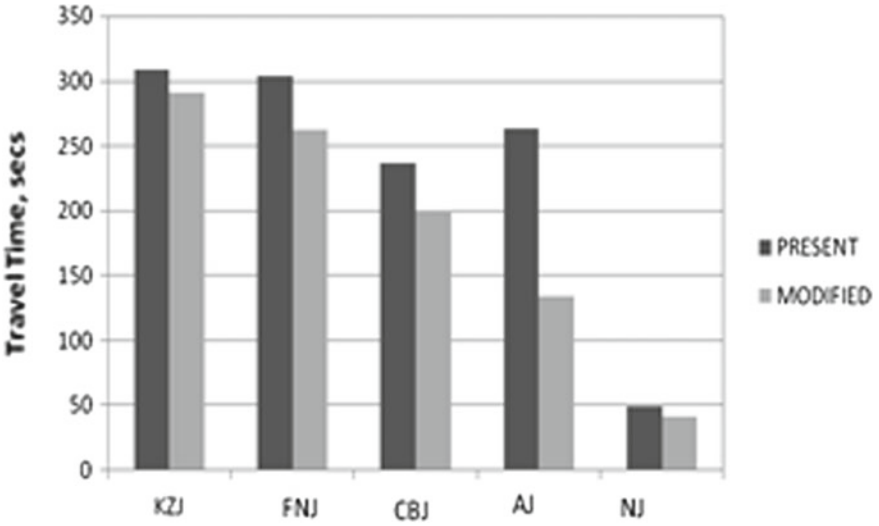

Fig. 1 Comparison of travel time after simultaneous coordination

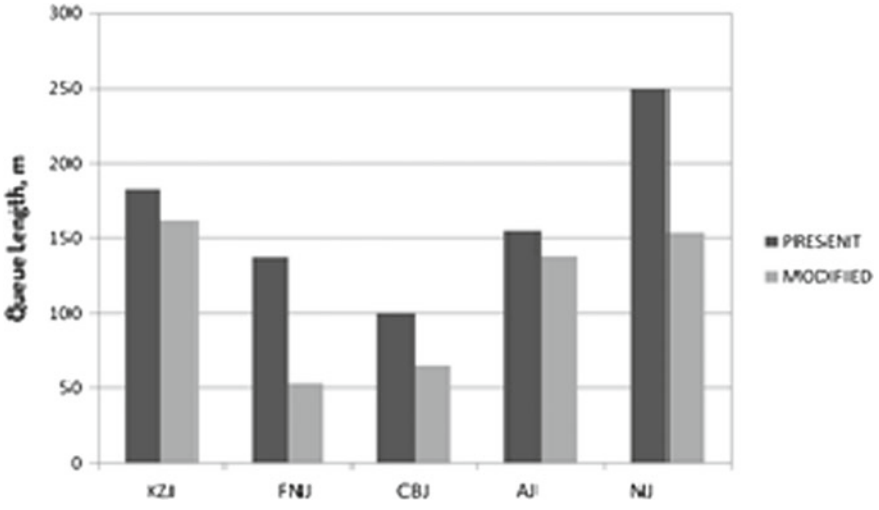

Fig. 2 Comparison of queue length after simultaneous coordination

decreases, and Fig. 3 also shows a decrease in the delay times for both the present and modified scenario at peak hour, and the average decrease is found to be 22%.

Next, the signals are then coordinated by simple progressive coordination, i.e. various signals along a street display green in such a manner so that continuous operation of platoons of vehicles along the street is possible. When the space-time diagram is drawn for this condition, 19s was observed as the bandwidth, and efficiency was calculated to be 23.75%. An efficiency of 40–50% is considered as good. So, the system is badly in need of retiming at least on the basis of bandwidth efficiency. Then, the signals were retimed according to the simple progressive coordination, and the comparison of the present and modified travel times in Fig. 4 showed a decrease in average travel time by 17.4%; delay times shown in Fig. 5 observed an average decrease in delay time as 20.36%. Figure 6 shows the decrease in queue lengths for all the intersections.

Finally, the signals along the corridor are coordinated by the third signal plan which is alternate signal coordination, i.e. consecutive signal installations along a

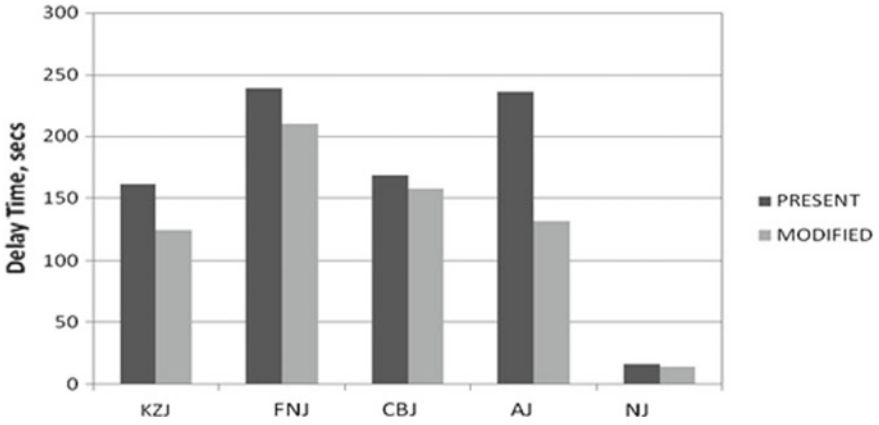

Fig. 3 Comparison of delay time after simultaneous coordination

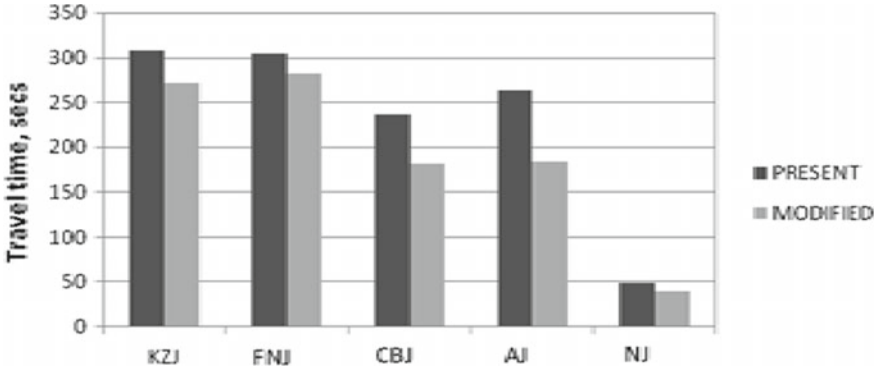

Fig. 4 Comparison of travel time after simple progressive coordination

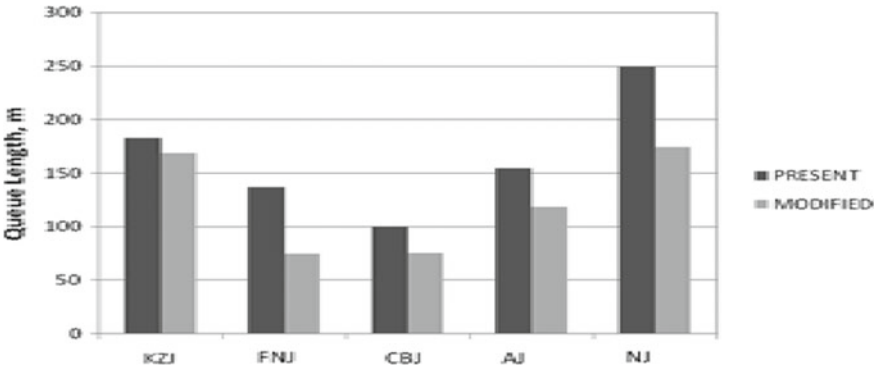

Fig. 5 Comparison of queue length after simple progressive coordination

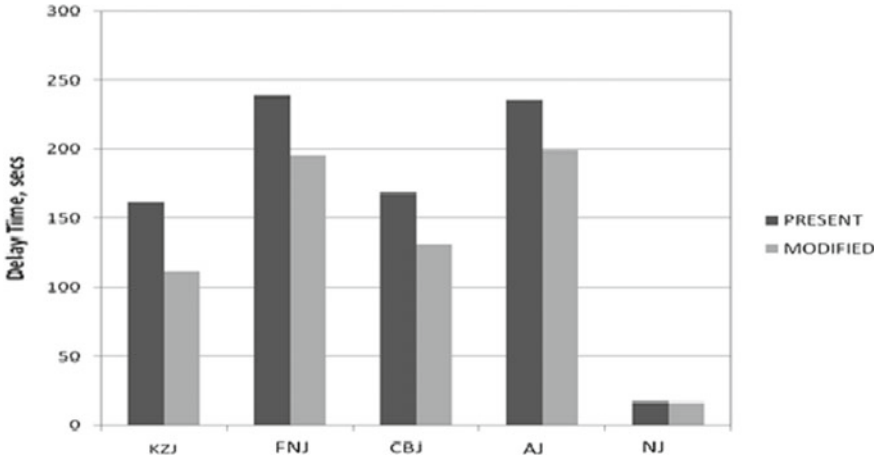

Fig. 6 Comparison of delay time after simple progressive coordination

given road show contrary indications at the same time. In this case, also the space-time diagram is drawn, and the bandwidth is observed as 33s. The bandwidth efficiency is calculated to be 41.85%. From Fig. 7, it is quite evident that the travel times are gradually decreasing in the case of modified signal timings. Hence, the impact of providing alternate signal timing is suitable for travel time evaluation. It leads to a decrease in the average travel time for the entire corridor by 26.92%. As seen from the graph in Fig. 8 almost at each intersection, there is a decrease in the queue length formation as compared to the present field condition. The queue length is decreased by about 41.27%. There is a substantial decrease in the delay times while travelling across the corridor, as shown in Fig. 9. The average delay times are also decreased by 34.90%.

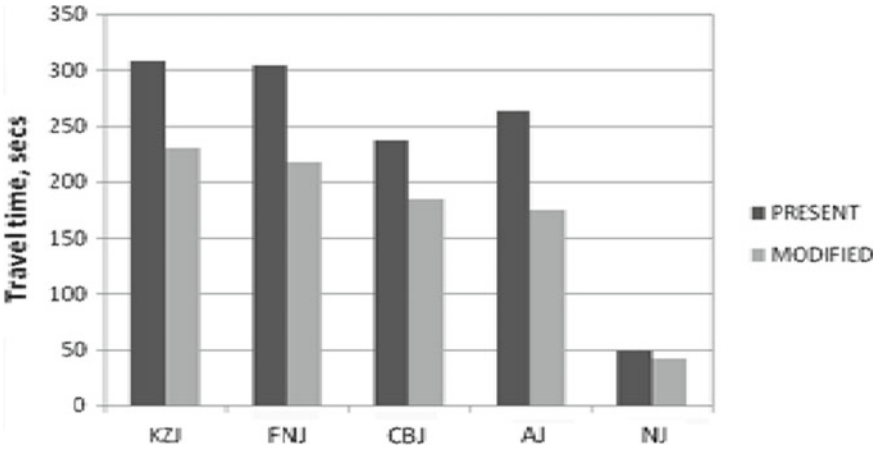

Fig. 7 Comparison of travel time after alternate coordination

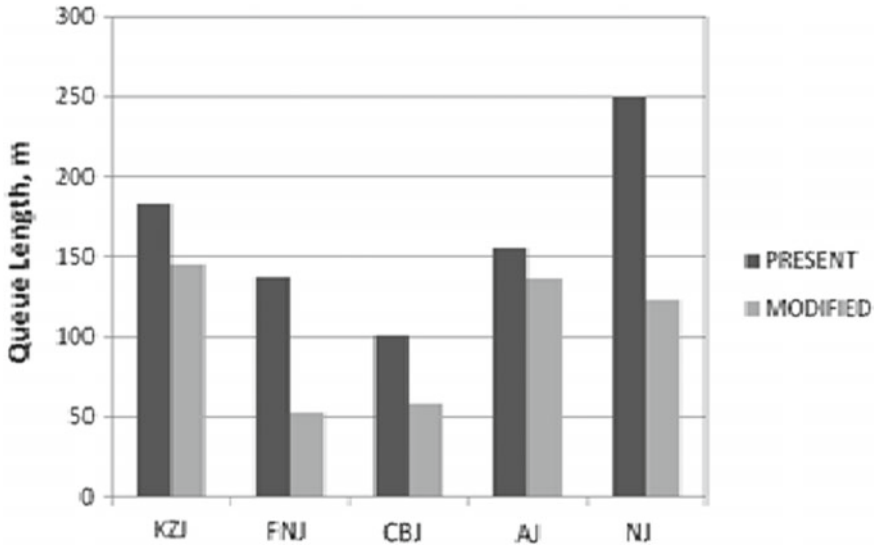

Fig. 8 Comparison of queue length after alternate coordination

To get the average speed along the study corridor, spot speed studies were conducted. The average speed of all the vehicles along the corridor is then compared with the average speeds obtained after the simulation is done for the alternate signal coordination. The average speed of the vehicles along the corridor is increased by around 13.42%. The change in the average speed for the alternate signal program is shown in Fig. 10.

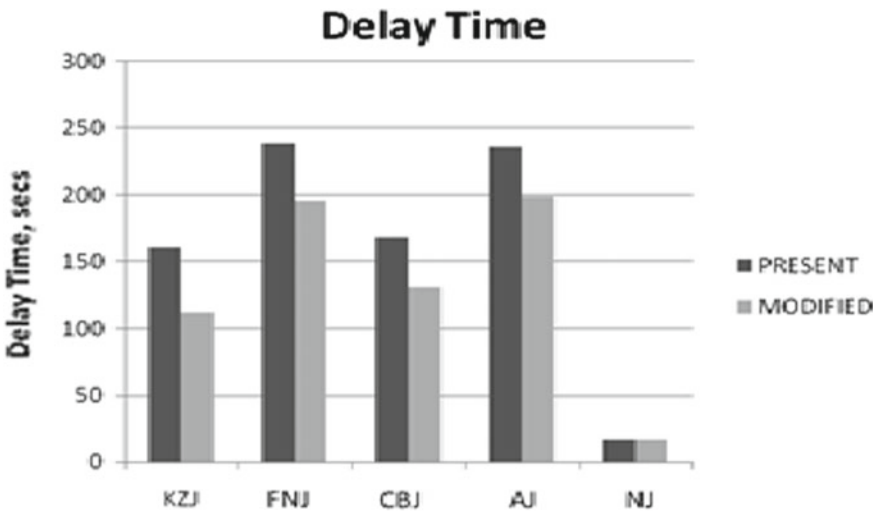

Fig. 9 Comparison of delay times after alternate coordination

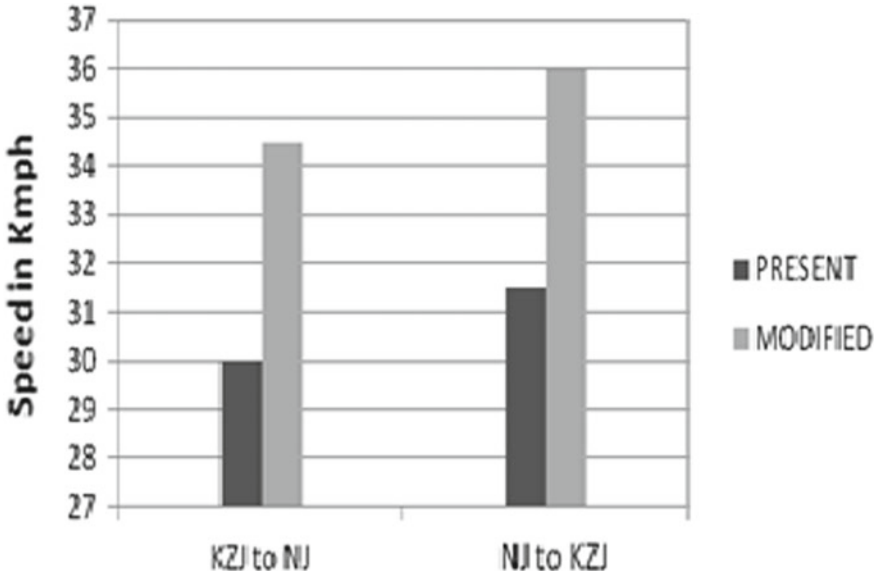

Fig. 10 Comparison of average speed along the corridor after alternate signal coordination

4 Conclusions

Analysis has been done in three phases, which includes model formation according to the present conditions, calibration of model and evaluation of different signal coordination plans for the given study corridor.

- Out of all the three alternatives for signal coordination plans, alternative signal coordination or limited progressive system shows a maximum impact on all the evaluation parameters.
- Alternate signal coordination plan shows the maximum decrease in the delay times of 28.87%.
- Alternate signal coordination shows a considerable decrease in travel times by 21.96%.
- There is a significant decrease in queue length by 41.27% when compared to the present field conditions.
- The alternative signal program also shows the maximum bandwidth as compared to the other two signal plans, which also leads to a better bandwidth efficiency of 41.85%.
- There is also an increase in the average speed along the corridor by 13.42%.

References

1. Parikh RI (2006) Effectiveness of signal coordination as an emission reduction measure for vehicles. M. S. Thesis, University of Texas, Arlington
2. Stevanovic AZ, Martin PT (2008) Assessment of the suitability of microsimulation as a tool for the evaluation of macroscopically optimized traffic signal timings. J Transp Eng 134(2):59–67
3. Stevanovic A, Martin PT (2008) Split-cycle offset optimization technique and coordinated actuated traffic control evaluated through microsimulation. Transp Res Rec: J Transp Res Board 2080(1):48–56
4. Ofosu K (2008) Traffic signal retiming study for Babcock street and Malabar road. Growth Management Department, Babcock, Palm Bay
5. Park B, Chen Y (2010) Quantifying the benefits of coordinated actuated traffic signal systems: a case study. Virginia Transport Research Council, Virginia
6. Gomes G, May A, Horowitz R (2004) Congested freeway microsimulation model using VISSIM. Transp Res Rec: J Transp Res Board 1876:71–81
7. Doina KSY, Chin HC (2007) Traffic simulation modeling: VISSIM. Undergraduate research opportunity project (UROP), National University of Singapore, Queenstown, Singapore
8. Zhizhou W, Jian S, Xiaoguang Y (2005) Calibration of VISSIM for shanghai expressway using genetic algorithm. Proceedings of the winter simulation conference, China, pp 2645–2648
9. Jie L, Fangfang Z, Zuylenb H, Shoufeng L (2011) Calibration of a microsimulation program for a Chinese city. Procedia Soc Behav Sci 20:263–272
10. Patel KM, Varia HR, Gundaliya PJ (2011) A methodology of signal coordination at network level. In: Proceedings of national conference on recent trends in engineering & technology, Gujarat, India
11. Cunningham A, Archer J (2003) Modelling the combined motorway and urban traffic conditions in the Norrtull-Brunnsviken network using VISSIM. Centre for Traffic Simulation Research, Royal Institute of Technology (KTH), Stockholm, Sweden

12. Woody T (2012) Calibrating freeway simulation models in VISSIM. M.S. Thesis, University of Washington, Seattle
13. Manjunatha P, Vortisch P (2012) Methodology for the calibration of VISSIM in mixed traffic. Transportation research board annual meeting

Rehabilitation of Breached Earth Dam Using GeoComposite—A Case Study

Randhir Kumar Choudhary

Abstract The 32.80 m high homogeneous earth dam at Gararda in Rajasthan, across the Dungari Nallah, was completed in 2010 and was breached during the first filling of its reservoir. The post-breach soil investigation carried out on existing unbreached portion of earth dam predicted large variation in in situ bulk density and permeability values of soil fill. Thus, rehabilitation measures were suggested in the entire length of dam. In view of investigation and analysis carried out based on field and laboratory tests results, the existing dam section was modified by cutting downstream slope in 2.25 (H): 1 (V) from the top left edge to introduce a downstream filter with geotextile. In Gararda dam, unexposed geocomposite (geotextile + HDPE geomembrane + geotextile) has been used in upstream slope of dam as seepage barrier. This study illustrates various investigations and analysis procedure used in the rehabilitation of Gararda earth dam. The FEM simulation shows that modified dam section is safe under all flow conditions prescribed in the IS code. Results from current case study and from monitoring of instruments in the dam shall lead to growth in confidence of practicing engineers in sustainable applications of geosynthetics in dams.

Keywords Embankment dam · Dam rehabilitation · Geosynthetic · HDPE geomembrane

1 Introduction

The Medium Irrigation Project with a 32.80 m high earth dam at Gararda in the Bundi district, Rajasthan, is meant to provide irrigation facilities to a culturable command area of 9161 ha. Three Chambal basin drainage channels, namely Mangli Nala (towards the left end across which there is a spillway site), Dungi River (in the middle) and the Ganeshi Nala (at the right end of Dam axis) have been tapped by the dam. These salient features of the project are presented in Table 1 and location in Fig. 1. The dam, for which construction was started in 2004, was completed in

R. K. Choudhary (✉)
Central Water Commission, MoWR, RD & GR, Sewa Bhawan, New Delhi 110066, India
e-mail: rkrchoudhary-cwc@gov.in

V. S. Kanwar and S. K. Shukla (eds.), *Sustainable Civil Engineering Practices*,
Lecture Notes in Civil Engineering 72,
https://doi.org/10.1007/978-981-15-3677-9_13

Table 1 Salient features of the Gararda Irrigation Project, Rajasthan (India)

A	**Location of dam**	
(1)	State	Rajasthan
(2)	District	Bundi
B	**Hydrology**	
(1)	Name of river	Mangli, Doongri and Ganeshi Nala
(2)	Basin	Chambal
(3)	Gross catchment area up to dam site	337.75 km^2
(4)	Design flood	3372.80 m^3/s
C	**Storage planning**	
(1)	Gross storage at FRL	44.38 M cum
(2)	Live storage	41.94 M cum
(3)	Dead storage	0.244 M cum
E	**Central elevation**	
(1)	Top bund level (TBL)	RL 300.80 m
(2)	Maximum water level (MWL)	RL 297.80 m
(3)	Flood reservoir level (FRL)	RL 295.90 m
(4)	Minimum draw down level (MDDL)	RL 277.00 m
(5)	Crest of spillway	RL 295.90 m
G	**Dam particulars**	
(1)	Type of dam	Earth Dam with central core
(2)	Total length of dam	4.3 km
(3)	Maximum height of dam	32.80 m
(4)	Free board above MWL	3.0 m
(5)	Deepest bed level of river	EL. 268 m
H	**Spillway**	
(1)	Type of spillway	Masonry Ogee shaped
(2)	Length of spillway	840.0 m
(3)	Maximum height of spillway	4.24 m
(4)	Crest level	EL. 295.90 m
(5)	Design flood	3372.80 m^3/s

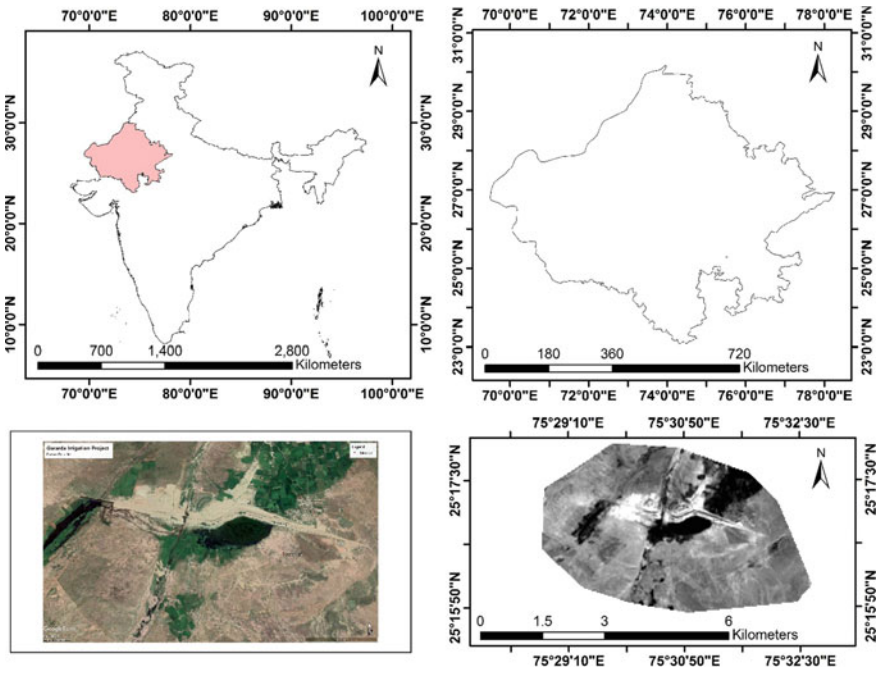

Fig. 1 Index map project site

2010 but breached in the central portion across the Dungari Nala in a length of about 100 m when the first filling-in of the reservoir during monsoon was attempted.

Contrada Sabetta rockfill dam (1959) in Italy and Dobsina earthfill dam (1960) in Slovakia were two new embankment dams where geomembrane was used because of being too permeable, thus requiring a separate element to provide imperviousness [5]. In several cases, geosynthetic barrier systems are much more sustainable, economical to use and their installation much easier than commonly used impervious materials [1].

Geosynthetics have been used widely and successfully in the rehabilitation, repair and retrofitting of existing concrete/masonry/earth dams. Imperviousness, flexibility, mechanical strength, frost and heat resistance, availability by industrial production and easy workability are the major factors for which geosynthetics are frequently used. The Kadamparai dam operated by Tamil Nadu Electricity Board (TNEB) in the state of Tamil Nadu was repaired recently by lining it's upstream face with PVC geomembrane to drastically reduce the seepage from 38,000 l per minute to about 30 l per minute [3]. Kandaleru reservoir earthen dam was eroded due to high current forces from the reservoir. Laying the drainage layer—using polypropylene instead of conventional filter materials [4].

In the current study, rehabilitation entails replacing the existing engineered material with another material of better characteristics, and function of watertightness is

transferred from the dam body (original design) to a geomembrane on the upstream face. In this way, both the unbreached portion embankment and the new "rehabilitated zone" are insulated from any contact with reservoir water.

2 Geological and Geotechnical Investigations

Subsequent to breach, the enquiry committee headed by Divisional Commissioner, Kota, in consultation with the professors of College of Engineering, Rajasthan Technical University, Kota, identified locations for boreholes within the dam body for investigation and testing of soil used for its construction and collected construction documentation and records. The foundation mapping and borehole logging of the dam foundation in the breached reaches revealed that foundation rock consisted of two sets of very widely spaced vertical to sub-vertical joints and few sporadic random joints. The spacing of the joints varied from 1.0 m to even more than 3.0 m and mostly occurred as clusters, and some of them open with an opening up to 10.0 cm. The joints trending parallel to the flow of the Nala were more prominent and continuous, and the other set which was less developed and mostly discontinuous was almost parallel to the dam axis. The report recommended that the strata exposed on the present surface were quite strong and competent with low to very low permeability (1.07×10^{-4} cm/s–6.98×10^{-4} cm/s).

The test results from geotechnical investigations of the dam indicated that entire dam is composed of an identical type of soil which implied that a homogeneous section has been constructed instead of a zoned section as envisaged. Since the material used differed from its tender specifications, its design should have been reviewed to account for the available quality of material. Also, soil test results of filter material showed that about 25–30% of the material was finer than 75 μm, whereas it should not have contained more than 5% of material passing 75 μm IS sieve. This showed that the proper filter material was not used, and constructed filter was not matching with the specifications. The shear strength parameters, compressibility characteristics and classification of shell material were found to be similar to core material. The gradation analysis of filter material indicated that the percentage passing by weight of particle size less than 75 μm was 23.7 and 29.5% which is too high to be used in the filter. The committee also presented the approved designed cross section and executed cross section of Gararda Dam as shown in Fig. 2.

In situ dry/bulk densities from different locations indicated significant variability in compaction characteristics of different layers, i.e. from very loose to dense state suggested uneven and insufficient compaction in various layers of the dam body. Permeability values of dam body material were inconsistent and had high variability. The drainage characteristics of both clay and filter material varied from highly pervious to impervious material in different layers. Standard penetration test (SPT) was carried out to assess the compactness and indirect strength characteristics of soils. The observed '*N*' values are varied from 9 to 50 (average *N* value 20) at the different depth.

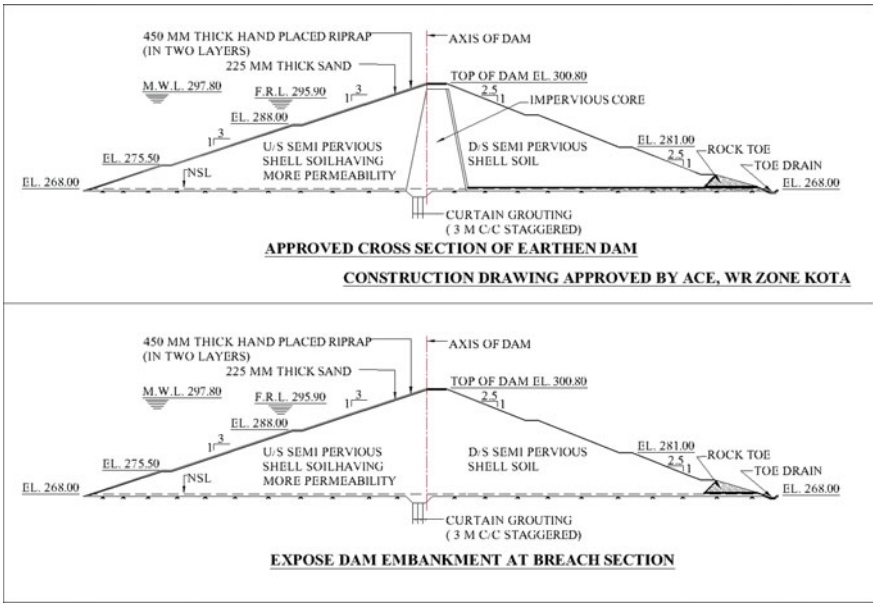

Fig. 2 Designed cross section and executed cross section of Gararda Dam

3 Analysis of Unbreached Dam Portion [2]

Above test results suggested that primarily dam was made of CL type soil. The result of triaxial tests of soil samples indicated that effective values of angle of shearing resistance (ϕ') and effective cohesion (c') for soil samples varied from 25° to 30° and 18–25 kPa, respectively. Most of the *N*-values ranged from 9 to 30 indicated that the consistency of soil can be defined as stiff to very stiff. One-dimensional consolidation test results indicated that the shell materials were likely to undergo low to medium compression depending upon the imposed stress levels.

In view of this, two-dimensional finite element model (2D-FEM)-based seepage and stress analysis of the existing unreached portion of earthen dam was carried out by utilizing RS2 (formerly RS^2 or $Phase^2$) without considering central clay core and downstream drainage filters under different flow condition at breach water level and flood reservoir level (FRL). This study showed that in the absence of downstream drainage filter, downstream slope of the existing dam becomes the seeping face. Also, existing section provided factor of safety of 1.3 in steady-state condition (Fig. 3) which is less than 1.5 as required by BIS code. Further, during breach, even existing dam section was subjected to sudden drawdown condition which resulted in local slope failure in upstream face at discrete location. The FEM analysis also depicted local slope failure near toe and first berm on the upstream slope (Fig. 4).

In view of above analysis, the unbreached dam section was modified by cutting downstream slope in 2.25 (H): 1 (V) from the edge of the upstream crest to introduce

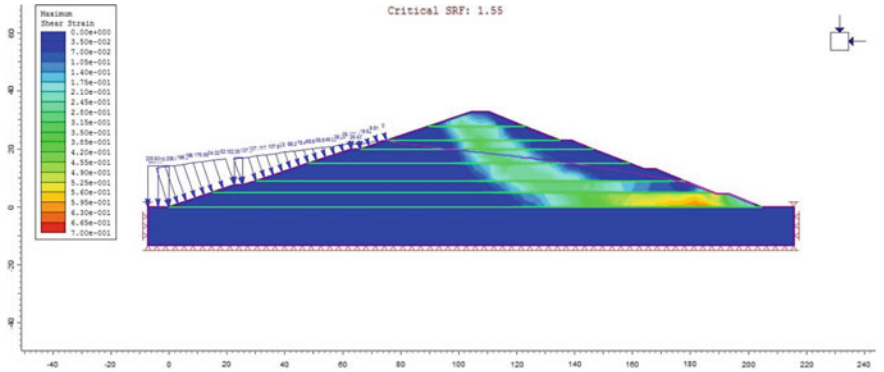

Fig. 3 Stress analysis under downstream steady seepage condition

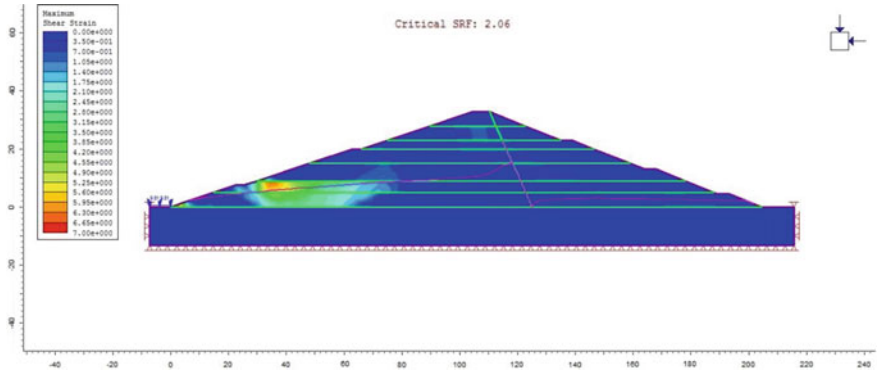

Fig. 4 Stress analysis under sudden drawdown condition

a downstream filter. The downstream filter was designed as per IS 9429. The modified section is shown in Fig. 5. The seepage analysis of modified section estimated that phreatic line was now within the dam and follows the filter. The FEM analysis showed that the modified dam section was safe under all flow conditions prescribed in IS 7894.

4 Rehabilitation Works Design

Based on the site investigations and testing of the unbreached portions of Gararda dam, slope stability analysis, seepage analysis and load-deformation analysis were carried out. It was inferred from the results of the above analysis that the dam can be made stable with the rehabilitation of slopes. However, a large variation in values of permeability and field density was observed during the field investigation, which

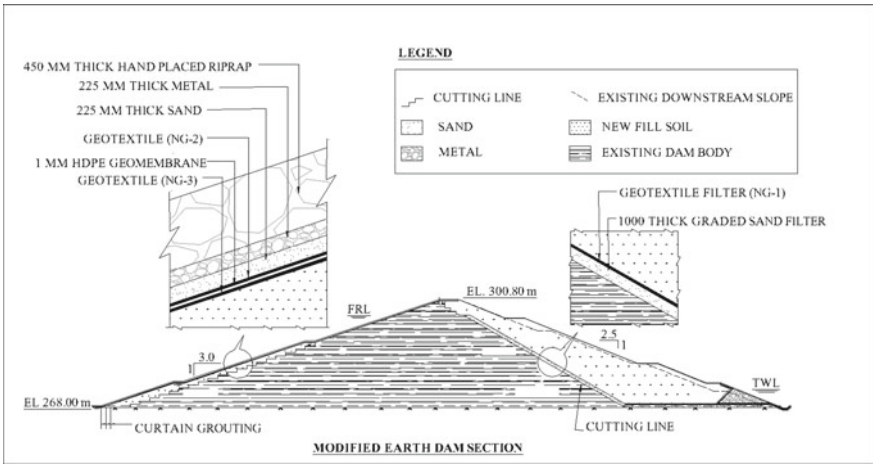

Fig. 5 Modified earth dam section

created doubt regarding the degree of compaction of the earth material of the existing dam body. To reduce ingress of water in the dam body, an impervious system of 1.0 mm thick HDPE geomembrane was provided in the upstream slope of the dam. Both upstream and downstream slopes were reinforced by providing 3.2 mm thick non-woven geotextile (NG-2 and NG-3) in upstream and a layer of geotextile filter (NG-1) of 0.7 mm apparent opening size and permeability of 5.5×10^{-4} cm/s in downstream. Physical properties of geotextiles (NG-1, NG-2 and NG-3) used for rehabilitation works are presented in Table 1. To provide downstream chimney filters and horizontal filter (both 1000 mm Sand + NG-1), the downstream slope was proposed to be cut in 2.25 H: 1.0 V slope from the edge of the upstream crest of the existing dam body. The remaining downstream slope was to be built up by providing better soil.

5 Status

The construction and installation works started in October 2017. The work is under progress as per specification and design and till date, approximately 75% of rehabilitation works have been completed (Fig. 6). The stipulated date of completion of the dam is February 2020.

Table 2 Physical properties of geotextiles (NG-1, NG-2 and NG-3) used for rehabilitation works

S. No.	Tests/Properties	Units	Method	NG-1	NG-2	NG-3
1.	Mass per unit area	g/m^2	ENISO-9864	250	400	100–125
2.	Wide width tensile strength	kN/m	ENISO-10319	15.5/18.5	26.5/32	6/7.5
3.	Wide width elongation at break strength (MD/CD)	%	ENISO-10319	50/50	50/50	–
4.	Puncture strength (CBR)	N	ENISO-12236	2300	4000	1000
5.	Dynamic performance resistance-cone drop	mm	ENISO-13433	22	10	35
6.	Permittivity/flow rate	10^{-3} m/s	ENISO-11058	35	20	–
7.	Apparent opening size (AOS)	mm	ENISO-12956	0.075	0.075	–

Fig. 6 Rehabilitation works in progress

6 Conclusion

Both upstream and downstream slopes have been provided with geosynthetic material. The geosynthetic material would offer protection against piping during the critical first filling of reservoir and during the first few operating years when post-construction settlement could be expected. There is an apprehension that due to the earlier poor construction quality, there could be pockets/layers of low shear strength which might lead to a large settlement. In view of this, a geosynthetic membrane is provided on the upstream face to substantially reduce the flow in the dam body, and a three-layer 200 mm thick curtain grout is also proposed on the upstream to reduce the flow in rock-foundation beneath the dam.

Geosynthetics provide a lot of flexibility in design works, wherein their different functional capabilities such as seepage barrier, separation, filtration, drainage and reinforcement can be utilized effectively. In many cases, due to lack of availability of good quality of construction materials in vicinity of project sites, geosynthetics provide an excellent and sustainable alternative. Geosynthetics have been found to be very useful in repair, retrofitting and rehabilitations of dams and reservoirs.

References

1. Cazzuffi DG (2010) Geosynthetic barriers systems for dams. In: 9th International conference on geosynthetics, vol 1, Keynote Lecture, Guarujá, São Paulo state, Brazil, pp 115–163
2. Choudhary RK (2018) Rehabilitation measures to un-breached portion of Gararda Earth Embankment Dam, Bundi (Rajasthan). In: International dam safety conference. Central Water Commission, Kerala, pp 529–538
3. Rajagopal KA (2015) State-of-the-art on the applications of geosynthetics for dam repair and rehabilitation. In: First national dam safety conference. Central Water Commission, IC&SR Auditorium, IITM, Chennai
4. Raju NR (2010) Case Studies on the Usage of Geosynthetics in Earthen dams and embankments. In: Indian geotechnical conference—2010, GEOtrendz. IIT Bombay, IGS Mumbai Chapter, pp 149–154
5. Scuero AM (2011) Development of geomembrane systems for watertightness of dams in Europe. In: The international symposium on dams and reservoirs under changing challenges—79 Annual meeting of ICOLD, Swiss Committee on Dams. Taylor & Francis Group, London, Lucerne, Switzerland, pp 203–210

Improvement of Subgrade Characteristics with Inclusion of Geotextiles

Madhu Sudan Negi and S. K. Singh

Abstract An experimental program has been undertaken to study the effect of geotextile as a tensional material used for subgrade reinforcement. The standard laboratory California bearing ratio (CBR) test under both soaked and unsoaked conditions was conducted on the unreinforced soils as well as reinforced ones with geotextile layer(s). Two different types of subgrade soil, sandy and clayey soil having soaked CBR value of 19.6 and 1.7%, respectively, and two types of geotextiles were used in this study. The geotextile reinforcements were placed in samples in seven different cases. The effects of geotextile reinforcement on the bearing capacity of soil which is taken in terms of CBR value were investigated. The results show an increase in CBR value for most of the cases due to placing the geotextile layer(s). Geotextile reinforcement is found to be most effective in the case of weak soil, i.e. clayey soil. It was also observed that woven geotextile performed better than nonwoven geotextile in all the cases.

Keywords Reinforcement · Woven geotextile · Nonwoven geotextile · CBR · Subgrade · Soft soils

1 Introduction

Subgrade stabilization becomes important where the local soil available is weak to support the traffic loads. There are several methods available for subgrade stabilization, either mechanical or chemical, but all of these methods require skilled manpower and costly equipment. The use of geosynthetics has proven to be an effective means of soil improvement. Different types of geosynthetics materials are used for subgrade stabilization in various forms such as geogrid, geotextile, geocell and geonet. These are used in the pavement for performing various functions such as

M. S. Negi (✉) · S. K. Singh
Punjab Engineering College (Deemed to Be University), Chandigarh 160012, India
e-mail: madhusudan.metrn17@pec.edu.in

S. K. Singh
e-mail: sksingh@pec.ac.in

V. S. Kanwar and S. K. Shukla (eds.), *Sustainable Civil Engineering Practices*,
Lecture Notes in Civil Engineering 72,
https://doi.org/10.1007/978-981-15-3677-9_14

separation, filtration, lateral drainage and reinforcement. Several researchers [12, 15, 21] recommended that the performance of pavement can be improved due to the geosynthetic reinforcement. Geotextiles and geogrid are among the two types of geosynthetics which are widely used in pavement. To increase the tensile property of the soil, geotextile has also been used in the flexible pavement as reinforcement.

Laboratory experiments have been conducted by many researchers to understand the effect of geotextile as a reinforcing material in terms of improvement of the bearing capacity of the subgrade [29]. CBR tests were conducted by introducing geotextiles and geogrid in granular soil [2, 18, 30]. The benefits of using geotextiles as a reinforcement are found to be most significant in weak subgrades of California bearing ratio (CBR) <3% as shown by [17, 30]. The effect of geotextile and geogrid is investigated in clay with low or medium compressibility [3, 16, 19, 28] as soft subgrade in an unpaved road system.

Resl and Werner [24] carried out laboratory tests under an axisymmetric loading condition using geotextiles. The results showed that the geotextile layer placed between the soil layers can significantly increase the bearing capacity of soft subgrades. Many researchers indicate that geotextiles which possess high tensile capacity will provide more load spreading ability for the same rut depth [9, 10, 13, 25]. The placement position of reinforcement is one of the main factors affecting the bearing capacity of reinforced soil. Higher bearing capacity has been observed when the depth of placement of reinforcement is decreased [1, 11, 23, 26]. Bergado et al. [4] performed CBR tests on soft clay overlain by compacted sand. The specimens were reinforced by geotextile with different stiffness between clay and sand. The results indicated that using geotextile in soil increase bearing capacity of soil.

In most of the studies, the geotextile layer had been used as a separator, i.e. at the interface of subgrade and subbase layer. Very few studies had used the geotextile as reinforcing element within subgrade soil in single layer only. The present study investigates the effect of geotextile in single/multiple layers at different placement levels. Two different types of soils, viz. sandy soil and clayey soil, have been selected and tested with and without geotextile reinforcement under both soaked and unsoaked conditions. Laboratory California bearing ratio (CBR) tests have been conducted on two types of soils to measure the effectiveness of using woven and nonwoven geotextiles for reinforcing the subgrade soil. The effect of number, placement and type of geotextile on the CBR value for both the soil is discussed.

2 Experimental Programs

2.1 Material

Two types of soils have been chosen for conducting the CBR test. Soil 1 and soil 2 were classified as SP-SM (silty sand) and CI (clay with medium compressibility), respectively, according to the Indian Standard Classification System IS 1498 (1970).

The grain size distributions for soil 1 were determined based on wet sieve analysis. By wet sieve analysis percentage, finer comes out to be 10%. In soil 2, the percentage of particles passing 0.075 mm sieve was more than 50%; hence, hydrometer test was used for the grain size distribution. Figure 1 shows the grain size distribution curves for the soils.

Standard proctor test conforming to IS 2720 (Part 7) was used for determining the optimum moisture content (OMC) and maximum dry density (MDD) of soils. The index properties and compaction characteristic of soils are given in Table 1.

Two types of geotextile, i.e. woven and nonwoven, were used in this study. Woven geotextiles have visible distinct construction pattern having tensile strength of 30

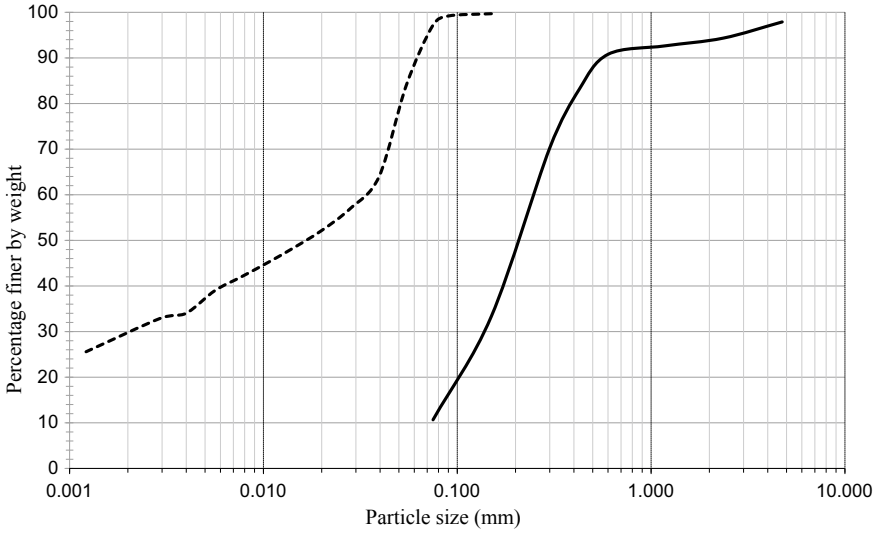

Fig. 1 Grain size distribution curve for soil

Table 1 Geotechnical properties of soil

Properties	Soil 1	Soil 2
Cu	3.33	–
Cc	1.20	–
Specific gravity	2.67	2.71
Optimum moisture content (%)	12	18
Maximum dry density (kN/m^3)	17.20	15.10
Liquid limit (%)	–	46
Plastic limit (%)	–	23
Plasticity index (%)	–	23
Free swell index, FSI (%)	–	22.70
Soil classification	SP-SM	CI

Table 2 Properties of geotextile

Properties	Woven geotextile	Nonwoven geotextile
Weight (g/m^3)	400	150
Thickness (mm)	0.88	0.86
Modulus of elasticity E (MPa)	60	25
Tensile strength (kN/m)	30	13
Elongation at peak stress (%)	15–20	45–50

kN/m, and nonwoven geotextiles have a random pattern and have tensile strength of 13 kN/m. The physical and mechanical properties of geotextiles are summarized in Table 2.

2.2 CBR Testing

In order to understand the strength improvement of reinforced soil, laboratory CBR test using soil samples reinforced with woven and nonwoven geotextile was conducted. CBR test on soils was performed by standard procedure mentioned in IS 2720 (Part 16) by compacting the specimen in three equal layers on optimum moisture content to achieve the desired density. Both soaked and unsoaked CBR tests were performed. For conducting the soaked CBR test, the soil sample with surcharge of 2.5 kg was submerged in water under controlled conditions for 96 h and then tested.

The placement position of the geotextile layer was chosen as per the study conducted by Rashidian et al. [22] in which for preparing reinforced specimens, geotextile was to be placed in the middle of each compacted layer. Hence, the geotextile was to be placed at a height of $H/6$, $H/2$ and $5H/6$ from top of sample where H is the height of the sample in CBR mould. Seven cases were considered for placing geotextile as shown in Fig. 2. Notations used in this study for various combinations of placement of geotextile in CBR mould are given in Table 3.

The strength improvement of the reinforced soil is quantified through a nondimensional parameter: Bearing capacity ratio (BCR). It is defined here as the ratio of CBR of reinforced soil (CBR_r) to the CBR of the unreinforced soil (CBR_u) as follows:

$$BCR = \frac{CBR_r}{CBR_u}$$

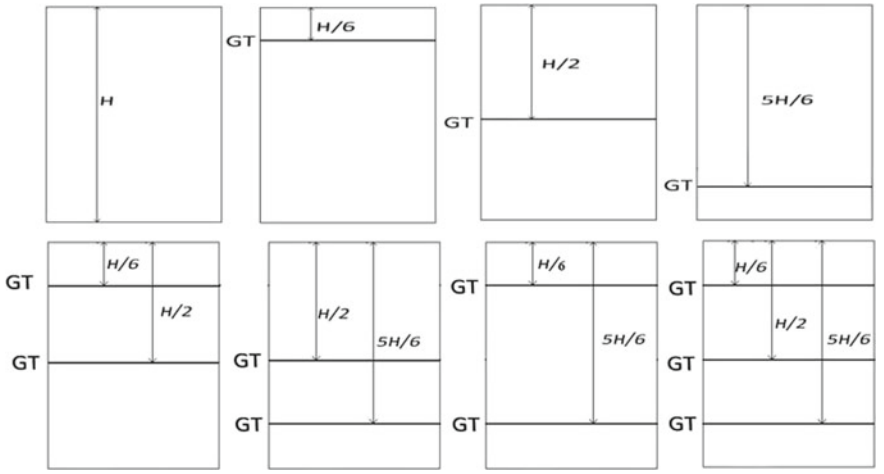

Fig. 2 Placement of geotextile in CBR mould

Table 3 Notations used for different combinations of placement of geotextile

Placement of geotextile at height (from top)	Woven geotextile	Nonwoven geotextile
H/6	wgt1	nwgt1
H/2	wgt2	nwgt2
5*H*/6	wgt3	nwgt3
H/6 and *H*/2	wgt12	nwgt12
H/6 and 5*H*/6	wgt13	nwgt13
H/2 and 5*H*/6	wgt23	nwgt23
H/6, *H*/2 and 5*H*/6	wgt123	nwgt123
Unreinforced	unr/f	

2.2.1 CBR Test on Soil 1

Both soaked and unsoaked CBR tests were performed on soil 1. The results of CBR tests on soil 1 are given in Table 4. A typical load vs penetration graph is shown in Fig. 3 for the case when geotextile placed at height *H*/6 and *H*/2 from top showing the increase in penetration resistance of the soil with geotextile inclusion.

As soil 1 is of sandy type, there is not much difference between the CBR values under unsoaked and soaked conditions as it can be seen from Fig. 4. However, the CBR value comes out to be slightly more in soaked condition as compared to unsoaked condition.

Woven geotextile shows better reinforcing capacity as compared to nonwoven geotextile as shown in Fig. 5.

Table 4 CBR test result on soil 1

	Soaked CBR (%)	BCR	Unsoaked CBR (%)	BCR		Soaked CBR (%)	BCR	Unsoaked CBR (%)	BCR
unr/f	19.66	–	18.52	–	wgt12	27.55	1.40	28.41	1.53
wgt1	23.23	1.18	23.82	1.29	ngt12	22.63	1.15	25.71	1.39
nwgt1	20.96	1.07	20.04	1.08	wgt13	22.96	1.17	21.71	1.17
wgt2	27.6	1.40	26.74	1.44	nwgt13	20.58	1.05	19.39	1.05
nwgt2	25.44	1.29	22.69	1.23	wgt23	20.8	1.06	18.47	1.00
wgt3	24.54	1.25	24.63	1.33	nwgt23	18.96	0.96	17.39	0.94
nwgt3	22.63	1.15	22.47	1.21	wgt123	26.09	1.33	25.44	1.37
					nwt123	20.58	1.05	20.2	1.09

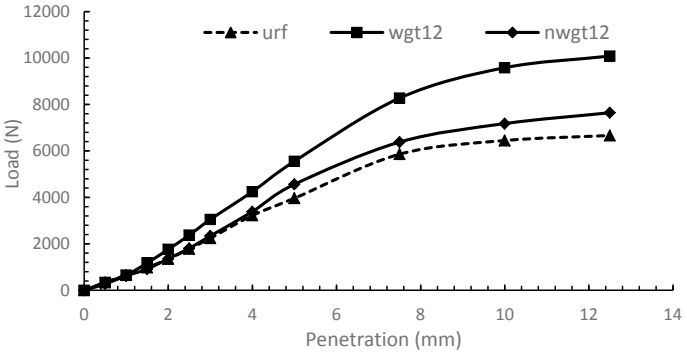

Fig. 3 Load versus penetration graph for soil 1; unreinforced and when geotextile placed at a distance *H*/6 and *H*/2 from top

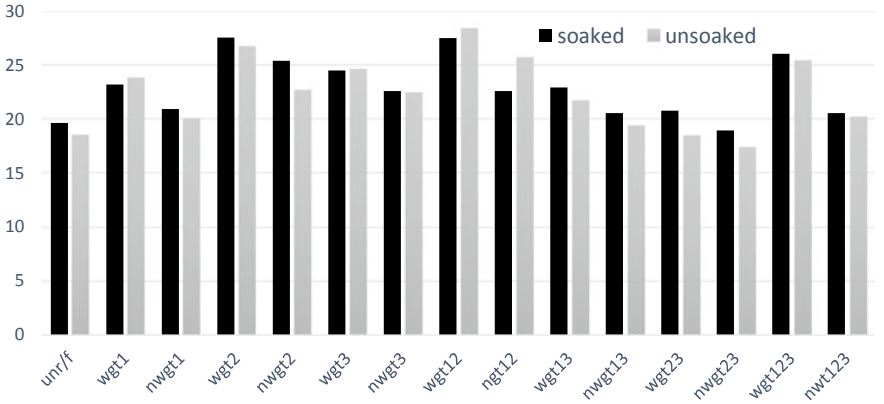

Fig. 4 Comparison of soaked and unsoaked CBR tests on soil 1

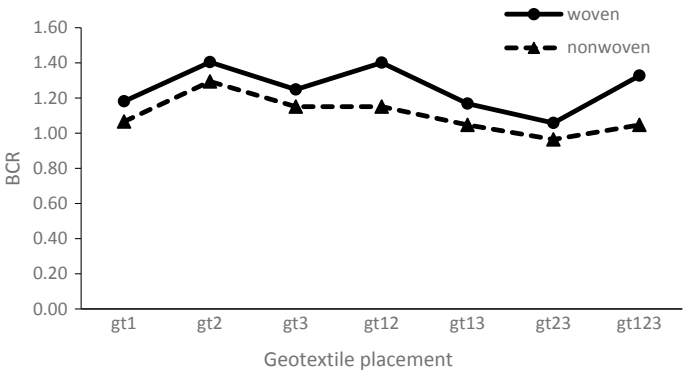

Fig. 5 Comparison of BCR between woven and nonwoven geotextile

Table 5 CBR test results on soil 2

	Soaked CBR (%)	BCR		Soaked CBR (%)	BCR
unr/f	1.78	–	wgt12	4.87	2.74
wgt1	2.48	1.39	ngt12	3.29	1.85
nwgt1	1.94	1.09	wgt13	3.78	2.12
wgt2	3.08	1.73	nwgt13	3.35	1.88
nwgt2	2.92	1.64	wgt23	3.46	1.94
wgt3	3.94	2.21	nwgt23	3.19	1.79
nwgt3	3.67	2.06	wgt123	4	2.25
			nwt123	3.62	2.03

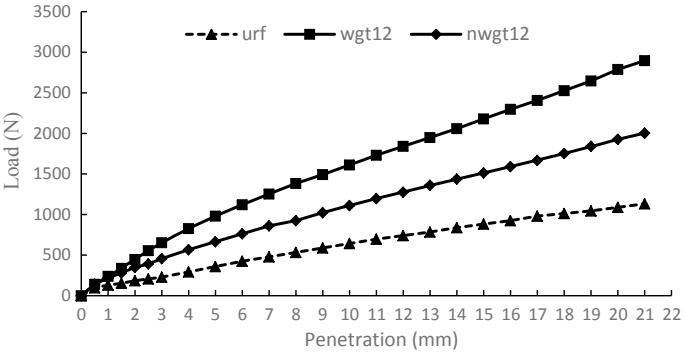

Fig. 6 Load vs penetration graph for soil 2; unreinforced and geotextile placed at a distance $H/6$ and $H/2$ from top

2.2.2 CBR Test on Soil 2

For simulating worst conditions, only soaked CBR tests were conducted for soil 2 as it is of clayey type. For clayey soil, moisture variation is of critical importance. The results of soaked CBR tests on soil 2 are given in Table 5. A typical load vs penetration graph is shown in Fig. 6 for the case when geotextile placed at height $H/6$ and $H/2$ from top. Figure 7 shows the comparison of BCR between woven and nonwoven geotextile for soil 2; it indicates the effectiveness of woven geotextile in reinforcing the soil as compared of nonwoven geotextile.

3 Results and Discussion

The results from the experimental study show that geotextile can be successfully used for reinforcement of subgrade soil as the increase in CBR value of soil is

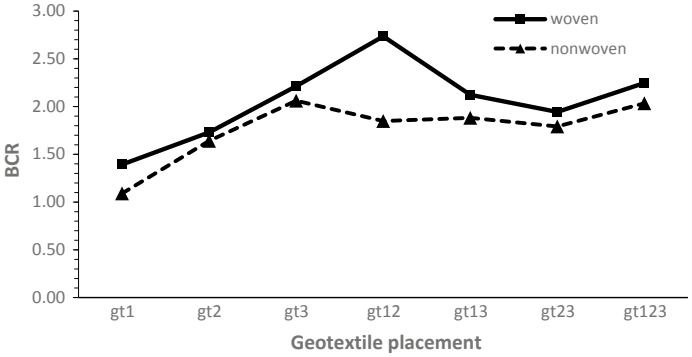

Fig. 7 Comparison of BCR between woven and nonwoven geotextile

seen by reinforcing it with geotextile, which is also observed by many researchers [8, 22, 27]. As it can be seen from Figs. 5 and 7 that woven geotextile always gives more BCR than nonwoven geotextile; this is because the tensile strength of woven geotextile is more than nonwoven geotextile. It is also observed that, increasing the number of geotextiles does not necessarily increase the BCR. Best reinforcement benefit is generally achieved when two layers of woven geotextile is placed at height $H/6$ and $H/2$ from top for both types of soils. Maximum BCR obtained for soil 1 is 1.40 under soaked condition and 1.53 under unsoaked condition when two layers of woven geotextile are placed at a height of $H/6$ and $H/2$ from top. For the case of soil 2, maximum BCR of 2.74 under soaked condition is obtained when two layers of woven geotextile are placed at a height of $H/6$ and $H/2$ from top. Maximum BCR is obtained for the case of soil 2 which is a weak soil of clayey type which is in good agreement with the results obtained by Williams and Okine [30]. This observation confirms the strength mobilization principle of the geosynthetic materials in general which emphasized that the strength mobilization of geosynthetic material depends on the range of CBR of soil sample. The smaller the soil CBR, the more effective is the strength mobilization effects of geosynthetic material. Since the woven geotextile used for the experiment has a high tensile strength of 30 kN/m, tensile stresses develop in the geotextile and the vertical component of the membrane stress was able to help the weak soil to support the applied stress due to loading.

The stronger the subgrade (higher CBR), lesser is the thickness of pavement, which gives a considerable cost saving. Conversely if subgrade is weak (low CBR), it requires to construct a suitable thicker road pavement to spread the wheel load over a greater area of the weak subgrade. According to MORTH [20], it is specified that the minimum CBR value of subbase should be more than 20% for the case of traffic less than 2 million standard axles. In the present study, for the case of soil 1 as the soaked CBR values come out to be 19.66% and by reinforcing it with woven geotextile placed at height $H/2$ and $H/6$ from top gives the CBR of 27.6% showing an increase of 40% from unreinforced case. Hence, in such case base course layer

can be directly applied on reinforced subgrade layer which can also act as subbase thus decreasing the cost of construction.

IRC 37 [14] states that, if the CBR value of subgrade in any site comes to be less than 2%, then a capping layer of 150 mm thickness having CBR value of more than 10% is to be used over subgrade. In the case of soil 2 (clayey soil) as a subgrade material, as the soaked CBR value comes out to be 1.78% which is less than 2%, and by reinforcing it with geotextile, the soaked CBR value goes up to 4.8% as such the capping layer will not be required. The benefit of using geotextile in this case for reinforcement of subgrade is thus supported by the fact that a sufficient amount of cost and effort related to providing capping layer can be saved using geotextile as reinforcing material.

4 Conclusions

An extensive laboratory CBR tests were performed on two different types of subgrade soils by reinforcing them with woven and nonwoven geotextiles under different placement conditions. It was observed that the bearing capacity of subgrade soil can be efficiently improved by inclusion of geotextile layer.

The main conclusions that can be drawn from the experimental study are:

- Woven geotextile shows better reinforcement than nonwoven geotextile since it has higher tensile capacity as compared to nonwoven geotextile.
- The strength improvement of soil when reinforced with geotextile depends on the CBR of the soil. Soils with low CBR have higher benefits in terms of improved strength (BCR) than those with higher in situ CBR values. As in this case, soil 2, which is clayey soil having soaked CBR of 1.78% which increased to 4.8% after placing woven geotextile in two layers at a distance of $H/6$ and $H/2$ from top showing an increase of 121% from the unreinforced case.
- Effect of number and position of geotextile is an important parameter for the subgrade reinforcement. Increasing number of geotextile does not necessarily increase the bearing capacity of subgrade. Two layers of woven geotextile placed at height of $H/6$ and $H/2$ from top gives maximum bearing capacity ratio for both the soils.
- Reinforcing subgrade soil by geotextile can significantly reduce the cost of construction of road. In the case of sandy soil, the requirement of granular subbase may be dispensed. The base course may be directly laid over the subgrade as CBR of reinforced soil is more than 20%. In the case of clayey soil, the capping layer will not be required as the CBR value increases from 1.78 to 4.8% after reinforcing with geotextile.

References

1. Akinmusuru JO, Akinbolade JA (1981) Stability of loaded footings on reinforced soil. J Geotech Eng Div ASCE 107:819–827
2. Al-Qadi IL, Brandon TL, Valentine RJ, Smith TE (1994) Laboratory evaluation of geosynthetic reinforced pavement sections. Transportation Research Board., No. 1439, 73rd Annual meeting, Washington DC, pp 25–31
3. Asha MN, Madhavi G (2010) Modified CBR tests on geosynthetic reinforced soil-aggregate systems. In: Proceedings of the Indian geotechnical conference, IGS Mumbai Chapter
4. Bergado DT, Youwai S, Hai CN, Voottipruex P (2001) Interaction of nonwoven needle-punched geotextiles under axisymmetric loading conditions. Geotext Geomembr 19:299–328
5. Bureau of Indian Standards (1990) IS 1948: classification and identification of soils for general engineering purposes. Bureau of Indian Standards, New Delhi
6. Bureau of Indian Standards (1980) IS 2720 (Part 7) methods of test for soils: determination of water content-dry density relation using light compaction. Bureau of Indian Standards, New Delhi
7. Bureau of Indian Standards (1987) IS 2720 (Part 16) methods of test for soils: laboratory determination of CBR. Bureau of Indian Standards, New Delhi
8. Choudhary A, Gill K, Jha J, Shukla SK (2012) Improvement in CBR of the expansive soil subgrades with a single reinforcement layer. In: Proceedings of Indian geotechnical conference, New Delhi, India, pp 289–292
9. Christopher BR, Holtz RR (1985) Geotextile engineering manual. Report No. FHWA-TS-86/203, Federal Highway Administration, Washington, DC
10. De Groat M, Janse E, Maagdenberg TAC, Vandenberg C (1986) Design methods and guidelines for geotextile applications in road construction. In: Proceedings on third international conference on geotextiles, Vienna, Austria, pp 741–746
11. Fragaszy RJ, Lawton E (1984) Bearing capacity of reinforced sand subgrades. J Geotech Eng 110(10):1500–1507
12. Giroud JP, Noiray L (1981) Geotextile reinforced unpaved road design. J Geotech Div ASCE 107:1233–1254
13. Hausmann MR (1987) Geotextiles for unpaved roads—a review of design procedures. Geotext Geomembr 5(3):201–233
14. Indian Road Congress (2001) IRC 37 guideline for the design of flexible pavements. Indian Road Congress, New Delhi
15. Keller GR (2016) Application of geosynthetics on low-volume roads. Transport Geotech. https://doi.org/10.1016/j.trgeo.2016.04.002
16. Latha G, Nair A, Hemalatha M (2013) Performance of geosynthetics in unpaved roads. Int J Geotech Eng. https://doi.org/10.3328/IJGE.2010.04.03.337-349
17. Moayed R, Nazari M (2011) Effect of utilization of geosynthetic on reducing the required thickness of subbase layer of a two layered soil. World Acad Sci Eng Technol 73(49):963–967
18. Naeini SA, Mirzakhanlari M (2008) The effect of geotextile and grading on the bearing ratio of the soils. Electron J Geotech Eng 13J:1–10
19. Naeini SA, Moayed RZ (2009) Effect of plasticity index and reinforcement on the CBR value of soft clay. Int J Civil Eng 7(2):124–130
20. MORTH (2001) Specifications for road and bridge works, 5th edn. Ministry of Road Transport and Highways, New Delhi
21. Perkins SW (2001) Mechanistic empirical modelling and design model development of geosynthetics reinforced flexible pavements. FHWA/MT-01-002/99160-1A, U.S. Department of Transportation, Federal Highway Administration, Washington, DC
22. Rashidian V, Naeini SA, Mirzakhanlari M (2016) Laboratory testing and numerical modelling on bearing capacity of geotextile reinforced granular soils. Int J Geotech Eng. https://doi.org/10.1080/19386362.2016.1269042
23. Raymond GP (1992) Reinforced sand behavior overlying compressible sub-grades. J Geotech Eng ASCE 118(11):1663–1695

24. Resl S, Werner G (1986) The influence of nonwoven needle-punched geotextiles on the ultimate bearing capacity of the subgrade. In: Proceedings of the third international conference on geotextiles, Vienna, No. 4, pp 1009–1013
25. Robnett Q, Lai J (1982) Effect of fabric properties on the performance and design of aggregate-fabric-soil-systems. In: Proceedings of the second international conference on geotextiles, vol II, Las Vegas, pp 381–386
26. Sankariah B, Narahari R (1988) Bearing capacity of reinforced sand beds. In: Proceeding of first Indian geotextile conference on reinforced soil and geotextiles, Bombay, India, pp C11–C13
27. Sivapragasam C, Vanitha S, Arun VM, Sutharsanam S (2010) Study on synthetic geotextiles for road pavements. In: Indian geotechnical conference—2010, GEOtrendz, IGS Mumbai Chapter
28. Srivastava RK, Jalota AV, Singh R (1995) Model studies on geotextile reinforced pavements. Indian Highw 23(9):31–39
29. Som N, Sahu R (1999) Bearing capacity of a geotextile-reinforced unpaved road as a function of deformation: a model study. Geosynthetics Int 6(1):1–17
30. Williams ED, Okine NA (2008) Effect of geogrid in granular base strength—an experimental investigation. Constr Build Mater 22:2180–2184

The Contribution of Bottom Ash Toward Filler Effect with Respect to Mortar

Lomesh S. Mahajan and S. R. Bhagat

Abstract The most widely used construction material is concrete. Concrete requires a large number of ingredients. Now the time has been changed, which inspire researchers to encourage alternative materials for replacing traditional concrete-making materials. Even though the mortar makes up as minor as 7–8% of the total volume of a masonry wall and in mortar volume, the content of fine aggregate is about 85%. The sources of natural sand are depleting very fast; hence, some alternative materials have to be identified to make replacement of natural sand. One such material which can be used as replacement of natural sand for making mortar is identified as bottom ash. The present work addresses the use of bottom ash as sand in making cement mortar. Five different grades are considered for this study with different proportions of cement–bottom ash or natural sand ranging from 1:2 to 1:8. The effect of incorporating bottom ash as fine aggregates on mortar properties at different replacement level was assessed. The obtained compressive strength of altered grades of mortar is higher than that of specified as per IS 1905–1987; it shows addictive features of bottom ash to develop sustainable mortar future.

Keywords Alternative material · Mortar · Fine aggregate · Bottom ash

1 Introduction

A large quantity of various natural resources is required for different applications in construction industry. Through out the world, approximately 3 billion tonnes of initial raw materials have been used yearly for manufacturing of cement [20].

L. S. Mahajan (✉)
Dr. Babasaheb, Ambedkar Technological University, Lonere, Maharashtra, India
e-mail: loms786@gmail.com

S. R. Bhagat
Department of Civil Engineering, Dr. Babasaheb Ambedkar Technological University, Lonere, Maharashtra, India
e-mail: srbhagat@dbatu.ac.in

V. S. Kanwar and S. K. Shukla (eds.), *Sustainable Civil Engineering Practices*,
Lecture Notes in Civil Engineering 72,
https://doi.org/10.1007/978-981-15-3677-9_15

The fast developments and expansion of the construction field requires huge quantity of natural river sand. Nowadays, construction business are facing problems due to paucity of river sand as an important ingredient of concrete. This requirement has lead to unstainable sand mining and has severely affected the flow of rivers. Mining of sand also lead to an increase in water pollution and impact biodiversity. Considering this important issue of environmental sustainability and at the same time fulfilling the requirements of fine aggregate for construction industry it becomes essential to find new solutions for a sustainable future. In the present situation of insufficient sources of naturally available river sand and booming in infrastructure development, it is necessary and noteworthy to find out its alternative material or method.

On the other facts according to Central Electricity Authority [8], a huge quantity of coal bottom ash has been produced by thermal power station (TPS) in India which accounts to 35 million tons annually. About 173 million tons of TPS coal ash including bottom ash and fly ash are generated by 143 TPS after 524 million tons of coal combustion. Figure 1 shows the gathered quantity and utilization of coal ash in India for a period of seven years. The main cause of a surroundings risk to the soil is the present method of disposing on open land [15]. Apart from this, sustainability can be achieved by increased use of resources effectively. This is possible by saving on the energy use, materials, and environmental approachability [20]. The few solutions are optional in concrete technologies. The solution is the deployments of industrial by-products into concrete constituents like bottom ash, slag, fly ash, waste glass, rice husk ash, and silica fume [12, 23, 25, 26]. TPS by-products bottom ash if used in the form of fine aggregate may increase the degree of absorbency of concrete. It is auspicious to produce concrete which is durable by consuming non-ground blast furnace slag and bottom ash as a replacement of natural sand. For normal concretes,

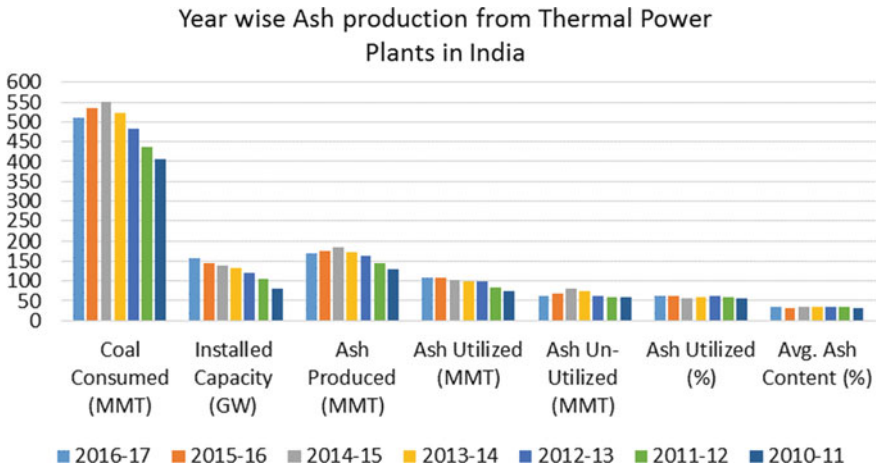

Fig. 1 Last 7 years ash production from thermal power plants in India. *Source* CEA Report [[7, 8] (2010–11 and 2016–17)]

bottom ash utilization of 20% sand replaced the favors of the compressive test results [24].

The use of TPS bottom ash has been found substantial up to 30–50% for non-superplasticizer to superplasticizer in concrete. 100% of coal bottom ash can be used in concrete specimens where workability is not a significant factor; like paving blocks and pavements [15]. Low calcium bottom ash has more strengthen properties than normal concrete [21]. Cheriaf et al. [9], also illustrated bottom ash advantageous merits for solution to fine aggregates and has met the requirements of European standard EN 450 [10]. The strength aspect is a critical issue due to some economic and environmental views [16–20].

Kim and Lee [13], investigated bottom ash effects on high strength concrete and did not notice any considerable change but slightly modulus of elasticity reduces. The key advantage of TPS bottom ash in concrete is dead weight reduction. The low specific gravity resulted in a low density as compared to normal control concrete. Many investigations did on coal ash utilization as cement replacement along with fine and coarse aggregate [1, 11, 22]. Mahdi et al. [14], suggested that good results of fresh phase and hardened phase properties of concrete were possible but results of workability reduce when bottom ash percentage increases. Based on the review of available literature, till having mechanical properties of incorporated bottom ash reporting minor in the preparation of mortar, we want to introduce sustainable material in the form of bottom ash, and its need to asses all other important parameters missing in existing. Therefore, intentionally the present study focused on determining the optimum use of bottom ash in mortar as fine aggregates and finding the optimum utility level by multiple replacements in mortar. The assessment of compressive strength and workability of mortar specimens were taken as the key elements for sustainability approach.

2 Materials Used

The present exploration deals with the materials used in this study work. The following paragraphs presents the materials and their properties used in the experimental work. Tests were performed to know the materials properties. The characterizations, as per appropriate codes of practices, were used for production the Mortar.

As per the following IS:12269-2008 [3], the cement was used for experimental study. To achieve the targeted strength levels, the misting researcher has chosen ordinary Portland cement of grade 53 instead of grade 43 and grade 33. Therefore, 53 MPa grade OPC of Chettinad company cement was used for all testing, before actual experimentation cement was tested for physical and chemical characteristics. The initial setting time and final setting time were found 240 and 330 min, respectively, and the consistency performed between ranges 32–33. The mean particle dia (μm) of cement was 22. The major chemical oxides CaO, SiO_2, Al_2O_3 were 65.39%, 20.61%, and 5.31%, respectively.

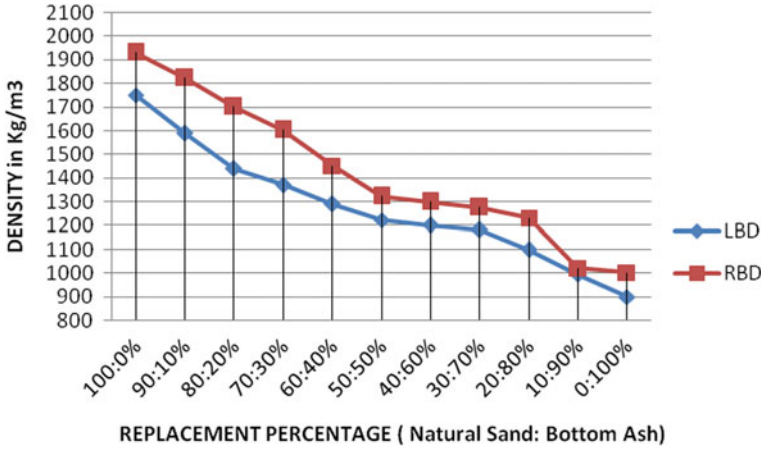

Fig. 2 Effect of replacement of natural sand with bottom ash on LBD and RBD

Fresh drinkable tap water according to IS 456: 2000 [5] is used for preparing mortar mix and all testing. Natural river sand obatined from a local river and conforming to IS 2116–1980 [4] has been used as fine aggregate for preparing mortar cube specimens. The specific gravity of natural river sand used was found to be 2.75. The bottom ash also has taken into account as fine aggregate for restricted replacement of FA. The TPS bottom ash was collected from Eklahare Thermal Power Station. Loose bulk density (LBD) was found 1750 kg/m^3 for zero percentage replacement (BA); as a percentage of bottom ash increases, LBD was slowly down up to 45%, and for 100%, bottom ash LBD was 900 kg/m^3. The similar behavior was seen in RBD, 1930 kg/m^3 was found for zero percentage replacement (BA) and 1002 kg/m^3 for 100% replacement. The details of LBD and RBD are graphically given in Fig. 2.

3 Experimental Program

The research work was carried out on mortar mixes that made from cement and bottom ash. This was followed by the bottom ash mortar mixes of different grades and percentage replacement. The effect of incorporating bottom ash by partial or full replacement of fine aggregates on the mortar hardened state was assessed. For the easy in experimentation, the identification was given to specimens of different proportion mixes. The specimens were designated as CM-B, i.e. CM(2, 3, 4, 6, 8)-B(0, 25, 50, 75, 100). 0, 25, 50, 75, and 100 represent the replacement percentage of sand by bottom ash, and 2, 3, 4, 6, 8 represented the mortar mix proportions of range 1:2, 1:3, 1:4, 1:6, and 1:8. The study area comprises of higher to lean mortar mixes with flow table test at broad trials of w/c ratios.

Fig. 3 Failure pattern of mortar cube testing in CTM

Compressive strength of mortar cubes of size (70.6 × 70.6 × 70.6) mm was estimated as per IS 2250–1981 [2]. The specimens were casted and tested in compressive testing machine (CTM) (Fig. 3) as per the standard procedures. Instantaneously after de-molding, cube specimens are cured in water for 7 days, 14 days, and 28 days. For CTM, the cube specimens are carefully aligned with the center of the thrust of steel rounded plates of the testing machine, and loading was applied at the same rate of 3.5 kN/s till failure seen. The ultimate load at failure was recorded for every specimen.

4 Results and Discussion

During BRCM mixes, it was needed to extra additional water to the proposed mixes (in the relation of correction for water absorption of bottom ash) to form the required flow. The workability of mortar was measured in terms of flow table test and reported graphically in Fig. 4. From the workability observations with flow table test of BRCM mixes at various percentage replacements and critic it with that of normal cement mortar (NCM: zero replacement level of bottom ash), the few comments are made. All the tested BRCM mixes achieved the workability requirements in terms of flow test for different BRCM mixes. They found good results even ranging from 90 to 100%. However, it is experiential of the replacement, percentage of bottom ash increases; workability in relation to the flow regularly decreases due to the richness of mortar. The BRCM mixes for higher grades of 1:2, 1:3, and 1:4 also fulfilled the percentage flow range from 94 to 100 till 75% replacement level. If looking into remaining BRCM mixes, they have percentage flow value between 90 and 100.

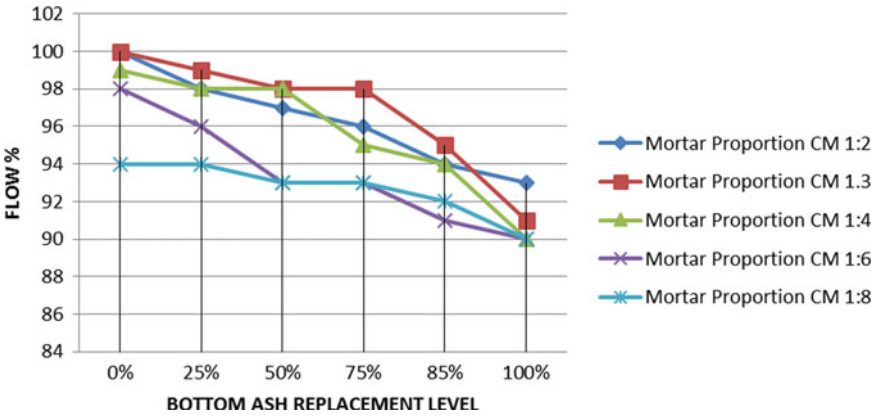

Fig. 4 Workability in flow term of BRCM mixes

The demand for water proportionally increases by bottom ash replacement level. The inclination of bottom ash to absorbed water and necessary more water during proper mixing. The call of water (or increased *w/c* ratio) is much greater obvious for leaner grades of mortar as compared to superior grades of the mortar due to the percentage of bottom ash particles rises in leaner mortar mixes resultant in increased water absorption. The alternate reason for increased water quantity is because of higher surface area occupied by bottom ash, as it covers more particle content than natural river bed sand.

The compressive strength of Bottom Ash Replaced Cement Mortar (BARCM) and (zero replacement level of bottom ash) ZRCM mixes were considered and presented in Table 1 at curing periods of 7 days, 14 days, and 28 days. In the experimentation trials, the behavior of Bottom Ash Replaced Cement Mortar (BARCM) and normal cement mortar (NCM: zero replacement level of bottom ash) studied and plotted relations between them in Fig. 5 and its normalized nature of graph plotted in Fig. 6. The compressive strength of BARCM mixes is seen less than that of ZRCM mixes. However, the obtained compressive strength of altered grades of mortar is higher than that specified as per IS 1905–1987 [6]. As the replacement of bottom ash by natural sand increases from 0 to 100% at 25% intervals, there is seen a reduction in the compressive strength results in all grades of mortar. The rates of reduction are reliant on the grades of mortar, cement, and bottom ash content in each mix. Reduction in compressive strength observed is 8.32%, 9.36%, 14.54, 31.88, and 23.21% For CM (1:2, 1:3, 1:4, 1:6, and 1:8), respectively, at 25% bottom ash replacement, noticeable reduction is detected when the replacement level is enlarged from 25 to 50%. An average reduction in the strength is in the range of 46% (range is 36–52%) at RL of 50%. Similarly, average strength is 53.31% reduction at RL of 75 and 63.51% reduction at RL of 100%, respectively. The rate of reduction of compressive strength is much greater in leaner mortar mixes that at rich mortar mix. But the obtained compressive strength of altered grades of mortar is higher than that of specified as

Table 1 Results of compressive strength for different mortar grades

Mortar type (C:FA)	Replacement %	Mortar proportion			Designation of mix	Compressive strength (MPa) at curing age		
		C	NS	BA		7	14	28
CM(1:2)	0	1	2	0	2M-B0	10.68	11.54	13.58
CM(1:2)	25	1	1.5	0.5	2M-B25	7.39	8.14	12.45
CM(1:2)	50	1	1	1	2M-B50	4.56	5.31	6.5
CM(1:2)	75	1	0.5	1.5	2M-B75	3.99	4.41	6.21
CM(1:2)	100	1	0	2	2M-B100	3.42	3.89	4.23
CM(1:3)	0	1	3	0	2M-B0	9.09	10.49	12.17
CM(1:3)	25	1	2.25	0.75	3M-B25	5.13	6.11	11.03
CM(1:3)	50	1	1.5	1.5	3M-B50	4.28	4.87	6.47
CM(1:3)	75	1	0.75	2.25	3M-B75	2.29	3.04	5.23
CM(1:3)	100	1	0	3	3M-B100	2.01	2.76	3.83
CM(1:4)	0	1	4	0	4M-B0	4.76	5.87	7.63
CM(1:4)	25	1	3	1	4M-B25	3.02	3.75	6.52
CM(1:4)	50	1	2	2	4M-B50	2.86	3.6	3.92
CM(1:4)	75	1	1	3	4M-B75	2.29	2.9	3.62
CM(1:4)	100	1	0	4	4M-B100	1.71	2.47	2.78
CM(1:6)	0	1	6	0	6M-B0	3.59	5.59	6.21
CM(1:6)	25	1	4.5	1.5	6M-B25	2.57	3.24	4.23
CM(1:6)	50	1	3	3	6M-B50	2.15	2.47	3.38
CM(1:6)	75	1	1.5	4.5	6M-B75	1.84	2.37	3.22
CM(1:6)	100	1	0	6	6M-B100	1.84	2.31	2.61
CM(1:8)	0	1	8	0	8M-B0	2.69	3.69	4.91
CM(1:8)	25	1	6	2	8M-B25	2.38	2.75	3.77
CM(1:8)	50	1	4	4	8M-B50	1.86	2.19	3.1
CM(1:8)	75	1	2	6	8M-B75	1.71	2.02	2.23
CM(1:8)	100	1	0	8	8M-B100	1.58	1.9	2.03

per IS 1905–1987; it shows addictive features of bottom ash to develop sustainable mortar future (Table 2).

Even though only if 25% of bottom ash is utilized as replacement of natural sand for preparation of cement mortar, the exploitation of resources can be maintained at a certain level and play an important role to achieve a sustainable future. Finding new unconventional materials for sustainable progress so as to noticeably decrease the utilization of accepted resources became necessary to safeguard the comforts of future construction activities.

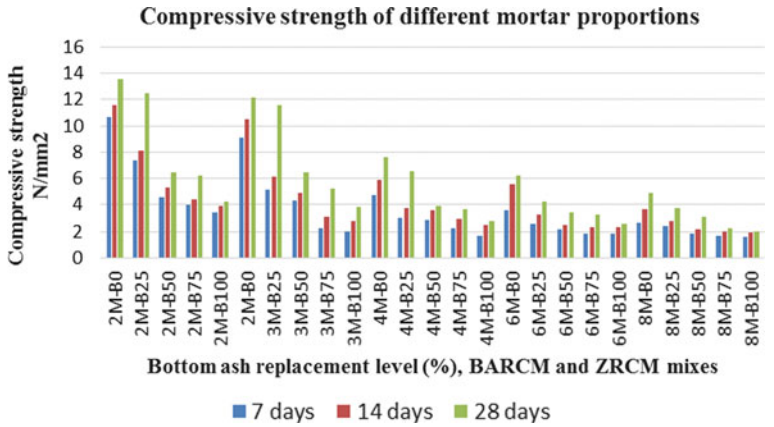

Fig. 5 Compressive strength of BARCM and ZRCM

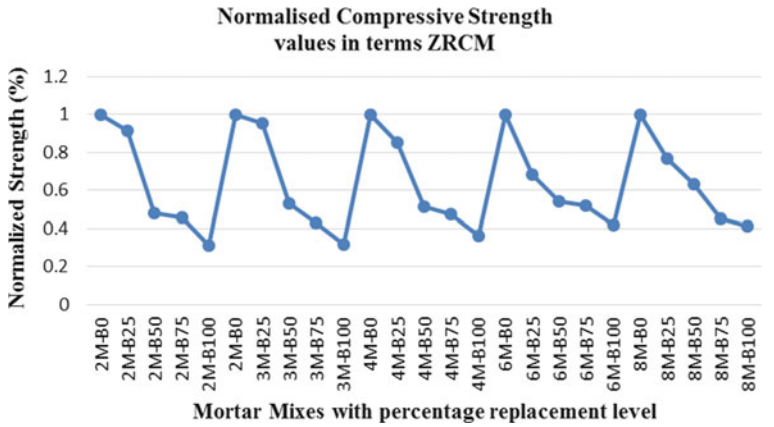

Fig. 6 Normalization strength percentage of bottom ash replacement at curing age 28 days

5 Concluding Remark

- Mortar mixes up to 75% replacement level are workable and fulfilling the flow requirement for all mixes excluding CM 1:8 may be due to tough mix nature.
- Growth of strength over age of BARCM mixes at different cement proportions, and also, it is similar in nature to normal mortar mixes.
- Compressive strength reduction is seen; as bottom ash percentage increases, but all results satisfy the strength margin described in IS 1905-1987.
- Bottom ash with particles lesser than 4.75 mm is recommended for use in the mortar.

Table 2 Normalized values of compressive strength of BARCM mixes in terms of strength of ZRCM mixes

Designation of mix	Normalized compressive strength			Designation of mix	Normalized compressive strength		
	7 days	14 days	28 days		7 days	14 days	28 days
2M-B0	1.00	1.00	1.00	4M-B0	1.00	1.00	1.00
2M-B25	0.69	0.71	0.92	4M-B25	0.63	0.64	0.85
2M-B50	0.43	0.46	0.48	4M-B50	0.60	0.61	0.51
2M-B75	0.37	0.38	0.46	4M-B75	0.48	0.49	0.47
2M-B100	0.32	0.34	0.31	4M-B100	0.36	0.42	0.36
2M-B0	1.00	1.00	1.00	6M-B0	1.00	1.00	1.00
3M-B25	0.56	0.58	0.95	6M-B25	0.72	0.58	0.68
3M-B50	0.47	0.46	0.53	6M-B50	0.60	0.44	0.54
3M-B75	0.25	0.29	0.43	6M-B75	0.51	0.42	0.52
3M-B100	0.22	0.26	0.31	6M-B100	0.51	0.41	0.42

- Bottom ash can be used for making mortar of all grades between CM (1:2) to CM (1:8) replacing sand up to 25% without negotiation in compressive strength.
- Involvement of pozzolanic effect on the strength at curing period is not visible. Inclusion of bottom ash does not call for prolonged curing in link to that of normal mortar mixes.
- The bottom ash advantages have eye catching toward environmental impacts and substituent to traditional mortar with cost economic.

References

1. Aggarwal Y, Siddique R (2014) Microstructure and properties of concrete using bottom ash and waste foundry sand as partial replacement of fine aggregates. Constr Build Mater 54:210–223
2. Bureau of Indian Standards (1981) IS 2250: code of practice for preparation and use of masonry mortars. Bureau of Indian Standards, New Delhi
3. Bureau of Indian Standards (Reaffirmed 2008) IS 12269-1987: specification for 53 grade ordinary Portland cement. Bureau of Indian Standards, New Delhi
4. Bureau of Indian Standards (Reaffirmed 2007) IS 2116-1980: sand for masonry mortars. Bureau of Indian Standards, New Delhi
5. Bureau of Indian Standards (2000) IS 456: code of practice for plain and reinforced concrete. Bureau of Indian Standards, New Delhi
6. Bureau of Indian Standards (Reaffirmed 2007) IS 1905-1987: code of practice for structural use of unreinforced masonry. Bureau of Indian Standards, New Delhi
7. Central Electricity Authority (2011) Report on fly ash generation at coal/lignite based thermal power stations and its utilization in the country for the year 2010–11. CEAI, New Delhi, India
8. Central Electricity Authority (2017) Report on fly ash generation at coal/lignite based thermal power stations and its utilization in the country for 1st half of the year 2016–17. CEAI, New Delhi, India

9. Cheriaf M, Rocka JC, Pera J (1999) Pozzolanic properties of pulverized coal combustion bottom ash. Cem Concr Res 29:1387–1391
10. EN 450-1 (2012) Fly ash for concrete—Part 1: definition, specifications and conformity criteria, Comite Europeen de Normalisation
11. Ghafoori N, Bucholc J (1997) Properties of high-calcium dry bottom ash concrete. ACI Mater J 94:90–101
12. Ghafoori N, Bulholc J (1999) Investigation of lignite-based bottom ash for structural concrete. J Mater Civil Eng 8(3):128–137
13. Kim HK, Lee HK (2011) Use of power plant bottom ash as fine and coarse aggregate in high-strength concrete. Constr Build Mater 25:1115–1122
14. Mahdi R, Jahangir M, Mohd RS, Mohd WH, Elnaz K (2016) Investigation of coal bottom ash and fly ash in concrete as replacement for sand and cement. Constr Build Mater 116:15–24
15. Malkit S, Rafat S (2015) Effect of coal bottom ash as partial replacement of sand on workability and strength properties of concrete. J Clean Prod xxx:1–11
16. Mehta PK (1997) Durability critical issues for the future. Concr Int 19(7):69–76
17. Mehta PK (1999) Advancements in concrete technology. Concr Int 21(6):27–33
18. Mehta PK (2001) Reducing the environmental impact of concrete. Concr Int 23(10):61–65
19. Mehta PK (2001) Building durable structures in the 21st century. Concr Int 23(11):57–63
20. Mehta PK (2002) Greening of the concrete industry for sustainable development. Concr Int 24(7):23–27
21. Singh M, Siddique R (2014) Strength properties and micro-structural properties of concrete containing coal bottom ash as partial replacement of fine aggregate. Constr Build Mater 50:246–256
22. Sua-iam G, Makul N (2014) Utilization of high volumes of unprocessed lignite-coal fly ash and rice husk ash in self-consolidating concrete. J Clean Prod 78:184–194
23. Topc-u IB, Canbaz M (2004) Properties of concrete containing waste glass. Cem Concr Res 34(2):267–274
24. Yuksel I, Turhan B, Omer O (2007) Durability of concrete incorporating non-ground blast furnace slag and bottom ash as fine aggregate. Build Environ 42:2651–2659
25. Yuksel I, Bilir T (2005) Usage of blast furnace slag to produce concrete pavement blocks and kerbs. In: Özer MF (ed) Kocaeli national symposium on earthquake. Kocaeli University, pp 870–880 (in Turkish (CD))
26. Yuksel I, Ozkan O, Bilir T (2003) Usage of granulated blast furnace slag as fine aggregate in concrete. In: Ozkul MH (ed) Proceedings of fifth national congress on concrete (durability of concrete). Turkish Chamber of Civil Engineers, pp 471–481

Comparative Study Between Weighted Overlay and Fuzzy Logic Models for Landslide Vulnerability Mapping—A Case Study of Rampur Tehsil, Himachal Pradesh

C. Prakasam, R. Aravinth, Varinder S. Kanwar and B. Nagarajan

Abstract The present research paper is an attempt to assess the vulnerability of Rampur Tehsil to landslides using weighted overlay and fuzzy logic methods. Causative factors such as land use, land cover, slope, geology, soil, and geomorphology have been used to assess landslide vulnerability. Survey of India Toposheets, Geological Survey of India Maps, ASTER GDEM, and LANDSAT 8 OLI/TIRS sensors are used as data sources. The causative factors were analyzed and processed in GIS environment. Fuzzy logic and weighted overlay method have been used to categorize the vulnerability zones of the study area. The weightages were assigned based on fuzzy logic rule of for macroscale landslide mapping and weighted overlay scale ranging from 1 to 5 for very low vulnerability to very high vulnerability. From the results, it can be interpreted that most of the study areas come under very high vulnerability class. The fuzzy values for each class vary from 0.6 to 0.8 for high vulnerability and from 0.81 to 0.96 for very high vulnerability class. About 57% of the area comes under very high vulnerability class, and rest 47% accounts for high vulnerability class. When it comes to weighted overlay model, nearly 80.24% and 13.68% of the area fall and under high and moderately vulnerable category. The rest minor quantities fall under very high and low categories.

Keywords Vulnerability mapping · Fuzzy logic · Fuzzy gamma operator · Weighted overlay · LULC · Soil

C. Prakasam (✉) · R. Aravinth · V. S. Kanwar
Department of Civil Engineering, Chitkara University, Solan, Himachal Pradesh, India
e-mail: cprakasam@gmail.com

B. Nagarajan
Department of Civil Engineering, Indian Institute of Technology Kanpur, Kanpur, Uttar Pradesh, India

V. S. Kanwar and S. K. Shukla (eds.), *Sustainable Civil Engineering Practices*,
Lecture Notes in Civil Engineering 72,
https://doi.org/10.1007/978-981-15-3677-9_16

1 Introduction

Hill ecosystem is one of the most fragile ecosystems in the world, leading to various geohazard and environmental problems due to various natural and anthropogenic causes [1]. Landslides are among one of the important catastrophic disasters occurring in mountain region leading to the change of surface geomorphology [2]. In India, 0.14 million km^2 is prone to landslide hazards falls under northeast Himalayas (Darjeeling and Sikkim) (GSI Web site). The Himalayan region is more prone to slope instability due to its rugged terrain [3]. Every year the state is affected by huge number of landslides that cause loss of life, damages to houses, roads, communication lines, and agricultural lands, where some of the examples [4]. Recent incidents such as landslide occurred on Mandi–Pathankot NH 154 with 46 life lost and damage to the road; landslides occurred near Dhalli Tunnel along the Kalka–Shimla NH 5A leading to damaged buildings, parked vehicles, and roads are some of the examples for the intensity of the landslides.

Prakash [5] compiled a list of historical socioeconomically significant landslides around India, where 371 events of reported landslides event occurred from the year 1800–2011. Based on his findings, he concluded that west and northwest of Himalayas are highly prone to landslides accounting for about 49% of the people killed and 51% of the landslide occurrences. The data on various occurrences and fatalities is given in Table 1.

Many researchers and scientists have previously analyzed landslide vulnerability for multiple areas. Anbalagan and Parida [6] studied the geo-environmental problems of harmony landslide in Uttarakhand. Anbalagan and Singh [7] studied landslide vulnerability mapping for Kumaun Himalayas using various causative factors such as geomorphology, geology, slope, and soil rainfall. Kanungo et al. [8], Martha et al. [1], Naithani [9], Rawat et al. [10], Saha et al. [11] were some other researchers who made notable contribution in the field of landslide vulnerability mapping. Anbalagan et al. [12], Bibi et al. [13], Leonardi et al. [14], Mijani and Samani [15], Rahaman et al. [16], these papers were studied and interpreted more for the current landslide analysis.

Table 1 Data on various events and fatalities between (1800–2011)

Sl. No.	Year	No. of socioeconomically significant events	Persons killed	No. of fatal events
1	2011	26	74	19
2	2010	85	368	53
3	2009	47	270	46
4	2008	36	220	30
5	2007	54	409	39
6	1800–2007	123	2630	61

Source Prakash [5]

1.1 Objectives

1. Preparation of various thematic layers such as land use, land cover, relative relief, and slope morphometry.
2. To categorize the various layers into vulnerable hazards, using fuzzy logic and weighted overlay method.
3. To delineate landslide vulnerable zones using fuzzy logic and weighted overlay method through remote sensing and GIS techniques.

2 Study Area

Rampur Tehsil (Fig. 1) is located between 31°15′3″ to 31°44′10″ north latitude and 77°30′19″ to 77°59′21″ east longitude. The total geographical extent of Rampur Tehsil is 987 km^2. According to the 2011 census, Rampur Tehsil consists of two hundred and eighteen villages and a total population is 77,542. The literacy rate stands at 93.63% which is greater than the literacy rate of Himachal Pradesh is 91.4%. Sutlej is the main river that drains through the Rampur Tehsil. The soil features of Rampur have been classified into three main types, namely coarse loam, fine loam, and glaciers. The geology of the study area can be differentiated into schist, slate, alluvium, and glacier. Timber and charcoal are the important forest producers. Besides them, resins, grass, medicinal herbs, and bamboos are also produced at minor quantity. Agriculture and horticulture are the important economic activities of the Rampur Tehsil. Along with that tourism and other small-scale industrial jobs bring a boon to Rampur Tehsil. Most of Tehsil's agriculture is dependent on rainfall. The climate is suitable for growing cereals, off-season vegetables, temperate, and stone fruits. The study area has subtropical highland climate under Koppen climate classification. The climate is subtropical in the valleys and temperate in the hilltops. The average annual rainfall of the study area is 999.4 mm out of which 75% occurs during the monsoon period from June to September. The temperature can go as low as 0 °C during winter times and as much as 40 °C during summer times.

3 Data Used

The base map was created using Survey of India Toposheets 53E/10, 53E/11, 53E/14, 53E/15 at 1: 50,000 scale. The land use and land cover were prepared using LANDSAT 8 OLI/TIRS sensor obtained from United States Geological Survey (USGS) Web site. The geology, geomorphology, and soil map was prepared using data obtained from soil and land use Survey of India. The slope morphometry was prepared from ASTER GDEM data obtained from USGS Web site. Table 2 depicts the data used for the study.

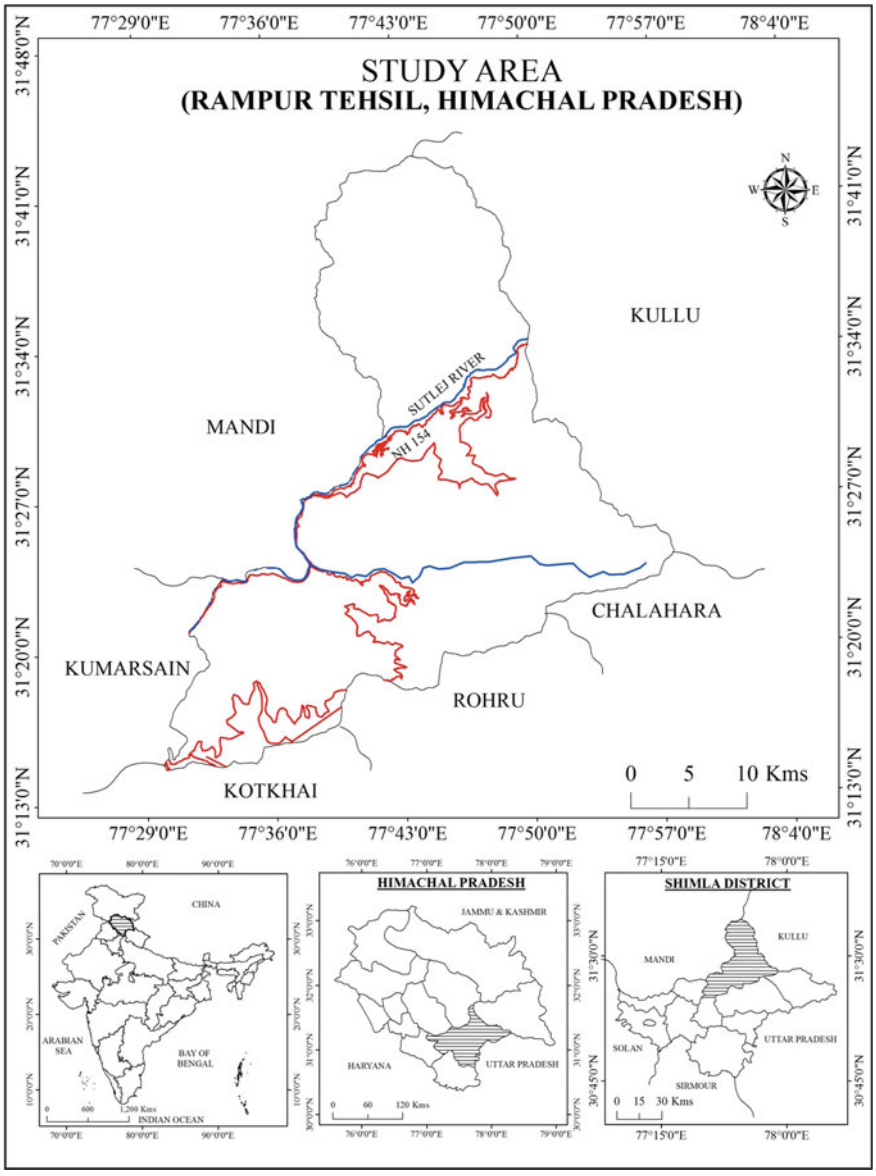

Fig. 1 Study area (*source* Authors)

Table 2 Data used

Sl. No.	Data	Source	Year	Resolution
1	Toposheets	Survey of India (53E/10, 53E/11, 53E/14, 53E/15)	1974	1:50,000
2	Land use and land cover	Earth explorer (USGS)	26/01/2018	30 mts
3	Geology	Soil and land use survey of India	–	1:50,000
4	Geomorphology	Soil and land use survey of India	–	1:50,000
5	Soil	Soil and land use survey of India	–	30 mts
6	Slope	ASTER GDEM	2009	30 mts

4 Research Methodology

The methodology adopted in the research is fuzzy logic and weighted overlay models (Fig. 2). In fuzzy logic method, each explanatory landslide causes assigned with a value from 0 to 1 based on the degree of association of landslide occurrences. These values are then integrated using fuzzy gamma operator or fuzzy algebraic sum to produce landslide hazard zonation maps. The data was analyzed and processed in GIS environment to find the vulnerability extent of the landslide in Rampur Tehsil. The vulnerable zones were categorized into five zones ranging from very low hazard zone

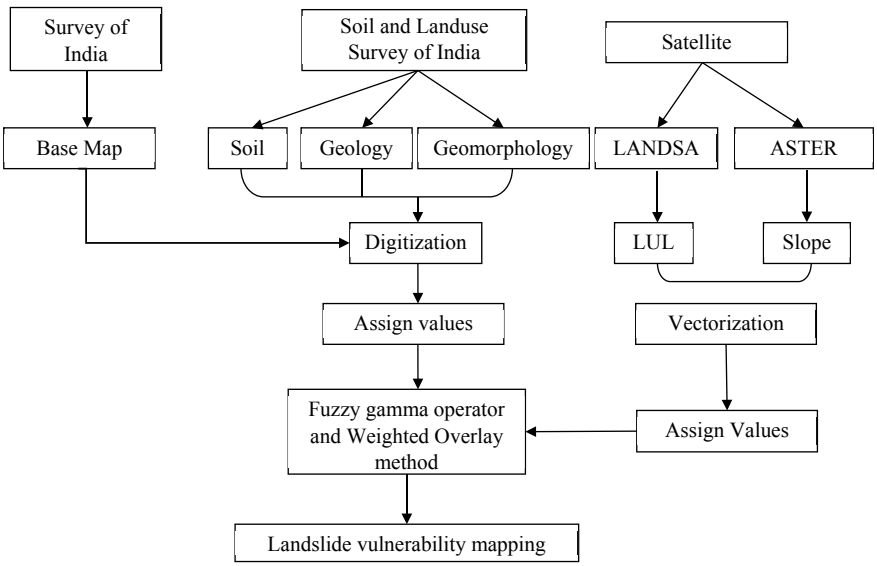

Fig. 2 Research methodology

to very high hazard zone. The weighted overlay model uses a ranking method in order to classify their landslide causing factors. Values from 1 to 5 are ranked depending upon their relation with landslide initiation factors where 5 denotes severely prone to landslide and value of 1 denotes least prone to landslides [17–19]. These values were then integrated into GIS environment to produce final vulnerability maps. Many other authors also studied landslide vulnerability using weighted overlay models [20–25] (Figs. 3 and 4).

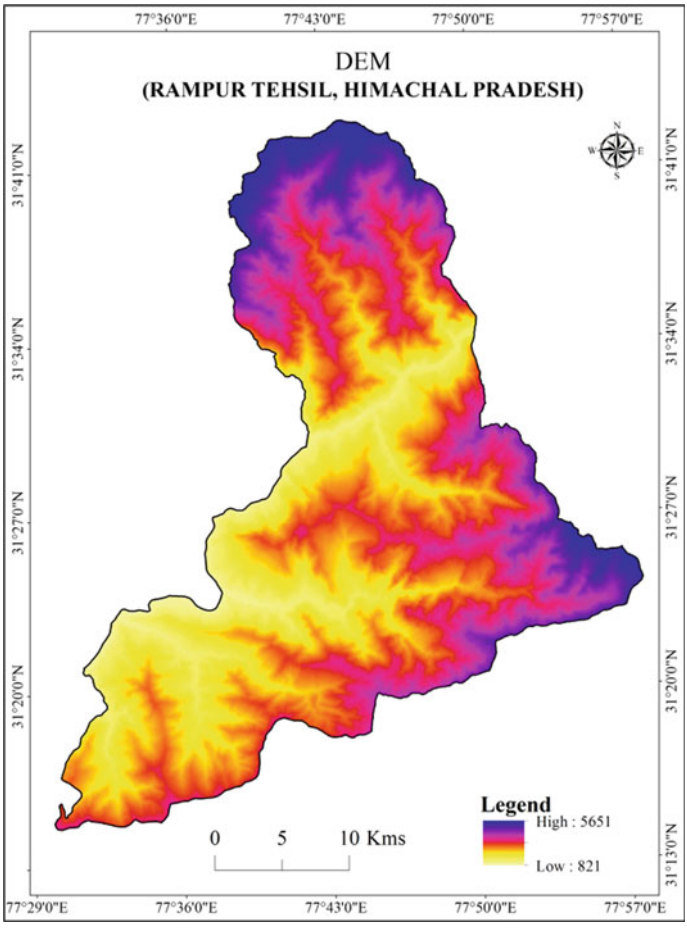

Fig. 3 DEM

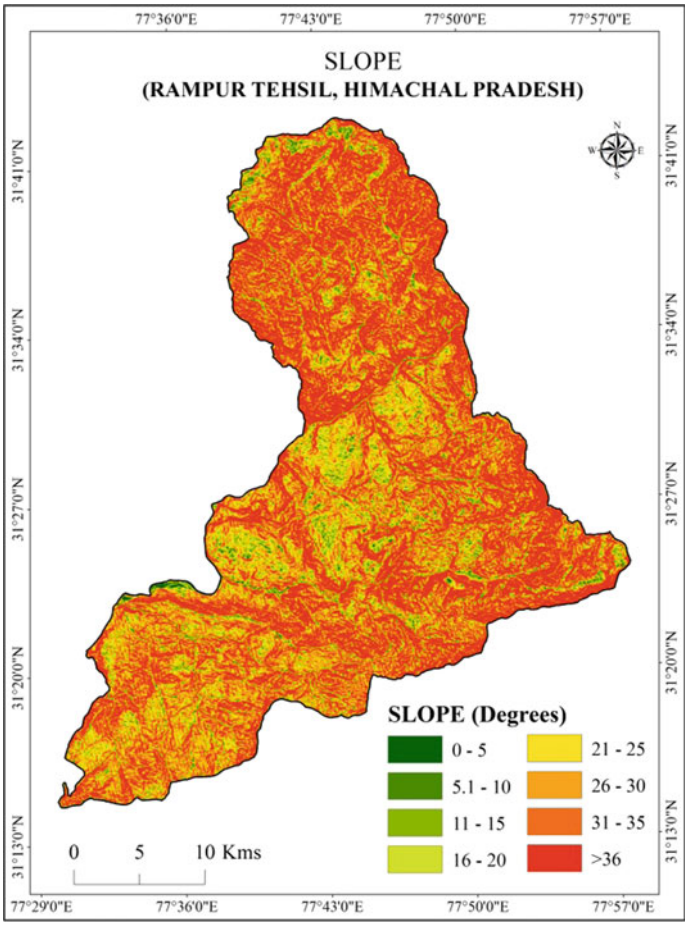

Fig. 4 Slope

5 Data Analysis

5.1 Land Use and Land Cover

Land use and land cover are important causative factors in landslide vulnerability. Extensive deforestation and construction of buildings may reduce the cohesion between soils and can cause slope instability leading to mass movements and landslides [26]. Land use and land cover were prepared from LANDSAT 8 OLI/TIRS sensor for the year 2018 (Table 3). The data was layer stacked and processed through supervised classification using maximum likelihood classifier method. Rampur Tehsil was classified into four classes, namely glacier, forest, agriculture, barren land, and build-up area. Land use and land cover were classified using NRSC level

Table 3 Total area coverage and fuzzy and weighted overlay values for LULC

Sl. No.	LULC	Area in km^2	Percent (%)	Fuzzy values	Weighted overlay
1	Agricultural land	114.14	11.55	0.3	3
2	Barren land	138.89	14.06	0.4	4
3	Build-up land	12.58	1.27	0.2	5
4	Forest	661.77	66.99	0.1	2
5	Glacier	60.52	6.13	0	1
	Total	987	100.00		

1 classification system (Fig. 5). Forest plays the least vulnerable role in landslide occurrences. Forest has the ability to hold the soils in place through the binding of roots to the soil. Agriculture lands are prone to landslide occurrences due to their shallow root penetration, lessening the ability to hold the soil particles in place. Barren land is highly exposed with no vegetation and hence has higher chances of landslide initiation due to various landslide inducing factors such as rainfall and earthquake. Rampur is highly mountainous region and most of the area falls under forest and glaciers—66.99% of the area falls under forest cover, 14.06% of the area falls under agriculture, and glacier covers about 11.55 and 6.13%, respectively (Fig. 6).

5.2 Geology

Geology is the study of physical characteristics of rocks such as size, texture, core samples. Geology was digitized from soil and land use Survey of India maps at 1:50,000 scales (Table 4). The geology of the study area mainly covers four distinct types, namely glacier, alluvium, schist, and slate (Fig. 7). Both schist and slate account for 29.48% and 59.60%. Glacier accounts for about 10.3%, and the rest are present in minor quantities.

5.3 Soil

The soil class in the study area is diversified into three classes, namely coarse loam, fine loamy, and glacier (Table 5, Fig. 8). Fine loamy covers about 84.5% while glacier and coarse loamy cover about 10.4 and 5.03%. Coarse loamy and fine loamy soils play a huge role in landslide occurrences. The soils vary in size ranging from 2 to 63 micrometers according to the soil classification system. These particles can be easily eroded and transported due to external forces. They are susceptible to landslides during rainfall season or any major earthquakes where the ground deformation is high. Glaciers are huge ice sheets that are usually covered up with snow formed materials at several meters. These features are the least prone to landslide occurrences.

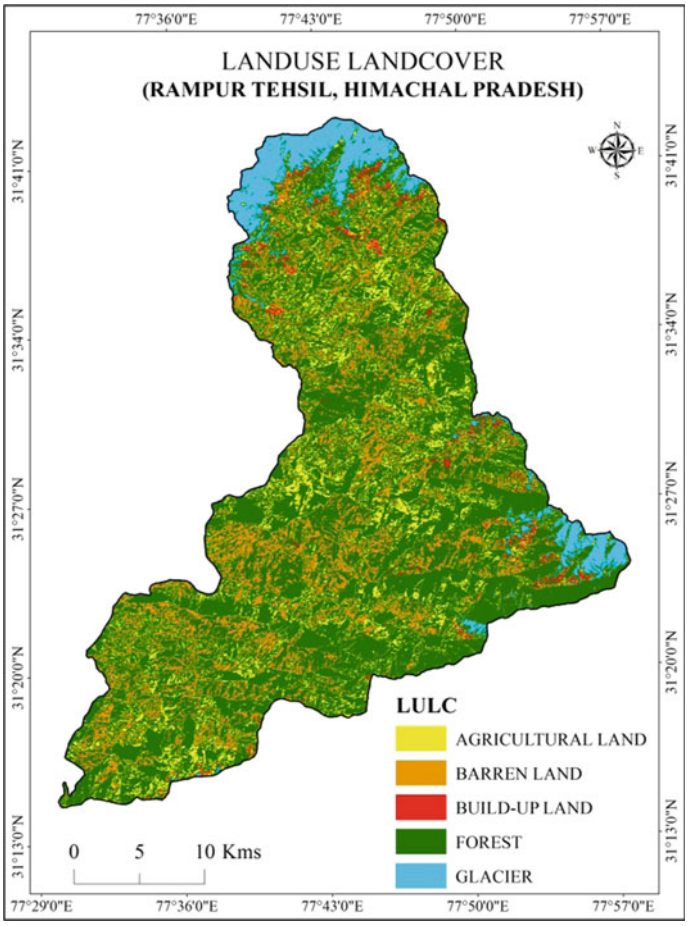

Fig. 5 LULC

5.4 Geomorphology

The geomorphology of the study area is classified into four types, namely glaciers, river terraces, undifferentiated hillside slopes, and undifferentiated mountainside slopes (Table 6). Nearly 83.52% of the study area falls under undifferentiated mountainside slopes. Undifferentiated hillside slopes and glaciers cover about 10.41 and 5.54%.

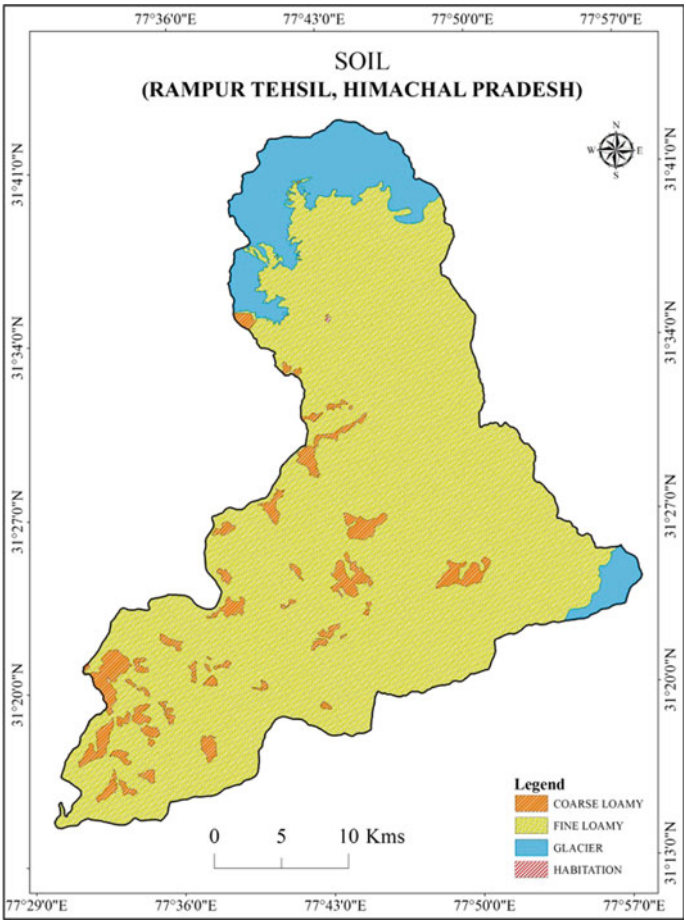

Fig. 6 Soil

Table 4 Total area coverage and fuzzy and weighted overlay values for geology

Sl. No.	Geology	Area in km^2	Percent (%)	Fuzzy values	Weighted overlay
1	Alluvium	5.08	0.51	0.3	4
2	Glacier	102.65	10.39	0.08	1
3	Habitation	0.14	0.01	0.1	5
4	Schist	291.22	29.48	0.5	2
5	Slate	588.81	59.60	0.4	2
	Total	987	100.00		

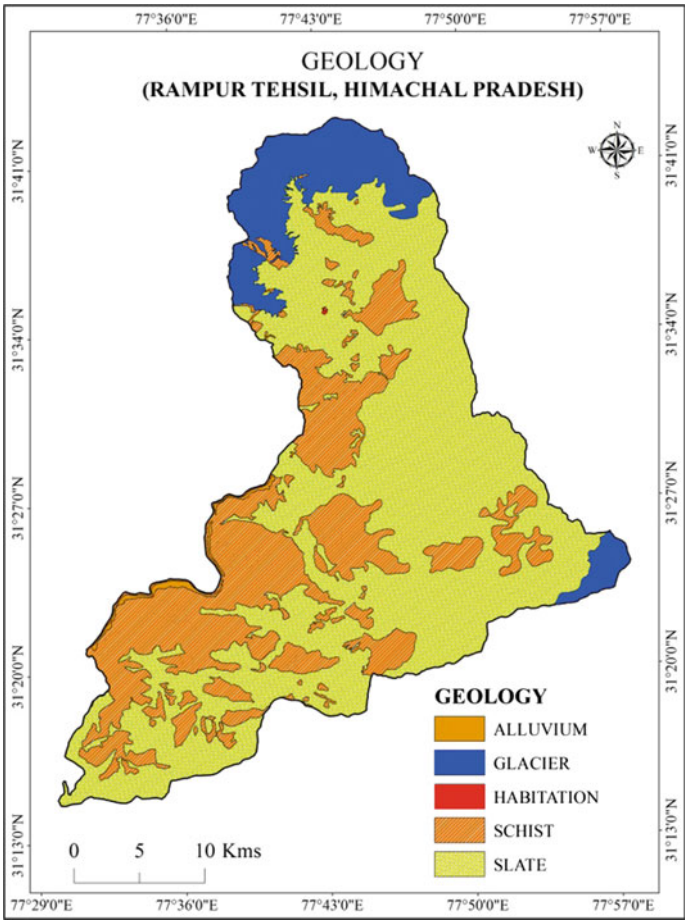

Fig. 7 Geology

Table 5 Total area coverage and fuzzy and weighted overlay values for soil

Sl. No.	Soil	Area in km^2	Percent (%)	Fuzzy values	Weighted overlay
1	Coarse loamy	49.69	5.03	0.12	3
2	Fine loamy	835.22	84.55	0.15	4
3	Glacier	102.85	10.41	0	1
4	Habitation	0.14	0.01	0.09	5
	Total	987	100.00		

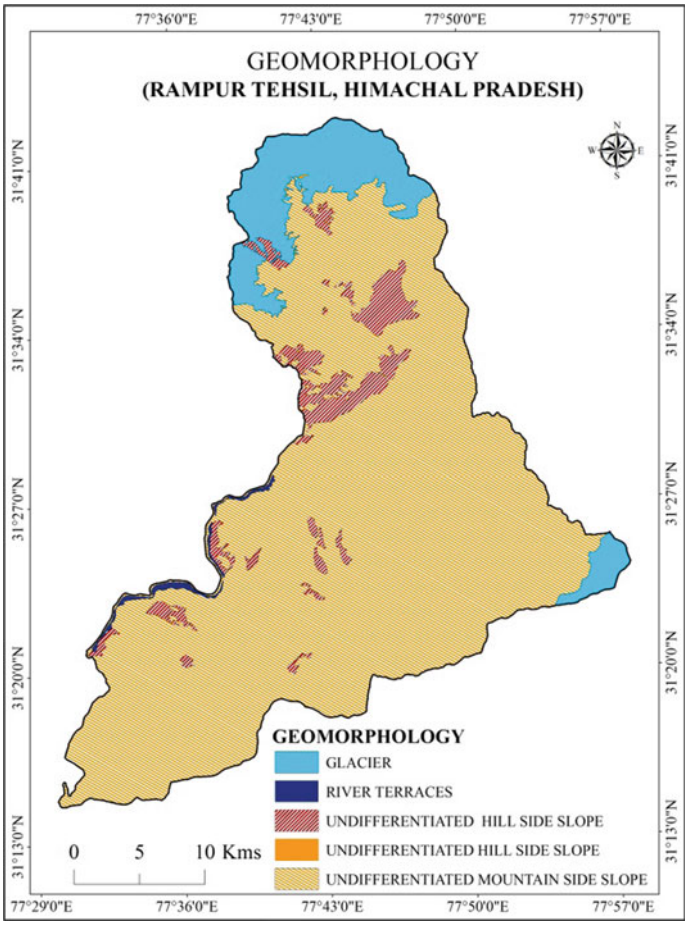

Fig. 8 Geomorphology

Table 6 Total area coverage and fuzzy and weighted overlay values for geomorphology

Sl. No.	Geomorphology	Area in km^2	Percent (%)	Fuzzy values	Weighted overlay
1	Glacier	102.85	10.41	0	1
2	River terraces	5.19	0.53	0.3	4
3	undifferentiated hill side slope	54.77	5.54	0.22	3
4	Undifferentiated mountain side slope	825.08	83.52	0.19	3
	Total	987	100.00		

Table 7 Total area coverage and fuzzy and weighted overlay values for slope

Sl. No.	Slope (degrees)	Fuzzy values	Weighted overlay
1	0–18	0.12	1
2	19–28	0.15	2
3	29–37	0	3
4	38–47	0.09	4
5	48	1	5

5.5 Slope

Slope plays an important aspect in landslide vulnerability mapping. The steeper the slope of an area, the more it is prone to landslides under gravity conditions. The slope is derived from ASTER GDEM with a spatial resolution of 30 mts. The slope has been categorized into five types (Fig. 4) based on vulnerability (Table 7).

6 Results and Discussion

In the present study, fuzzy logic and weighted overlay method were used to calculate the landslide vulnerability assessment. Various factors such as slope, LULC, geology, geomorphology, and soil were used as causative factors to derive the final conclusion. The factors were then assigned their respective fuzzy values referred from various literature reviews. Then these values were analyzed through fuzzy gamma logic to produce final landslide vulnerability maps (Fig. 9). Assigned fuzzy classes and their corresponding area coverage are given in Table 8.

The weighted overlay analysis was carried out in GIS environment using overlay statistics method (Fig. 10). Five causative factors such as soil, geology, geomorphology, slope, and LULC were considered as landslide causative factors. Each sub-category of factors has been ranked from 1 to 5 depending upon their relation with landslide activities. The layers were then integrated by giving equal weightage to all the layers to produce landslide vulnerability map. Assigned weighted values and their corresponding area coverage are given in Table 9.

7 Conclusions

a. The fuzzy values for each class vary from 0.6 to 0.8 for high vulnerability and 0.81 to 0.96 for very high vulnerability class. About 57% of the area comes under very high vulnerability class, and rest 47% accounts for high vulnerability class.

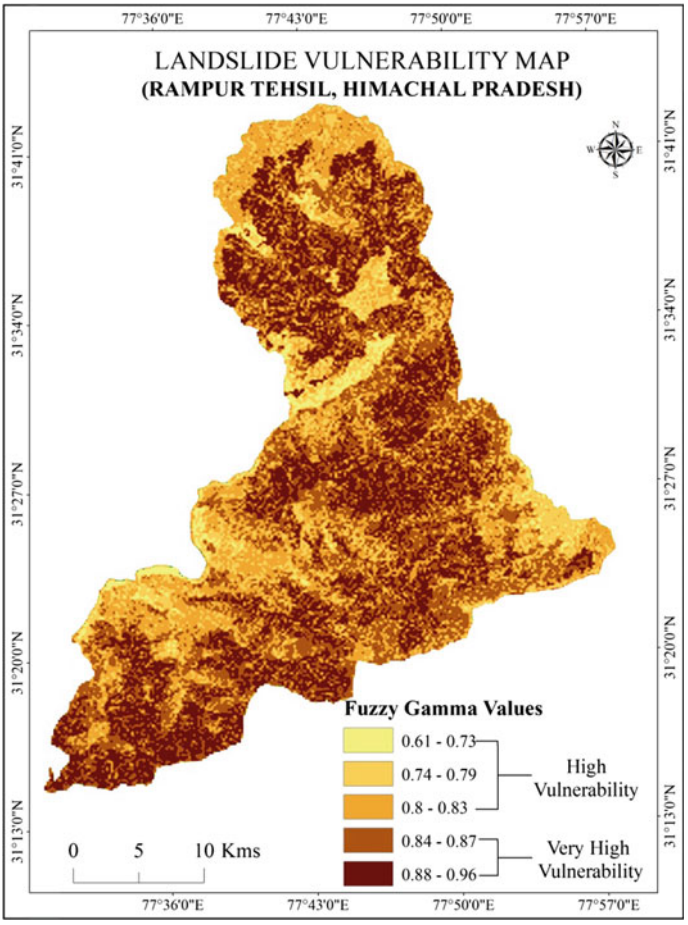

Fig. 9 Landslide vulnerability (fuzzy model)

Table 8 Fuzzy gamma-based landslide vulnerability classes

Sl. No.	Fuzzy values	Vulnerability class	Area in km^2	Percent (%)
1	0.61– 0.73	High vulnerability	20.9	2.12
2	0.74–0.79		132.76	13.45
3	0.80–0.83		270.88	27.44
4	0.84–0.87	Very high vulnerability	304.55	30.85
5	0.88–0.96		258.25	26.16
		Total	987	100.00

Source Authors calculation

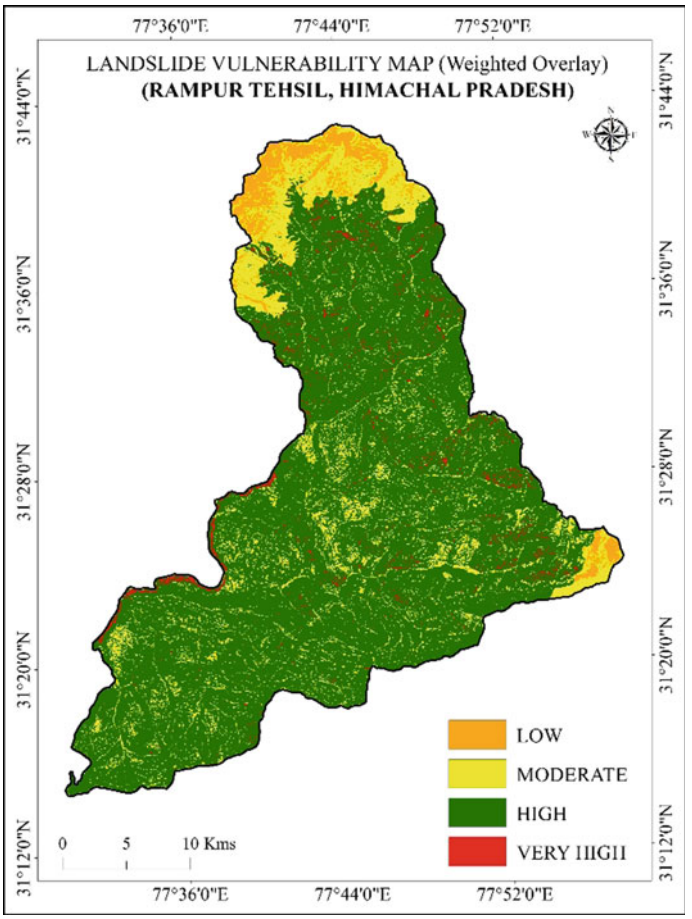

Fig. 10 Landslide vulnerability (WOM model)

Table 9 Weighted overlay-based landslide vulnerability classes

Sl. No.	Vulnerability class	WOM value	Area in km^2	Percent coverage (%)
1	Low	1	44	4.46
2	Moderate	2	135	13.68
3	High	3	792	80.24
4	Very high	4	16	1.62
	Total		987	100.00

Source Authors calculation

b. When it comes to weighted overlay model nearly 80.24% and 13.68% of the area fall and under high and moderately vulnerable categories. The rest minor quantities fall under very high and low categories. The very higher areas in the WOM model fall along with the river banks of Sutlej River where the banks are more prone to landslide activities leading to landslide damming activities. The higher vulnerable areas cover mostly the forest, agriculture as well as build-up lands along the study area.
c. The present study demonstrates the application of fuzzy logic and weighted overlay models for landslide hazard mapping using remote sensing and GIS for Rampur Tehsil.
d. High-resolution satellite imageries and real-time climatic data have increased the level of accuracy of LHZ maps in time. Even though the high hazard areas are only few percent compared to moderate and low hazards, they can easily become prone to landslide through unplanned anthropogenic activities.
e. This approach of landslide hazard zonation using remote sensing and GIS is advantageous for rapid assessment when the area is not accessible. Use of high-resolution images and DEM data can increase the accuracy of the landslide hazard assessments.

Acknowledgements The research work done is a part of NRDMS-DST funded research project. We would like to express our sincerest gratitude to NRDMS-DST, GOI, New Delhi, India, for funding this research project.

References

1. Martha TR, Kerle N, van Westen CJ, Jetten V, Vinod Kumar K (2012) Object-oriented analysis of multi-temporal panchromatic images for creation of historical landslide inventories. ISPRS J Photogramm Remote Sens 67(1):105–119. https://doi.org/10.1016/j.isprsjprs.2011.11.004
2. Gupta RP, Joshi BC (1990) Landslide hazard zoning using the GIS approach-A case study from the Ramganga catchment, Himalayas. Eng Geol 28(1–2):119–131. https://doi.org/10.1016/0013-7952(90)90037-2
3. Panikkar SV, Subramanyan V (1996) A geomorphic evaluation of the landslides around Dehradun and Mussoorie, Uttar Pradesh, India. Geomorphology 15(2):169–181. https://doi.org/10.1016/0169-555X(95)00121-K
4. Champati Ray PK, Dimri S, Lakhera RC, Sati Sa (2007) Fuzzy-based method for landslide hazard assessment in active seismic zone of Himalaya. Landslides 4(2):101–111. https://doi.org/10.1007/s10346-006-0068-6
5. Prakash S (2016) Historical records of socio-economically significant Landslides in India. J South Asian Stud 4(2):177–204
6. Anbalagan R, Parida S (2013) Geoenvironmental problems due to harmony landslide in Garhwal Himalaya, Uttarakhand, India. Int J Emerg Technol Adv Eng 3(3):553–559
7. Anbalagan R, Singh B (1996) Landslide hazard and risk assessment mapping of mountainous terrains-a case study from Kumaun Himalaya, India. Eng Geol 43:237–246. https://doi.org/10.1016/S0013-7952(96)00033-6
8. Kanungo D, Arrora M, Sarkar S, Gupta R (2009) Landslide Susceptibility Zonation (LSZ) mapping-a review. J South Asia Disaster Stud 2:81–105

9. Naithani A (2007) Macro landslide hazard zonation mapping using univariate statistical analysis in parts of Garhwal Himalaya. J Geol Soc India 70:353–368
10. Rawat MS, Uniyal DP, Dobhal R, Joshi V, Rawat BS, Bartwal A, Aswal A (2015) Study of landslide hazard zonation in Mandakini Valley, Rudraprayag district, Uttarakhand using remote sensing and GIS. Curr Sci 109(1):158–170
11. Saha AK, Gupta RP, Arora MK (2002) GIS-based landslide hazard zonation in the Bhagirathi (Ganga) Valley, Himalayas. Int J Remote Sens 23(2):357–369
12. Anbalagan R, Kumar R, Lakshmanan K, Parida S, Neethu S (2015) Landslide hazard zonation mapping using frequency ratio and fuzzy logic approach, a case study of Lachung valley, Sikkim. Geoenvironmental Disasters 2(1):6. https://doi.org/10.1186/s40677-014-0009-y
13. Bibi T, Gul Y, Abdul Rahman A, Riaz M (2016) Landslide susceptibility assessment through fuzzy logic inference system (FLIS). Int Arch Photogramm, Remote Sens Spat Inf sciences—ISPRS Arch 42(4W1):355–360. https://doi.org/10.5194/isprs-archives-XLII-4-W1-355-2016
14. Leonardi G, Palamara R, Cirianni F (2016) Landslide susceptibility mapping using a fuzzy approach. Procedia Eng 161:380–387. https://doi.org/10.1016/j.proeng.2016.08.578
15. Mijani N, Samani NN (2017) Comparison of fuzzy-based models in landslide hazard mapping XLII(October):7–10
16. Rahaman S, Abdul S, Aruchamy S, Jegankumar R (2014) Geospatial approach on landslide hazard zonation mapping using multicriteria decision analysis: a study on Coonoor and Ooty, Part of Kallar Watershed, the Nilgiris, Tamil Nadu. Int Arch Photogramm, Remote Sens Spat Inf Sci-ISPRS Arch 40(8):1417–1422. https://doi.org/10.5194/isprsarchives-XL-8-1417-2014
17. Othman, AN, Mohd W. Naim WM, Noraini S (2012) GIS based multi-criteria decision making for landslide hazard zonation. Procedia—Soc Behav Sci 35(December 2011):595–602. https://doi.org/10.1016/j.sbspro.2012.02.126
18. Raghuvanshi TK, Negassa L, Kala PM (2015) GIS based grid overlay method versus modeling approach—a comparative study for landslide hazard zonation (LHZ) in meta robi District of West Showa Zone in Ethiopia. Egypt J Remote Sens Space Sci 18(2):235–250. https://doi.org/10.1016/j.ejrs.2015.08.001
19. Elmahdy SI, Marghany MM, Mohamed MM (2016) Application of a weighted spatial probability model in GIS to analyse landslides in Penang Island, Malaysia. Geomatics, Nat Hazards Risk 7(1):345–359. https://doi.org/10.1080/19475705.2014.904825
20. Ahmed B (2015) Landslide susceptibility mapping using multi-criteria evaluation techniques in Chittagong metropolitan area, Bangladesh. Landslides 12(6):1077–1095. https://doi.org/10.1007/s10346-014-0521-x
21. Ding MT, Miao C (2015) GIS-based assessment of vulnerability to landslide hazards in Lushan earthquake-stricken areas. J Risk Anal Cris Response 5(2):93–106. https://doi.org/10.2991/jrarc.2015.5.2.3
22. Michael EA, Samanta S (2016) Landslide vulnerability mapping (LVM) using weighted linear combination (WLC) model through remote sensing and GIS techniques. Model Earth Syst Environ 2(2):81–88. https://doi.org/10.1007/s40808-016-0141-7
23. Wang, J, Peng XG (2009) GIS-based landslide hazard zonation model and its application. Procedia Earth Planet Sci 1(1):1198–1204. https://doi.org/10.1016/j.proeps.2009.09.184
24. Shit PK, Bhunia GS, Maiti R (2016) Potential landslide susceptibility mapping using weighted overlay model (WOM). Model Earth Syst Environ 2(1):11–21. https://doi.org/10.1007/s40808-016-0078-x
25. Lari S, Frattini P, Crosta GB (2014) A Probabilistic approach for landslide hazard analysis. Eng Geol 182(PA):3–14. https://doi.org/10.1016/j.enggeo.2014.07.015
26. Panikkar S, Subramaniyan V (1997) Landslide hazard analysis of the area around Dehra Dun and Mussoorie, Uttar Pradesh. Curr Sci 73:1117–1123
27. Bureau of Indian Standards (1998) Preparation of landslide hazard zonation maps in mountainous terrain—Guidelines (Part2-Macrozonation), vol 14496, 2nd edn. BIS, New Delhi, pp 1–19

Effect of Cell Height and Infill Density on the Performance of Geocell-Reinforced Beds of Brahmaputra River Sand

Chirajyoti Doley, Utpal Kumar Das and Sanjay Kumar Shukla

Abstract Geocells, which are three-dimensional interconnected cells, are laid over foundation bases to provide lateral confinement to the infill material and thus improve the load-bearing capacity of the bases. Some experimental and mathematical studies have been reported in the literature in this regard. In this research, a laboratory experimental program was undertaken to study the improvement of bearing capacity of geocell-reinforced granular bases made from Brahmaputra river sand. In a laboratory model test, a steel tank was filled with Brahmaputra river sand, reinforced with geocell of different heights (made from woven geotextile), and progressively loaded to record the load versus settlement response. The infill density of sand was also varied to evaluate the effect on performance of geocell-reinforced sand beds. A square steel plate placed on the geocell-reinforced sand bed was incrementally loaded till failure to quantify the positive effects of geocell height and density of infill soil on the resultant bearing capacity. Enhancement of bearing capacity of geocell-reinforced sand bed with the increase in geocell height and density of infill material was evident from the test results. The bearing capacity of the geocell-reinforced bed, as compared to an unreinforced bed, is found to be increased by 1.8–4.3 times for normalized height of 0.33–1, having infill soil relative density of 70%, and 4.3–8.6 times for normalized height of 0.33–1, having infill soil relative density of 90%. The test results also show that significant reduction of settlement is achieved by the use of geocell reinforcement.

Keywords Geocell · Bearing capacity · Woven geotextile · Geocell height · Infill density

C. Doley (✉) · U. K. Das
Department of Civil Engineering, Tezpur University, Napam, Sonitpur, Assam 784028, India
e-mail: chirajd@tezu.ernet.in

U. K. Das
e-mail: ukrdas@tezu.ernet.in

S. K. Shukla
School of Engineering, Edith Cowan University, Joondalup, Perth, WA 6027, Australia
e-mail: s.shukla@ecu.edu.au

V. S. Kanwar and S. K. Shukla (eds.), *Sustainable Civil Engineering Practices*,
Lecture Notes in Civil Engineering 72,
https://doi.org/10.1007/978-981-15-3677-9_17

1 Introduction

Geosynthetics are extensively used for soil reinforcements. Geocell, a type of geosynthetics, is three-dimensional cells and is produced from polyethylene, polyester or other polymers. Geocell can be applied in reinforcement of weak sub-grade soil, earth retaining structures, stabilization of steep earth slopes, etc. The geocells provide an all-round confinement to the infilled soil due to its three-dimensional nature and enhanced the overall stability of the foundation bed. In recent years, many researchers have studied the beneficial effects of the geocell reinforcement through small-scale and large-scale physical model tests [1–3, 5–9]. However, most of those studies are related to geocell made from geogrids or factory-made geocell of polymeric material. In spite of the potential of geotextile as geocell material, very limited study on such geocell is available in published literature (e.g., [6, 10]). Laboratory prepared geocells have advantage of varying geocell geometry as compared to commercially available geocells.

Similarly, another important aspect of geocell that requires more investigation is the effect of the infill soil density on the performance of geocell. Generally, granular materials such as sand or gravel are used to fill the geocell pockets. Compacting the geocell infill soil to high density is key to effective utilization of geocell reinforcement [8].

In the present study, the effect of cell height and infill soil density on the performance of the geocell has been studied under the action of static load. Contrary to use of factory manufactured geocell in many previous researches, the geocells used in this work were made from strips of woven geotextile (W.G.) with different height, and Brahmaputra river sand was used as a base and infill material.

2 Laboratory Model Tests

2.1 Test Tank and Footing

The internal dimensions of the steel tank made for the experimental tests of the model are 1200 mm × 980 mm × 1010 mm (L × B × H). The sides of the tank were braced with the help of mild steel angles in vertical and horizontal directions to avoid lateral deformation. The tank was connected to the loading frame, which was attached to a manually operated hydraulic jack of capacity 100 kN. A square steel plate of size 150 mm × 150 mm × 20 mm was used as the model footing. A thin layer of sand was glued to the bottom face of the steel plate to induce surface roughness. The model footing was subjected to reaction load applied vertically through steel balls. A hydraulic jack was used to manually control the applied reaction load. The load

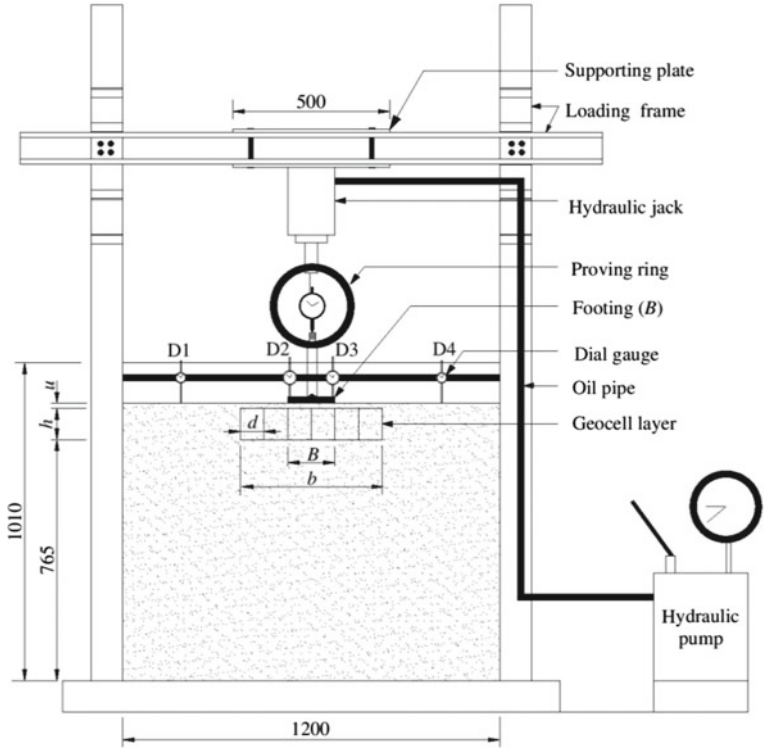

Fig. 1 Schematic view of the test setup. *Note* All dimensions are in mm

carried by the footing was measured with a proving ring. The loading arrangement is illustrated in Fig. 1.

2.2 Test Materials

The sand used in the experimental program was collected from the Brahmaputra river bed. It was made free from roots, organic matters, etc., by washing and cleaning. The above sample was then air dried in the laboratory before it was used in the experimental work. The specific gravity of the sand was found to be 2.66. The dry unit weight in the densest state was found to be 16.95 kN/m^3 and that in the loosest state was 14.78 kN/m^3. The particle size distribution was determined using the dry sieving method, and the results are shown in Fig. 2.

The following values are found from Fig. 2.

The effective size (D_{10}) = 0.30 mm, the mean particle size (D_{50}) = 0.60 mm, the uniformity coefficient (C_u) = 2.33 and the coefficient of curvature (C_c) = 0.964.

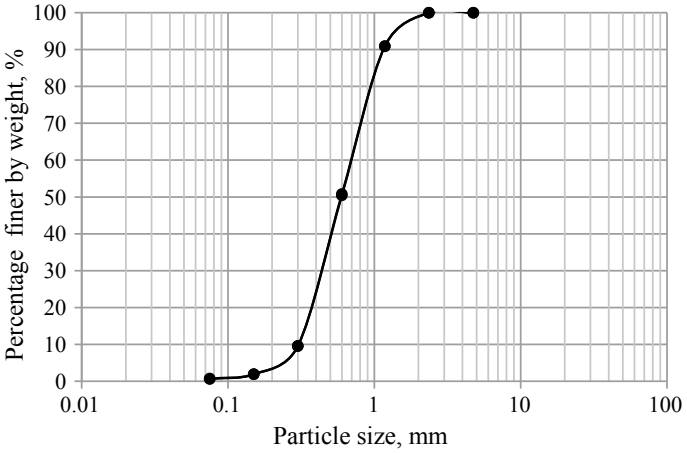

Fig. 2 Particle size distribution of the Brahmaputra sand used

The soil was classified as SP as per USCS. The model footing tests were performed using sand with a relative density (R_d) of 70%. The peak friction angle of the sand obtained from direct shear tests was 40.9° at 70% of relative density.

3 Geocell Reinforcement

In this research, woven geotextile was used to prepare geocells with different cell heights. The engineering properties of geotextile material used in this study are given in Table 1. In order to fabricate geocells of desired dimensions, paper templates were first made. Strips of curtains were then cut and stitched with nylon thread as per the template. The strength of the seam was also tested, and the strength was found to be as strong as curtain material.

Table 1 Properties of geocell material

Parameter	Description
Geocell material type	Woven geotextile
Polymer	Polyester
Thickness, t (mm)	0.8
Ultimate tensile strength, T_u (kN/m)	24
Failure strain (%)	7.0

4 Preparation of Test Setup and Procedure

An extensive test program was carried out to study the settlement behavior of square model footings supported on geocell-reinforced sand under the effect of monotonic load. A Brahmaputra sand bed of 500 mm thickness was prepared using the pluviation technique (raining of sand through air). The density obtained through rainfall technique depends on the height through which the sand is allowed to fall. The system was calibrated by measuring the respective densities achieved for different preset heights of fall during a pluviation test series. The height of fall required to maintain a relative density of 70% of the test sand bed was obtained from the calibration curve. The average density achieved during pluviation was 1.66 g/cm^3, and less than 2% difference was observed in the measured densities at different locations of the bed. Reinforcements with width equal to $3B$ were placed at the depth of $0.1B$ (B is the width of the footing) below the bottom of the footing. Moghaddas Tafreshi and Dawson [6] reported that the optimum depth of placement of the geocell would be $0.1B$ below the footing. The same Brahmaputra sand was used to fill the geocell pockets by pluviation technique to maintain uniform relative density. Any unevenness of the final sand surface over the geocell was leveled taking care to avoid change in the relative density.

The footing was then placed at the top of the bed exactly at the center of the test tank. In order to find the average settlement of the footing, the settlements of the footing at its two opposite edges were measured with the help of two dial gauges. The footing settlement (s) was normalized by the footing width (B) to express them in non-dimensional form as s/B (%). The height of geocell (h) was also normalized with respect to footing width (B). Three different series of tests have been conducted as listed in Table 2. Test series I on unreinforced sand was conducted to quantify the improvement due to the provision of geocell. Test series II to III were conducted to evaluate the effect of cell height and infill soil density on the performance of geocell-reinforced beds of Brahmaputra river sand.

Table 2 Model tests program

Test series	Constant parameters	Variable parameter
I	Monotonic, unreinforced sand, R_d = 70%	–
II	Monotonic, reinforced sand, $d/B = 0.50$, $b/B = 3$, $u/B = 0.1$, *Woven geotextile*	$h/B = 0.33$, 0.5, 0.66 and 1
III	Monotonic, reinforced sand, $d/B = 0.50$, $h/B = 0.66$, $u/B = 0.1$, *Woven geotextile*	*Infill soil density*, R_d = 70 and 90%

Note See Fig. 1 for definition of the variable. Square footing width (B) = 150 mm, depth of top geocell layer (u/B) = 0.10, Geocell pocket size d/B = 0.5, width of geocell layer b/B = 3 and relative density of footing bed (R_d) = 70% were taken in this test series

5 Results and Discussions

The performance improvements due to provision of geocell-reinforced sand foundation are quantified through two non-dimensional parameters as below:

- Bearing capacity improvement factor (I_f): It indicates the relative improvement of bearing pressure of sand bed with geocell (q_r) in comparison with that of sand bed without geocell (q_{unrein}) at the same reference settlement.

$$I_f = q_r/q_{unrein} \tag{1}$$

- Percentage reduction of settlement (PRS): Improvement in footing settlement which compares the settlement of the geocell-reinforced bed to that of the unreinforced bed at same level of bearing pressure, i.e.,

$$\text{PRS} = (1 - s_r/s_{unrein}) \times 100 \tag{2}$$

where s_r is settlement of a reinforced foundation bed and s_{unrein} is the settlement of unreinforced foundation bed at the same level of bearing pressure.

6 Effect of Cell Height

The pressure settlement response of footings on unreinforced sand and that on reinforced sand with different geocell heights is plotted in Fig. 3. It shows that for unreinforced foundation bed, the local shear failure has taken place. Also, a clearly defined failure was observed for the unreinforced sand bed. The slope of the pressure settlement curve becomes nearly vertical beyond $s/B = 5\%$, indicating the failure of the foundation. In contrary, no clear-cut failure was observed for the geocell-reinforced sand bed even for as low as normalized height 0.33. Since there was no clear-cut indication of failure in the pressure settlement response, hence, the tests were carried out up to footing settlement level 30% of the footing width. It is observed from Fig. 3 that for a given applied pressure, the corresponding settlements decrease with increase in geocell height indicating increase in stiffness of geocell-reinforced soil with cell height. Moreover, geocell-reinforced soil is capable of bearing higher load with increase in cell height. A similar trend was also observed by Dash et al. [1].

Figure 4a represents the variation of bearing capacity improvement factor (I_f) with geocell height at footing settlement equals 30% of footing width. It shows that I_f initially increases with greater slope (up to $h/B = 0.66$), and thereafter, it increases with gentle slope indicating the optimum level of cell height. It also indicates that by increasing height of geocell from $h/B = 0.33$ to $h/B = 1$, I_f increases from 1.8 to 4.3 at maximum measured footing settlement level, i.e., $s = 0.3B$. Figure 4b shows the variation of the bearing capacity improvement factors (I_f) versus the footing

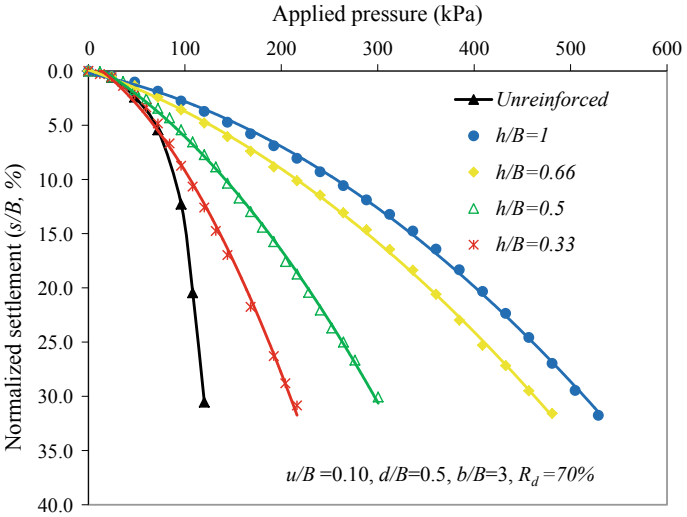

Fig. 3 Variation of footing settlement with bearing pressure for different heights of geocell

settlement for different geocell heights. It is evident that by using a geocell even for $h/B = 0.33$, I_f increases from 1.0 to 1.8.

The plot between PRS and normalized settlement for different geocell heights is shown in Fig. 5. Since settlement of footing on unreinforced sand bed is taken as reference in assessment of improvement of settlement and many of the small-scale model tests [4, 6, 11] suggest an allowable bearing capacity at footing settlement of 5–10% of foundation width, hence the maximum investigated settlement in Fig. 5 is considered as 12% of the footing width. The test results show that PRS value increases with increasing geocell height. It is also apparent from Fig. 5 that the variation of the PRS value even for $h/B = 0.33$ at $s/B = 12\%$ is 52%.

7 Effect of Infill Soil Density

Bearing pressure versus settlement response of unreinforced and reinforced sand with different infill soil densities is shown in Fig. 6. The pressure settlement responses, depicted in Fig. 6, show that great improvement can be achieved by increasing the relative density of infill soil.

Figure 7 represents the variation of the bearing capacity improvement factor (I_f) with relative density of infill soil (R_d), at different settlement levels of the footing s/B. It is seen from the plots that I_f value gets better with the increase in relative density of the infill soil. The test results show that I_f increases 4.3 and 8.6 folds at settlement level of 30% of footing width for relative density of 70% and 90%, respectively. This observation points to a mechanism where the frictional stress between infill soil

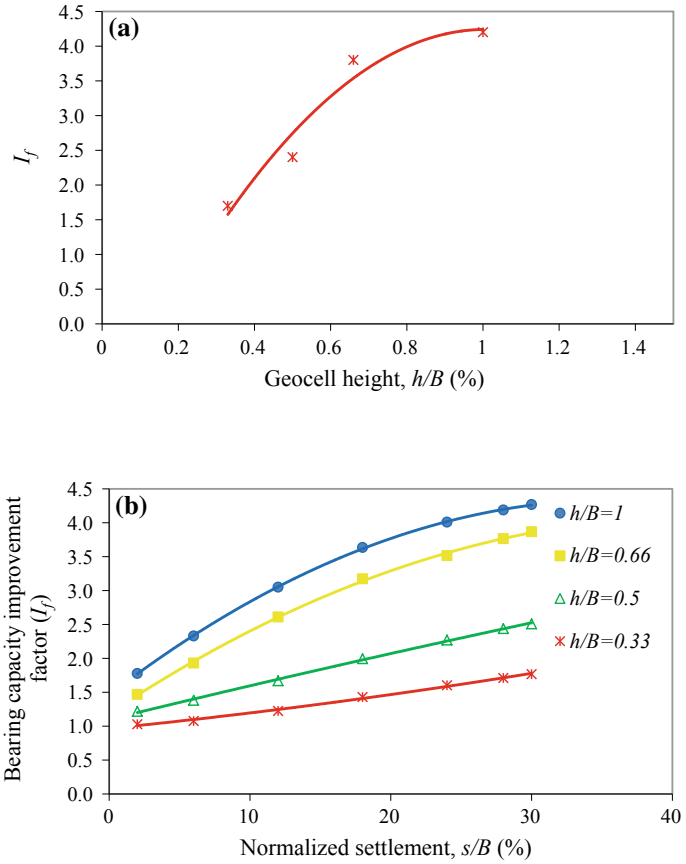

Fig. 4 Variation of (**a**) bearing capacity improvement factor with geocell height at $s/B = 30\%$ (**b**) bearing capacity improvement factor with footing settlement

and geocell provides to additional strength to the reinforced soil. The loose infill soil consumes the applied displacement in readjustment of the void space thereby inducing lesser frictional drag along the soil–geocell interface. On the other hand, in soil with higher relative density, there is less redistribution of void space, and consequently, there is a tendency of expansion of infill soil under loading. This leads to mobilization of shear resistance along the soil–geocell interface and improvement of the load-carrying capacity of the reinforced soil. Similar observations were reported by Dash [8].

The variation of PRS at different levels of footing settlement (s/B) for different infill soil density is presented in Fig. 8. It is observed that the PRS value increases with an increase of infill soil density.

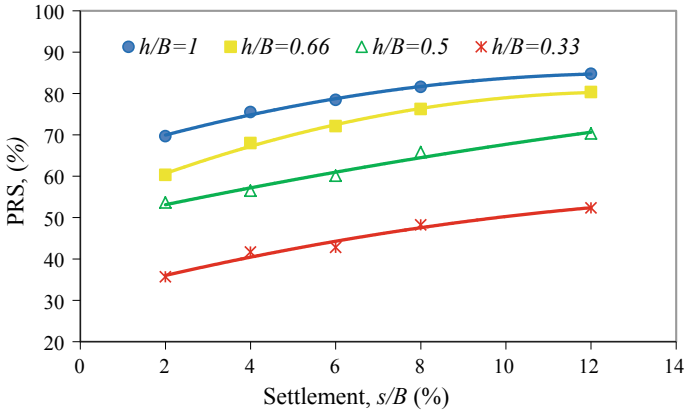

Fig. 5 Variation of the percentage reduction of settlement (PRS) with normalized settlement of footing on unreinforced sand for different geocell heights

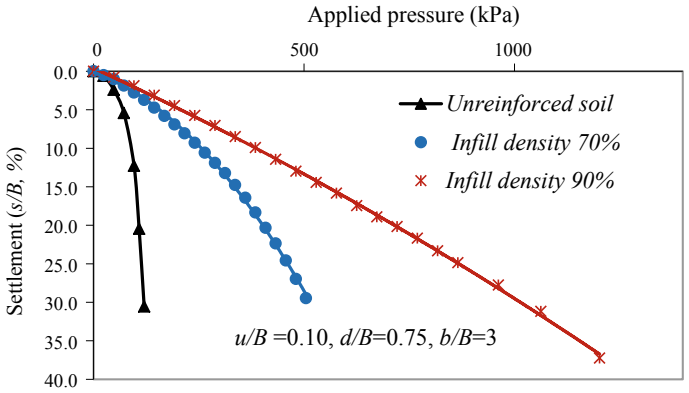

Fig. 6 Variation of settlement with bearing pressure for varying infill density of geocell mattress

8 Conclusions

In this paper, the effect of cell height and infill soil density on the performance of geocell-reinforced beds of Brahmaputra river sand is studied by constructing a model test setup and conducting a series of tests in this laboratory test setup. The model square footing, when under monotonically increasing load, resulted in increase in load-carrying capacity and decrease in settlement with the introduction of geocell as base soil reinforcement. The conclusions drawn from analysis of the test results are as follows:

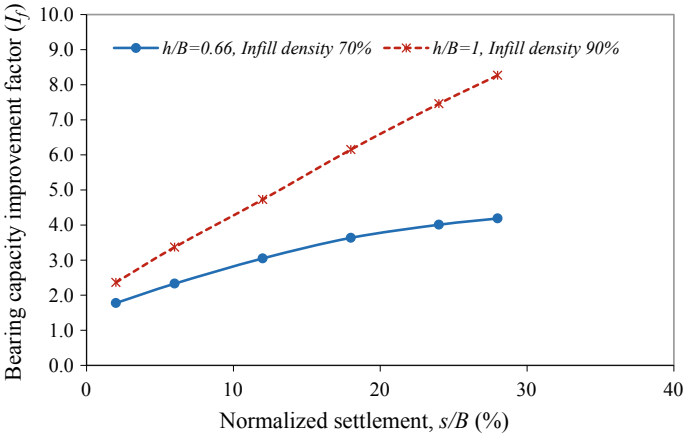

Fig. 7 Variation of I_f with footing settlement for different infill soil densities

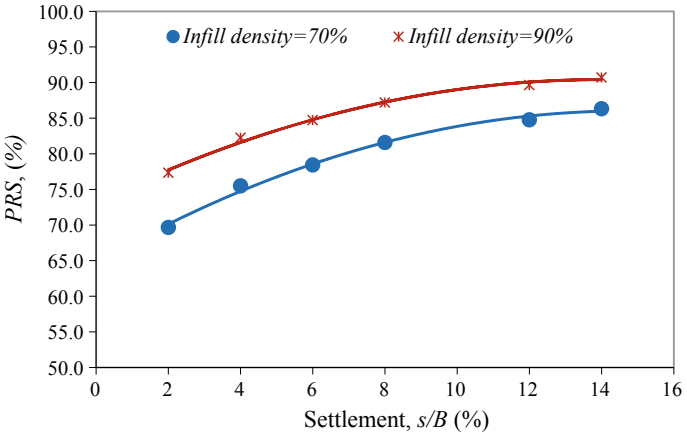

Fig. 8 Variation of the percentage reduction in settlement (PRS) with footing settlement for infill soil density

- In comparison with unreinforced condition, geocell-reinforced granular soil produces higher load-carrying capacity and decreased settlement of the foundation bed.
- Height of geocell plays a crucial role in increasing the bearing capacity of geocell-reinforced sand beds. In this study, by increasing the geocell height from $h/B =$ 0.33 to 1 (i.e., Aspect ratio from $h/d = 0.66$–2), the bearing capacity improvement factor increases from 1.8 to 4.3 at the footing settlement level of 30% of footing width. Moreover, the percentage reduction in settlement of footing for $h/B = 0.33$ to $h/B = 1$ at $s/B = 12\%$ is found to be increased from 52 to 85%.

- Infill soil having higher relative density enhances the performance of the geocell-reinforced bed in terms of its load-carrying capacity and settlement. The result shows that the bearing capacity improvement factor (I_f) increases from 4.3 to 8.6 folds having $h/B = 1$ at $s/B = 30\%$ for relative density of infill soil from 70 to 90%. It is, therefore, concluded that the highest possible compaction of the infill soil is a key to achieving effective performance of geocell reinforcement of soil.

References

1. Dash SK, Krishnaswamy NR, Rajagopal K (2001) Bearing capacity of strip footings supported on geocell reinforced sand. Geotext Geomembr 19:235–256
2. Dash SK, Sireesh S, Sitharam TG (2003) Model studies on circular footing supported on geocell reinforced sand underlain by soft clay. Geotext Geomembr 21:197–219
3. Sitharam TG, Sireesh S, Dash SK (2005) Model studies of a circular footing supported on geocell-reinforced clay. Can Geotech J 42:693–703
4. Cerato AB, Lutenegger AJ (2007) Scale effects of shallow foundation bearing capacity on granular material. J Geotech Geoenviron Eng ASCE 133(10):1192–1202
5. Madhavi Latha G, Somwanshi A (2009) Effect of reinforcement form on the bearing capacity of square footing on sand. Geotext Geomembr 27:409–422
6. Moghaddas Tafreshi SN, Dawson AR (2010) Behavior of footings on reinforced sand subjected to repeated loading comparing use of 3D and planar geotextile. Geotext Geomembr 28:434–447
7. Pokharel SK, Han J, Leshchinsky D, Parsons RL, Halahmi I (2010) Investigation of factors influencing behaviour of single geocell reinforced bases under static loading. Geotext Geomembr 28(6):570–578
8. Dash SK (2010) Influence of relative density of soil on performance of geocell-reinforced sand foundations. Geotext Geomembr 19:235–256
9. Hedge A, Sitharam TG (2013) Experimental and numerical studies on footings supported on geocell reinforced sand and clay beds. Int J Geotech Eng 7(4):346–354
10. Kargar M, Mir Mohammad Hosseini SM (2017) Effect of reinforcement geometry onthe performance of a reduced-scale strip footing model supported on geocell reinforced sand. Sci Iran 24(1):96–109
11. Boiko IL, Alhassan M (2013) Effect of vertical cross-sectional shape of foundation on settlement and bearing capacity of soils. In: Procedia engineering 2013: 11th international conference on modern building materials, structures and techniques, vol 57, pp 207–212

A Study on Subsurface Drainage of Mountain Roads in Bhutan

Dorji Tshering, Leki Dorji and Sanjay Kumar Shukla

Abstract There are many problems associated with hill roads in Bhutan. Since most roads are constructed through steep terrains, there are significant problems related to the slope stability and drainage system. The slope stability problem is massively localized and may not be easily avoided. On the other hand, the drainage problem which affects the larger portion of road stretches than any other factor might be reduced through proper construction of drainage systems itself. In the light of these facts, an attempt is made in this paper to recognize the sources of drainage problems and proposes a design of an economically viable subsurface drain for hill roads in Bhutan. It also presents the discharge calculation of a watershed for the design of roadside drainage system and discusses about determination of the rainfall intensity in Bhutan in order to understand the influence of rainfall on the stability of roads located on mountain hills, and mitigations measures methods are adopted to prevent amount of rainfall run-off reaching towards the roads.

Keywords Hill roads · Drainage problems · Seepages · Subsurface drainage systems · Mountain roads

D. Tshering
Ministry of Works and Human Settlement, Royal Government of Bhutan, Thimphu, Bhutan

L. Dorji (✉)
Department of Civil and Architecture, College of Science and Technology, Thimphu, Bhutan
e-mail: lekidorji.cst@rub.edu.bt

S. K. Shukla
Founding Research Group Leader, Geotechnical and Geoenvironmental Engineering, School of Engineering, Edith Cowan University, Perth, Australia

Fiji National University, Suva, Fiji

V. S. Kanwar and S. K. Shukla (eds.), *Sustainable Civil Engineering Practices*,
Lecture Notes in Civil Engineering 72,
https://doi.org/10.1007/978-981-15-3677-9_18

1 Introduction

Bhutan is a small Himalayan country which shares a border with China in north and India in south. The gentle valleys and small strip of plains supporting a larger portion of population are separated by mountains ranging as high as 7000 m above mean sea level (MSL) in north and 100 m in the southern areas [14]. The regions and valleys which support the population are connected by road networks of various categories or grades as shown in Fig. 1. Since Bhutan is a mountainous country, most of the highways and roads connecting different districts within Bhutan or connecting India in south pass amongst mountains and hilly areas, and thus, it can be generalized that the roads in Bhutan are hill roads.

The road construction in mountains and hilly areas is mostly accompanied with large-scale slope excavation with complex geological conditions, which often threaten the smooth construction schedule and safety. It also causes huge economic losses and serious impacts on the environment and society due to slope instability [7]. The road construction in Bhutan is not an exception. There are several problems associated with the construction and maintenance of hill roads in Bhutan, such as the risks involved in cutting steep terrain and fragile slopes. There are also serious water management problems including formation of undulation of road pavements and pilling off of bituminous layer due to uncontrolled seepage, attacking the subgrade soils and slowly reaching to the layers above it. The compacted subgrade soil is sensitive to moisture; thus, the moisture in subgrade has long been considered as an important factor for the new road construction as well as maintenance of old roads [2].

Therefore, in this paper, an attempt is made mainly to focus on managing the seepage from the hillside or higher ground escaping beneath structures like walls or open roadside drains/kerbs and reaching to the subgrade soil and slowly weakening

Fig. 1 Map of Bhutan showing road networks. Courtesy of MoWHS

the above layers. This paper also presents the possible depth of subsurface drainage, so that the seepage flow lines escaping below these structures will be flowing deep enough to avoid its influence on the performance of road pavements.

2 Hill Road Drainage Problems in Bhutan

Some of the major highways in Bhutan are Thimphu–Trashigang Highway, Thimphu–Phuntsholing Highway, Wangdi–Gelephu Highway, Trongsa–Gelephu Highway, and Trashigang to Samdrupjongkhar Highway, as indicated by 1, 2, 3, 4, and 5, respectively, in Fig. 1. All these roads are constructed in mountain areas, often passing through steep terrains, fragile, and unstable slopes, along the river and through marshy areas as the favourable ground condition is not always found along the highway alignment. Therefore, given these geological constraints, the roads in Bhutan are not always constructed or maintained effectively. Despite normal types of pavement failures such as formation of rutting and cracks due to age and some material defects [8], the hill roads in Bhutan are always accompanied by an untimely formation of undulation on the road surface, pilling off of bituminous surface, and seepage leaks from subgrade soils as shown in Figs. 2 and 3. These failures occur either within the design period or soon after the completion of the road construction works. In Fig. 2, it can be seen that either water from the road surface-run-off or uncontrolled seepage entering from the other side of road (higher ground) and making the subgrade soil saturated and weak is triggering cracks and sliding of road edges. It is also noticed that seepage flowing through subgrade soils and subbase layers breaks out, it causes landslides and erosion due to high gradient of slopes. The presence of water in subgrade also reduces the vertical compressive strength at the top of subgrade layer,

Fig. 2 Sliding of road edges due to uncontrolled seepage in subgrade soils or surface run-off from road surface on Thinphu–Trashigang Highway. Courtesy of Mr. Karma Dorji, Deputy Executive Engineer, Lobesa

Fig. 3 Pilling-off bituminous layers and segregation of coarse aggregates and bitumen on Thimphu–Trashigang Highway. Courtesy of Mr. Karma Dorji, Deputy Executive Engineer, Lobesa

and thus, the deformation at this level is reflected up on the road surface as serious undulation and sinking.

Pilling off of bituminous surface and separation of aggregates with bitumen are seen commonly in newly constructed or resurfaced roads in Bhutan. When the seepage flow lines are close enough to surface or lie within subgrade or subbase layers, the moisture moving up within the pavement layers reaches easily to the bituminous layer. This causes the surface layer to lose the bonding with other layers and also induces a segregation of bitumen and coarse aggregates within itself [16]. This finally leads to pilling off of bituminous layer from road surface or segregation of aggregates and bitumen. This type of phenomenon is noticed in Fig. 3. Therefore, these types of pavement distresses associated with the hill roads in Bhutan are strongly interlinked, and for effective remedial measures, the cause of the distresses has to be detected first.

2.1 Drainage Problems and Source of Seepage

Although the method of road construction, including the maintenance approaches, is adopted in the similar ways for all the roads in Bhutan, the formation of undulation right after construction or leaking of seepage water from subgrade soil as stated above is commonly found between Thimphu and Wangdi on Thimphu–Trashigang Highway, Yotongla areas, and stretches between Thrumshingla to Mongar. These types of defects are also found in many areas on other highways and roads connecting the districts within Bhutan. The main cause of such failures is the uncontrolled seepage from the mountainside as the above-mentioned particular distresses are specially observed in marshy areas. In the similar geological conditions, the road construction in mountains in Canada has observed that water management through proper

Fig. 4 Road sides allowing water to freely move on the road surface. **a** Trashigang–Trashiyangtse road (courtesy of Mr. Sonam, Surveyor, Trashiyangtse), **b** Wangdi–Gelephu Highway (courtesy of Mr. Bishnu Dital, Engineer, Gelephu)

drainage system is found to be a key factor for both good construction of roads and for maintenance of existing roads [13]. Further, it is not an uncommon scene to see that road drainage system in Bhutan has not always received a good level of care as shown in Fig. 4, despite its great influence on the performance of the road pavement. In Fig. 4a, it can be noticed that the hillside is saturated and the water has even littered on the road surface. In Fig. 4b, there is no side drain at all despite the road being one of the major highways. In addition, the highways in Bhutan are not provided with the underground drainage or subsurface drainage systems for better trapping of seepage infiltrating through subgrade soils and pavements layers.

It is also important to define the source of seepage and its nature. The source of the seepage that deteriorates the road surface or pavement layers in Bhutan is either one of the following three sources or combination of them. The first is presence of water bodies in the uphill side of the roads such as lake or pond, the second source is due to marshy areas on the mountainside of the road, and finally, the seepage occurring due to long rainfall season is indicated in Fig. 5.

The first two sources of seepage tend to influence the highways throughout the year, but in some areas, their influence may not be noticeable in dry season or in winter. On the other hand, seepage occurring due to heavy rainfall lasts only for short period but may also bring a noticeable amount of deterioration to the road pavements. However, in general, the atmospheric precipitation such as rain, snow, melting ice, condensing mist, and hail is considered to be the most abundant source of water entering substructures or pavement [11].

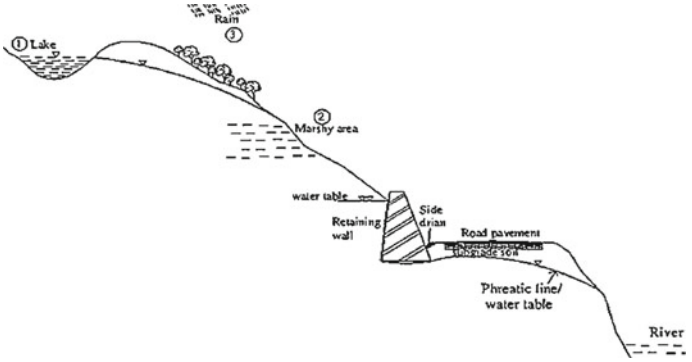

Fig. 5 Hill road section showing the sources of seepage from higher ground

2.2 Subsurface Drain as a Solution

The open side drains that form only the drainage system for hill roads in Bhutan fail to intercept the seepage water infiltrating through the subgrade soils and subbase layers. The seepage which flows either due to hydrostatic pressure or under gravity raises the water table below the road pavements. Furthermore, the upward migration of water by capillary action through soil medium wets the lower pavement layers resulting in the loss of its bearing capacity. To effectively intercept the seepage and to keep the subgrade layer above the capillary fringe, a subsurface drainage depth 1.5–1.8 m is recommended as per the Indian Roads Congress [9]. A depth of 2 m for subsurface drainage is also recommended [16] for effective draining of groundwater in highways. As per the AASHTO methods [1, 5], a subsurface drainage with longitudinal grades of minimum of 0.2–0.5% is recommended and the depth depends on the factors such as permeability, the moisture characteristics of pavement soil, the water table elevation, and the amount of drawdown to achieve the stability. Therefore, the determination of depth of subsurface drainage is a complex problem and may never be accurately estimated. The most economical depth has to be adopted for the construction, which is further discussed in detail.

3 Design of Subsurface Drain

There are various methods of designing subsurface drainage system with use of geosynthetics. However, fundamentally, there are two common requirements of such drains: firstly, the geotextile filter or granular filter enclosing the drain must be fine enough to prevent the substantial migration of fine particles from the adjacent soil medium in order to avoid contamination and clogging of drain. Secondly, the drainage medium should be coarse enough to be more permeable than the adjacent soil mass for effective movement of water through it [1]. Moreover, the subsurface drainage

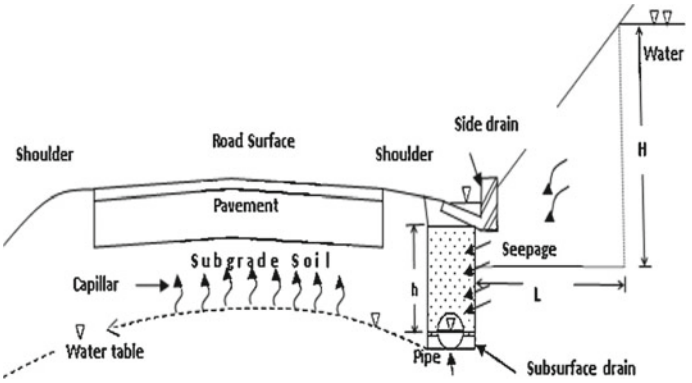

Fig. 6 Subsurface drainage system

should have two functional aspects: the pipe used inside the drain must quickly drain out the entrapped seepage to outlet point. On the other hand, subsurface drainage must effectively intercept all the seepages that will affect the strength of the pavement layers. Figure 6 shows the arrangement of subsurface drainage system for hill roads in Bhutan.

A typical transverse discharge drain of spacing of minimum of 60–100 m is recommended in Austroads, Part-5; however, given the geological condition of Bhutan, it does not form a sensitive part of the design. This is because the hill roads in Bhutan have on an average of about 2–4% longitudinal gradient for better transporting of water, and there are also natural gullies often occurring within 50–100 m of road length for discharging water. The spacing of such outlet points also depends on the size of drain and amount of seepage. Therefore, the spacing and longitudinal gradients are naturally taken care by the virtue of its steep terrains in Bhutan.

3.1 Carrying Capacity of Drainage Pipe and Rate of Infiltration of Seepage

The first functional aspect of the subsurface drain is that the carrying capacity must be higher than the rate of infiltration of seepage into it through the soil facing the seepage side as indicated in Fig. 6. The following ways to determine the discharge capacity of drainage pipe and height of pipe to be installed are:

the rate of flow in a pipe as per the Manning's formula is given as [6]:

$$Q_{\mathrm{p}} = \frac{1}{n} A R^{2/3} S^{1/2} \tag{1}$$

where Q_p = discharge in pipe and n = coefficient of roughness ($n \approx 0.02$ approx. for pvc pipe), as per [4], and it is further found suitable for corrugated pipes used in the similar conditions [3].

A = cross-sectional area of flow ($\pi r^2/2$, since the maximum flow is half full as the upper half of the pipe is perforated).

R = hydraulic radius = $\frac{A}{P}$ ($= 1/2\pi r^2/2\pi r = r/4$). P = wetted perimeter ($2\pi r$)

s = slope of pipe (2–4% slope, $s \approx 0.03$ average)

If the pipe used in the drain is 150 mm, the flow is half full since the upper half of the pipe is perforated as shown in Fig. 6. Therefore, the rate of flow in pipe from Eq. (1) gives

$$Q_p = \frac{1}{n} A R^{2/3} S^{1/2} = \frac{1}{0.01} \pi \frac{75^2}{2} \left(\frac{75}{4}\right)^{2/3} \times 0.03^{1/2} \tag{2}$$

$= 1.08 \times 10^6$ mm^3/s.

3.2 Rate of Infiltration of Seepage into the Drain

The rate of flow of seepage into the drain is given by the Darcy's law [6]:

$$Q_d = k\, i\, A \tag{3}$$

Q_d = discharge into the drain through the soil face of the drain.

k = hydraulic conductivity (for soil types: fine sands, silts, sand–silt–clays mixtures have k value ranges from 10^{-2} to 10^{-6} mm/sec (see Table 1). Assume value 10^{-3} mm/sec) for saver purpose.

Table 1 Typical ranges for coefficient of permeability (hydraulic conductivity, k) in different types of soil

Soil type	Relative degree of permeability	K_{hyd}, coefficient of permeability or hydraulic conductivity (mm/s)
Clean gravel	High	10 to 100
Clean sand, sand and gravel mixtures	Medium	10 to 10^{-2}
Fine sands, silts	Low	10^{-2} to 10^{-4}
Sand-silt, clay mixtures, glacial tills	Very low	10^{-3} to 10^{-6}
Homogeneous clay	Very low to practically impermeable	10^{-3} to 10^{-6} 10^{-6} to 10^{-10}

After McCarthy [10]

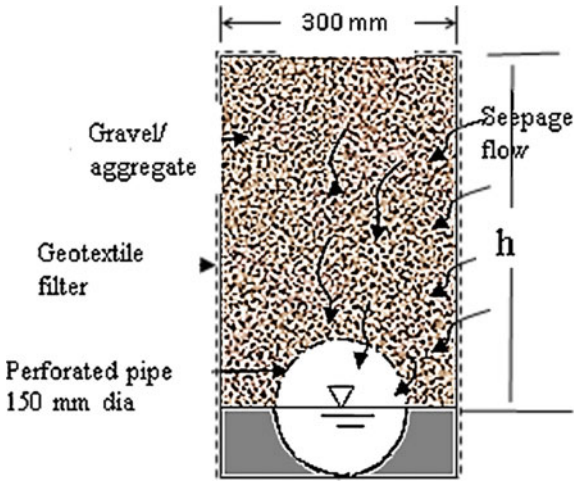

Fig. 7 Geotextile wrapped subsurface drainage

i = hydraulic gradient (H/L, approximately equal to 1 from Fig. 7)

A = cross-sectional area of drain wall through which seepage is occurring = $h \times S$ (since the seepage occurs from one face of wall of the drain only).

S = length of drain between two outlet points/spacing (maximum of 100 m as per Austroads standards).

Therefore, the maximum rate of flow of seepage into the drain at outlet point from Eq. (3) gives

$$Q_{\mathrm{d}} = 10^{-3} \times 1 \times 100000 \times h = 100\ h\ \mathrm{mm}^2/\mathrm{sec}(h \text{ in mm}) \tag{4}$$

From Eqs. (2) and (4), the height or location of the drain can be found out. $1.08 \times 10^6\ \mathrm{mm}^3/\mathrm{sec} = 100\ h\ \mathrm{mm}^2/\mathrm{sec}$, $h = 10.8$ m (approximately).

Theoretically, this value shows that a polyvinyl chloride (PVC) pipe of diameter 150 mm can discharge a seepage intercepted by a drain having dimensions 34 m height and 100 m length, which practically can never be the height of subsurface drain. The carrying capacity of pipe is much higher than the rate of seepage entering into it. Therefore, the size of pipe inside the drain discharging the intercepted seepage does not form a sensitive part of the design of the subsurface drainage. Even a PVC pipe of smaller size can easily transport the entrapped seepage. Figure 7 shows an economically vibrant size of the geotextile wrapped subsurface drain, since the economic factor always plays an important role in most construction fields in Bhutan. Gravel/aggregate is used as a granular filter, and PVC pipe with upper half perforated is installed to facilitate the faster draining of seepage water. The width of the drain and diameter of pipe are 300 and 150 mm, respectively, as suggested by Brockenbrough and Boedecker [5] for economic reasons, although a greater width is suggested by some other researchers [16]. The construction procedures suggested by Shukla and Yin [12] can be adopted for construction of such geotextile wrapped drains. The drain can be filled with gravel material [1]; however, care must be taken to avoid entering

of small particles into pipe as clogging of drain may occur in long run. The location of drain will depend on the site condition as indicated in Fig. 7. It can be installed below road shoulder or beneath the side drain depending on the space availability at site. The top of the drain can be sealed with ordinary soil or by a concrete slab.

3.3 Determining the Depth of Subsurface Drainage

As seen above, a small pipe can easily transport the intercepted seepage water with given gradients of roads in Bhutan, yet the depth, the other important functional requirement, of subsurface drainage to effectively remove the seepages affecting the pavement layers remains at large. The higher the depth of drain, it can more effectively intercept the seepage water infiltrating through subgrade soils, but going as deep as 1.5–2 m as suggested by Mathur and Uppal [9] and Yuan et al. [16] may be economically unsound for hill roads in Bhutan. As mentioned earlier, since the economic factor plays an important role in Bhutan, the depth and size of drain have to be economically feasible and serving the basic functions. Thus, a functionally minimum depth of a subsurface drain will be the single most important governing factor for designing the subsurface drainage.

As noted in Fig. 7, the subsurface drainage must be well below subgrade soil, so that its top layer is not within the capillary fringe. On the other hand, the capillary rise depends on type of soil and the temperature that make the accurate prediction of the height of capillary rise almost impossible [10]. In addition, the type of soil along the road varies with varying water table which make the height of capillary rise vary along the length of road as the capillary rise decreases with the increase in the depth of water table [15].

Therefore, in Bhutan, providing 1–1.5 m height of subsurface drainage will be economically and functionally a balanced design. This is because the soil types are mostly fine sands, and the capillary water does not rise as high as 1 m (see Table 2). In addition, the soils in the upper zone of the capillary fringe remain relatively dry, and the bearing capacity is not lost significantly.

Table 2 Representing height of capillary rise in different types of soil

Soil type	Meter
Small gravel	0.02–0.1
Course sand	0.15
Fine sand	0.3–1
Silt	1–10
Clay	10–30

Courtesy McCarthy (2007)

Table 3 Standard dimensions of catch water drain

Catch drain type	Max. top width of flow (T) [m]	Max. floe depth (y) [m]
Type-A	1.0	0.15
Type-B	1.8	0.30
Type-C	3.0	0.50

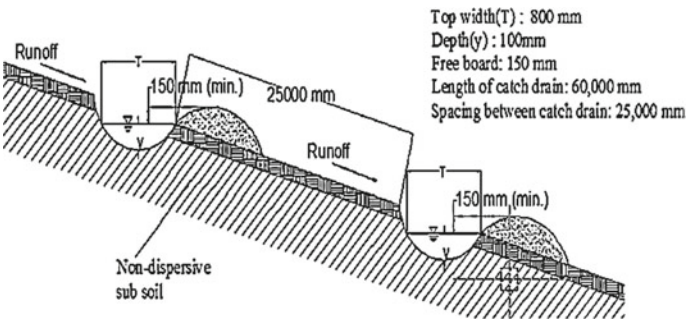

Fig. 8 Catch water drain

4 Mitigations Measures for Surface Water Flow

Catch drains are drainage structures which are generally constructed to collect water from upper side of the road and divert to the other drainage systems usually to the culverts. Catch drains must have sufficient cross-sectional dimensions to fully collect the design flow with a minimum freeboard of 0.15 m. The cross-sectional profile can be parabolic (U-shaped), trapezoidal, or triangular (V-drain). But, parabolic drains have a greater hydraulic capacity and are generally less susceptible to invert erosion. Table 3 gives the design standard dimensions of catch water drains. Types of catch drain will be chosen based on the soil types and rainfall intensity. The principal purpose of catch drain is to divert storm water run-off around the soil disturbance and to collect run-off from the unstable slope before it is allowed to concentrate and cause soil erosion. These drains will reduce the amount of water flowing towards the roads which ultimately minimize the water stress at the subsurface of the roads (Fig. 8).

5 Conclusions

In general, the drainage plays an important role in the performance of the road pavements as the strength of pavement layer is affected mainly by the presence of water. The following general conclusions can be made:

- In particular, the road problems as discussed here are either created by the capillary rise from the seepage water or the seepage itself. To minimize the amount of seepage water through roads, construction of catch water drains are necessary.
- In order to keep the upper layer of the subgrade soil relatively dry so that its bearing capacity is not compromised against the wheel load, the depth of the subsurface drainage should be high enough to keep its path well below the pavement layers.
- Thus, considering the economic benefits and the minimum functional requirements, the depth of 1 m subsurface drainage can also keep the seepage flow lines below the pavement layers.
- For important highways and in areas where there is huge marshy area along the road pavement, the construction of subsurface drainage system will be the most feasible solution for hill roads in Bhutan aside from surface drainage system

References

1. Austroads (2005) Guide to pavement technology-part 5: pavement evaluation and treatment design. Austroads, Sydney
2. Bae A, Stoffels SM, Antle CE, Lee SW (2008) Observed evidence of subgrade moisture influence on pavement longitudinal profile. Can J Civ Eng 35(10):1050–1063. https://doi.org/10.1139/l08-047
3. Bayat E, Kouchakzadeh S, Azimi R (2011) Evaluating the carrying capacity of a subsurface drainage network based on a spatially varied flow regime. Irrig Drain 60(5):668–681. https://doi.org/10.1002/ird.603
4. Bedient PB, Huber WC, Vieux BE (2008) Hydrology and floodplain analysis. Prentice Hall, Upper Saddle River, N.J
5. Brockenbrough RL, Boedecker KJ (2003) Highway engineering handbook: building and rehabilitating the infrastructure. McGraw-Hill, New York
6. Cedergren HR (1989) Seepage, drainage, and flow nets. Wiley, New York
7. Ju N, Zhao J, Huang R, Duan H (2011) Dynamic design and construction of highway cut slopes in Huangshan area, China. J Mount Sci 8(2):154–165. https://doi.org/10.1007/s11629-011-2113-8
8. Khedr SA, Breakah TM (2011) Rutting parameters for asphalt concrete for different aggregate structures. Int J Pavement Eng 12(1):13–23. https://doi.org/10.1080/10298430903578960
9. Mathur BD, Uppal DHL (2001) Recommendation for road constrcution in waterlogged areas. The Indian Road Congress, Delhi
10. McCarthy DF (2007) Essentials of soil mechanics and foundations: basic geotechnics. Pearson/Prentice Hall, Upper Saddle River, N.J
11. Robert YC, Paul C (1999) Modeling subsoil drainage systems for urban roadways. Can J Civ Eng 26(6):799–809. https://doi.org/10.1139/l99-048
12. Shukla SK, Yin J-H (2006) Fundamentals of geosynthetic engineering. Taylor & Francis, London
13. Treena H (2010) Moving mountains. Aggregates Roadbuild 24(4):24
14. Wangchhuk L (2010) Facts about Bhutan. Absolute Bhutan Books, Thimphu
15. Yang F, Zhang G, Yin X, Liu Z, Huang Z (2011) Study on capillary rise from shallow groundwater and critical water table depth of a saline-sodic soil in western Songnen plain of China. Environ Earth Sci 64(8):2119–2126. https://doi.org/10.1007/s12665-011-1038-4
16. Yuan R, Yang YS, Qiu X, Ma FS (2007) Environmental hazard analysis and effective remediation of highway seepage. J Hazard Mater 142(1–2):381–388. https://doi.org/10.1016/j.jhazmat.2006.08.025

Comparison of Modules for Water Distribution System Design—A Case Study of Ramapuram Chennai Tamil Nadu

C. Prakasam and R. Saravanan

Abstract The water supply and distribution planning is an important aspect of urban planning and development of it and also very important for livelihood. The key goal is to supply a uniform water supply from the first point to the end user with constant pressure and quantity. The increasing urbanization demands to design an efficient and broaden the existing network to fill the gaps between supply and consumer demand. Ramapuram is a growing part of the city whose water distribution system is being renewed with a ductile iron pipe. The water supply design was done with the help of Loop Software with 2018 as the base year. The pressure in the network nodes is identified to be lower than the standard requirement. Current work discusses the simulation performed by using the WaterGEMS tool for the existing system of Ramapuram Zone 1. The design of the distribution system varies with many factors such as topography, population, water, and demand. The water distribution system is designed using Loop 4.0 and WaterGEMS software. WaterGEMS is a hydraulic modeling module that uses the discharge, headloss, and velocity parameters for the design and analysis of water distribution network. The research focuses on identifying the pipe connections with an inadequate water supply and design it with adequate supply pressure. The results show that the water pressure is uniform and feasible at all junctions, the flow parameters to supply uniform water supply in the study area.

Keywords WaterGEMS · Loop 4.0 · Ramapuram · Water distribution design

1 Introduction

The sorted out water supply system to Chennai was started in the late 1800s which was the core of the secured system for water supply now in presence in Chennai Corporation City. With a 2573 Mcft limit, Poondi Reservoir was established over

C. Prakasam · R. Saravanan (✉)
Department of Civil Engineering, Chitkara University, Haryana, Himachal Pradesh, India
e-mail: saravana8689@gmail.com

C. Prakasam
e-mail: cprakasam@gmail.com

V. S. Kanwar and S. K. Shukla (eds.), *Sustainable Civil Engineering Practices*,
Lecture Notes in Civil Engineering 72,
https://doi.org/10.1007/978-981-15-3677-9_19

the Kosathalaiyar River and put in a facility for interrupting and storage of the river water. In the year 1961, with an intended water supply of 115 lpcd, the system was designed for an assessed population approximately 0.66 million. Source: http://www.chennaimetrowater.tn.nic.in/. Chennai Metropolitan Water Supply and Sewerage Board (CMWSSB) is now implementing the supply of water plans/Under Ground Sewerage Schemes in a portion of the nearby bodies in Chennai Metropolitan Area. There is a number of nearby bodies which are without holistic infrastructure offices both in sewerage and water supply system in the recently expanded City. Therefore, it progresses toward becoming a need for the Board to cover the implementation of water supply plans/Under Ground Sewage Schemes in the recently attached 42 nearby bodies and additionally to the Chennai Metropolitan Area. With that objective, numerous spots were restructured with the assistance of new pipe material, effective appropriation system, for the anticipated population. One such place is Ramapuram, where the restoration of the system was completed.

Bhaskar et al. [1] investigated the water system of Yavatmal city and proposed measures for the enhancement of the conveyance system using WaterGEMS. The results show that the existing conveyance system will not have the capacity to take the heap of the equivalent to another pipelines to be proposed that guarantee essential water for drinking for quickly developing population. Menapace et al. [2] overcame the drawback by proposing a new application of EPANET-2. This new application is equipped with water requirement distributed uniformly along the pipes and also a precise depiction of the distribution of pressure and lets to recognize precisely the point of minimum head. Ramana and Sudheer Chekka [3] conducted a detailed study to circumvent various present problems encountered and leakage losses. EPANET tool was used to analyze and design the water supply system. In addition to the tool, WaterGEMS and AutoCAD were also used to support the cause and results show that the pipe diameter has to be revised. Mehta et al. [4] simulated the hydraulic analysis of the pipeline system of Punagam area close Surat city using EPANET 2.0. The result shows that the load at all intersections and the flows are adequate with their speeds at all channels and water is sufficient in the study area. Paneria and Bhatt [5] stated that because of fast urbanization in an urban area, the water demand is quickly increasing. Therefore, the weight on the existing system is growing. This may result in the hole among supply and buyer chain in a various way. The work investigates the distinctive model tools that can be connected in the system to eradicate the hole. Vaghela and Bhagat [6] did the hydraulic analysis of Laxmi Nagar territory of the west zone, Rajkot city using WaterGEMS. The outcome obtained confirmed that weight at the intersections and the water flows with the respective speeds at the channels is sufficiently attainable for giving sufficient water to the people.

The present investigation attempts to structure the system with the parameters involved using Loop 4.0 and WaterGEMS and contrast the proficiency of both and their favorable position and detriment.

2 Study Area

Ramapuram area has been furnished with the water supply distribution system, with 50 mm and 75 mm dia PVC main. Ramapuram Village Panchayat presently being converged with Chennai city, it is proposed to give enhancement to water supply plan to supply water @150 lpcd and to supplant the whole PVC main with new D.I main for conveyance system. Consequently, to give an exhaustive water supply plot, it requires to supplant the whole dispersion system, providing extra storage structures for the limit according to the Central Public Health and Environmental Engineering Organization standards (CPHEEO). The present work imagines for providing appropriation system to the whole Ramapuram area and providing new overhead tanks/underground tanks for ensuring the storage office for 33% of the intermediate demand of the year 2033 and providing a conveying main from the existing 1200 mm Dia. Pre-Stressed Concrete (PSC) main in Arcot street to the existing underground tank (UGT) at Kurinji Nagar (Fig. 1).

The whole area has been divided into two zones of which the design is carried out for Zone 1. At present, the Local body is providing water supply to its residents through the existing source of 20 Lakh Liters sump, through 50 and 75 mm dia polyvinyl chloride (PVC) pipe main. The existing sump receives water through 250 mm dia cast iron(CI) main. Water is being tapped at Dr. Ambedkhar street, from

Fig. 1 Layout on Ramapuram zone 1

the existing 1200 mm dia PSC main in Arcot road which is utilized as a source for water supply to Ramapuram. Twenty overhead tanks exist at various locations in the area.

3 Materials and Methods

From two distinct directions, where the development of the town has not been organized arranged, with a few productive and impartial circulation of water, the matrix configuration where various water mains are intersected making sure that impasses to a lowest is prescribed. The framework simplifies for the water supply to any intersection in the network not less than sacks just in emerging phase, a few zones as yet left over empty lands, circulation framework was intended future demand in an approach to supply water from the adjoining matrix to the later improvements. With the help of CPHEEO Manual for Treatment and Water supply, the framework was intended for anticipated population for the year 2048, for supply at 155 lpcd per capita and peak factor of 2.5. Taking the population per unit length of the road as 2.92 for the ultimate year, the utilization at each nodal point according to the above utilization rate has been worked out. Hydraulic plan for the conveyance framework was conveyed using Loop variant 4.0. to such an extent that the proposed Head Works might cover the area by supplying water from the overhead tank (OHT) with staging tallness 17 m and capable yield remaining weight of 12.0 m at the last part.

Following steps have been carried out. The primary step in creating the model for water supply distribution system using WaterGEMS is to create a model by using a base map of the existing system. The water distribution system model is geo-referenced using AutoCAD module to delineate the water demand provision at each node/junction. After the georeferencing, the elevation values are assigned to all nodes/junction using the Trex function. Elevated storage reservoir (ESR) data or overhead tank data input such as diameter, capacity and base elevation value of the tank is entered.

3.1 Population Projected for Ramapuram

The population details were acquired from the Census Department for the 1981 to 2011 years are provided in the table as follows (Table 1)

The population was projected for the 30 years' design period as per the norms. The various types of population projection methods are arithmetical method, geometrical progression, incremental increase, and method of least squares. With 2018, 2033, and 2048 as a base, intermediate, and ultimate year, respectively, the calculation was carried out. Taking the population of 54665 for the year 2011 as the base value, adopt the annual growth rate of 3.525% for Thiruvallur district as given in the census department.

Table 1 Population projected for Ramapuram

Sl. No.	Statistical year	Population for Ramapuram
1	1981	9000
2	1991	23,000
3	2001	72,000
4	2011	54,665 (provisional)

Table 2 Water demand for Ramapuram

Sl No.	Design years	Population	Water demand in MLD (rate of water supply @ 150 lpcd + 3% for the unaccounted-for water)
1	2018 (Base year)	60,652	9.4
2	2033(Intermediate year)	101,982	15.81
3	2048 (Ultimate year)	171,476	26.58

The projected population for base year 2018 = (54665 * (1 + 0.03525) ^ 4) = 70,605.

The population for the intermediate period of 2033 = (54665 × (1 + 0.03525) ^ 22) = 117,140.

The population for the year 2048 = (54665 × (1 + 0.03525) ^ 37) = 196962.

3.2 Water Demand

As 150 lpcd as per capita supply according to CPHEEO rules [7], the water demands for 2018, 2033, and 2048 years for Ramapuram area are worked out as follows (Table 2).

3.3 Design of Water Distribution System Using Loop Version 4.0

With the hydraulic criteria 30 years of design period, 155 lpcd (include the ng 3% for UFW (Unaccounted-for Water)) of per capita, 30 years' design period (2048) with base year as 2018, 12 m of minimum residual head, for ductile iron pipes Hazen Williams coefficient of 140 and a peak factor of 2.5 used for the network analysis using the Loop version 4.0 (Fig. 2).

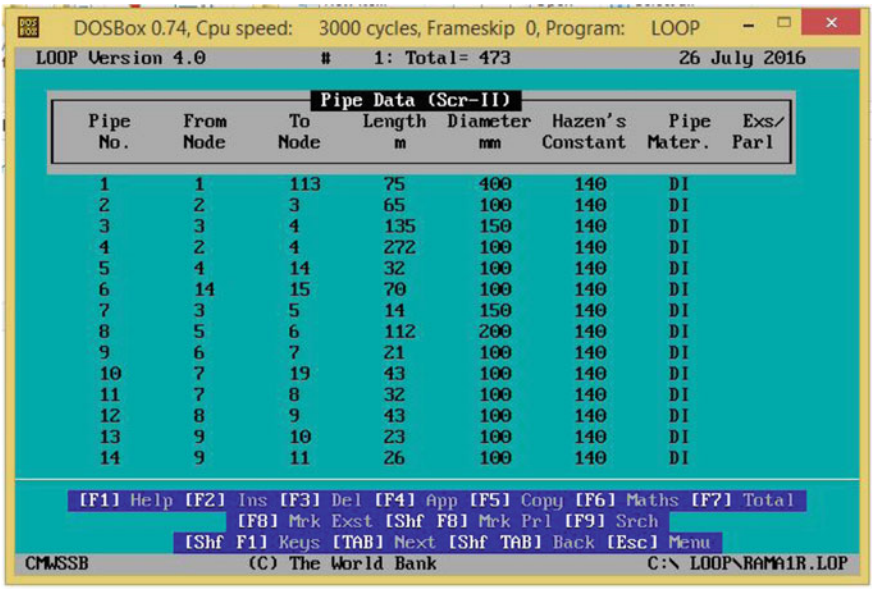

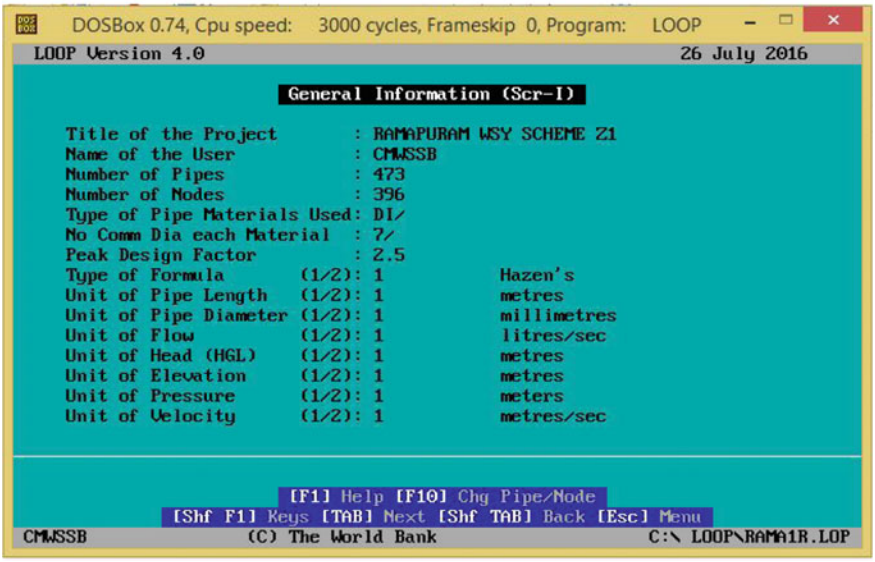

Fig. 2 Hydraulic design using Loop 4.0

3.4 Appurtenances

Sluice valves of 71 in number are used in Zone I in a way that separates the distribution part to control the flow of water that permitted preservation in an easy way for future. Total number of five air valves are provided each in Zone I as a part of the design at suitable locations wherever it is warranted. Provision has been made for 2812 numbers of House Service connections for Zone I. Provision has also been made for fixing Water Meters in all House Service Connections for collecting water charges on a volumetric basis.

4 Results and Discussion

The node data at the end of pipes are about 784 in numbers with a peak of 2.50 and flow value in negative liters per second (lps) and elevation ranging from 12.11 m with minimum and a maximum pressure of 12.00 and 30.00 m correspondingly. The fixed head reservoir has the source node 1 with the head as 29.11 m. The diameter of the pipe varies from 100.00 to 700.00 mm with Hazen's constant 140.000. The allowable pressure is 30.00 m for the ductile iron pipe material. Run out for distribution network was carried out according to the loop 4.0 design for the road length of 30667 m including 10 m of pipe inside the water distribution station in Zone I and for the road length of 28490 m including approximately 10 m of pipe inside the water distribution station in Zone I. After computing successfully, the flux table of pipe and junction is studied out. There are 104 pipes and 73 junctions in the area. Considering the various aspects of designing, the pressure has been designated. For the water distribution system, the existing system is replaced with the ductile pipes owing to various reasons such as C (Flow coefficient) factor is 140 which is a realistic, long term for sustainable practices. It also possesses less head loss and also smooth in nature. Another main reason is the cost; DI pipes saves a lot of money as it as larger inside diameter helping in pumping cost.

The network of the existing distribution system in WaterGEMS is given below. In some cases, there is a backflow in the system in a number of pipes. The whole system is looped so that there is a possibility of backflow. To satisfy the water requirement in the area, water main is directly supplied from the tank by pumping service. Also, injunctions, the pressure at the starting node is kept 2.2 kg/cm^2 but at the end consumer, it is 0.8 kg/cm^2, which is low and flow supplied is less than the starting node. The parameters, for example, the diameter of the pipe and length are entered physically, while the head loss and velocity flow are estimated by the WaterGEMS. For DI material, the velocity may change in—0.0 m/sec. to 0.8 Mt./sec based on the water demand, topography, and kind of system. As the kind of system is circled in Ramapuram Zone 1, negative flow is available in the pipe. The length of channels had variation from a minimum 5–618 m having a total length of the system as 30,667 m. The pipe widths were in scope of 100–700 mm having roundabout

shape in the material of flexible iron and the main lines installed of gentle steel. The flow in the courses was ranging from −79.62 to 233.61 L/sec. The water demand and elevation are the data input parameters for the intersection calculation. The estimation generates estimations of hydraulic review and density. The total area of the water system is high, thus at the initial intersections, the pressure is great as 1.9 kg/cm^2, as the remoteness from the tank increases, the weight gets dropped down as low as 0.5 kg/cm^2. It demonstrates that the amount of water in the conveyance by the system has tremendous variations and the dispersion is not equivalent.

4.1 Conclusions

- The water plays a vital role as a basic requirement for existence and is essential in a sufficient amount to stay hale and hearty. Growing development, increasing requirement of water, contamination of close-by sources of water, and exhaustion of sources because of overexploitation have all added to the momentum emergency of consumable water.
- With urban areas growing quickly, more up to date wellsprings of water must be controlled, and these are frequently added far from the municipal. A portion of the urban areas, that relied upon adjacent wellsprings of water supply prior, need to go a lot further later on to supply water to their residents.
- Thus, my work is concentrated on equal and uninterrupted water supply. I also witnessed that all the water supply network components should abide by the guidelines of CPHEEO manual. All valuable experiences and knowledge that I have gained helped me for a better understanding of water distribution and supply network.
- The use of WaterGEMS in real-time monitoring will allow for quality of network and quantity of water delivery monitoring. It certainly will elevate the service delivery levels for the Ramapuram Municipal Corporation uplifting the status of the Chennai as a smarter city.

References

1. Bhaskar SP, More Ashok B, Rout AK, Rajendra GM (2017) Feasibility analysis of water distribution system for Yavatmal City using WaterGEMS software. IJIRSET 6(7)
2. Menapace A, Avesani D, Righetti Maurizio, Bellin A, Pisaturo G (2018) Uniformly distributed demand EPANET extension. Water Resour Manage 32(6):2165–2180
3. Ramana GV, Sudheer Chekka VSS (2018) Validation and examination of existing water distribution network for continuous supply of water using epanet. Water Resour Manag 32(6):1993–2011
4. Mehta D, Waikhom S, Yadav V, Lakhani K (2016) Simulation of hydraulic parameters in water distribution network using EPANET: a case study of surat city
5. Paneria DB, Bhatt BV (2017) Modernization in water distribution system

6. Vaghela PV, Bhagat SS (2016) Analysis of existing water distribution network by using watergems: a case study of Rajkot City. Water Supply (lpcd) 150(135):180
7. Ministry of Urban Development (1999) Manual on Water supply and treatment. Central Public Health and Environmental Engineering Organization, New Delhi
8. http://www.chennaimetrowater.tn.nic.in/

Environmental Flow—A Mitigation Measure for Impact of Hydropower Projects

C. Prakasam and R. Saravanan

Abstract Hydropower is considered a standout among the most economical and nonpolluting sources of energy. One of the principal sources of water for agribusiness and livelihood is the dam. To tap the hydropower potential, water is extricated from the dam at a more prominent level, time and again to meet the maximum capacity. Water is excessively misused because of some unavoidable situations because of which, the water which is important for the agricultural reason for existing usage is not adequate; thus, the agricultural sector suffers. The potential impacts of this would be decreased in agricultural efficiency and loss of agrarian land. The present research explores the impact of hydropower project upon agriculture with the help of GIS techniques to understand the impact of spatially and temporally. The vegetation index calculation and the land use land cover study that helps in understanding the impacts of a hydropower project in the study area for the land use change spatially and temporally. Following the impact assessment, mitigation measures were provided to cope up the agricultural practices in the study area.

Keywords Hydropower project · Beas · Vegetation index · Minimal flow

1 Introduction

Himachal Pradesh is known for hydropower production as the snow and river serves as the source in abundance. Himachal Pradesh is known as the "Power state" with a respectable potential to pass hydropower energy. Despite the fact that the major and medium hydropower projects have been noted for their risky environmental impacts, the little hydroelectric projects of mere 6 MW limits appear to have turned out to impact the environment as well. The concentration was more on constructing number of projects; anyway what influences neighborhood living of remotely

C. Prakasam · R. Saravanan (✉)
Department of Civil Engineering, Chitkara University, Baddi, Himachal Pradesh, India
e-mail: saravana8689@gmail.com

C. Prakasam
e-mail: cprakasam@gmail.com

V. S. Kanwar and S. K. Shukla (eds.), *Sustainable Civil Engineering Practices*,
Lecture Notes in Civil Engineering 72,
https://doi.org/10.1007/978-981-15-3677-9_20

located individuals and effect upon ecosystems in different means are overlooked by government.

Ramachandra et al. [1] utilized the GIS application along with the various hydrological parameters to quantify the environmental flow in the Western Ghats region. The LULC analysis shows that there is a larger potential for water storage in the study area. Hadeel et al. [2] highlighted the environmental change signs in south Iraq for the past 20 years. Indices like NDVI, Normalized Difference Water Index (NDWI), Normalized Difference Built-up Index (NDBI) were analyzed resulting in spatial and temporal vegetation degradation took place in the study area. Lin et al. [3] studied the variation in the greenness seasonal wise for the years between 2001 and 2012 by analyzing the MODIS Terra Level 1 Product. The result shows that about 34.63% of the vegetation was degraded, and the vegetation starts again in the month of April and degrades in September. Wong et al. [4] used the Sentinel-2 images of 10 m resolution to compute the NDVI in the Pearl River Delta (PRD) region. The Google satellite images with some adjustments show relatively higher accurate results than the Sentinel-2 images. Palmate et al. [5] assess the climate change effect upon vegetation in the River Yamuna (a tributary), Betwa River Basin using the Normalized Difference Vegetation Index (NDVI) using the Landsat images imported in the ArcGIS and ERDAS for analysis. The results were divided into pre- and post-monsoon season, whereas the post-monsoon shows a negative response to the vegetation.

This paper tries to bring the limelight upon the environmental flow as a mitigation measure as the environmental impact occurs irrespective of the potential of the hydropower project by assessing the vegetation index in the study area.

2 Study Area

To represent the Beas River Basin, two hydropower projects were chosen such as Larji (126 MW) and Binwa Hydropower Project (6 MW) to represent a large and small hydropower project. Larji Hydropower Project (126 MW) was constructed in 1984 on Beas River Basin as a hydropower station to produce the vast hydropower potential.

The catchment area of the hydropower project is spread over an area of 4921 sq.km. The large dam site is located at an altitude of 2299 m MSL. The project was completed in September 2007. As a 56.84 m of design head and discharging capacity of 250 m^3/s and 230 ha m of live storage capacity the power project is functioning.

Binwa watershed is situated between 76° 34′ 08″ to 76° 45′ 53″ E longitude and 31° 53′ 15″ to 32° 11′ 58″ N latitude in Kangra district of Himachal Pradesh, comprising of a bit of Lesser Himalayas and Shivalik hilly slopes. It has a place with agro-eco region, i.e., Western Himalayas, warm and substicky to humid eco region with dark-colored backwoods and podzolic soils [8]. The watershed spread over an

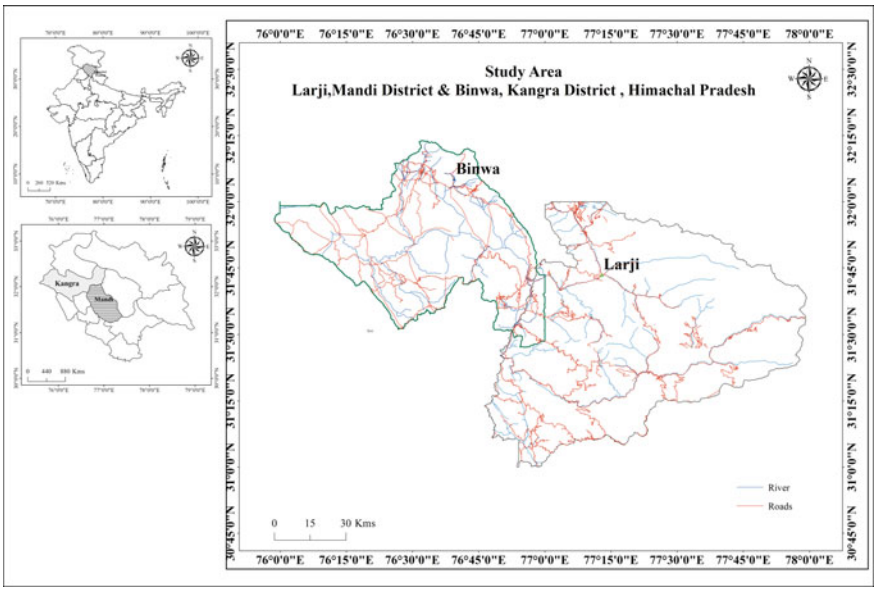

Fig. 1 Study area map

area of around 340.1 km^2 with an elevation ranging from 600 to 4286 m above mean sea level (Fig. 1 shows the study area map).

3 Materials and Methods

Present research centers around the Binwa hydroelectric power venture located in the Beas River Basin and its impact upon the area condition, farming, living and so forth. The hydropower activities can be named reservoir-based hydro tasks and run-of-river-based hydro ventures. A vast majority of the activities in the state depend on the run-of-river ventures. Run-of-the-river hydroelectricity is a kind of hydropower generation wherein the natural flow of the river is made to drop from the elevation to deliver hydropower. In a general sense depending on inconsistent river flows, power stations of this type are installed on rivers with a strong and enduring flow, either natural or using a colossal reservoir at the head of the river. The common assumption is that there is only an environmental impact due to large hydropower project, whereas the impact due to small hydropower projects is overlooked.

Hydropower headway forcefully influences the profitability of agribusiness methods for degrading or goes through different natural resources that contain imperative agrarian inputs. The water is necessary for the irrigation, and if overexploited for the power generation purpose, then the agribusiness will be a question mark. Losing

of timberland and vegetation cover, both have an immediate impact on the environment. Deforestation influences agribusiness by varying the river flow and drought events and destabilizing soil. All through district individuals feature the lessening in agriculture producing limit, air contamination, diminished rainfall, water filtration and nonappearance of soil dampness on account of the foundation of hydropower ventures.

4 Results and Discussion

4.1 The Normalized Difference Vegetation Index (NDVI)

It helps in understanding vegetation changes occurred in a region spatially and temporally.

NDVI indicates the health of vegetation and its density

$$\text{NDVI} = \left(\frac{(\lambda_{\text{NIR}} - \lambda_{\text{red}})}{(\lambda_{\text{NIR}} + \lambda_{\text{red}})} \right) \tag{1}$$

where λ_{NIR} and λ_{red} represent the reflectance in the near-infrared and red bands, respectively.

5 Importance of E-Flow

Amrit et al. [6] showed that there is relation between the environmental flows and the drought conditions. Tonkin et al. [7] say that the e-flows are the solution to the increasing alteration in the hydrological regime and parameters. Normalized Difference Vegetation Index (NDVI) calculated using Eq. (1) helps in understanding vegetation changes occurred in a region spatially and temporally. NDVI analysis was done for two hydropower projects, Larji (126 MW) and Binwa (6 MW). These three were chosen to represent a large and small hydropower project. NDVI demonstrates the temporal and spatial difference in vegetation spread as average and poor vegetation. Considering the study area which is located near perennial water resources, the vegetation must be best of its nature, but the outcome indicated that the natural vegetation of the study area is declining as such it is average after the construction of the hydropower dam. This is mainly because of the over exploitation of the water resources from the dam, leaving no water behind for the agricultural purpose. This implies that numerous areas which were vegetative in nature are now affected by the construction and operation of the dam. Irrespective of the potential of the project being it large or small, the impact prevails if e-flow is not maintained in the study area. As of solution and recommendation, 15% minimal flow has to be maintained

in the project for agriculture purpose. NDVI is estimated from reflectance estimated in the visible red and infrared channels of the Landsat 8 data. NDVI demonstrates the temporal and spatial difference in vegetation spread. The vegetation change is the difference between two pictures which is calculated by finding the difference of pixel contrast between each pixel in each picture. Considering the study area which is located near perennial water resources, the vegetation must be best of its nature, but the outcome indicated that the natural vegetation of the study area is declining as such it is average after the construction of the hydropower dam.

This is mainly because of the over exploitation of the water resources from the dam, leaving no water behind for the agricultural purpose. The development of cultured areas, exposed farms and developed areas are evident in the NDVI study. These zones were shown as dark red, and NDVI values are less than 0.0 as an average ranging near the negative values. This implies that numerous areas which were vegetative in nature are now affected by the construction and operation of the dam.

6 Conclusions

Hydroelectric Projects can cause a few issues, despite the fact that they consume no fuel. Figure 2 represents the vegetation index in the study area. The common assumption is that there is only an environmental impact due to large hydropower project, whereas the impact due to small hydropower projects is overlooked. This paper tried to bring the limelight upon the environmental flow as a mitigation measure as the environmental impact occurs irrespective of the potential of the hydropower project. This research is an example that even small hydropower project can impact the environment if the norms are not maintained with standards. By building dams on rivers may for all time change river frameworks and wildlife habitats. Fishes and other river fauna may never again have the capacity to swim upstream. Following recommendations are provided as part of mitigation measure:

- Considering the study area is located near perennial water resources, the vegetation must be best of its nature, but the outcome indicated that the natural vegetation of the study area is declining as such it is average after the construction of the hydropower dam.
- The water resource in the region is also very meager, and barren lands have also increased in range due to poor maintenance of minimal flow in the dam.
- The neighborhood issues must be mulled over. The strategies ought to be confined by accurate examination of nearby destinations with the goal that the proportionate harmony among biotic and its segments of the mother earth can be maintained and the potential rivers can be used legitimately.
- As of now, the production of hydropower might be a greater goal, but in a long run for a sustainable environment and agricultural aspect, the environmental flow has to be taken into serious consideration and followed with strict adherence.

- Hence, irrespective of the potential, 15% of minimal flow has to be maintained in the dam for better health of the ecosystem.

Acknowledgements The research work done is a part of DOES&T, Himachal Pradesh funded research project. We would like to express our sincerest gratitude to DOES&T, Himachal Pradesh for funding this research project.

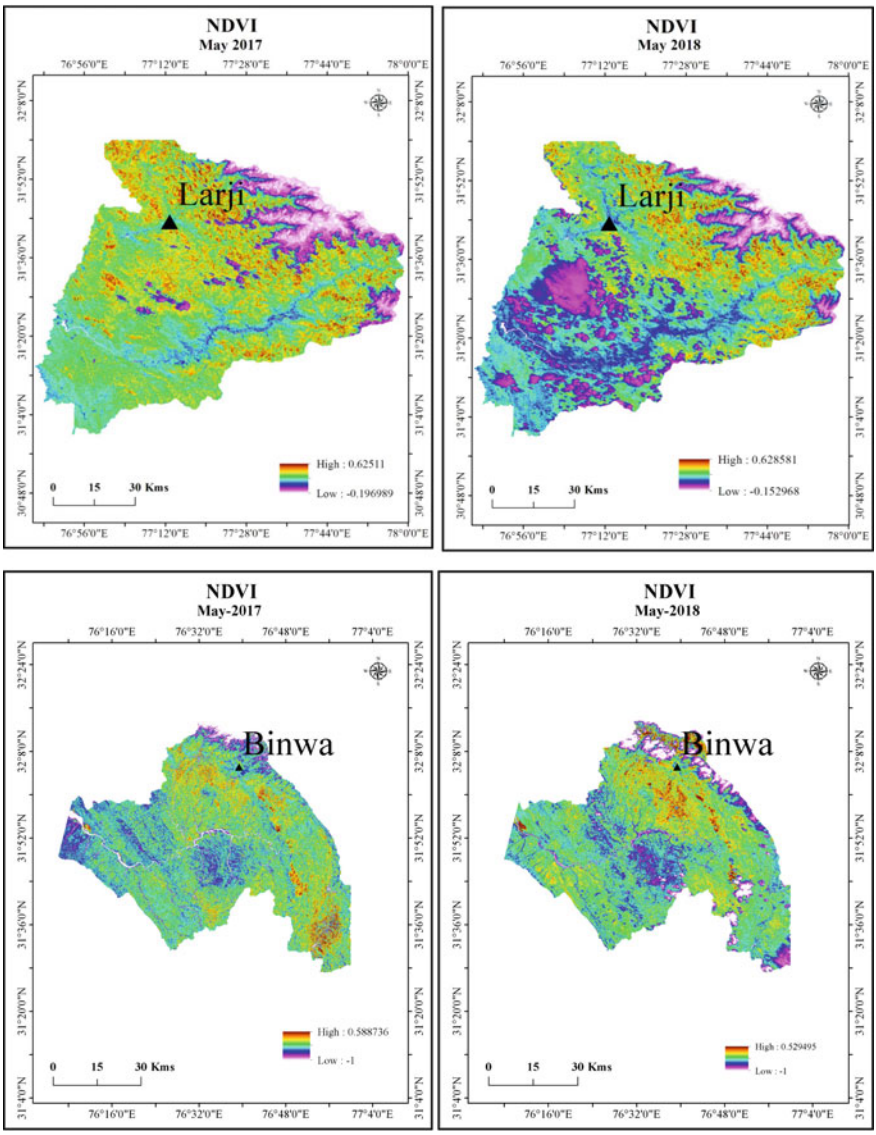

Fig. 2 Larji and Binwa NDVI analysis (2017–2018)

References

1. Ramachandra TV, Vinay S, Bharath HA, Bharath S, Shashishankar A (2014) Environmental flow assessment in the rivers originating at the Western Ghats. In: Proceeding of bi-annual lake conference, Sirsi, Karnataka, India
2. Hadeel A, Jabbar M, Chen X (2011) Remote sensing and GIS application in the detection of environmental degradation indicators. Geo-spatial Inf Sci 14(1):39–47
3. Lin X-S, Tang J, Li Z-Y, Li H-Y (2016) Vegetation greenness modelling in response to interannual precipitation and temperature changes between 2001 and 2012 in Liao River Basin in Jilin Province, China. SpringerPlus 5(1):1173
4. Wong MM, Fung JCH, Yeung PP (2019) High-resolution calculation of the urban vegetation fraction in the Pearl River Delta from the Sentinel-2 NDVI for urban climate model parameterization. Geosci Lett 6(1):2
5. Palmate SS, Pandey A, Kumar D, Pandey RP, Mishra SK (2017) Climate change impact on forest cover and vegetation in Betwa Basin, India. Appl Water Sci 7(1):103–114
6. Amrit K, Mishra SK, Pandey RP (2018) Coupling of tennant concept with standardized precipitation index (SPI) for the prediction of environmental flow condition from rainfall in upper Narmada Basin. In: Climate change impacts, Springer, Singapore, pp 265–272
7. Tonkin JD, Jähnig SC, Haase P (2014) The rise of riverine flow-ecology and environmental flow research. Environ Proc 1(3):323–330
8. Sehgal J, Mndal DK, Mandal C (1992) Agro-ecological regions of India, 2nd edn., NBSS Publ. 24. Oxford & IBH New Delhi

RBI Grade 81 Commercial Chemical Stabilizer for Sustainable Highway Construction

Gaurav Gupta, Hemant Sood and Pardeep Kumar Gupta

Abstract Weak soils cannot be used in subgrade course of pavements and need to be stabilized, for which different commercial chemical stabilizers are available that claim their superiority over traditional stabilizers like lime and cement. RBI Grade 81 is one such patented soil stabilizer, and this paper aims to review the geotechnical and geo-environmental properties of RBI Grade 81 stabilized soils for use in the construction of sustainable highways. Regarding the stabilized soils, strength parameters (unconfined compressive strength, California bearing ratio and Brazilian tensile strength), compaction parameters (optimum moisture content and maximum dry density), consolidation parameters (void ratio and compression index), fatigue life, plasticity, durability, chemical composition, mineralogical composition and surface morphology through scanning electron microscopy were reviewed. The effects of the dosage of the stabilizer, curing period and time of elapse were also reviewed along with its efficiency to stabilize soils of different plasticity. The toxicity characteristics of the stabilized soils were reviewed to evaluate the potential damage to the groundwater through leaching of heavy metals. Gaps in the literature were identified that limit the application of the soil stabilizer and are therefore required to be studied in the future.

Keywords Chemical soil stabilization · Commercial chemical stabilizer · RBI grade 81 · Sustainable highway construction · Unconfined compressive strength · California bearing ratio (CBR) · Toxicity characteristic leachate procedure

G. Gupta (✉) · H. Sood
National Institute of Technical Teachers' Training and Research, Chandigarh, India
e-mail: gaurav007gupta@gmail.com

H. Sood
e-mail: sood_hemant@yahoo.co.in

P. K. Gupta
Punjab Engineering College (Deemed to be University), Chandigarh, India
e-mail: p_gupta_2000@yahoo.com

V. S. Kanwar and S. K. Shukla (eds.), *Sustainable Civil Engineering Practices*,
Lecture Notes in Civil Engineering 72,
https://doi.org/10.1007/978-981-15-3677-9_21

1 Introduction

The rise in population, all across the globe, has generated a simultaneous demand for more infrastructure, the building of which consumes natural resources and leads to the deterioration of the environment. The practice of construction of roads is no different and relies on natural resources such as bitumen, aggregates and soil. The subgrade course of flexible pavements serves as the foundation and must have enough bearing strength and stiffness to bear the stresses generated due to the movement of traffic on the surface layer and the overburden pressure of overlying base course and surface course. It is not often that the bearing strength of the soil fulfils the minimum criteria of 8% 4-day soaked California bearing ratio (CBR) value, for use in the construction of the subgrade layer of national highways of India, as directed by the Indian Road Congress [4]. Therefore, either the in situ soil needs to be replaced with soil having a 4-day soaked CBR >8%, or the in situ soil shall be stabilized. The soil replacement option consumes scarcely available natural resources and deteriorates the environment, making it a non-sustainable practice. In order to achieve sustainable highway construction, the in situ soil for the subgrade must be utilized on-site and hence needs to be strengthened through stabilization. The soil stabilization option needs a proper evaluation of the properties of the stabilized soils to ensure sustainable benefits of the stabilization. Construction on the strengthened subgrade reduces the thickness of overlying granular layers and thereby mitigates consumption of natural aggregates and its haulage requirement, making it a sustainable practice. The fact that greenhouse gas emission associated with pavement construction is mitigated as the carbon dioxide emission released during the processing of granular material, and its transportation is reduced in another sustainable aspect of the stabilization. Though traditional stabilizers like cement and lime have been used for soil stabilization, they carry their own set of limitations in their application. Regarding lime stabilization, the method is effectual for soils having plasticity index higher than 10% or soils having material >25% finer than 75-micron sieve size, and hence, has a very limited application range. The cement stabilization method is effectual for low plasticity index soils. Cement is self-hardening in its behaviour and performs the role of filler and does not directly make a bond with grains of quartz present in non-plastic soils. The inclusion of cement to a plastic soil results in, after hydration, expansive ettringite crystallization that generates expansive forces beyond the bearing capacity of the soil and inescapably leads to cracking. The generation of crack in any layer of pavement allows water to percolate through the layer and leads to irrevocable damage. In view of these limitations of new commercial chemical stabilizers (CCS) are being promoted by a number of companies that claim to perform better than traditional stabilizers. Recently in the year of 2018, the IRC released the guidelines for the design of stabilized pavements (Part 2) that deal with different aspects of CCS that are necessary to be ascertained before the application of CCS in large-scale road construction [5].

Invented in the early 1990s in South Africa, Road Building International (RBI) Grade 81 is a soil stabilizer for use in the stabilization of weak soils for road construction. Anyway, Solid Environmental Solutions Ltd. Kerem Maharal Corporation manufactures RBI Grade 81 in countries such as Canada and Israel. The product is limitedly made available by M/S Alchemist Technology in India. RBI Grade 81 has attained a precise global acknowledgement as a stabilizer of road pavement layers such as the base, subbase and subgrade. RBI Grade 81 has found its application in different countries located in the continent of Africa and Europe, but unfortunately, RBI Grade 81 has found little application in India, limited to the base course and the subbase course of flexible pavement. As claimed by the manufacturer, RBI Grade 81 can be used to stabilize soil of varying plasticity ranging from clay to sand, but these need to be verified by independent studies.

This paper reviews the geotechnical characteristics such as strength parameters [3, 13], compaction and plasticity parameters [1, 7] and consolidation parameters [7] of RBI Grade 81 stabilized soils. Also, the effect of curing period on the strength of the stabilized soils [11, 8], the effect of elapsed time on the strength of the stabilized soils [10], durability of the stabilized soils [12] and Anjaneyappa and Amarnath [1] and the performance of the stabilized soils under cyclic loading [8] and Anjaneyappa and Amarnath [1] were reviewed along with the mineralogical, microstructural and geo-environmental properties of RBI Grade 81 stabilized soils [3]. RBI Grade 81 stabilized soils were studied in detail for their extensive application in the field, and research gaps were identified to work upon in future, for a better understanding of the behaviour of stabilized soil and a broader application of the stabilizer in building sustainable highway construction.

2 Properties of RBI Grade 81

RBI Grade 81 comprises inorganic substances that stabilize soil to develop strength and stiffness against stress from repeated traffic loading. The main components that are used to formulate RBI Grade 81 are a series of inorganic hydration-activated powders comprising a specific type of cement, a lime, several pozzolanas, rate governing additives and unique polypropylene fibre. The fibre has a diameter of 20 μm and a length of 2 cm and is randomly distributed. The fibre imparts ductility and tensile strength to the stabilized soil mixtures. Gupta et al. [3] observed the surface morphology of the particles of RBI Grade 81 through Scanning Electron Microscopy (SEM) and concluded that the particles were angular in shape as shown in Fig. 1.

Regarding physical properties, RBI Grade 81 is an odourless, grey-coloured and a non-self-inflammable powder. A saturate paste of RBI Grade 81 has a pH of 12.5, and its grains possess a unit weight of 25 kN/m^3. The main chemical elements forming the product and their respective variation range in terms of percentage are listed in Table 1 [2]. The soil stabilizer is sold in the form of grains, packed in a pack of 25 kg weight and in one-ton weight container, having a shelf life of 12 months.

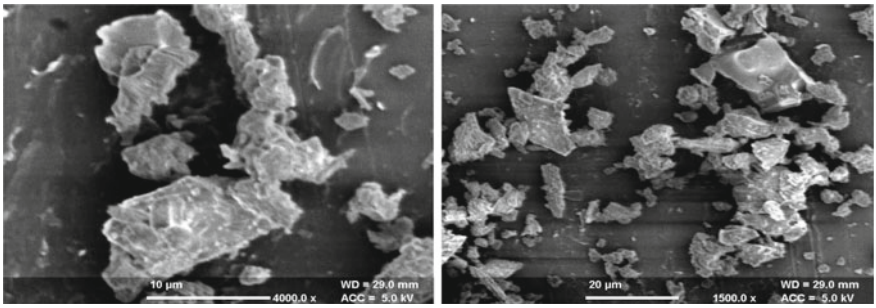

Fig. 1 RBI Grade 81 images from SEM at 4000× and 1500× magnification

Table 1 Chemical composition of RBI Grade 81

Calcium (%)	Silica (%)	Sulphur (%)	Magnesium (%)
25–45	5–15	0–10	0–10
Iron (%)	Potassium (%)	Aluminium (%)	Manganese (%)
0–5	0–5	0–5	0–2

3 Geotechnical Properties of the Stabilized Soils

The soils stabilized with RBI Grade 81 were reviewed for their strength parameters like Brazilian tensile strength (BTS), CBR and Unconfined Compressive Strength (UCS), compaction parameters like Optimum Moisture Content (OMC) and Maximum Dry Density (MDD), consolidation parameters such as void ratio and compression index, plasticity and behaviour under repeated loading. For uniformity, the soils reviewed in this paper were classified according to the Unified Soil Classification System (USCS).

3.1 Strength Parameters of the Stabilized Soils

Trindade [13] performed CBR, UCS and BTS tests on three soils (USCS classification: MH, SM and SC) stabilized with RBI Grade 81 (2%, 4% and 6% content). The samples were cured for seven days followed by 4-day water immersion for CBR test and 4-hour water immersion for UCS and BTS test, following the Brazilian standards. RBI Grade 81 emerged as an effective soil stabilizer producing a gain in the mechanical strength and reduction in swelling for all the soils. Prepared at modified compaction effort, the unsoaked CBR specimens depicted a gain of 293% (SC soil), 249% (SM soil) and 349% (MH soil), while for the soaked condition a gain of 600% (SC soil), 698% (SM soil) and 374% (MH soil) was observed. The

largest improvement in UCS of the stabilized was 946% (SC soil), 258% (SM soil) and 376% (MH soil), whereas a gain of 1296% (SC soil), 329% (SM soil) and 502% (MH soil) was attained in the BTS test for soils stabilized with 6% RBI Grade 81 content. Immersion of samples in water leads to a diminution of BTS and UCS by 48% and 54%, respectively.

Trindade [14] stabilized three soils (USCS classification: MH, SM and SC), with 2%, 4% and 6% RBI Grade 81 content, at three compaction efforts (standard, intermediate and modified) and subjected to un-consolidated un-drained triaxial tests. The authors concluded that the shear strength of the soils enhances with the rise in the stabilizer content as well as the compaction effort, but the impact of the confining pressure continuously reduces for the shear strength. The cementitious action of the stabilizer had a noteworthy impact on the soil deformation parameters producing a more rigid soil mass with a brittle behaviour.

Lekha and Shankar [8] stabilized black cotton soil (USCS classification: CH) with 2, 4 and 6% RBI Grade 81 content and evaluated CBR and UCS of the stabilized samples. The CBR samples were subjected to 7 days curing followed by 4 days soaking. The UCS samples were cured for 4 h, and 1, 3, 7 and 28 days and soaked for 1 day. The CBR increased from 0.3 to 12.5% at 6% RBI Grade 81 content depicting an appreciable increase in the bearing strength of the soil. The UCS first decreased with increase in curing time from 4 h to 1 day followed by an increase with increasing curing time for any RBI Grade 81 content. The unsoaked UCS was significantly higher than the soaked UCS. The 4 h and 1 day cured samples showed almost nil strength under soaked condition. The unsoaked UCS (28 days cured) of soil increased from 350 kPa to 830 kPa, 1350 kPa and 1800 kPa on the addition of 2%, 4% and 8% RBI Grade 81 content, respectively. The soaked UCS (28 days cured) of soil increased from 0 kPa to 140 kPa, 370 kPa and 680 kPa on the addition of 2%, 4% and 8% RBI Grade 81 content, respectively.

Anjaneyappa and Amarnath [1] evaluated the potential of RBI Grade 81 (2%, 4% and 6% content) to stabilize three soils (USCS classification: MH, ML and SM). The experimental programme comprises CBR (7 days cured and 4 days soaked) and UCS tests (4 h, and 1, 3 and 7 days curing; unsoaked and 2 h soaked). An increase in the CBR from 5% to 30% (MH soil), 10 to 45% (ML soil) and 14 to 40% (SM soil) was attained at 6% RBI Grade 81 content. The increase in UCS for 7 day cured MH soil is 270%, 353% and 360% at 2%, 4% and 6% stabilizer content, respectively. Likewise, in the ML and SM soils, the increases in UCS are 138%, 148% and 167% and 115%, 393% and 643%, respectively. Increase in strength with curing time is observed for all types of soils. Stabilization of MH soil with 2 and 4% RBI Grade 81 content leads to 32 and 39% reduction in the vertical compressive strain at the top of the subgrade, respectively.

Kumar and Janewoo [7] used RBI Grade 81 (2, 4 and 6% content) to stabilize an expansive soil (USCS classification: CH) mixed with 5, 10 and 15% cement kiln dust (CKD). The authors stated that for any fixed CKD content (5, 10% or 15%), with the rise in the content of the stabilizer. CBR tests were carried out in the unsoaked and uncured conditions. The CBR increased from 2.41% to 19.02%, 3.88% to 20.02% and 4.35% to 21.7% on adding 6% RBI Grade 81 content to soils containing 5%, 10%

and 15% CKD, respectively. The UCS (28 days cured) increased from 107.5 kPa to 662.3 kPa, 125.7 kPa to 770.5 kPa and 139.5 kPa to 770.5 kPa on adding 6% RBI Grade 81 content to soils containing 5%, 10% and 15% CKD, respectively. On average, the 3 days UCS increased by 40% and 132% on the 14th and 28th day depicting significant UCS gain.

Taib et al. [9] stabilized a clay soil obtained from Serian (USCS classification: MH) with 2, 4, 6 and 8 RBI Grade 81 content. UCS test was carried out on samples cured for 7, 14 and 28 days. The UCS (28 days cured) increased from 193.5 kPa to 374.7 kPa, 346.6 kPa to 551.3 kPa, 636.1 kPa to 864.8 kPa and 682.4 kPa to 975.2 kPa on adding 8% RBI Grade 81 content to soil cured for 7, 14 and 28 days, respectively. On average, the 3 days UCS increased by 50 and 57% on the 14th and 28th day depicting an insignificant gain in the UCS during the period of 14 to 28 days.

Kodicherla and Nandyala [6] stabilized a clay soil (USCS classification: CL) with 2, 4, 6 and 8% RBI Grade 81 content. The CBR enhanced from 3 to 13.8% at 4% RBI Grade 81 content beyond which no further increase in CBR was observed up to 8% RBI Grade 81 content. The UCS increased almost linearly with the increasing contents of the stabilizer. The UCS increased from 100 to 375 kPa, whereas the axial strain fell from 9.7 to 3.9% on treatment with 8% stabilizer content. The reduced failure strain depicts the brittle behaviour of the stabilized soil specimens. Overall, it was concluded that RBI Grade 81 could be used effectively for soil stabilization.

Gupta et al. [3] stabilized two soils (USCS classification: CL and SM) with 1%, 2%, 3%, 4% RBI Grade 81 content to establish the efficacy of the stabilizer for varying plasticity soils. The 4-day soaked CBR increased with the increase in the contents of the stabilizer. On treatment with 4% stabilizer content, the CBR value of sand and clay enhanced from 9.4% and 3.2% to 28.8% and 25.3%, respectively. Regarding the UCS test, the highest axial stress increased radically with rising stabilizer content. On treatment with 4% stabilizer content, the failure strain reduced from 2.0% to 0.65% and 0.80% in sand and clay, respectively, due to imparted brittleness by the soil stabilizer.

3.2 Compaction Parameters of the Stabilized Soils

Trindade [13–15] stabilized three soils (USCS classification: MH, SM and SC) with RBI Grade 81 and reported that the stabilized samples exhibited reduced MDD and increased OMC. The authors stated that the increase in the MDD was due to the formation of flocs and grouping of smaller aggregates (by the chemical stabilizer) to form large aggregates, possessing a more porous structure. The increase in OMC was cited as a higher water requirement for hydration of RBI Grade 81, as in the case of hydraulic cement.

Anjaneyappa and Amarnath [1], Kumar and Janewoo [7], Kodicherla and Nandyala [6] and Gupta et al. [3] also reported the same trend.

3.3 Plasticity of the Stabilized Soils

Trindade [15] reported the physical characterization of three soils (USCS classification: MH, SM and SC) mixed with 2, 4 and 6% RBI Grade 81 content. The results show that RBI Grade 81 altered the plasticity and grain size distribution of the soils. With the rise in the stabilizer content, the plastic limit slightly increased and the liquid limit and the plasticity index value decreased, reporting a reduction in the plasticity of the soils. The grain size distribution showed increases in coarse grain fraction with increasing stabilizer content due to the linking of fine particles.

Anjaneyappa and Amarnath [1] evaluated the potential of RBI Grade 81 (2, 4 and 6%) to stabilize three soils (USCS classification: MH, ML and). The authors stated a noteworthy decrease in the plasticity index. A decline of 15%, 20% and 35% and 8%, 16% and 25% in plasticity index was observed in MH and ML soil samples stabilized with 2%, 4% and 6% content of RBI Grade 81, respectively.

Kumar and Janewoo [7] used RBI Grade 81 (2, 4 and 6%) to stabilize an expansive soil (USCS classification: CH) mixed with 5, 10 and 15% CKD. The authors stated that for any fixed CKD content (5, 10 or 15%), the liquid limit and plasticity index decreased, whereas the plastic limit increased up to 4% RBI Grade 81 content, beyond which there was a reversal of a trend.

Kodicherla and Nandyala [6] stabilized a clay soil (USCS classification: CL) with 2,4, 6 and 8% RBI Grade 81 content, and the authors stated that the stabilization process increases the plastic limit and decreases the plasticity index and liquid limit of the clay soil. The effects were almost linear with the increasing dosage of RBI Grade 81 where at 8% stabilizer content the soil turned non-plastic with plasticity index <1%.

3.4 Consolidation Parameters of the Stabilized Soils

Kumar and Janewoo [7] used RBI Grade 81 (2%, 4% and 6% content) to stabilize an expansive soil (USCS classification: CH) mixed with 5%, 10% and 15% CKD. The optimum mix of 81% soil + 15% CKD and 4% RBI Grade 81 was subjected to consolidation test. The optimized mixture had reduced void ratio and volume compressibility.

3.5 The Effect of Curing Period on the Strength of the Stabilized Soils

Trindade et al. [11] studied the effect of different types of curing conditions and water immersion on the UCS of three soils stabilized with RBI Grade 81 (2%, 4% and 6% content). The samples were cured for seven days in an air-conditioned room, with

Table 2 Fatigue life test observations for RBI Grade 81 stabilized black cotton soil

Curing period	Applied load (kg)	Fatigue life (Number of cycles)			
		0%[a]	2%[a]	4%[a]	6%[a]
7 Days	23	3	1811	3628	4172
	34	2	1126	2277	2987
28 Days	31	5	2931	5719	8005
	47	3	1318	2193	3860

[a]content of RBI Grade 81

and without plastic wrap covering. Results show that specimens cured without plastic covering showed better mechanical strength than the plastic wrapped samples. Also, the immersion of specimens in water resulted in reduced UCS.

Lekha and Shankar [8] stabilized black cotton soil (USCS classification: CH) with 2, 4 and 6% RBI Grade 81 content, and the authors reported that the UCS first decreased with increase in curing time from 4 h to 1 day followed by an increase with increasing curing time. The fatigue life was enhanced with rising in the content of the stabilizer and time of curing, the results of which are reported in Table 2 under Sect. 10.

Kumar and Janewoo [7] and Taib et al. [9] reported a gain in UCS with an increase in the curing period of 3, 14 and 28 days.

3.6 The Effect of Elapsed Time on the UCS of Stabilized Soils

Trindade et al. [10] stabilized three soils (USCS classification: MH, SM and SC) with 4% RBI Grade 81 content and evaluated the effect of elapsed time (0, 4, 8 and 24 h) on their UCS. The samples were prepared at modified compaction effort and cured for seven days prior to testing. The elapsed time between a mixture and specimen compaction had a significant effect on the mechanical strength of the mixtures. The most substantial rise in UCS was attained at 4 h for MH soil (877–1330 kPa) and SM soil (638–1341 kPa), whereas in case of the SC soil, the specimens compacted immediately showed the highest UCS gain (292–1622 kPa). Also, the SC soil showed higher UCS gain (455.8%) than SM soil (110.2%) and MH soil (51.7%) at their respective optimum elapsed time.

3.7 Durability of the Stabilized Soils

Trindade et al. [12] determined the durability of RBI Grade 81 stabilized soils (USCS classification: MH, SM and SC), for which the soils were mixed with 6% stabilizer content and at three compaction efforts (standard, intermediate and modified) and

subjected to twelve wet and dry cycles. Results show that only the samples compacted at modified effort (MH and SC soils) and intermediate effort (SM and SC soils) were able to endure all the twelve wetting and drying cycles. Under the modified effort, the lowest mass loss was reported for SC soil (<13%) after undergoing 12 cycles, whereas the MH and SM soil report a loss of 21% after 10 cycles and 22% after 12 cycles, respectively.

Anjaneyappa and Amarnath [1] evaluated the potential of RBI Grade 81 (2%, 4% and 6%) to stabilize three soils (USCS classification: MH, ML and SM) and performed wetting and drying test. The loss in weight due to wetting and drying tests carried out on clayey soil found to be in the range of 10% and 30% for first and second cycles.

3.8 Performance of the Stabilized Soils Under Cyclic Loading

Lekha and Shankar [8] stabilized a black cotton soil (USCS classification: CH) with 2, 4 and 6% RBI Grade 81 content and evaluated the fatigue life of the stabilized samples. In order to evaluate the fatigue life of the stabilized soil specimens, 7 days and 28 days cured specimens were subject to repeated loading of 1 Hz frequency. The tests were performed at loadings corresponding to 1/3rd and half of the UCS of the soil treated 2% chemical stabilizer. The fatigue life increased with rising RBI Grade 81 content and time of curing, the results of which are reported in Table 2.

Anjaneyappa and Amarnath [1] evaluated the potential of RBI Grade 81 (2%, 4% and 6%) to stabilize three soils (USCS classification: MH, ML and SM) and performed a repeated load test. Concerning repeated load tests conducted at different stress ratios, the percentage increase in a number of cycles to failure was about 100, 300 and 850% at the stress ratio of 0.9, 0.8 and 0.5, respectively, for MH soil samples stabilized with 2% content of the chemical stabilizer.

4 Mineralogical Characterization of the Stabilized Soils

Trindade [15] reported the chemical and mineralogical characterization of three soils (USCS classification: MH, SM and SC) mixed with 6% RBI Grade 81 content. Energy-dispersive X-ray spectrometry (EDS) result depicted that the stabilization process leads to a decrease in the contents of silica and aluminium oxides, noticeably due to solubilization of these oxides and calcium aluminates and silicates creation through hydration and pozzolanic reactions of the soils stabilized with RBI Grade 81. The findings of the EDS were corroborated by the X-ray diffraction (XRD) analysis that depicted a lowering of all clay minerals and the creation of rankinite (a calcium silicate) in a well-crystalline form for the stabilized soil mixes. The authors hypothesized that soil stabilization with RBI Grade 81 resulted in the formation of an inter-particle cementing matrix of a very durable, sturdy and established mixture.

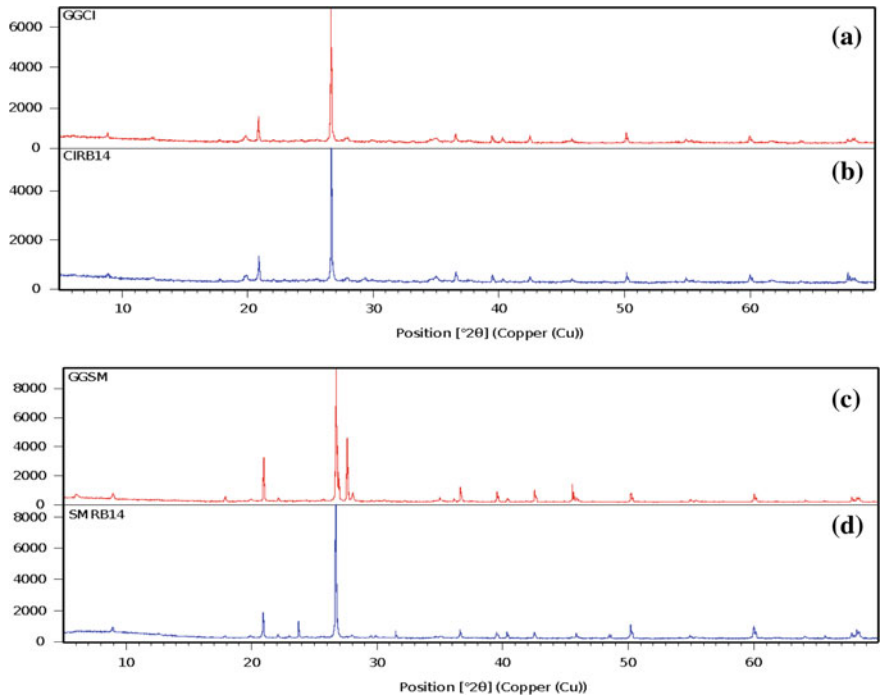

Fig. 2 XRD intensity plots: **a** untreated clay; **b** stabilized clay; **c** sand; **d** stabilized sand

Kumar and Janewoo [7] reported higher silica and calcium components RBI Grade 81 treated expansive soil (USCS classification: CH), through EDS test.

Gupta et al. [3] performed the XRD test on clay and sand stabilized with 4% RBI Grade 81 content, and the XRD patterns are shown in Fig. 2. The mineral of quartz was seen in the XRD intensity plot of the untreated soils. The RBI Grade 81 stabilized soils showed a decrease in the concentration of the peaks of quartz, representing utilization of the mineral during the stabilization process. Furthermore, soil stabilization with RBI Grade 81 resulted in the generation of new minerals, albite and muscovite in the sandy soil and tri-calcium di-yttrium and muscovite in the clay soil, which most likely enhanced the capacity of the soil to bear the peak stresses.

5 Microstructural Characterization of the stabilized soils

Trindade [15] reported the microstructural characterization of three soils (USCS classification: MH, SM and SC) stabilized with 6% content of the stabilizer. The SEM images reveal that raising the compaction effort resulted in the manifestation of fractures all along the surfaces of the stabilized soils.

Kumar and Janewoo [7] presented SEM images depicting the formation of needle-like structures (cementitious compounds) in RBI Grade 81 treated expansive soil (USCS classification: CH).

Taib et al. [9] stabilized a clay soil obtained from Serian (USCS classification: MH) with 2, 4, 6 and 8% RBI Grade 81 content and presented its SEM images, providing sufficient evidence of the formation of cementitious compounds in the stabilized soil samples.

Gupta et al. [3] performed SEM test on 4% RBI Grade 81 content admixed clay (USCS classification: CL) and sand (USCS classification: SM), and the images are shown in Figs. 3 and 4. The authors stated that soil stabilization with RBI Grade 81 resulted in the manifestation of cementation nuclei amongst the micro-particles of the soil, probably due to solubilization of SiO_2 and Al_2O_3 to produce calcium silicate

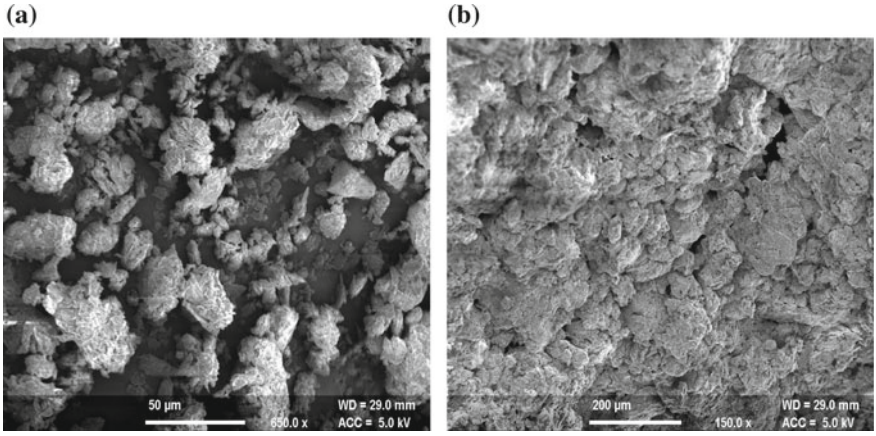

Fig. 3 SEM images of un-stabilized clay **a** and stabilized clay **b**

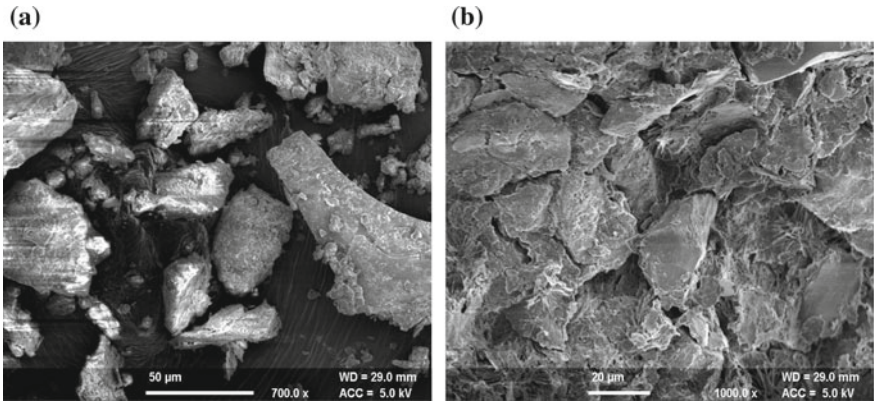

Fig. 4 SEM images of un-stabilized sand **a** and stabilized sand **b**

Table 3 Heavy metal concentration in the stabilized soils

	Concentration (mg/l)							
	Zn	Hg	As	Pb	Ni	Cr	Cu	Ni
Regulatory level for hazardous waste, USEPA	NR	0.2	5.0	5.0	NR	5.0	NR	NR
Stabilized sand	0.56	BDL	0.12	0.11	BDL	BDL	BDL	BDL
Stabilized clay	0.81	BDL	0.15	0.12	BDL	BDL	BDL	BDL

Note NR: Not reported, BDL: below detection level with detection limit <0.1 mg/l

and aluminates. The SEM images show the strong linkage of RBI Grade 81 hydrated products and inert sand particles that eventually provide the mechanical strength to the mixture.

6 Geo-environmental Properties of the stabilized soils

The guidelines for the design of stabilized pavements [5] state that the soils stabilized with CCS must be investigated for possible leaching of toxic heavy metals. The concentration of heavy metals shall be determined in the leachate of the stabilized soil, obtained through toxicity characteristics leachate procedure (TCLP). The TCLP test should be performed in accordance with the United States Environmental Protection Agency (USEPA) guidelines [16]. The leachate obtained through TCLP is tested for the concentrations of heavy metals, namely zinc (Zn), mercury (Hg), arsenic (As), lead (Pb), copper (Cu), nickel (Ni), cadmium (Cd) and chromium (Cr), by making the use of MP-atomic emission spectrophotometer. Gupta et al. [3] performed the above-stated tests on two soils (USCS classification: CL and SM) stabilized with 4% RBI Grade 81 content, the results for the same are reported in Table 3, together with the USEPA provided limits of the concentration of heavy metals for hazardous materials.

The authors concluded that the RBI Grade 81 stabilized soils are non-toxic and non-hazardous for the environment and do not possess the potential to contaminate groundwater. Hence, RBI Grade 81 can be potentially used for sustainable highway construction.

7 Conclusions

Based on the review of the literature, the following conclusion could be drawn:

1. RBI Grade 81 emerged as an effective stabilizer for soils of varying plasticity including the expansive soils.

2. A large number of studies depict RBI Grade 81 as a potential soil stabilizer that can improve the CBR, UCS, BTS and the shear strength of in situ soils.
3. RBI Grade 81 stabilization reduced the plasticity and MDD but increased the OMC of the stabilized soil.
4. The mechanism of the stabilization has been well understood by the EDS, XRD and SEM analysis that confirm the formation of cementitious hydrated products in the stabilized soils.
5. The geo-environment properties of the stabilized soils show that the concentrations of heavy metals were well inside the permissible limits and hence safe for use in highway construction.

Following gaps were identified in the literature survey:

1. Limited studies are available on the dynamic response of the RBI Grade 81 treated soils. No study was found that determine the resilient modulus of RBI Grade 81 soils that is required for ascertaining the behaviour of the pavement layers under repeated traffic loading.
2. The studies done up till now have been performed on a maximum of three soils of varying plasticity, and hence, studies incorporating more types of soils are required to be performed.
3. No study has been performed that evaluates the benefit–cost ratio of pavements constructed with RBI Grade 81 stabilized pavements.
4. No study has attempted to determine the optimum dosage of RBI Grade 81, based on strength, economics and sustainability aspects of road construction.
5. No study has been performed to evaluate the permeability of RBI Grade 81 stabilized soils.
6. No study has been performed to validate the laboratory test results with the performance of RBI Grade 81 stabilized soil in the field.
7. The majority of work, carried out by Trindade et al. [10–12] and Trindade [13–15], was done on soils available in Brazil. Similar studies are required to be performed on Indian soils for mass application of the stabilizer in India.

References

1. Anjaneyappa V, Amarnath MS (2011) Studies on soils treated with non-traditional stabilizer for pavements. Indian Geotech J 41(3):162–167
2. Anyway Solid Environmental Solutions Ltd. Kerem Maharal (2004) In: Materials safety data sheet. Israeli Office, 50 Bezalel Street, Ramat-Gan, 52521 Israel. Available at http://www.anywaysolutions.com/. Access on 22 Mar 2019, p 2
3. Gupta G, Sood H, Gupta PK (2019) Geotechnical and geo-environmental properties of discrete polyester fibre-reinforced and RBI Grade-81-stabilized clay and sand. In: IOP conference series: earth and environmental science, vol 219, p 012019
4. Indian Road Congress. IRC 37 (2012) Guidelines for the design of flexible pavements. Indian Road Congress, New Delhi, India
5. Indian Road Congress. IRC SP 89 (Part 2) (2018) Guidelines for the design of stabilized pavements. Indian Road Congress, New Delhi, India

6. Kodicherla SPK, Nandyala DK (2017) Effect of RBI Grade 81 on strength characteristics of clayey subgrade. Int J Geo-Eng 8(1):1–11. https://doi.org/10.1186/s40703-017-0061-z
7. Kumar JS, Janewoo U (2016) Stabilization of expansive soil with cement kiln dust and RBI Grade 81 at subgrade level. Geotech Geol Eng 34(4):1037–1046
8. Lekha BM, Shankar AR (2014) Laboratory performance of RBI 81 stabilized soil for pavements. Int J Civ Eng Res 5(2):105–110
9. Taib SNL, Striprabu S, Ahmad F, Charmaine HJ, Patricia NE (2016) Investigation on strength development in RBI Grade 81 stabilized Serian soil with microstructural considerations. In: IOP conference series: materials science and engineering, vol 136, p 012016
10. Trindade TPD, Lima DCD, Machado CC, Carvalho CABD, Fontes MPF, Schaefer CEGR, Caneschi FP (2005) Chemical stabilization of road subgrade: influence of elapsed time between mixture and compaction on mechanical strength of soil-RBI Grade 81 mixtures. Revista Árvore 29(3):413–418. https://doi.org/10.1590/S0100-67622005000300008
11. Trindade TPD, Lima DCD, Machado CC, Carvalho CABD, Fontes MPF, Schaefer CEGR, Caneschi FP (2005) Influence of the curing type (sealed and exposed) and water submersion on the mechanical strength of soil-RBI grade 81 mixtures for forest roads applications. Revista Árvore 29(4):601–606. https://doi.org/10.1590/S0100-67622005000400012
12. Trindade TPD, Lima DCD, Machado CC, Carvalho CABD, Fontes MPF, Schaefer CEGR, Caneschi FP (2005) Study of the durability of soil-RBI Grade 81 mixtures for application on forest roads and conventional pavement layers. Revista Árvore 29(4):591–600. https://doi.org/10.1590/S0100-67622005000400011
13. Trindade TPD (2006) Chemical stabilization of tropical soils: mechanical characterization using CBR, unconfined compression and Brazilian tensile strength laboratory tests. In: Technological characterization of three residual soils chemically stabilized for highway and environmental geotechnical applications (Dissertation). University of Vicosa, Brazil. Available from: http://alexandria.cpd.ufv.br:8000/teses/engenharia%20civil/2006/195010f.pdf#page=57. Accessed on 24 Mar 2019
14. Trindade TPD (2006) Chemical stabilization of tropical soils: shear strength and elastic properties characterization using triaxial tests. In: Technological characterization of three residual soils chemically stabilized for highway and environmental geotechnical applications (Dissertation). University of Vicosa, Brazil. Available from: http://alexandria.cpd.ufv.br:8000/teses/engenharia%20civil/2006/195010f.pdf#page=57. Accessed on March 24 Mar 2019
15. Trindade TPD (2006) Chemical stabilization of tropical soils: physical, chemical, mineralogical and microstructural characterization. In: Technological characterization of three residual soils chemically stabilized for highway and environmental geotechnical applications (Dissertation), University of Vicosa, Brazil. Available from: http://alexandria.cpd.ufv.br:8000/teses/engenharia%20civil/2006/195010f.pdf#page=57. Accessed on 24 Mar 2019
16. United States Environmental Protection Agency. USEPA Method 1311:1992 (1992) Toxicity characteristic leachate procedure, part of test methods for evaluating solid waste, physical/chemical methods. USEPA, Washington, US

Evaluation of Moisture Susceptibility of HMA Modified with Waste Sludge

Abhishek Kanoungo, Varinder S. Kanwar and Sanjay Kumar Shukla

Abstract Damage caused by the moisture induction is one of the major causes of distress in hot mix asphalt (HMA), which affects the durability of asphalt pavement. Due to the presence of water, the bond between binder and aggregate becomes weak, resulting in stripping of the pavement. To reduce the probability of failure due to moisture, anti-stripping additives are added into the HMA mixtures. The present study investigates the use of waste lime sludge as an additive in HMA to assess the moisture susceptibility of the mixtures. The performance of HMA was evaluated by performing the retained Marshall stability ratio test, indirect tensile strength test and tensile strength ratio test. It was found that the lime sludge acts as an anti-stripping agent. The results indicate that the addition of lime sludge in the HMA effectively increases the resistance of these mixtures against the damage caused by moisture.

Keywords Modified bituminous mix · Waste sludge · Indirect tensile test · Retained marshall stability test

1 Introduction

In current construction practice, the asphaltic/bituminous mixes are often used in pavement construction globally. Pavement design is a process that involves many steps. The selection of binder is one important step, which depends on the climatic condition of the region where road is intended to be constructed. The aggregate gradation depends on the selection of the mix as specified in MoRTH and also takes into account the effects of traffic loading. As the traffic intensity is exponentially

A. Kanoungo (✉) · V. S. Kanwar · S. K. Shukla
Chitkara University School of Engineering and Technology, Chitkara University, Baddi, Himachal Pradesh 173220, India
e-mail: abhishek.kanoungo@chitkarauniversity.edu.in

V. S. Kanwar
e-mail: vc@chitkarauniversity.edu.in

S. K. Shukla
e-mail: s.shukla@ecu.edu.au

V. S. Kanwar and S. K. Shukla (eds.), *Sustainable Civil Engineering Practices*,
Lecture Notes in Civil Engineering 72,
https://doi.org/10.1007/978-981-15-3677-9_22

increasing and the variation in temperature is rising, there is a need to think of an alternative solution for improvement of pavement characteristics. These problems have a damaging effect on the preferred properties of bituminous pavement, such as flexibility, resistance to fatigue, resistance to rutting, stripping and ravelling. The tendency towards stripping occurs due to the retention of moisture in the hot mix asphalt (HMA) mixture. Stripping is explained as the loss of bond between the asphalt and aggregate. The damage caused by moisture can often lead to permanent failures in pavements. This is one of the major concerns for pavement deterioration and hence needs to be addressed. Numerous tests have been evolved to evaluate the moisture susceptibility of asphaltic mixture and the researchers are working to improvise the same.

The road network in India predominantly consists of bituminous (flexible pavements) roads which have a design life span of 15–20 years [1]. These pavements do not have sufficient flexural strength and thus deform under repetitive or higher loads. The stress pattern is not the same for each layer of the pavement [2]. As we move down in the structure of pavement, the stress values decrease from being maximum at the top layer to least at the bottom [3]. These pavements are designed in such a way that the load which reaches the subgrade does not exceed the bearing capacity of the subgrade soil. Therefore, the thickness of different layers above the subgrade varies depending upon strength of soil [4]. Commonly, the performance of a flexible pavement is governed by various factors such as traffic, moisture, subgrade properties, construction quality and maintenance. However, it is known that the pavement will certainly deteriorate over time, no matter how well the pavement is constructed. In India, about 98% of the pavements are bituminous in nature as they require low initial cost and less time to construct [5]. Although, during the first few years after the construction, bituminous roads tend to deteriorate at a very slow rate but with time there is a rapid increase in deterioration rate. Therefore, these roads highly demand for regular and frequent maintenance to check the deterioration rate and increase the serviceability of the road [6]. Generally, this type of pavement fails due to structural or functional factors or their combinations [7]. If the pavement is insufficient to absorb and transfer the wheel load, it leads to the structural failure of the pavement [8]. However, the pavement failure is not only the result of poor design and construction but also it is caused by the unavoidable wear and tear that occurs with time, variation in climate, increasing vehicular load and heavy traffic [9]. Therefore, the pavement condition is usually monitored based on its riding quality, the presence of surface distress, the structural capacity and resistance to skid [10]. The occurrence of surface distresses is an indication of poor or unfavourable road performance or signs of approaching failure. To establish an organized maintenance management system, the evaluation of the surface distresses is one of the prerequisites for selecting appropriate maintenance operations. The four major categories of defects in flexible pavements are cracking, surface deformation, surface defects and disintegration) [10]. The failure in flexible pavements occurs normally because of structural, functional or a combination of both [9, 11]. The four major categories of distresses in flexible pavements are cracking, surface deformation, surface defects and disintegration. The presence of surface cracks significantly reduces

the life of flexible pavements. This is because the surface cracks are one of the main contributors to the development of other different types of cracks in the subsequent layers which eventually lead to early failure of the pavement. These distresses are the external indicators of pavement condition, and therefore, their evaluation is the most common way to evaluate road surface condition.

Hameed and Merawi [12] discussed the two common reasons of premature failure of flexible pavements. They are the moisture-induced and stripping. This research involved an extensive experimental investigation on two types of polymers (Novolac and PVA) as modifiers to produce the polymer modified bitumen (PMB). Different ratios of both additives were investigated for rheological properties of binder and mechanical properties of hot mix asphalt (HMA). The mechanical properties of HMA were assessed by the Marshall stability test, retained Marshall stability test, indirect tensile strength test, tensile strength ratio (TSR) and striping test. The results of tests showed that the Novolac modifier improves the cohesion properties of binder and the adhesion of binder to aggregate.

It was observed that the gradation of aggregate also affects the moisture damage in bituminous mixes. The bituminous concrete mix with VG30 binder showed lower values of the retained Marshall stability than dense bituminous macadam (DBM) with VG 30 binder [13]. Affrin and Anand Babu [14] discussed that one of the main causes of distress in asphalt pavements is moisture damage. The effectiveness of hydrated lime in improving the resistance of asphalt mixtures to moisture susceptibility is evaluated to determine the influence of compaction technique (Marshall and roller compaction) on the moisture susceptibility of asphalt mixtures. The asphalt mixtures were prepared using aggregate (granite), and asphalt binder (VG-30). In addition, one of the common anti-stripping additive, hydrated lime, is used to improve the asphalt mixture resistance to moisture damage. Asphalt mixes prepared at optimum binder content were tested for indirect tensile strength and retained stability. An optimum hydrated lime content of 2% is expected to improve the resistance of asphalt mixtures to moisture-induced damage.

One such solution to this problem is the use of modified bitumen that satisfies both the strength and economic aspects. The generation of waste material is analogous to the population growth in the world. Paper manufacturing and toothpaste industry generate the sludge in large quantities. This waste sludge from the industry is generally dumped of as landfills or directly into river and streams causing huge harm to the environment. Due to space constraint, the sludge is generally left untreated and causes health concern. Therefore, it is the prime necessity to find a substitute to dispose of this humongous amount of waste. Many researchers works have been intended to evaluate the moisture damage of pavements but not much work has been done with sludge modified mixes. The objective of this study is to assess the resistance to moisture-induced damage of sludge modified asphalt mixes by conducting indirect tensile strength and retained Marshall stability test.

2 Experimental Programme

The research is intended to assess the result of moisture damage on lime sludge modified HMA specimens. Several tests were carried out to determine the optimum sludge content. The Marshall specimens were prepared using optimum sludge and bitumen and the specified mix. In this paper, the results of different moisture susceptibility tests are discussed. The overall methodology used in this study is described in Fig. 1.

2.1 Lime Sludge

The waste sludge sample is collected from toothpaste and paper industry as shown in Figs. 2 and 3, respectively. The characterization of the waste material was done prior to its use. The specimen is found to be unreactive with water as no fumes or explosive gases were evolved. The chemical characteristics of lime sludge after laboratory tests are given in Table 1.

The SEM image of the sludge specimen is given in Fig. 4. It is observed that the structure of sludge is highly porous and has a rough surface.

2.2 Bituminous Binder

Bituminous binder type is selected in India based on the guidelines given in MoRTH (2013), IRC: 111 (2009) and IRC: SP-53 (2010). Bitumen is classified into four grades

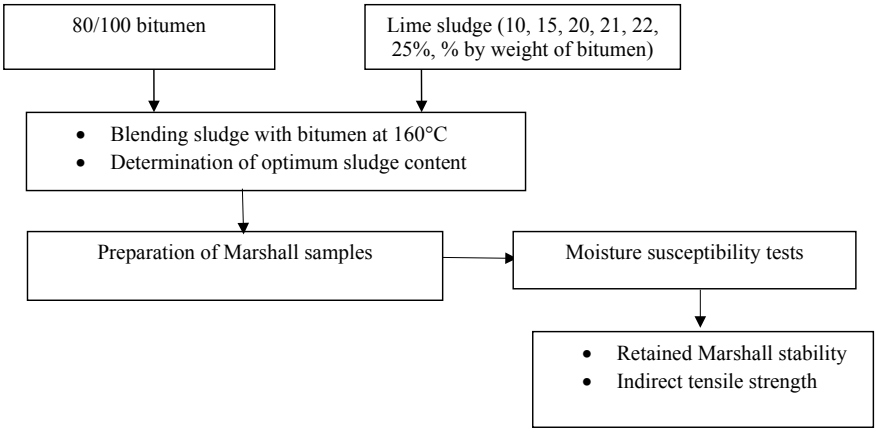

Fig. 1 Methodology adopted in the current research

Fig. 2 Lime sludge from toothpaste industry

Fig. 3 Lime sludge from paper industry

Table 1 Chemical characteristics of lime sludge

Test carried out	Test value
$CaCo_3$ by mass	40%
Loss on ignition% by mass (@900° ± 25°)	63.5
Iron as Fe_2O_3 % by mass	0.04
Alumina as Al_2O_3 % by mass	0.36
Magnesium as MgO % by mass	0.93
Calcium as CaO % by mass	34.2
Sodium as Na_2O % by mass	0.11
Potassium as K_2O % by mass	0.07

based on the viscosity, and suitability recommended for maximum air temperature as given by IS 73:2013 and is described in Table 2. VG 10 grade bitumen is used for carrying out research work. The properties of neat bituminous binder used and the specifications provided by standard are summarized in Table 3.

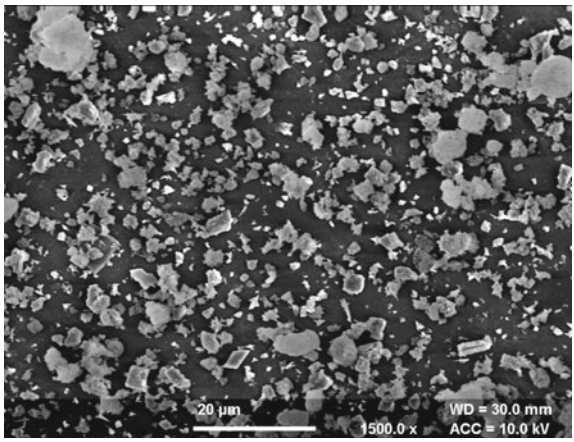

Fig. 4 SEM analysis of sludge sample

Table 2 Grades of bitumen

Grade	Average maximum day temperature (°C)
VG 10	<30
VG 20	30–38
VG 30	38–45
VG 40	>45

Table 3 Properties of unmodified bitumen

Grade of bitumen	VG 10	
	Result	Spec (min)
Penetration value (0.1 mm, 5 s) @ 25 °C	95.3	80
Ductility (cm) @ 25 °C	78.7	75
Absolute viscosity @ 60 °C (poise)	1079	800–1200
Kinematic viscosity @ 135 °C, cSt	257	250
Softening point (°C)	51	40

The waste sludge was added in contents of 10, 15, 20, 21, 22 and 25% to the binder after it was heated to a temperature of 160 °C. The blend was then manually mixed for about 5–10 min. The prepared sample is shown in Fig. 5. The SEM images of modified bitumen in given in Fig. 6.

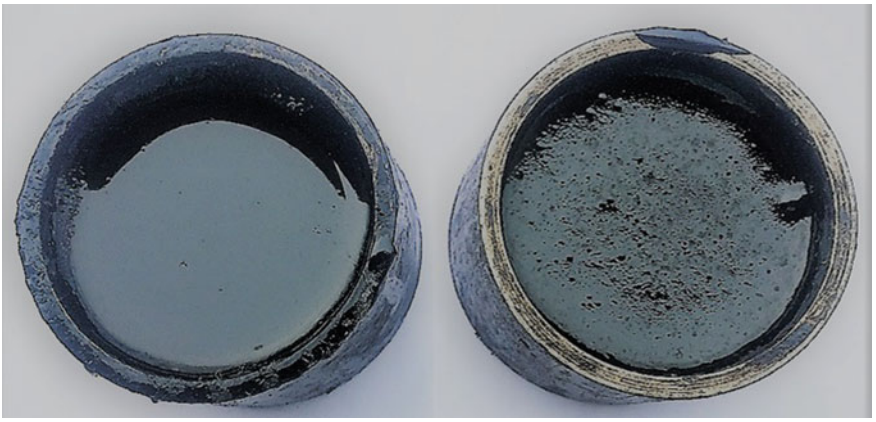

Fig. 5 Unmodified and modified bitumen samples

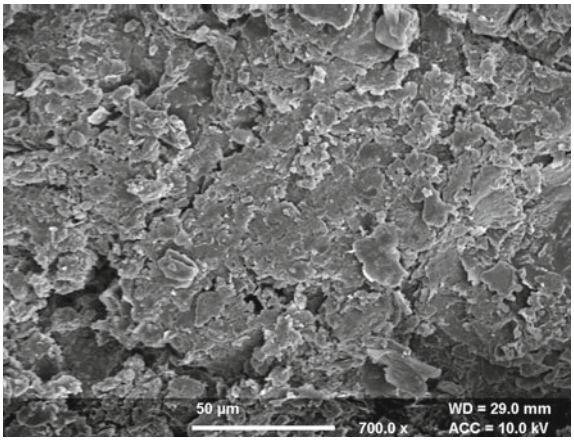

Fig. 6 SEM analysis of modified bitumen

2.3 Aggregates

Fresh aggregates were collected from construction site near the university situated in Baddi district of Himachal Pradesh, India. The crushed stone aggregate of limestone type with maximum nominal size of 26.5 mm was used to prepare the bituminous mix specimens. Bituminous concrete (BC) is commonly used as a surfacing layer for high traffic volume roads in India. The gradation of aggregate as specified in MoRTH specifications for BC was used. Tests were performed to determine the aptness of aggregate and results are presented in Table 4. The gradation of aggregate used is given in Fig. 7.

Table 4 Properties of aggregates

Properties	Coarse aggregates	Test method
Aggregate crushing value (%)	22	BIS:2386 (Part IV)—1963
Aggregate impact value (%)	18	BIS:2386 (Part IV)—1963
Specific gravity	2.7	BIS:2386 (Part IV)—1963
LA abrasion value	17	BIS:2386 (Part IV)—1963
Water absorption (%)	0.9	BIS:2386 (Part IV)—1963
Combined flakiness and elongation index (%)	19	BIS:2386 (Part IV)—1963

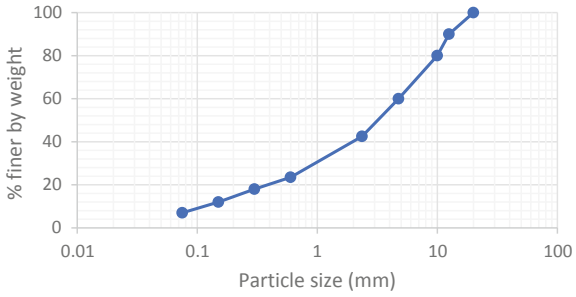

Fig. 7 Gradation of aggregate used

2.4 Test Method

Marshall method of mix design was used in the design of asphalt mixture, and optimum bitumen content was found as 6.5% by weight. The optimum sludge content was calculated by varying the amount of sludge as 10, 15, 20, 21, 22, 25% and performing different tests.

Retained Marshall stability

The resistance to moisture damage in asphaltic pavements can be determined using the retained Marshall stability method. The test is specified in IRC: SP 53-2002 and is conducted as per ASTM D 1075–1979 specifications. The Marshall specimens were prepared by varying the percentage of sludge and corresponding bitumen content. The retained Marshall stability is calculated using Eq. 1.

$$\text{RMS} = \frac{100 \times \text{MS(wet)}}{\text{MS(dry)}}. \tag{1}$$

where RMS = Retained Marshall stability of the specimen
MS_{dry} = Marshall stability of unconditioned specimen (kN)
MS_{wet} = Marshall stability of conditioned specimen (kN)

The conditioned specimen is the one which is kept in water bath for 24 h at a maintained temperature of 60 °C before testing. The results are expressed as percentage. The higher the value of RMS, the greater is the moisture resistance of the mix.

Indirect tensile strength (ITS)
The test is conducted on Marshall specimens prepared with different percentages of sludge and corresponding bitumen content. The test is conducted in accordance with ASTM D6931. The loading develops an indirect tensile stress in the direction perpendicular to the direction of application of load. The indirect tensile strength of the mix is evaluated based upon the maximum load that can be carried by the specimen using Eq. 2.

$$\mathrm{St} = \frac{2000 \times P}{\pi \times t \times D} \tag{2}$$

where St = Indirect tensile strength, kPa
P = maximum load, N
T = specimen height, mm
D = specimen diameter, mm

This is a performance test used to determine the resistance to moisture of the mix. It is further required to calculate the tensile strength ratio (TSR) of the mix which is a measure of sensitivity of the mix to moisture. The conditioning of specimen is done to calculate the wet tensile strength. The specimen is immersed in water for 24 h at a maintained temperature of 60 °C. TSR can be determined using Eq. 3.

$$\mathrm{TSR} = 100 \times \frac{\mathrm{ITS\ (wet)}}{\mathrm{ITS\ (dry)}} \tag{3}$$

The results are expressed in percentage. The greater the value of TSR, the higher is the resistance to moisture damage of the mix. MoRTH specifies a minimum value of 80% TSR for use in pavements.

3 Results and Discussion

The presence of moisture can affect the performance of the mix adversely. The results for various tests conducted to determine moisture susceptibility are thus discussed below.

Retained Marshall Stability test
The results of the retained Marshall stability are presented in Table 5 and Fig. 10 for different values of sludge. As the percentage of sludge added increases, it is

Table 5 Retained Marshall stability test results

Percentage sludge (by wt. of bitumen) (%)	Unconditioned sample	Conditioned sample	Retained stability (%)
0	1601.4	1435	89.61
10	1459.4	1290	88.39
15	1553.4	1280	82.40
20	1988.3	1867	93.90
21	1997.5	1900	95.12
22	1875.4	1656	88.30
25	1754.5	1467	83.61

observed that the values of the retained Marshall stability show fluctuating trend with maximum value at 21%. The values do not follow a constant increasing or decreasing trend.

Sample calculation for retained stability

For 21% sludge,

Unconditioned Marshall stability = 1997.5 kN

Conditioned Marshall stability = 1900 kN

Retained Marshall stability (RMS) $= \frac{100 \times 1900}{1997.5} = 95\%$

Indirect Tensile strength

Figures 8 and 9 show the indirect tensile strength and tensile strength ratio, respectively, at different percentages of sludge added to asphalt mixture. The mixes with 21% lime sludge showed better performance than the rest of the mixture. The reason for the same can be explained here. The viscosity of the bituminous binder was high with 21% sludge than others, and it is known that high viscosity of binder resists displacement by water and provides a better retention of binder on aggregate surface. Higher tensile ratio shows that the mixture has a better resistance to water damage (Fig. 10).

Sample calculation for tensile strength ratio:-

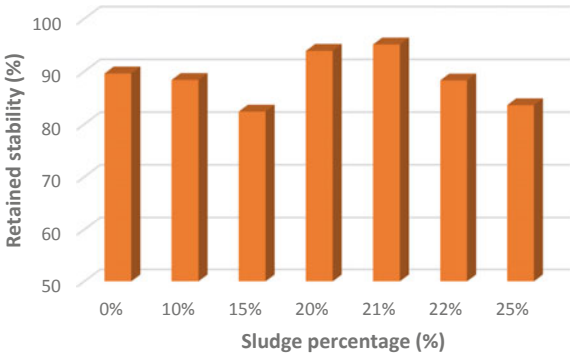

Fig. 8 Variation of retained stability with sludge

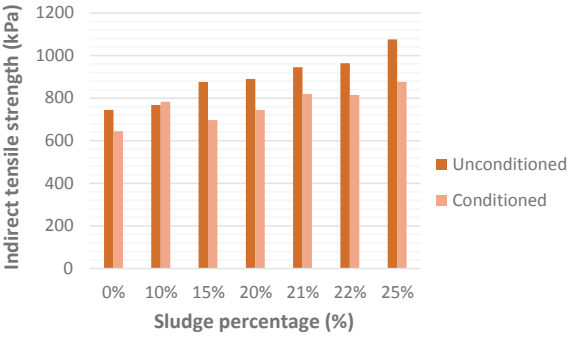

Fig. 9 Variation of indirect tensile strength with sludge

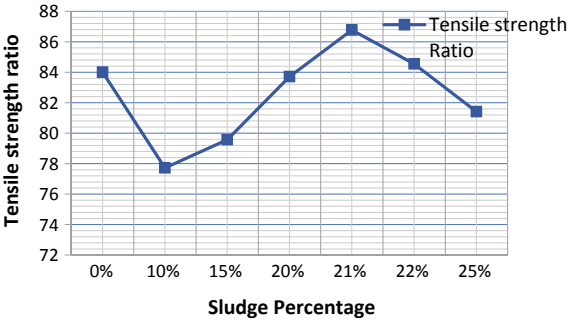

Fig. 10 Variation of tensile strength ratio with sludge

For 21% sludge value,
Unconditioned indirect tensile strength (ITS_{dry}) = 945 kPa
Conditioned indirect tensile strength (ITS_{wet}) = 820 kPa
Tensile strength ratio (TSR) = $\frac{100\times820}{945}$ = 87%

4 Conclusions

The addition of sludge improves the properties of the mix as mentioned in the literature. Different moisture susceptibility tests were conducted so as to determine the resistance of the mix to moisture damage. The conclusions drawn from the study are as follows-

- The addition of waste sludge to pure bitumen has been studied to improve its characteristics and performance of sludge modified bituminous mix. The moisture susceptibility of binder was evaluated by conducting the retained marshall stability and the tensile strength ratio test. The ideal value of sludge added to the mix comes out to be 21% by weight of bitumen.
- The retained Marshall stability of the mix with 21% sludge was found to be 95%. Higher the value of retained stability, greater is the resistance to moisture damage.

- The indirect tensile strength of the mix with 21% sludge was found to be 87%. According to Ministry of Road Transport and Highway (MoRTH) standards, tensile strength ratio (TSR) values above 80% are considered to be minimum threshold for HMA. The value of TSR corresponding to 21% sludge is maximum and hence optimum value for use.

Hence, it is found that addition of sludge increases the resistance to moisture damage of the binder and converts the soft grade bitumen to the hard grade bitumen.

Acknowledgements Authors are thankful to the Department of Environment, Science & Technology, Paryavaran Bhawan, US Club, Government of Himachal Pradesh, Shimla, for providing the financial assistance to carry out this research.

References

1. IRC 37 (2012) Guidelines for the design of flexible pavements. Indian Roads Congress. New Delhi, pp 1–94
2. Montepara A, Tebaldi G, Marradi A, Betti G (2012) Effect on pavement performance of a sub-base layer composed by natural aggregate and RAP. Proc Soc Behav Sci 53:981–990
3. Sayyed SS, Patil RP, Tapase A, Attar AC, Chandak PG (2018) Review and assessment of flexible pavement. Advancements on sustainable civil infrastructures. GeoChina sustainable civil infrastructures. HangZhou, China, 23–25 July, pp 139–149
4. Ranadive MS, Tapase AB (2013) Investigation of behavioral aspects of flexible pavement under various conditions by finite element method. Constitutive Model Geomater 48:765–770
5. Ghosh D, Marasteanu M, Falchetto AC, Turos M (2017) Testing protocol to obtain failure properties of asphalt binders at low temperature using creep compliance and stress-controlled strength test. Road Mater Pavement Des 18(2):352–367
6. Cheung LW, Kong PK, Leung GLM, Wong WG (2012) Structural assessment of cracked flexible pavement. In: 7th RILEM international conference on cracking in pavements, RILEM Bookseries. Springer, 4, Dordrecht, Netherlands, pp 277–285
7. Naik AM, Gupta R (2018) A review on evaluation of flexible pavement failures. Int Res J Eng Technol 5(8):1527–1529
8. Shah YU, Jain SS, Tiwari D, Jain MK (2013) Development of overall pavement condition index for urban roads networks. Proc Soc Behav Sci 104:332–41
9. Dangar RP, Zala LB, Umrigar FS (2011) Pavement deterioration-a case study on national highway 8b Section Rajkot-Bamanbore (Km 185/0-Km 216/8). In: National conference on recent trends in engineering & technology, Gujarat, India, 13–14 May, pp 45–51
10. Gupta A, Rastogi R (2011) Pavement deterioration and maintenance model for low volume roads. Int J Pavement Res Technol 4(4):195–202
11. Gonzalez RC, Woods RE (2002) Digital image processing, 2nd edn, Chap 3. Prentice Hall, New Jersey, pp 136, 164
12. Hameed KK, Merawi HA (2016) Evaluation of moisture damage and stripping of asphalt concrete prepared with new additives of polymer modified bitumen. J Univ Babylon 24(1):117–128. ISSN 19920652 23128135
13. Habeeb H, Chandra S, Nashaat Y (2013) Estimation of moisture damage and permanent deformation in asphalt mixture from aggregate gradation. July 12, 2012/Revised March 25, 2013/Accepted November 4, 2013/Published Online July 7, 2014
14. Affrin SKR, Anand Babu Y (2017) Study on improvement in performance of moisture damage in asphalt mixtures with various anti-stripping agents. Int J Sci Eng Technol Res (IJSETR) 6(6). ISSN 2278-7798